COMBRI DESIGN MANUAL

Part I: Application of Eurocode rules

A project carried out with a financial grant from the Research Fund for Coal and Steel (RFCS) of the European Community.

COMBRI DESIGN MANUAL

Part I: Application of Eurocode rules

Universität Stuttgart
Germany

RWTH AACHEN UNIVERSITY

cticm

LULEÅ UNIVERSITY OF TECHNOLOGY

Université de Liège

labein tecnalia

Sétra Service d'études sur les transports, les routes et leurs aménagements

A project carried out with a financial grant from the Research Fund for Coal and Steel (RFCS) of the European Community.

Although all care has been taken to ensure the integrity and quality of this publication and the information herein, no liability is assumed by the project partners and the publisher for any damage to property or persons as a result of the use of this publication and the information contained herein.

1st Edition
Copyright © 2008 by project partners
Reproduction for non-commercial purpose is authorised provided the source is acknowledged and notice is given to the project coordinator. Publicly available distribution of this publication through other sources than the web sites given below requires the prior permission of the project partners. Requests should be addressed to the project coordinator:

Universität Stuttgart
Institut für Konstruktion und Entwurf / Institute for Structural Design
Pfaffenwaldring 7
70569 Stuttgart
Germany
Phone: +49-(0)711-685-66245
Fax: +49-(0)711-685-66236
E-mail: sekretariat@ke.uni-stuttgart.de

The present document and others related to the research project COMBRI+RFS-CR-03018 “Competitive Steel and Composite Bridges by Improved Steel Plated Structures” and the successive dissemination project RFS2-CT-2007-00031 “Valorisation of Knowledge for Competitive Steel and Composite Bridges”, which have been co-funded by the Research Fund for Coal and Steel (RFCS) of the European Community, can be accessed for free on the following project partners’ web sites:

Belgium:	www.argenco.ulg.ac.be
France:	www.cticm.com
Germany:	www.uni-stuttgart.de/ke, www.stb.rwth-aachen.de
Spain:	www.labein.es, www.apta.org.es
Sweden:	cee.project.ltu.se

Cover pictures (from left to right):

Valley bridge Haseltal near Suhl, Germany, 2006 (© KE)
Valley bridge Dambachtal near Suhl, Germany, 2005 (© KE)
Viaduct over Dordogne river near Souillac, France, 2000 (© Sétra)

Preface

This design manual is an outcome of the research project RFS-CR-03018 “Competitive Steel and Composite Bridges by Improved Steel Plated Structures - COMBRI” [7] and the successive dissemination project RFS2-CT-2007-00031 “Valorisation of Knowledge for Competitive Steel and Composite Bridges - COMBRI+” which have been funded by the Research Fund for Coal and Steel (RFCS) of the European Community. Within the RFCS research project essential knowledge has been acquired to enhance the competitiveness of steel and composite bridges and this has been incorporated in the design manual at hand which has been also presented in the frame of several seminars and workshops. The manual is subdivided into two parts to provide the reader with clearly arranged and concise documents:

► Part I: Application of Eurocode rules

In the research project the different national background of each partner how to apply and interprete Eurocode rules was brought together and a European melting pot of background information and general knowledge has been created. In order to maintain this valuable information two composite bridge structures - a twin-girder and a box-girder bridge - are covered in this part of the COMBRI Design Manual on the basis of worked examples for which the knowledge is written down in a descriptive manner. The examples include references to current Eurocode rules.

► Part II: State-of-the-Art and Conceptual Design of Steel and Composite Bridges

The national state-of-the-art in bridge design can be different so that firstly bridge types of the project partners’ countries - Belgium, France, Germany, Spain and Sweden - are introduced. They reflect the current practice in those countries and common bridge types as well as unusual bridges intended to solve special problems and some solutions being part of development projects are presented in Part II of the COMBRI Design Manual [8]. Also, improvements which can be provided to the design of steel and composite bridges are discussed and the possibilities and restrictions given by the current Eurocode rules are highlighted.

Moreover, the features of software ***EB**Plate* [13] developed in the research project to determine the elastic critical buckling stresses are presented in its contributive application for bridge design.

Finally, the authors of this design manual gratefully acknowledge the support and financial grant of the Research Fund for Coal and Steel (RFCS) of the European Community.

Ulrike Kuhlmann, Benjamin Braun
Universität Stuttgart, Institute for Structural Design / Institut für Konstruktion und Entwurf (KE)

Markus Feldmann, Johannes Naumes
RWTH Aachen University, Institute for Steel Structures

Pierre-Olivier Martin, Yvan Galéa
Centre Technique Industriel de la Construction Métallique (CTICM)

Bernt Johansson, Peter Collin, Jörgen Eriksen
Luleå University of Technology, Division of Steel Structures (LTU)

Hervé Degée, Nicolas Hausoul
Université de Liège, ArGEnCo Département

José Chica
Fundación LABEIN

Joël Raoul, Laurence Davaine, Aude Petel
Service d'études sur les transports, les routes et leurs aménagements (Sétra)

October 2008

Table of Contents

Page

Notations V

1 Introduction and scope 1
  1.1 Introduction 1
  1.2 Structure of the document 3
2 Description of the deck and global analysis 5
  2.1 Twin-girder bridge 5
    2.1.1 Longitudinal elevation 5
    2.1.2 Transverse cross-section 5
    2.1.3 Structural steel distribution 5
    2.1.4 Construction phases 11
  2.2 Box-girder bridge 15
    2.2.1 Longitudinal elevation 15
    2.2.2 Transverse cross-section 15
    2.2.3 Structural steel distribution 17
    2.2.4 Construction phases 19
  2.3 General common data 25
    2.3.1 Reinforcement of the concrete slab 25
      2.3.1.1 Description of the slab reinforcement 25
      2.3.1.2 Modelling the slab to calculate the general longitudinal bending 25
    2.3.2 Material properties 29
      2.3.2.1 Structural steel 29
      2.3.2.2 Concrete 29
      2.3.2.3 Reinforcement 31
      2.3.2.4 Partial safety factors for materials 31
    2.3.3 Actions 31
      2.3.3.1 Permanent loads 33
      2.3.3.2 Concrete shrinkage 35
      2.3.3.3 Creep – Modular ratios 37
      2.3.3.4 Traffic loads 39
      2.3.3.5 Torque 47
      2.3.3.6 Thermal gradient 49
    2.3.4 Combinations of actions 49
      2.3.4.1 Design situations 49

2.3.4.2 General remarks 49
2.3.4.3 ULS combinations other than fatigue 51
2.3.4.4 SLS combinations 51
2.4 Global analysis....53
2.4.1 General 53
2.4.1.1 Concrete cracking 53
2.4.1.2 Shear lag in the concrete slab....53
2.4.2 Internal forces and moments – Stresses....53
2.4.2.1 Numerical model....53
2.4.2.2 Effective width....55
2.4.2.3 Determination of the cracked zones around internal supports 63
2.4.2.4 Shrinkage and cracked zones 65
2.4.2.5 Organisation of the global analysis calculations....65
2.4.2.6 Results....69
3 Cross-section verifications....79
3.1 Twin-girder bridge....79
3.1.1 General 79
3.1.2 Check of cross-section at the end support C0....81
3.1.2.1 Geometry....81
3.1.2.2 Material properties 83
3.1.2.3 Internal forces and moments 85
3.1.2.4 Determination of the cross-section class....85
3.1.2.5 Plastic section analysis....87
3.1.3 Check of cross-section at mid-span C0-P1....95
3.1.3.1 Geometry....95
3.1.3.2 Material properties 95
3.1.3.3 Internal forces and moments 95
3.1.3.4 Determination of the cross-section class....95
3.1.3.5 Plastic section analysis....95
3.1.4 Check of cross-section at mid-span P1-P2 97
3.1.4.1 Geometry....97
3.1.4.2 Material properties 99
3.1.4.3 Internal forces and moments 101
3.1.4.4 Determination of the cross-section class....101
3.1.4.5 Plastic section analysis....103
3.1.5 Check of cross-section at the internal support P2....107
3.1.5.1 Subpanel 1 - Geometry....107
3.1.5.2 Subpanel 1 - Material properties....111
3.1.5.3 Subpanel 1 - Internal forces and moments....111

3.1.5.4 Subpanel 1 - Determination of the cross-section class....111

3.1.5.5 Subpanel 1 - Elastic section analysis....115

3.1.5.6 Subpanel 2 - Geometry....128

3.1.5.7 Subpanel 2 - Material properties....128

3.1.5.8 Subpanel 2 - Internal forces and moments....128

3.1.5.9 Subpanel 2 - Determination of the cross-section class....128

3.1.5.10 Subpanel 2 - Elastic section analysis....128

3.1.5.11 Subpanel 3 - Geometry....132

3.1.5.12 Subpanel 3 - Material properties....134

3.1.5.13 Subpanel 3 - Internal forces and moments....134

3.1.5.14 Subpanel 3 - Determination of the cross-section class....134

3.1.5.15 Subpanel 3 - Elastic section analysis....134

3.2 Box-girder bridge....139

3.2.1 General....139

3.2.2 Check of cross-section at mid-span P1-P2....141

3.2.2.1 Geometry....141

3.2.2.2 Material properties....143

3.2.2.3 Internal forces and moments....143

3.2.2.4 Reduction due to shear lag effect....145

3.2.2.5 Determination of the cross-section class....145

3.2.2.6 Bending resistance verification....147

3.2.2.7 Shear resistance verification....147

3.2.2.8 Interaction between bending moment and shear force....153

3.2.3 Check of cross-section at the internal support P3....153

3.2.3.1 Geometry....153

3.2.3.2 Material properties....155

3.2.3.3 Internal forces and moments....157

3.2.3.4 Mechanical properties of the gross cross-section....157

3.2.3.5 Effective area of the bottom flange....159

3.2.3.6 Effective area of the web....175

3.2.3.7 Bending resistance verification....181

3.2.3.8 Shear resistance verification....181

3.2.3.9 Interaction between bending moment and shear force....191

4 Verifications during erection....195

4.1 Twin-girder bridge....195

4.1.1 General....195

4.1.2 Verifications according to Sections 6 and 7, EN 1993-1-5....199

4.1.3 Verifications according to Section 10, EN 1993-1-5....201

4.1.4 Results....209

4.2 Box-girder bridge 211
  4.2.1 General 211
  4.2.2 Verifications according to Section 6, EN 1993-1-5 217
    4.2.2.1 Launching situation “1” 217
    4.2.2.2 Launching situation “2” 223
    4.2.2.3 Launching situation “3” 223
  4.2.3 Verifications according to Section 10, EN 1993-1-5 225
    4.2.3.1 Webpanel (Launching situation “1” only) 225
    4.2.3.2 Bottom plate 243
  4.2.4 Results 263
5 Summary 267
References 271
List of figures 273
List of tables 277

Notations

Small Latin letters

a	Length of a web plate between adjacent vertical stiffeners (possible lower indices: p, w)
b_b	Width of the bottom flange
b_{bf}	Width of the bottom flange of the beam
b_{eff}	Effective width of the concrete slab
b_i	Actual geometric width of the slab associated to the main girder
b_{tf}	Width of the top flange of the beam
b_p	Width of the panel
b_{slab}	Thickness of the concrete slab
b_{sub}	Width of each subpanel of the bottom flange
b_0	Center-to-center distance between the outside stud rows
b_1	Distance between webs of stiffener
b_2	Width of stiffener flange
b_3	Width of each stiffener web
c_{bf}	Part of the bottom flange subject to compression
c_w	Part of the web subject to compression
c_{lr}	Distance between the centroid of each lower longitudinal reinforcing steel layer and the near free external surface
c_{ur}	Distance between the cenroid of each upper longitudinal reinforcing steel layer and the near free external surface
e	Thickness of the concrete slab
f_{cd}	Design value of concrete compressive strength
f_{ck}	Characteristic compressive cylinder strength at 28 days
$f_{ctk,0.05}$	5% fractile of the characteristic axial tensile strength
$f_{ctk,0.95}$	95% fractile of the characteristic axial tensile strength
f_{ctm}	Mean value of axial tensile strength
f_{cm}	Mean value of concrete cylinder strength at 28 days
f_{sk}	Yield strength of the reinforcing steel bars
f_u	Ultimate stress of the structural steel
f_y	Yield strength of the structural steel (possible lower indices: w, tf, tf1, tf2, tst, p)
f_{yd}	Design yield strength (possible lower indices: w, tf, tf1, tf2, tst, p)
h	Height of the beam
$h_{a,seff}$	Effective elastic neutral axis (ENA) of the structural steel part only
h_{eff}	Effective elastic neutral axis of the composite cross-section

h_w	Height of the web of the beam
$h_{w,eff}$	Effective height of the web in compression of the beam
$h_{we1,2}$	Distribution of the effective height of the web in compression of the beam
h_{st}	Height of stiffener
k_σ	Plate buckling coefficient for normal stress (possible lower indices: c, p, w, pw, pbf, LT, op)
k_τ	Plate buckling coefficient for shear stress
$k_{\tau,st}$	Plate buckling coefficient for shear stress for plate with longitudinal stiffeners
m_q	Torque loads due to distributed loads
n_{lr}	Total number of steel reinforcement in lower layer
n, n_0	Structural steel / concrete modular ratio for short-term loading
n_L	Structural steel / concrete modular ratio for long-term loading
n_{st}	Number of stiffeners (equally spaced) of the bottom flange
n_{ur}	Total number of steel reinforcement on in upper layer
p	Perimeter of the concrete slab
q	Eccentric distributed traffic loads
q_{fk}	Characteristic value of the uniformly distributed load due to pedestrian and cycle traffic
q_{min}	Minimum value of the line load due to bridge equipment
q_{max}	Maximum value of the line load due to bridge equipment
q_{nom}	Nominal value of the line load due to bridge equipement (safety devices, pavement, …)
s_{lr}	Spacing in lower layer of steel reinforcement of the concrete slab
s_{ur}	Spacing in upper layer of steel reinforcement of the concrete slab
t	Plate thickness (possible lower indices: tf, tf1, tf2, p, w, st)
t	Time
t_0	Age of the concrete put in place at each construction phase
t_f	Thickness of the flange of the beam (possible lower indices: 1, 2)
t_{ini}	Time at traffic opening
t_{slab}	Thickness of the concrete slab
t_{st}	Thickness of stiffener
$t_{st,eq}$	Equivalent thickness of stiffener web
t_w	Thickness of the web of the beam
w	Width of all traffic lanes
x	Abscissa of bridge
z	Position of the centre of gravity of the cross-section
z_{na}	Position of the centre of gravity of the composite cross-section
z_{pl}	Position of the plastic neutral axis (PNA) of the composite cross-section

Capital Latin Letters

A_a	Cross-sectional area of the structural steel section
A_{abf}	Cross-sectional area of the bottom flange
$A_{a,\,eff}$	Effective cross-sectional area of the steel structural part only
A_{atf}	Cross-sectional area of the top flange (possible lower indices: 1, 2)
A_{aw}	Cross-sectional area of the web
A_c	Total cross-sectional area of the concrete slab; Gross area of the bottom flange with stiffeners neglecting parts supported by adjacent plate elements
$A_{c.eff.loc}$	Effective local area of the bottom flange with stiffeners
A_{clr}	Cross-sectional area of the concrete located under the lower layer of steel reinforcement of the slab
A_{clur}	Cross-sectional area of the concrete located between the lower and upper layer of steel reinforcement of the slab
A_{cur}	Cross-sectional area of the concrete located above the upper layer of steel reinforcement of the slab
A_{eff}	Effective cross-sectional area of the composite cross-section
A_{slr}	Cross-sectional area of one steel reinforcement of the lower layer of the slab
A_{stw}	Cross-sectional area of the web stiffener
A_{sur}	Cross-sectional area of one steel reinforcement of the upper layer of the slab
A_{tot}	Gross cross-sectional area of the composite cross-section
A_{tslr}	Cross-sectional area of the total steel reinforcement of the lower layer of the slab
A_{tsur}	Cross-sectional area of the total steel reinforcement of the upper layer of the slab
E_a	Elasticity modulus of structural steel
E_{cm}	Elasticity modulus of concrete
E_s	Elasticity modulus of reinforcing steel
G_k	Characteristic (nominal) value of the effect of permanent actions
$G_{k,inf}$	Characteristic value of a *favourable* permanent action (nominal value of self-weight and minimum value of non-structural equipments) taking account of construction phases
$G_{k,sup}$	Characteristic value of an *unfavourable* permanent action (nominal value of self-weight and maximum value of non-structural equipments) taking account of construction phases
I	Second moment of area
$I_{a,eff}$	Effective second moment of area of the structural steel part
I_{eff}	Effective second moment of area of the cross-section
I_t	The St. Venant torsional stiffness
I_{tot}	Gross second moment of area of the composite bridge
I_{Δ}	Second moment of area (around a horizontal axis Δ located at the steel/concrete interface)
L_e	Equivalent span length in the considered cross-section
L_i	Length of the span i

$M_{a,Ed}$	Design bending moment acting on the structural steel cross-section
$M_{c,Ed}$	Design bending moment acting on the composite cross-section
$M_{f,Rd}$	Design value of the plastic resistance moment of a cross-section consisting of the flanges only
M_{Ed}	Design bending moment
$M_{pl,Rd}$	Design value of the plastic bending moment resistance
M_Q	Torque loads due to concentrated loads
N_a	Design value of the plastic normal force resistance of the structural steel cross-section
N_{abf}	Design value of the plastic normal force resistance of the structural steel bottom flange
N_{atf}	Design value of the plastic normal force resistance of the structural steel top flange
N_{aw}	Design value of the plastic normal force resistance of the structural steel web
N_c	Design value of the plastic normal force resistance of the concrete slab in compression
N_{clr}	Design value of the plastic normal force resistance of the concrete in compression located under lower layer of steel reinforcement
N_{cur}	Design value of the plastic normal force resistance of the concrete in compression located above upper layer of steel reinforcement
N_{clur}	Design value of the plastic normal force resistance of the concrete in compression located between lower and upper layer of steel reinforcement
N_{sl}	Design value of the plastic normal force resistance of the lower layer of steel reinforcement
N_{su}	Design value of the plastic normal force resistance of the upper layer of steel reinforcement
Q	Eccentric concentrated traffic loads
Q_{k1}	Characteristic value of the leading variable action 1
$Q_{ki,i\geq 2}$	Characteristic value of the accompagning variable action i
S	Envelope of characteristic values of internal forces and moments (or deformations) due to concrete shrinkage
S_{na}	Gross first moment of area of the composite cross-section
TS_k	Envelope of characteristic values of internal forces and moments (or deformations) due to the vertical concentrated loads from Load Model no. 1 in EN 1991-2
UDL_k	Envelope of characteristic values of internal forces and moments (or deformations) due to the vertical uniformly distributed loads from Load Model no. 1 in EN 1991-2
$V_{b,Rd}$	Design value of the shear resistance in case of shear plate buckling in the structural steel web
$V_{bf,Rd}$	Design value of the shear resistance of the flange in case of shear plate buckling in the structural steel web
$V_{bw,Rd}$	Design value of the shear resistance of the web in case of shear plate buckling in the structural steel web
V_{Ed}	Design shear force
$V_{Ed,\,proj}$	Projection of the design shear force in the direction of the web
V_{Rd}	Design value of the shear resistance
$V_{pl,Rd}$	Design value of the plastic shear resistance
$V_{pl,a,Rd}$	Design value of the plastic shear resistance of the structural steel cross-section

Small Greek letters

α	Factor; angle; compressed height percentage
α_{Qi}	Adjustment factor on concentrated load TS of LM1 on lanes i (i = 1, 2, …)
α_{qi}	Adjustment factor on uniformly distributed load UDL of LM1 on lanes i (i =1, 2,…)
α_{qr}	Adjustment factor on load model LM1 on the remaining area
β	Reduction factor for shear lag effect
γ_C	Partial safety factor for resistance of concrete
γ_M	Partial safety factor for resistance of structural steel
γ_{M0}	Partial safety factor for resistance of structural steel (Yielding, local instability)
γ_{M1}	Partial safety factor for resistance of structural steel (Resistance of members to instability)
γ_{M2}	Partial safety factor for resistance of structural steel (Resistance of joints)
$\gamma_{M,ser}$	Partial safety factor for resistance of structural steel at Serviceability Limit State (SLS)
γ_S	Partial safety factor for resistance of reinforcing steel
ε	Strain; factor $\sqrt{\frac{235N/mm^2}{f_y}}$ (possible lower indices: tf, tf1, tf2, p, w, st)
ε_{ca}	Autogenous shrinkage strain
ε_{cd}	Drying shrinkage strain
ε_{cs}	Total shrinkage strain
η	Coefficient of the yield strength of structural steel
η_1 ; η_3	Ratio between applied stress and yield strength in a structural steel cross-section
$\bar{\eta}_1$; $\bar{\eta}_3$	Ratio between applied force and resistance in a structural steel cross-section
θ_ω	Incline angle of the web with reference to the vertical direction
κ	Factor to take into account shear lag
$\bar{\lambda}$	Reduced slenderness (possible lower indices: c, p, w, pw, pbf, LT, op)
μ	Moment of area
ν	Poisson's ratio
σ_{abfu}	Stress at the upper edge of the bottom flange (possible lower indices: eff)
σ_{abfl}	Stress at the lower edge of the bottom flange (possible lower indices: eff)
σ_{atfl}	Stress at the lower edge of the top flange (possible lower indices: eff)
σ_{atfu}	Stress at the upper edge of the top flange (possible lower indices: eff)
σ_c	Longitudinal upper fibre tensile stress in the concrete slab
σ_{cr}	Elastic critical plate buckling stress
σ_E	Elastic critical Euler's stress
σ_{Ed}	Design value of a direct stress in a cross-section
σ_{tslr}	Stress in the lower reinforcement of the concrete slab (possible lower indices: eff)

σ_{tsur}	Stress in the upper reinforcement of the concrete slab (possible lower indices: eff)
$\sigma_{sup,reinf}$	Maximal ULS Stress in the upper reinforcement of the concrete slab in the cracked behaviour (sagging moment)
ρ	Reduction factor (≤ 1,0) for effective area of a structural steel cross-section
ρ_c	Reduction factor for effective^{p} width
ρ_s	Reinforcement ratio in a concrete cross-section
τ_{cr}	Elastic critical shear buckling stress
τ_{Ed}	Design value of a shear stress in a cross-section
φ	Creep function
ϕ	Diameter of the steel reinforcement of the concrete slab
ϕ_{lr}	Diameter of the upper steel reinforcement of the concrete slab
ϕ_{ur}	Diameter of the upper steel reinforcement of the concrete slab
χ	Reduction factor (≤ 1) for instability (possible lower indices: c, p, w)
ψ	Stress ratio between opposite edges of a structural steel plate (possible lower indices: w)
ψ_L	Creep multiplier for modular ratio
ψ_0	Factor for the combination value of a variable action
ψ_1	Factor for the frequent value of a variable action
ψ_2	Factor for the quasi-permanent value of a variable action
Ω	Area bordered by the mid-planes of the internal elements of the box cross-section

1 Introduction and scope

1.1 Introduction

In the COMBRI research project [7], in which this design manual has its origin, the different national background of each partner how to apply and interprete Eurocode rules was brought together and a European melting pot of background information and general knowledge has been created. In order to facilitate the implementation of Eurocodes EN 1993-1-5, EN 1993-2 and EN 1994-2 with regard to plate buckling verifications, it was decided to cover two steel-concrete composite bridges - a twin-girder and a box-girder bridge - in order to present the knowledge with the help of worked examples and in a very descriptive manner. As the examples focus in detail on the application and interpretation of Eurocode rules which are related to plate buckling verifications, the overall view on bridge design cannot be covered. In this context, Figure 1-1 shows how many standards can be involved in the design of a composite bridge. Here, we are mainly dealing with EN 1993-1-5 “Plated Structural Elements”, EN 1993-2 “Steel bridges” and EN 1994-2 “Composite bridges”.

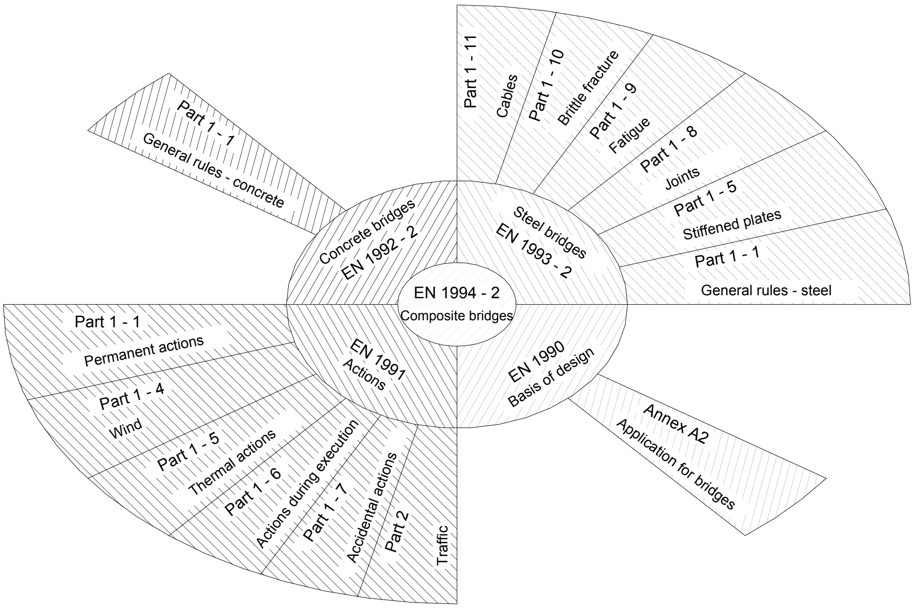
Part 1 - 1
General rules - concrete
Concrete bridges
EN 1992 - 2
Part 1 - 11
Cables
Part 1 - 10
Brittle fracture
Part 1 - 9
Fatigue
Part 1 - 8
Joints
Part 1 - 5
Stiffened plates
Part 1 - 1
General rules - steel
Steel bridges
EN 1993 - 2
EN 1994 - 2
Composite bridges
Part 1 - 1
Permanent actions
Part 1 - 4
Wind
Part 1 - 5
Thermal actions
Part 1 - 6
Actions during execution
Part 1 - 7
Accidental actions
Part 2
Traffic
EN 1991
Actions
EN 1990
Basis of design
Annex A2
Application for bridges

Figure 1-1: Eurocodes to be used in a composite bridge design.

In some parts, this design manual introduces general assumptions e.g. on actions without aiming to present the theoretical background or the modelling in detail. In addition to that, it is assumed that the reader is familiar with general design and modelling issues of bridges because this design manual gives a detailed view on plate buckling topics but it can of course not cover all other topics related to the verification of the design. For further information to the aforementioned topics, the reader is referred to e.g. [2], [4], [6], [32], [33], [34], [35], [36], [37], [39], [41]. However, this summary of references does not attempt to provide a comprehensive overview on available literature so that much more excellent work may exist which is not mentioned here.

The design of steel and composite bridges according to the Eurocodes

For the design of steel and composite bridges the following Eurocodes are mandatory [3]:

EN 1990/A1	Eurocode: Basis of structural design – Application for bridges [14]
EN 1991-1-1	Eurocode 1: Actions on structures – Part 1-1: General actions - Densities, self-weight, imposed loads for buildings [15]
EN 1991-1-3	Eurocode 1: Actions on structures – Part 1-3: General actions, Snow loads [16]
EN 1991-1-4	Eurocode 1: Actions on structures – Part 1-4: General actions, Wind actions [17]
EN 1991-1-5	Eurocode 1: Actions on structures – Part 1-5: General actions, Thermal actions [18]
EN 1991-1-6	Eurocode 1: Actions on structures – Part 1-6: General actions, Actions during execution [19]
EN 1991-1-7	Eurocode 1: Actions on structures – Part 1-7: General actions, Accidental actions [20]
EN 1991-2	Eurocode 1: Actions on structures – Part 2: Traffic loads on bridges [21]
EN 1993-1-1	Eurocode 3: Design of steel structures – Part 1-1: General rules and rules for buildings [22]
EN 1993-1-5	Eurocode 3: Design of steel structures – Part 1-5: Plated structural elements [23]
EN 1993-2	Eurocode 3: Design of steel structures – Part 2: Steel Bridges [24]
EN 1994-1-1	Eurocode 4: Design of composite steel and concrete structures – Part 1-1: General rules and rules for buildings [25]
EN 1994-2	Eurocode 4: Design of composite steel and concrete structures – Part 2: General rules and rules for bridges [26]
EN 1997-1	Eurocode 7: Geotechnical design – Part 1: General rules [27]
EN 1998-1	Eurocode 8: Design of structures for earthquake resistance – Part 1: General rules, seismic actions and rules for buildings [28]
EN 1998-2	Eurocode 8: Design of structures for earthquake resistance – Part 2: Bridges [29]
EN 1998-5	Eurocode 8: Design of structures for earthquake resistance – Part 5: Foundations, retaining structures and geotechnical aspects [30]

Throughout the document, references to the Eurocodes used herein is given.

1.2 Structure of the document

In the following, the worked examples are presented in a double-sided layout with comments, background information and interpretation issues on the left-hand side and the example calculation on the right. All relevant references to current Eurocode rules are provided. As mentioned above, the examples are a twin-girder and a box-girder bridge which allows to look basically at a design without and with longitudinal stiffeners.

In Chapter 2 the deck of the twin-girder and the box-girder bridge is described and the global analysis of both bridges is introduced. For this purpose, an overview on the bridge geometry, material distribution and construction sequences is given firstly. Secondly, a general section follows in which common data such as material properties and actions as well as combinations thereof are given. Last but not least, the global analysis is presented for both bridges and the relevant results - internal forces and moments - are summarised for the verifications. Based on that, Chapters 3 and 4 look at the verifications during the final stage and the execution stage. Here, each chapter is subdivided into a part dealing with the verifications of the twin-girder bridge or the box-girder bridge.

2 Description of the deck and global analysis

2.1 Twin-girder bridge

2.1.1 Longitudinal elevation

The bridge is a symmetrical twin-girder composite structure with three spans of 50 m, 60 m and 50 m (i.e. a total length between abutments of 160 m). This is a theoretical example for which a few geometrical simplifications have been made:

- Straight horizontal alignment
- Flat top face of the deck
- Straight bridge
- Constant height of 2400 mm for the structural steel main girders

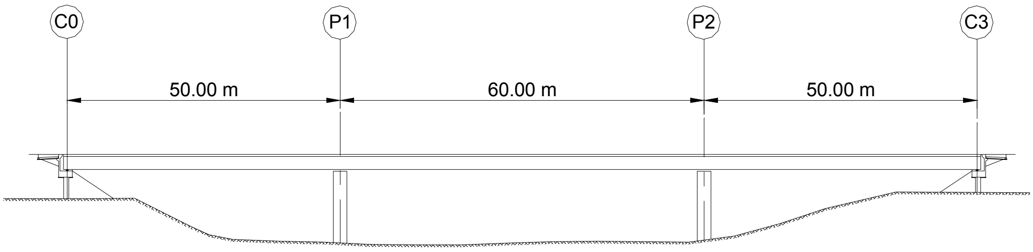

Figure 2-1: Elevation of the twin-girder bridge.

2.1.2 Transverse cross-section

The bridge carries a two-lane traffic road.with two 3.5 m wide lanes, hard shoulders of 2 m width on each side and a standard safety barrier (see Figure 2-2).

The transverse cross-section of the concrete slab and of the non-structural equipment is symmetrical with reference to the axis of the bridge. The slab thickness varies from 0.4 m above the main girders to 0.25 m at its free edges, but it has been modelled as a 0.325 m deep rectangular cross-section.

The total slab width is 12 m. The centre-to-centre spacing between main girders is 7 m and the slab cantilever on each side is 2.5 m.

2.1.3 Structural steel distribution

The structural steel distribution for a main girder is presented in Figure 2-4.

Each main girder has a constant depth of 2400 mm and the variations in thickness of the upper and lower flanges face towards the inside of the girder. The lower flange is 1000 mm wide whereas the upper flange is 800 mm wide.

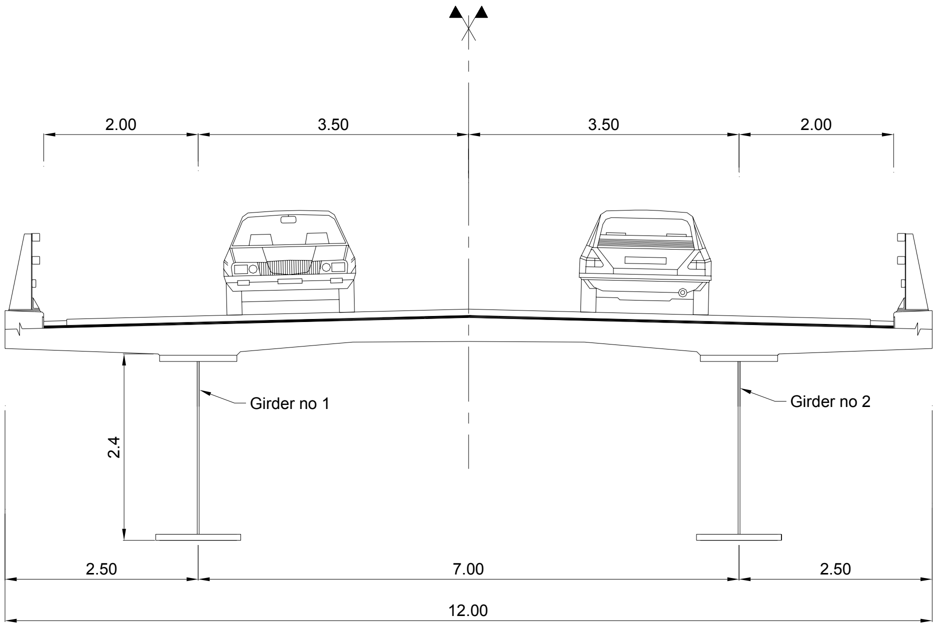

Figure 2-2: Cross-section with traffic data of the twin-girder bridge.

The two main girders have transverse bracings on abutments and on internal supports as well as every 8.333 m in side spans (C0-P1 and P2-C3) and every 7.5 m in the central span (P1-P2). Figure 2-3 illustrates the geometry adopted for this transverse cross-bracing on supports. In order to justify the shear resistance of the internal support sections, vertical stiffeners are added at 1.5 m and at about 4 m from the internal supports.

The optimisation of the stiffening will be discussed in Design Manual Part II [8], according to the results of COMBRI research project [7].

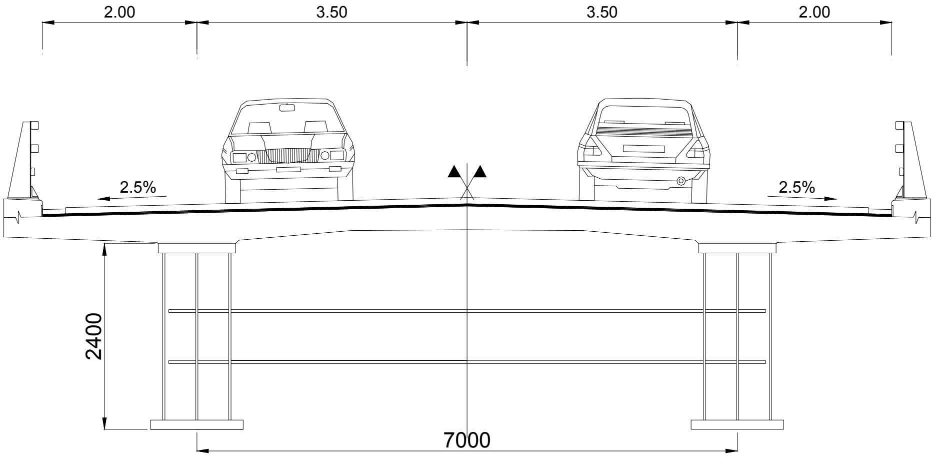

Figure 2-3: Transverse cross-bracing on supports of the twin-girder bridge.

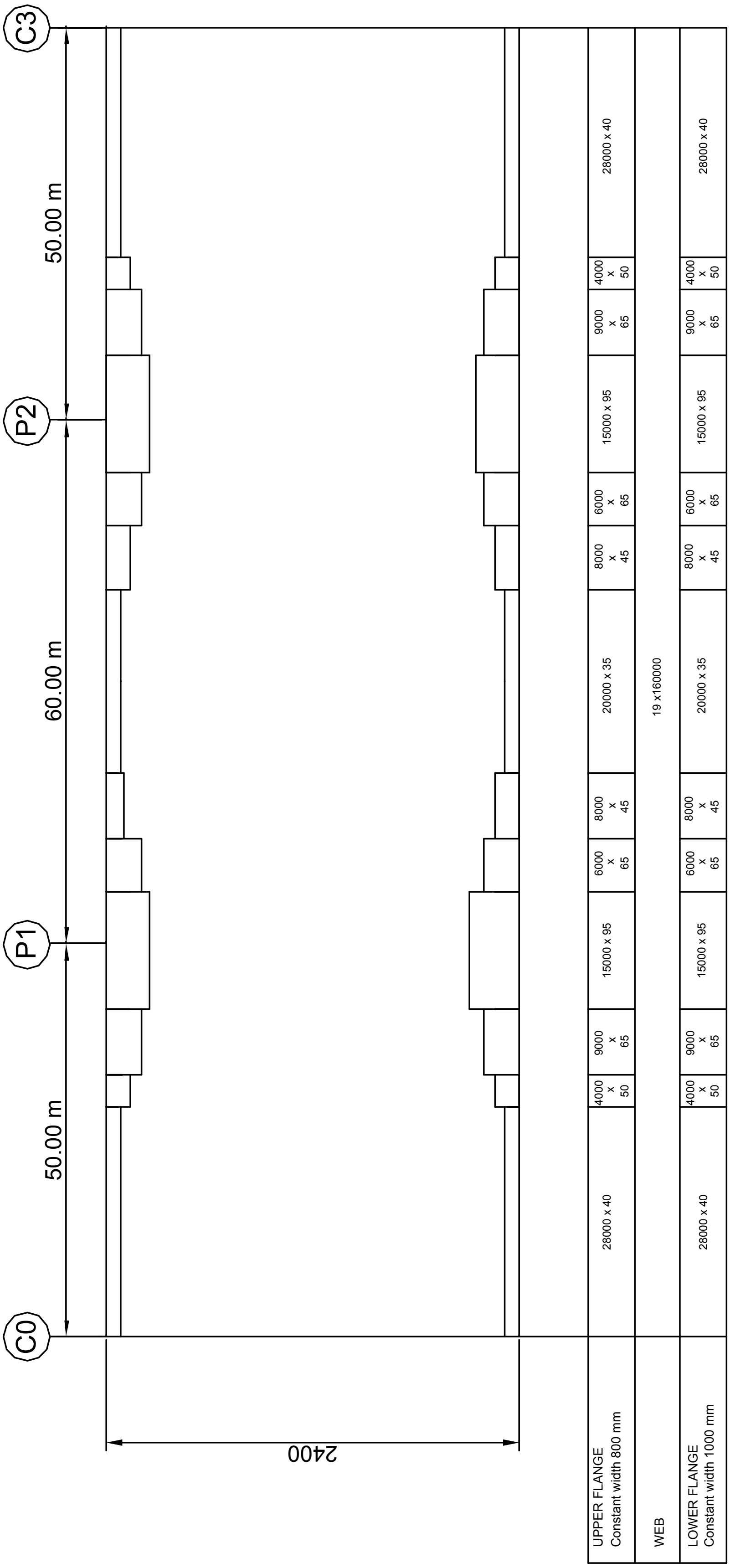
C0
P1
P2
C3
50.00 m
60.00 m
50.00 m
2400
UPPER FLANGE
Constant width 800 mm
28000 x 40
4000 x 50
9000 x 65
15000 x 95
6000 x 65
8000 x 45
20000 x 35
8000 x 45
6000 x 65
15000 x 95
9000 x 65
4000 x 50
28000 x 40
WEB
19 x160000
LOWER FLANGE
Constant width 1000 mm
28000 x 40
4000 x 50
9000 x 65
15000 x 95
6000 x 65
8000 x 45
20000 x 35
8000 x 45
6000 x 65
15000 x 95
9000 x 65
4000 x 50
28000 x 40

Figure 2-4: Structural steel distribution for a main girder of the twin-girder bridge.

EN 1994-2, 5.4.2.4, Stages and sequence of construction

(1)P Appropriate analysis shall be made to cover the effects of staged construction including where necessary separate effects of actions applied to structural steel and to wholly or partially composite members.

(2) The effects of sequence of construction may be neglected in analysis for ultimate limit states other than fatigue, for composite members where all cross-sections are in Class 1 or 2 and in which no allowance for lateral-torsional buckling is necessary.

EN 1994-2, 6.6.5.2(3)

(3) In execution, the rate and sequence of concreting should be required to be such that partly matured concrete is not damaged as a result of limited composite action occurring from deformation of the steel beams under subsequent concreting operations. Wherever possible, deformation should not be imposed on a shear connection until the concrete has reached a cylinder strength of at least 20 N/mm^2.

2.1.4 Construction phases

The assumptions regarding the construction phases are important for all the verifications during erection of the structural steel structure of the deck and during concreting. They are also necessary to determine the values of steel/concrete modular ratios (see Paragraph 2.3.3.3). Finally, the calculation of internal forces and moments in the deck should take construction phases into account (EN 1994-2, 5.4.2.4).

The following construction phases have been adopted:

- Erection of the structural steel structure by launching (see Section 4.1)
- On-site pouring of the concrete slab segments by casting them in a selected order:

  The total length of 160 m has been broken down into 16 identical 10-m-long concreting segments. They are poured in the order indicated in Figure 2-5. The start of pouring the first slab segment is the time origin ($t = 0$). Its definition is necessary for determining the respective ages of the concrete slab segments during the construction phasing.

  The time taken to pour each slab segment is assessed to three working days. The first day is devoted to the concreting, the second day to its hardening and the third day to moving the mobile formwork. The slab is thus completed within 48 days (EN 1994-2, 6.6.5.2(3)).
- Installation of non-structural equipments:

  It is assumed to be completed within 32 days, so that the deck is fully constructed at the date $t = 48 + 32 = 80$ days.

Given these choices, Table 2-1 shows the ages of the various slab segments and the mean value of the age t_0 for all the concrete put in place at each construction phase.

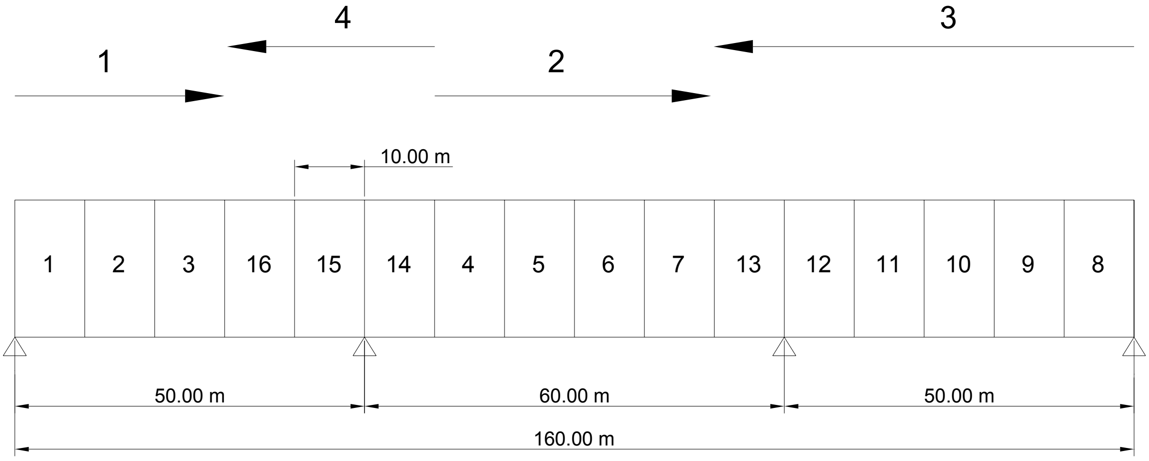

Figure 2-5: Order for concreting the slab segments of the twin-girder bridge.

Table 2-1: Age of concrete slab segments at the end of the construction phasing of the twin-girder bridge.

Loading	time t	segment 1	segment 2	segment 3	segment 4	segment 5	segment 6	segment 7	segment 8	segment 9	segment 10	segment 11	segment 12	segment 13	segment 14	segment 15	segment 16	Mean age t0 of the concrete at the time t
pouring of the segment 1	0																	
pouring of the segment 2	3	3																3
pouring of the segment 3	6	6	3															4.5
pouring of the segment 4	9	9	6	3														6
pouring of the segment 5	12	12	9	6	3													7.5
pouring of the segment 6	15	15	12	9	6	3												9
pouring of the segment 7	18	18	15	12	9	6	3											10.5
pouring of the segment 8	21	21	18	15	12	9	6	3										12
pouring of the segment 9	24	24	21	18	15	12	9	6	3									13.5
pouring of the segment 10	27	27	24	21	18	15	12	9	6	3								15
pouring of the segment 11	30	30	27	24	21	18	15	12	9	6	3							16.5
pouring of the segment 12	33	33	30	27	24	21	18	15	12	9	6	3						18
pouring of the segment 13	36	36	33	30	27	24	21	18	15	12	9	6	3					19.5
pouring of the segment 14	39	39	36	33	30	27	24	21	18	15	12	9	6	3				21
pouring of the segment 15	42	42	39	36	33	30	27	24	21	18	15	12	9	6	3			22.5
pouring of the segment 16	45	45	42	39	36	33	30	27	24	21	18	15	12	9	6	3		24
end of the slab hardening	48	48	45	42	39	36	33	30	27	24	21	18	15	12	9	6	3	25.5
superstructures	80	80	77	74	71	68	65	62	59	56	53	50	47	44	41	38	35	57.5
End of construction phasing	80	80	77	74	71	68	65	62	59	56	53	50	47	44	41	38	35	57.5

2.2 Box-girder bridge

2.2.1 Longitudinal elevation

The bridge is a symmetrical box-girder composite structure with five spans of 90 m, 3 x 120 m and 90 m (i.e. a total length between abutments of 540 m). This is a theoretical example for which a few geometrical simplifications have been made:

- Straight horizontal alignment
- Flat top face of the deck
- Straight bridge
- Constant height of 4000 mm for the structural steel box-girder

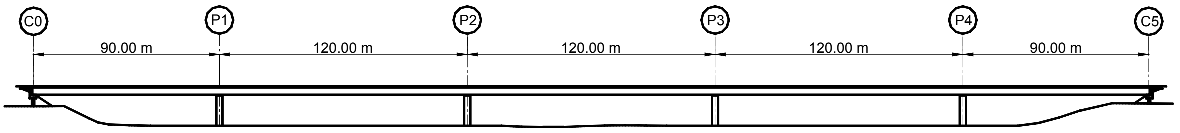

Figure 2-6: Elevation of the box-girder bridge.

2.2.2 Transverse cross-section

The bridge carries a four-lane traffic road. Each lane is 3.50 meter wide and the two outside ones are bordered by a 2.06 meter wide safety lane. Standard safety barriers are located outside the traffic lanes and at the middle of the slab width (see Figure 2-7).

The transverse cross-section of the concrete slab and of the non-structural equipment is symmetrical with reference to the axis of the bridge. The 21.50 m wide slab has been modelled with a theoretical constant thickness of 0.325 m. The centre-to-centre spacing between the webs in the upper part is 12.00 m and the slab cantilever on each side is 4.75 m.

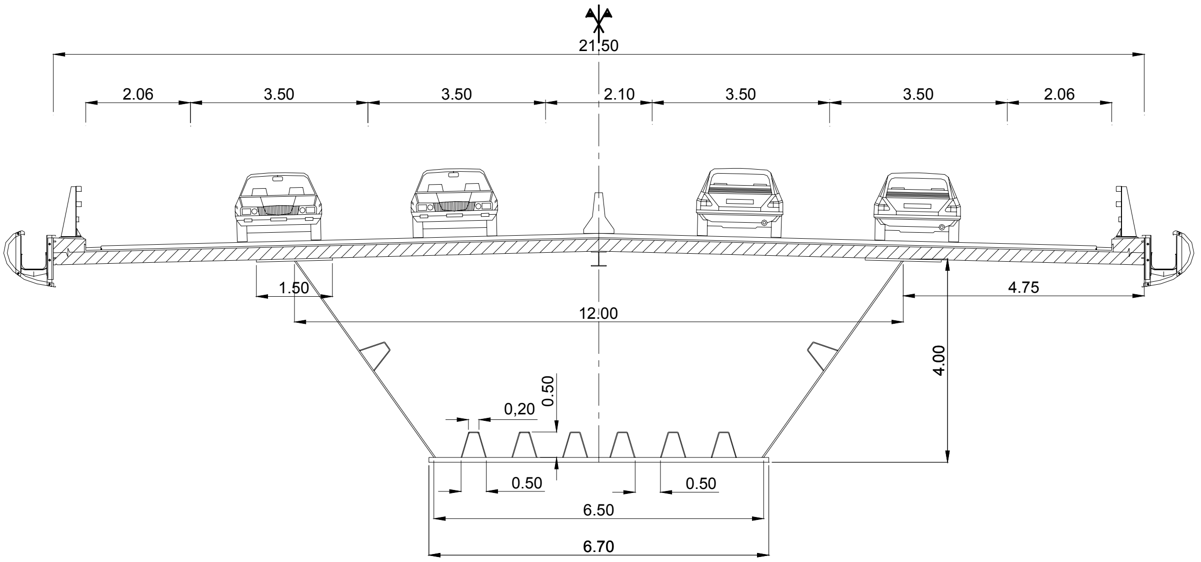

Figure 2-7: Cross-section with traffic data of the box-girder bridge.

The concrete slab is connected to an open box section with the following features:

- total depth: 4.00 m
- centre-to-centre distance between the webs in the upper part: 12.00 m
- centre-to-centre distance between the webs in the lower part: 6.50 m
- width of upper flanges: 1.50 m
- width of lower flange: 6.70 m

2.2.3 Structural steel distribution

The structural steel distribution is presented in Figure 2-10.

The box-girder has a constant depth of 4000 mm and the variations in thickness of the upper and lower flanges face towards the inside of the box-girder. The bottom flange is 6700 mm wide whereas the upper flanges are 1500 mm wide. An additional upper flange is necessary around the intermediate supports. It is located below the main upper flange, so that the total height of the box-girder is always equal to 4000 mm. The width of this additional upper flange is 1400 mm.

An additional steel rolled I-girder, which is located along the longitudinal bridge axis of symmetry, has been connected to the concrete slab. It helps during the concreting phases of the slab and participates in the resistance of the composite cross-section as additional section for the upper steel flanges.

The box section has transverse frames on abutments and on internal supports as well as every 4.0 m in side and central spans. Figure 2-8 illustrates the adopted geometry of this transverse cross-bracing on supports.

In order to justify the shear resistance in the webpanels adjacent to an intermediate support, transverse frames are added at 2.5 m from the internal supports.

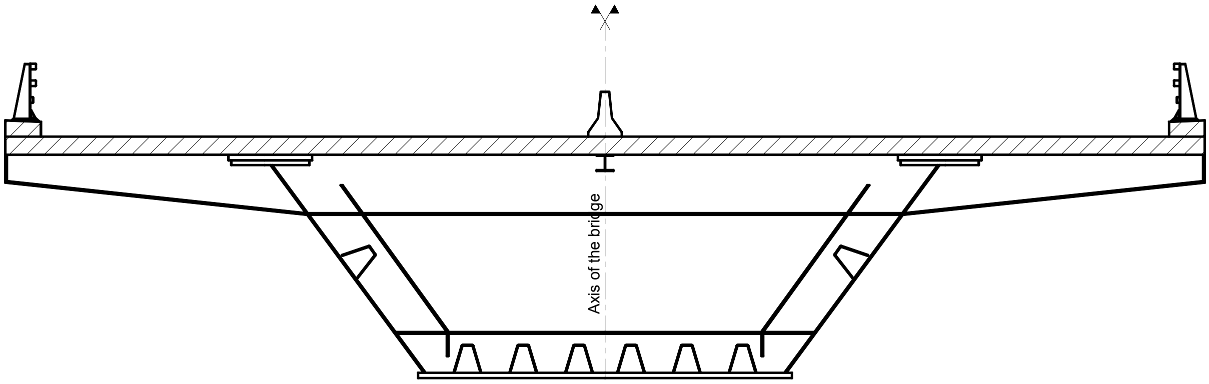

Figure 2-8: Transverse cross-bracings on supports of the box-girder bridge.

Figure 2-9 illustrates the dimensions of the bottom flange longitudinal trapezoidal stiffeners. The thickness is 15 mm for the webs and the flange of the stiffeners. They are continuous along the whole bridge, whereas web longitudinal stiffeners are only used for the panels surrounding the intermediate supports. The web longitudinal stiffeners have the same dimensions as the bottom flange longitudinal stiffeners; they are located at mid-depth of the webs. They have been added to justify the shear resistance of the web.

The stiffening design has been made following the recommendations of the COMBRI research project [7], leading to dimensions which are bigger than the classical ones.

EN 1993-1-10, Table 2.1

EN 1994-2, 5.4.2.4, Stages and sequence of construction

(1)P Appropriate analysis shall be made to cover the effects of staged construction including where necessary separate effects of actions applied to structural steel and to wholly or partially composite members.

(2) The effects of sequence of construction may be neglected in analysis for ultimate limit states other than fatigue, for composite members where all cross-sections are in Class 1 or 2 and in which no allowance for lateral-torsional buckling is necessary.

EN 1994-2, 6.6.5.2(3)

(3) In execution, the rate and sequence of concreting should be required to be such that partly matured concrete is not damaged as a result of limited composite action occurring from deformation of the steel beams under subsequent concreting operations. Wherever possible, deformation should not be imposed on a shear connection until the concrete has reached a cylinder strength of at least 20 N/mm^2.

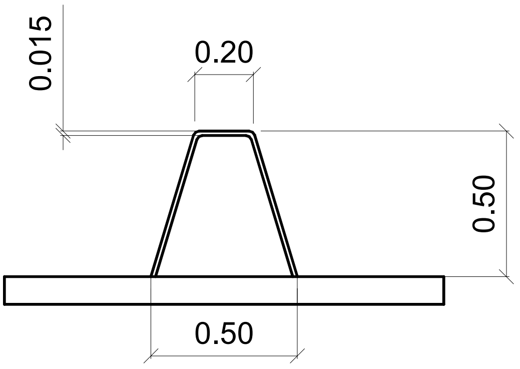

Figure 2-9: Detail of a bottom flange longitudinal stiffener of the box-girder bridge.

NOTE1: On the intermediate supports, an additional upper flange of 1400 mm x 90 mm is welded to the main upper flange.

NOTE2: Different thickness ratios could be obtained by using S355 with quality M or ML around the intermediate supports. Indeed, according to EN 10025-3, by using steel S355 N/NL the main upper flange thickness is limited to 100 mm to keep a yield strength equal to 315 MPa, whereas according to EN 10025-4 by using S355 M/ML the yield strength is equal to 320 MPa for up to 120 mm thick plates. So a design in steel S355 M/ML allows a main 120 mm thick upper flange and an additional 70 mm thick upper flange at intermediate supports. The choice of plate thickness should also fulfil the requirements of EN 1993-1-10, Table 2.1.

NOTE3: An alternative design with a single upper flange made of S 460 is studied in Design Manual Part II, Chapter 3 [8].

2.2.4 Construction phases

The assumptions regarding the construction phases are important for all verifications during erection of the structural steel structure of the deck and during concreting. They are also necessary to determine the values of steel/concrete modular ratios (see Paragraph 2.3.3.3). Finally the calculation of internal forces and moments in the deck should take construction phases into account (EN 1994-2, 5.4.2.4).

The following construction phasing has been adopted:

- Erection of the structural steel structure by launching (see Section 4.2);
- On-site pouring of the concrete slab segments by casting them in a selected order:

  The total length of 540 m has been broken down into 45 identical 12-m-long concreting segments. They are poured in the order indicated in Figure 2-11. The start of pouring the first slab segment is the time origin ($t = 0$). Its definition is necessary to determine the respective ages of the concrete slab segments during the construction phasing.

  The time taken to pour each slab segment is assessed to three working days. The first day is devoted to the concreting, the second day to its hardening and the third day to move the mobile formwork. The slab is thus completed within 135 days (EN 1994-2, 6.6.5.2(3)).

- Installation of non-structural equipments:

  It is assumed to be completed within 35 days, so that the deck is fully constructed at the date $t = 135 + 35 = 170$ days.

Given these choices Table 2-2 shows the ages of the various slab segments and the mean value of the age t_0 for all the concrete put in place at each construction phase. For simplification reasons, no allowance has been made to non-working days.

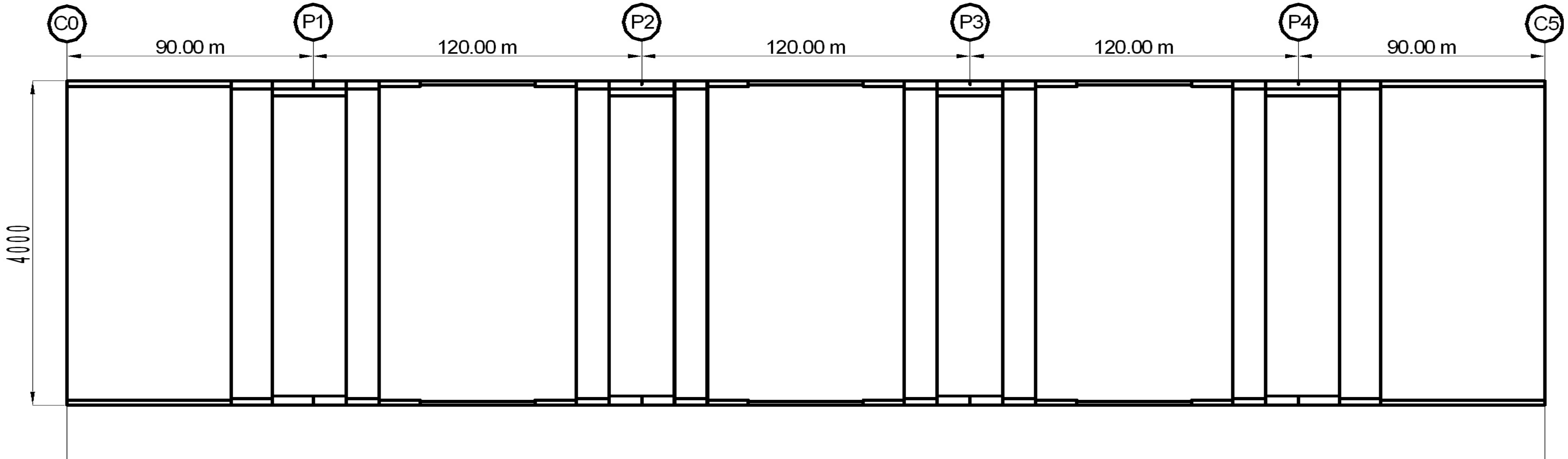

UPPER FLANGE Constant width 1500 mm	60000 x 70	15000 x 100	(15000+12000) x (100+90)		12000 x 100	15000 x 70	42000 x 50	15000 x 70	12000 x 100	24000 x (100+90)	12000 x 100	15000 x 70	42000 x 50	15000 x 70	12000 x 100	24000 x (100+90)	12000 x 100	15000 x 70	42000 x 50	15000 x 70	12000 x 100	(12000+15000) x (100+90)		15000 x 100	60000 x 70
WEB	20 x 60000	24 x 15000	27 x 15000	27 x 12000	24 x 12000	18 x 15000	18 x 42000	18 x 15000	24 x 12000	27 x 24000	24 x 12000	18 x 15000	18 x 42000	18 x 15000	24 x 12000	27 x 24000	24 x 12000	18 x 15000	18 x 42000	18 x 15000	24 x 12000	27 x 12000	27 x 15000	24 x 15000	20 x 60000
LOWER FLANGE Constant width 3350 mm	60000 x 35	15000 x 50	15000 x 75	12000 x 75	12000 x 50	15000 x 35	42000 x 25	15000 x 35	12000 x 50	24000 x 75	12000 x 50	15000 x 35	42000 x 25	15000 x 35	12000 x 50	24000 x 75	12000 x 50	15000 x 35	42000 x 25	15000 x 35	12000 x 50	12000 x 75	15000 x 75	15000 x 50	60000 x 35

Figure 2-10: Structural steel distribution for a main girder of the box-girder bridge.

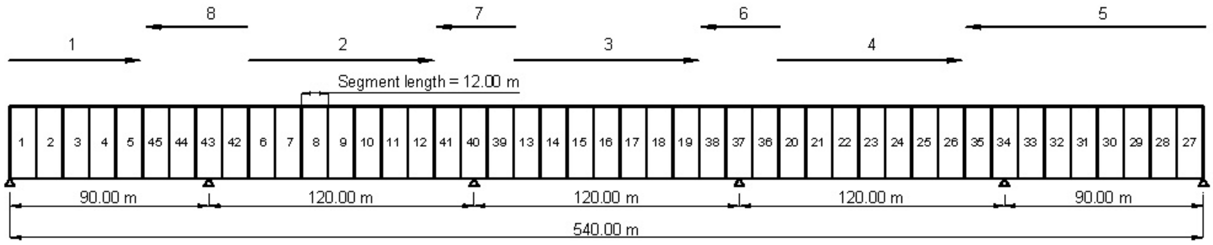
1
2
3
4
5
6
7
8
Segment length = 12.00 m
1 2 3 4 5 45 44 43 42 6 7 8 9 10 11 12 41 40 39 13 14 15 16 17 18 19 38 37 36 20 21 22 23 24 25 26 35 34 33 32 31 30 29 28 27
90.00 m
120.00 m
120.00 m
120.00 m
90.00 m
540.00 m

Figure 2-11: Order for concreting the slab segments of the box-girder bridge.

Table 2-2: Age of concrete slab segments at the end of the construction phasing of the box-girder bridge.

Loading	time t	segment 1	segment 2	segment 3	segment 4	segment 5	segment 6	segment 7	segment 8	…	segment 39	segment 40	segment 41	segment 42	segment 43	segment 44	segment 45	Mean age t0 of the concrete at the time t
pouring of the segment 1	0																	0
pouring of the segment 2	3	3																3
pouring of the segment 3	6	6	3															4.5
pouring of the segment 4	9	9	6	3														6
pouring of the segment 5	12	12	9	6	3													7.5
pouring of the segment 6	15	15	12	9	6	3												9
pouring of the segment 7	18	18	15	12	9	6	3											10.5
pouring of the segment 8	21	21	18	15	12	9	6	3										12
…	…	…	…	…	…	…	…	…	…									…
pouring of the segment 39	114	114	111	108	105	102	99	96	93	…								58.5
pouring of the segment 40	117	117	114	111	108	105	102	99	96	…	3							60
pouring of the segment 41	120	120	117	114	111	108	105	102	99	…	6	3						61.5
pouring of the segment 42	123	123	120	117	114	111	108	105	102	…	9	6	3					63
pouring of the segment 43	126	126	123	120	117	114	111	108	105	…	12	9	6	3				64.5
pouring of the segment 44	129	129	126	123	120	117	114	111	108	…	15	12	9	6	3			66
pouring of the segment 45	132	132	129	126	123	120	117	114	111	…	18	15	12	9	6	3		67.5
end of the slab hardening	135	135	132	129	126	123	120	117	114	…	21	18	15	12	9	6	3	69
superstructures	170	170	167	164	161	158	155	152	149	…	56	53	50	47	44	41	38	104
End of construction phasing	170	170	167	164	161	158	155	152	149	…	56	53	50	47	44	41	38	104

2.3 General common data

2.3.1 Reinforcement of the concrete slab

2.3.1.1 Description of the slab reinforcement

This report does not deal with the transverse reinforcement. Only longitudinal reinforcement is described.

For the example dealt with herein, the cross-sections have been classified between span regions and intermediate support regions for calculation of the longitudinal reinforcing steel. The lengths of these regions are illustrated in Figure 2-12 and Figure 2-13.

- Span regions:

  High bond bars with diameter $\Phi = 16$ mm and spacing $s = 130$ mm in upper and lower layers (i.e. in total $\rho_s = 0.96\%$ of the concrete section)

- Intermediate support regions:

  High bond bars with diameter $\Phi = 20$ mm and spacing $s = 130$ mm in upper layer; high bond bars with diameter $\Phi = 16$ mm and spacing $s = 130$ mm in lower layer (i.e. in total $\rho_s = 1.22\%$ of the concrete section)

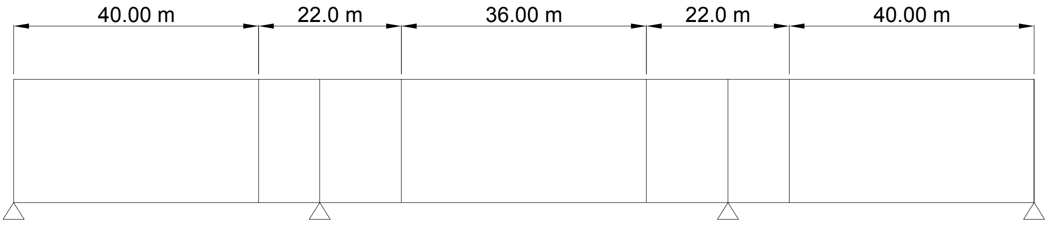

Figure 2-12: Location of mid-span and support sections for longitudinal reinforcing steel of the twin-girder bridge.

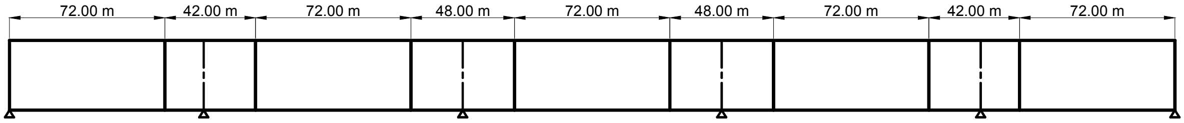

Figure 2-13: Location of mid-span and support sections for longitudinal reinforcing steel of the box-girder bridge.

2.3.1.2 Modelling the slab to calculate the general longitudinal bending

For simplification reasons the actual slab cross-section of a half-deck (see Figure 2-15) is modelled by a rectangular area with the actual width (i.e. 6 m). The height e of this rectangle is calculated so that the actual and modelled sections have the same area. This gives $e = 32.5$ cm.

The mechanical properties of the whole transverse cross-section of the slab are:

Twin-girder bridge

- Area: $A_b = 3.9$ m²
- Second moment of area (around a horizontal axis Δ located at the steel/concrete interface): $I_\Delta = 0.137\ \mathrm{m}^4$
- Perimeter: $p = 24.65$ m

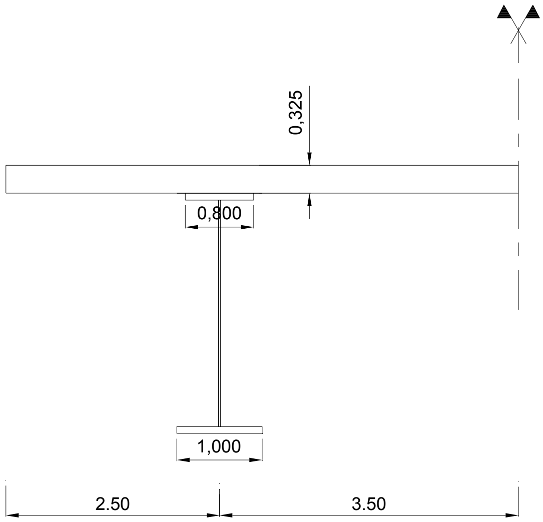

Figure 2-14: Modelling the concrete slab for the longitudinal global bending (twin-girder bridge).

Box-girder bridge

- Area: $A_b = 21.5 \cdot 0.325 = 6.99$ m²
- Second moment of area (around a horizontal axis Δ located at the steel/concrete interface): $I_\Delta = 21.5 \cdot 0.325^3 / 12 + A_b \cdot (0.325 / 2)^2 = 0.246\ \mathrm{m}^4$
- Perimeter : $p = (21.5 + 0.325) \cdot 2 = 43.65$ m

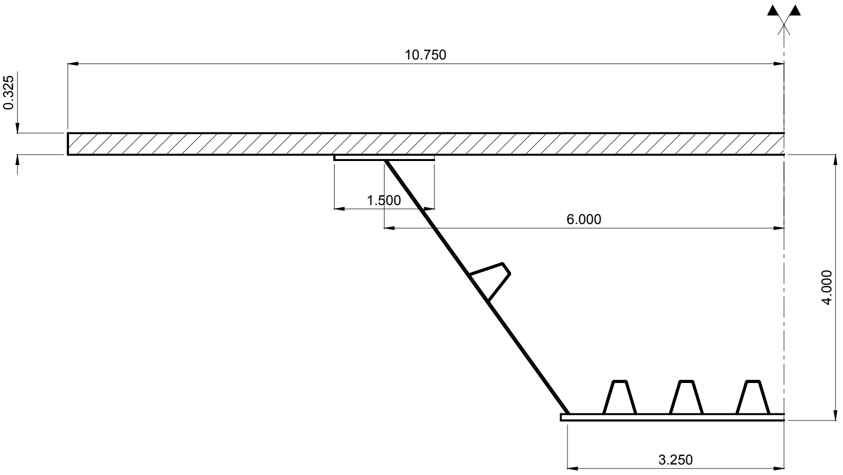

Figure 2-15: Modelling the concrete slab for the longitudinal global bending (box-girder bridge).

EN 1993-1-1, 3.2.6, Design values of material coefficients

(1) The material coefficients to be adopted in calculations for the structural steels covered by this Eurocode Part should be taken as follows:

- modulus of elasticity E = 210000 N/mm²
- shear modulus $G = \dfrac{E}{2\left(1+\nu\right)} \approx 81000$ N/mm²
- Poisson's ratio in elastic stage ν = 0,3
- coefficient of linear thermal expansion $\alpha = 12.10^{-6}$ per *K* (for T ≤ 100 °C)

NOTE: For calculating the structural effects of unequal temperatures in composite concrete-steel structures according to EN 1994 the coefficient of linear thermal expansion is taken as $\alpha = 10.10^{-6}$ *per K.*

EN 1993-1-10 and EN 10164

EN 1992-1-1, Table 3.1, Strength and deformation characteristics for concrete

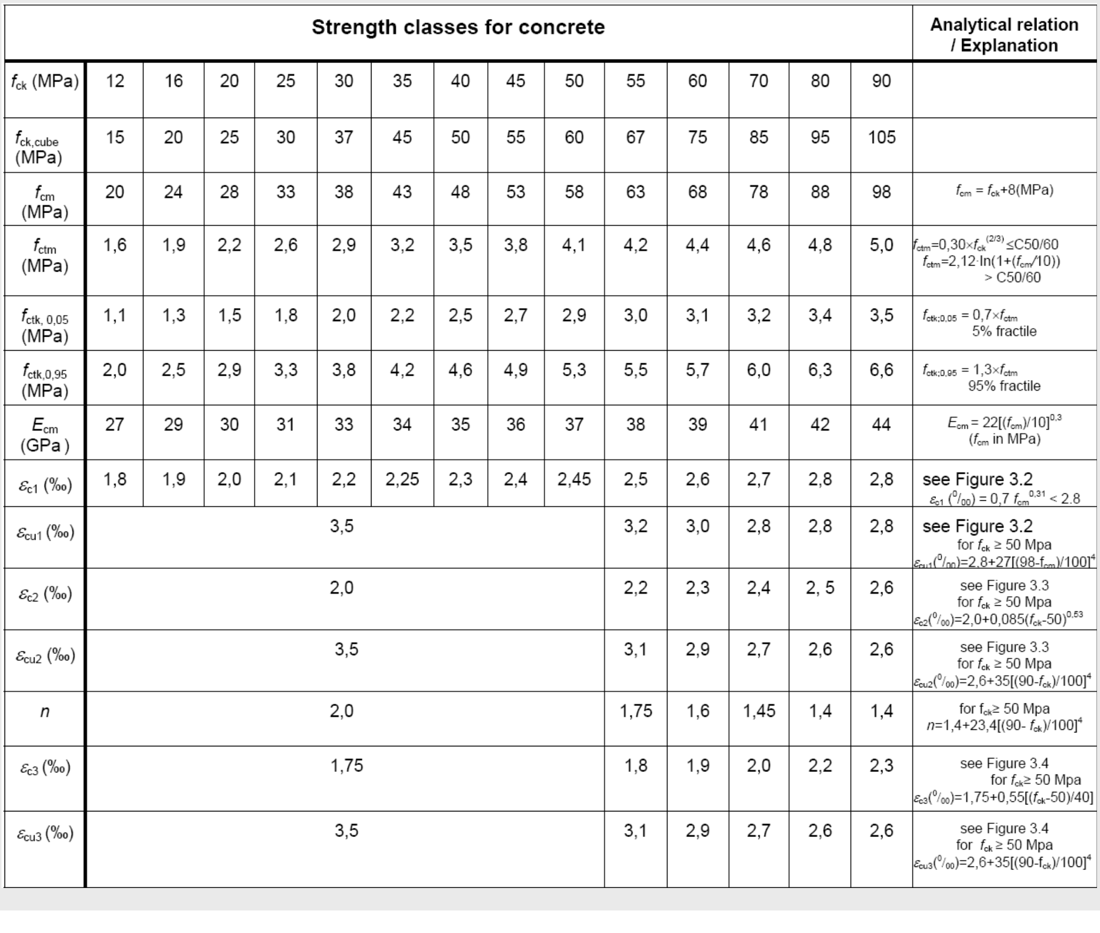

Strength classes for concrete															Analytical relation / Explanation
f_{ck} (MPa)	12	16	20	25	30	35	40	45	50	55	60	70	80	90	
$f_{ck,cube}$ (MPa)	15	20	25	30	37	45	50	55	60	67	75	85	95	105	
f_{cm} (MPa)	20	24	28	33	38	43	48	53	58	63	68	78	88	98	$f_{cm} = f_{ck}+8$(MPa)
f_{ctm} (MPa)	1,6	1,9	2,2	2,6	2,9	3,2	3,5	3,8	4,1	4,2	4,4	4,6	4,8	5,0	$f_{ctm}=0,30\times f_{ck}^{(2/3)} \leq$C50/60 $f_{ctm}=2,12\cdot\ln(1+(f_{cm}/10))$ > C50/60
$f_{ctk,\,0,05}$ (MPa)	1,1	1,3	1,5	1,8	2,0	2,2	2,5	2,7	2,9	3,0	3,1	3,2	3,4	3,5	$f_{ctk;0,05} = 0,7\times f_{ctm}$ 5% fractile
$f_{ctk,0,95}$ (MPa)	2,0	2,5	2,9	3,3	3,8	4,2	4,6	4,9	5,3	5,5	5,7	6,0	6,3	6,6	$f_{ctk;0,95} = 1,3\times f_{ctm}$ 95% fractile
E_{cm} (GPa)	27	29	30	31	33	34	35	36	37	38	39	41	42	44	$E_{cm} = 22[(f_{cm})/10]^{0,3}$ (f_{cm} in MPa)
ε_{c1} (‰)	1,8	1,9	2,0	2,1	2,2	2,25	2,3	2,4	2,45	2,5	2,6	2,7	2,8	2,8	see Figure 3.2 $\varepsilon_{c1}\ ({}^{0}/_{00}) = 0,7\ f_{cm}{}^{0,31} < 2.8$
ε_{cu1} (‰)	3,5									3,2	3,0	2,8	2,8	2,8	see Figure 3.2 for $f_{ck} \geq 50$ Mpa $\varepsilon_{cu1}({}^{0}/_{00})=2,8+27[(98-f_{cm})/100]^4$
ε_{c2} (‰)	2,0									2,2	2,3	2,4	2, 5	2,6	see Figure 3.3 for $f_{ck} \geq 50$ Mpa $\varepsilon_{c2}({}^{0}/_{00})=2,0+0,085(f_{ck}-50)^{0,53}$
ε_{cu2} (‰)	3,5									3,1	2,9	2,7	2,6	2,6	see Figure 3.3 for $f_{ck} \geq 50$ Mpa $\varepsilon_{cu2}({}^{0}/_{00})=2,6+35[(90-f_{ck})/100]^4$
n	2,0									1,75	1,6	1,45	1,4	1,4	for $f_{ck} \geq 50$ Mpa $n=1,4+23,4[(90- f_{ck})/100]^4$
ε_{c3} (‰)	1,75									1,8	1,9	2,0	2,2	2,3	see Figure 3.4 for $f_{ck} \geq 50$ Mpa $\varepsilon_{c3}({}^{0}/_{00})=1,75+0,55[(f_{ck}-50)/40]$
ε_{cu3} (‰)	3,5									3,1	2,9	2,7	2,6	2,6	see Figure 3.4 for $f_{ck} \geq 50$ Mpa $\varepsilon_{cu3}({}^{0}/_{00})=2,6+35[(90-f_{ck})/100]^4$

Similarly, to model the reinforcing bars, each longitudinal reinforcement layer is replaced by a single point-shaped bar with the same area and located in the plane of the main steel web. The reinforcing steel areas are introduced into the numerical model as percentages of the total area of the concrete slab:

Table 2-3: Areas of the steel reinforcement.

		ρ_s (%)
Mid-span cross-sections	top layer	0.48
	bottom layer	0.48
Support cross-sections	top layer	0.74
	bottom layer	0.48

The centroid of each longitudinal reinforcing steel layer has been assumed to be located at 60 mm away from the closest horizontal face of the concrete slab. This value takes account of the concrete cover and the fact that the transverse reinforcing bars are placed outside the longitudinal reinforcing bars (on the side of the slab free surface).

2.3.2 Material properties

2.3.2.1 Structural steel

Steel grade S355 is considered for this bridge. The subgrades (also called quality) N or NL have been adopted (depending on the plate thickness). The corresponding structural steel mechanical properties are given in EN 10025-3.

Table 2-4: Decrease of f_y and f_u according to the plate thickness t.

t [mm]	≤ 16	> 16 ≤ 40	> 40 ≤ 63	> 63 ≤ 80	> 80 ≤ 100	> 100 ≤ 150
f_y [MPa]	355	345	335	325	315	295
f_u [MPa]	470	470	470	470	470	450

The structural steel has a modulus of elasticity E_a = 210 000 MPa (EN 1993-1-1, 3.2.6). In order to avoid any lamellar tearing, the steel has a though-thickness ductility quality Z15 for the main web (when a transverse bracing is welded to it) according to EN 1993-1-10 and EN 10164.

2.3.2.2 Concrete

Normal concrete C35/45 is used for the reinforced slab. The main mechanical properties are as follows (EN 1992-1-1, 3.1.2, Table 3.1):

- Characteristic compressive cylinder strength at 28 days: f_{ck} = 35 MPa
- Mean value of axial tensile strength: f_{ctm} = -3.2 MPa
- 5% fractile of the characteristic axial tensile strength: $f_{ctk,0.05}$ = -2.2 MPa
- 95% fractile of the characteristic axial tensile strength: $f_{ctk,0.95}$ = -4.2 MPa
- Mean value of concrete cylinder strength at 28 days: $f_{cm} = f_{ck} + 8 = 43$ MPa
- Modulus of elasticity: E_{cm} = 22 000 (f_{cm} / 10)0.3 = 34 077 MPa

EN 1992-1-1, 3.2 and Annex C, Reinforcing steel

EN 1994-2, 3.2(2), Reinforcing steel

(2) For composite structures, the design value of the modulus of elasticity E_s may be taken as equal to the value for structural steel given in EN 1993-1-1, 3.2.6.

EN 1992-1-1, 2.4.2.4, Partial safety factors for materials

EN 1993-2, 6.1 and Table 6.2, General

EN 1993-2, 7.3(1), Limitations for stress

2.3.2.3 Reinforcement

The reinforcing steel bars used in this project are class B high bond bars with a yield strength f_{sk} = 500 MPa (EN 1992-1-1, 3.2 and Annex C).

In EN 1992-1-1 the elasticity modulus of reinforcing steel is E_s = 200 000 MPa. However, in order to simplify the modulus used for the structural steel, EN 1994-2 allows the use of $E_s = E_a$ = 210 000 MPa which will be done in this project (EN 1994-2, 3.2(2)).

2.3.2.4 Partial safety factors for materials

For Ultimate Limit State (ULS) see Table 2-5.

Table 2-5: Partial safety factors for materials (ULS).

Design situation	γ_C **(concrete)**	γ_S **(reinforcing steel)**	γ_M **(structural steel)**	
Persistent Transient	1.5	1.15	γ_{M0} =1.0	Yielding, local instability
			γ_{M1} =1.1	Resistance of members to instability
			γ_{M2} =1.25	Resistance of joints
Reference	EN 1992-1-1, 2.4.2.4.		EN 1993-2, 6.1 and Table 6.1	

For Serviceability Limit State (SLS) see Table 2-6.

Table 2-6: Partial safety factors for materials (SLS).

γ_C **(concrete)**	γ_S **(reinforcing steel)**	$\gamma_{M,ser}$ **(structural steel)**
1.0	1.0	1.0
EN 1992-1-1, 2.4.2.4		EN 1993-2, 7.3 (1)

2.3.3 Actions

In order to simplify the calculations, only six different load cases have been defined:

1. Self-weight of the structural steel
2. Self-weight of the reinforced concrete slab (with construction phasing, so in fact 16 load cases for the twin-girder bridges and 45 load cases for the box-girder bridge)
3. Self-weight of the non structural bridge equipments
4. Shrinkage
5. Creep
6. Traffic load LM1

Specifications to apply these loads on the bridge are explained below.

EN 1991-1-1, Table A.4, Construction materials-metals

Materials	Density γ [kN/m^3]
metals	
aluminium	27,0
brass	83,0 to 85,0
bronze	83,0 to 85,0
copper	87,0 to 89,0
iron, cast	71,0 to 72,5
iron, wrought	76,0
lead	112,0 to 114,0
steel	77,0 to 78,5
zinc	71,0 to 72,0

EN 1991-1-1, Table A.1, Construction materials-concrete and mortar

Materials	Density γ [kN/m^3]
concrete (see EN 206)	
lightweight	
density class LC 1,0	9,0 to 10,0 1)2)
density class LC 1,2	10,0 to 12,0 1)2)
density class LC 1,4	12,0 to 14,0 1)2)
density class LC 1,6	14,0 to 16,0 1)2)
density class LC 1,8	16,0 to 18,0 1)2)
density class LC 2,0	18,0 to 20,0 1)2)
normal weight	24,0 1)2)
heavy weight	> 1)2)
mortar	
cement mortar	19,0 to 23,0
gypsum mortar	12,0 to 18,0
lime-cement mortar	18,0 to 20,0
lime mortar	12,0 to 18,0

1) Increase by 1kN/m^3 for normal percentage of reinforcing and pre-stressing steel
2) Increase by 1kN/m^3 for unhardened concrete

NOTE See Section 4

2.3.3.1 Permanent loads

Distinction is made for permanent loads between the self-weights of the structural steel girders, of reinforced concrete slab and of non-structural equipments.

2.3.3.1.1 Self-weight

The density of the structural steel is taken as equal to 77 kN/m^3 (EN 1991-1-1, Table A-4). For calculation of the internal forces and moments and the stresses for the longitudinal bending global analysis, the self-weights are modelled as follows:

Twin-girder bridge

The self-weight of the in-span located transverse cross girders is modelled by a vertical uniformly distributed load of 1300 N/m applied on each main girder (about 12% of the weight of this main girder).

Box-girder bridge

The self-weight of the in-span located transverse frames is modelled by a vertical uniformly distributed load of 8000 N/m for the total width of the bridge (about 12.2 % of the weight of the full box-girder).

The density of the reinforced concrete is taken as equal to 25 kN/m^3 (EN 1991-1-1, Table A-1).

2.3.3.1.2 Non-structural equipment

The nominal value of the waterproofing layer is multiplied by ±20% and the nominal value of the asphalt layer by +40% / -20% for all spans (EN 1991-1-1, 5.2.3).

Table 2-7: Loads of the non-structural equipment (twin-girder bridge).

Item	Characteristics	Maximum multiplier	Minimum multiplier	q_{nom} (kN/m)	q_{max} (kN/m)	q_{min} (kN/m)
Waterproofing layer	3 cm thick, 25 kN/m^3	1.2	0.8	4.2	5.04	3.36
Asphalt	8 cm thick, 25 kN/m^3	1.4	0.8	11	15.4	8.8
Concrete support for the safety barrier	area 0.5 x 0.2 m, 25 kN/m^3	1	1	2.5	2.5	2.5
Safety barriers	65 kg/m	1	1	0.638	0.638	0.638
Cornice	25 kg/m	1	1	0.245	0.245	0.245
Total				**18.58**	**23.82**	**15.54**

Table 2-8: Loads of the non-structural equipment (box-girder bridge).

Item	Characteristics	Maximum multiplier	Minimum multiplier	q_{nom} (kN/m)	q_{max} (kN/m)	q_{min} (kN/m)
Waterproofing layer	3 cm thick, 25 kN/m3	1.2	0.8	7.66	9.19	6.13
Asphalt	8 cm thick, 25 kN/m3	1.4	0.8	20.22	28.31	16.18
Safety barrier ground girder	area 0.5 x 0.2 m, 25 kN/m3	1	1	2.50	2.50	2.50
Safety barrier	65 kg/m	1	1	0.64	0.64	0.64
Cornice	25 kg/m	1	1	0.25	0.25	0.25
Total				**31.26**	**40.88**	**25.68**

EN 1991-1-1, 5.2.3, Additional provisions specific for bridges

(1) The upper and lower characteristic values of densities for non structural parts, such as ballast on railway bridges, or fill above buried structures such as culverts, should be taken into account if the material is expected to consolidate, become saturated or otherwise change its properties, during use.

NOTE: Suitable values may be given in the National Annex.

(2) The nominal depth of ballast on railway bridges should be specified. To determine the upper and lower characteristic values of the depth of ballast on railway bridges a deviation from the nominal depth of ±30 % should be taken into account.

NOTE: A suitable value may be given in the National Annex

(3) To determine the upper and lower characteristic values of self-weight of waterproofing, surfacing and other coatings for bridges, where the variability of their thickness may be high, a deviation of the total thickness from the nominal or other specified values should be taken into account. Unless otherwise specified, this deviation should be taken equal to ± 20 % if a post-execution coating is included in the nominal value, and to + 40 % and – 20 % if such a coating is not included.

NOTE: Suitable specifications may be given in the National Annex.

(4) For the self-weight of cables, pipes and service ducts, the upper and lower characteristic values should be taken into account. Unless otherwise specified, a deviation from the mean value of the self-weight of ± 20 % should be taken into account.

NOTE: Suitable specifications may be given in the National Annex. See also EN 1990, 4.1.2(4)

(5) For the self-weight of other non structural elements such as:

- hand rails, safety barriers, parapets, kerbs and other bridge funiture,
- joints/fasteners,
- void formers,

the characteristic values should be taken equal to the nominal values unless otherwise specified.

NOTE: Suitable specifications may be given in the National annex. An allowance for voids filling with water may be made depending on the project.

Figure 2-16 details the non-structural bridge equipment used for the example.

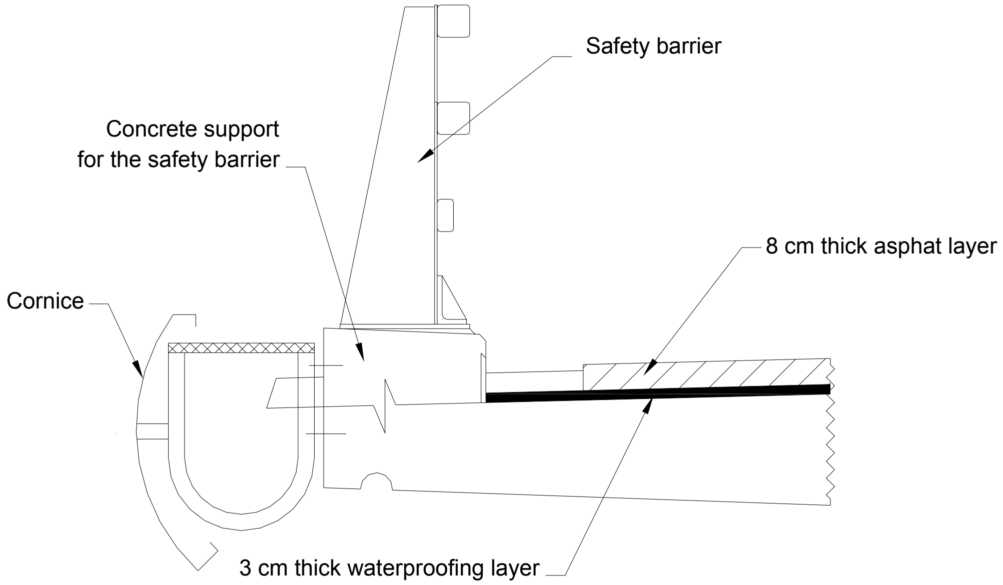

Figure 2-16: Non-structural bridge equipment details.

2.3.3.2 Concrete shrinkage

According to Eurocode 4, three different concrete shrinkage deformations should be considered in the design. In order to simplify the analysis and because thermal shrinkage at early age is part of national choices, it has been decided not to consider it in the calculations. Only autogenous and drying shrinkage deformations ($\varepsilon_{cs} = \varepsilon_{ca} + \varepsilon_{cd}$ with notations from EN 1992-1-1, 3.1.4(6)) have been taken into account. Two values of the total deformation ε_{cs} have been then calculated:

Shrinkage deformation for persistent design situation at traffic opening
(for the twin-girder bridge date t_{ini} = 80 days, for the box-girder bridge date t_{ini} = 170 days)

Table 2-9 summarises the values of autogenous and drying shrinkage deformation for persistent design situation at traffic opening for the twin-girder bridge and the box-girder bridge respectively.

Table 2-9: Shrinkage at traffic opening for the persistent design situation at traffic opening (t_{ini}).

	twin-girder bridge	**box-girder bridge**
Autogenous shrinkage	4.88E-05	5.44E-05
Drying shrinkage	1.36E-05	2.23E-05
Total	**6.20E-05**	**7.67E-05**

Shrinkage deformation for persistent design situation at infinite time

Table 2-10 summarises the values of autogenous and drying shrinkage deformation for persistent design situation at infinite time for the twin-girder bridge and the box-girder bridge.

EN 1994-2, 5.4.2.2 (2), Creep and shrinkage

(2) Except for members with both flanges composite, the effects of creep may be taken into account by using modular ratios n_L for the concrete. The modular ratios depending on the type of loading (subscript L) are given by:

$$n_L = n_0 \, (1 + \psi_L / \varphi_t) \qquad (5.6)$$

where:

n_0 is the modular ratio E_a / E_{cm} for short-term loading;

E_{cm} is the secant modulus of elasticity of the concrete for short-term loading according to EN 1992-1-1, Table 3.1 or Table 11.3.1;

φ_t is the creep coefficient $\varphi\,(t,t_0)$ according to EN 1992-1-1, 3.1.4 or 11.3.3, depending on the age (t) of concrete at the moment considered and the age (t_0) at loading;

ψ_L is the creep multiplier depending on the type of loading, which be taken as 1.1 for permanent loads, 0.55 for primary and secondary effects of shrinkage and 1.5 for prestressing by imposed deformations

Table 2-10: Shrinkage at infinite time.

	t=infinite
Autogenous shrinkage	6.25E-05
Drying shrinkage	1.77E-04
Total	**2.40E-04**

Finally for calculating the internal forces and moments for the persistent design situation at traffic opening, a shrinkage deformation of $6.2 \cdot 10^{-5}$ (for the twin-girder-bridge) and $7.67 \cdot 10^{-5}$ (for the box-girder-bridge) is applied to each slab segment following the concreting order. For the persistent design situation at infinite time, a shrinkage deformation of $2.4 \cdot 10^{-4}$ (for the 2 bridges) is applied to the whole slab after finishing all concreting phases.

2.3.3.3 Creep – Modular ratios

2.3.3.3.1 Modular ratio for short-term loading

$$n_0 = \frac{E_a}{E_{cm}} = \frac{210000}{22000\left(\frac{f_{cm}}{10}\right)^{0.3}} = 6.1625$$

2.3.3.3.2 Modular ratio for long-term loading

For a given long-term loading L applied to the bridge when the mean age of concrete is equal to t_0, the modular ratio is defined by the following equation for the calculations of the bridge at infinite time (EN 1994-2, 5.4.2.2(2)):

$$n_L = n_0\left(1 + \psi_L \varphi(\infty, t_0)\right)$$

Table 2-11 and Table 2-12 summarise the intermediate values for the calculation of the creep factor $\varphi(\infty, t_0)$ and the modular ratio values n_L used in the design of the twin-girder bridge and the box-girder bridge. See Table 2-1 and Table 2-2 for further details on the ages t_0.

Table 2-11: Modular ratio for long-term loading (twin-girder bridge).

Load case	ψ_L	t_0 (days)	$\varphi(\infty, t_0)$	n_L
Concreting	1.1	24	1.484	16.22
Shrinkage	0.55	1	2.683	15.25
Non structural bridge equipments	1.1	57.5	1.256	14.68

Table 2-12: Modular ratio for long-term loading (box-girder bridge).

Load case	ψ_L	t_0 (days)	$\varphi(\infty, t_0)$	n_L
Concreting	1.1	67.5	1.215	14.40
Shrinkage	0.55	1	2.674	15.23
Non structural bridge equipments	1.1	104	1.118	13.74

EN 1991-2, 4.2.3, Divisions of the carriageway into notional lanes

(1) The carriageway width, *w*, should be measured between kerbs or between the inner limits of vehicle restraint systems, and should not include the distance between fixed vehicle restraint systems or kerbs of a central reservation nor the widths of these vehicle restraint systems.

NOTE: The National Annex may define the minimum value of the height of the kerbs to be taken into account. The recommended minimum value of this height is 100 mm.

(2) The width w_l of notional lanes on a carriageway and the greatest possible whole (integer) number n_l of such lanes on this carriageway are defined in Table 4.1.

Table 4.1: Number and width of notional lanes

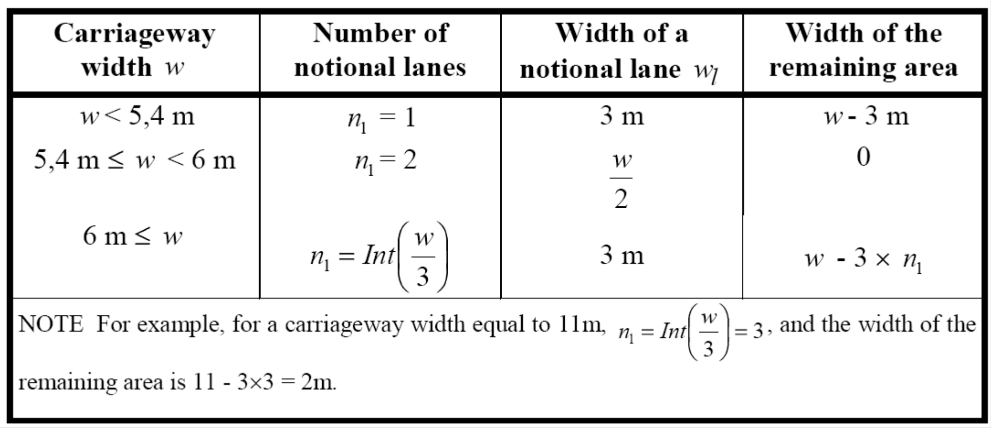

Carriageway width w	Number of notional lanes	Width of a notional lane w_l	Width of the remaining area
$w < 5{,}4$ m	$n_1 = 1$	3 m	w - 3 m
5,4 m $\leq w < 6$ m	$n_1 = 2$	$\frac{w}{2}$	0
6 m $\leq w$	$n_1 = Int\left(\frac{w}{3}\right)$	3 m	$w - 3 \times n_1$
NOTE For example, for a carriageway width equal to 11m, $n_1 = Int\left(\frac{w}{3}\right) = 3$, and the width of the remaining area is 11 - 3×3 = 2m.			

(3) For variable carriageway widths, the number of notional lanes should be defined in accordance with the principles used for Table 4.1.

NOTE: For example, the number of notional lanes will be:

- *1 where w < 5,4 m*
- *2 where 5,4 ≤ w < 9 m*
- *3 where 9 m ≤ w < 12 m, etc.*

(4) Where the carriageway on a bridge deck is physically divided into two parts separated by a central reservation, then:

(a) each part, including all hard shoulders or strips, should be separately divided into notional lanes if the parts are separated by a permanent road restraint system ;

(b) the whole carriageway, central reservation included, should be divided into notional lanes if the parts are separated by a temporary road restraint system.

NOTE: The rules given in 4.2.3(4) may be adjusted for the individual project, allowing for envisaged future modifications of the traffic lanes on the deck, e.g. for repair.

The hyperstatic effects (also called “secondary effects” in Eurocode 4) of creep are negligible compared to the other action effects. So they have not been considered in the calculations (and the corresponding modular ratio is not mentioned here).

2.3.3.4 Traffic loads

2.3.3.4.1 Adjustment coefficients

The definition of the LM1 vertical loads (consiting of the tandem system TS and the uniformly distributed load UDL) includes a series of adjustment coefficients α_{Qi}, α_{qi} and α_{qr}. These coefficients are given in the National Annex of each country. Only minimum recommended values are given in EN 1991-2. Here, the following values have been assumed (coming from the French National Annex to EN 1991-2, for a highway or motorway traffic category) (EN 1991-2, 4.3.2 (3)):

Table 2-13: Adjustment coefficients for LM1.

Lane no.	α_{Qi} (for TS)	α_{qi} (for UDL)	α_{qr}
1	0.9	0.7	/
2 or more	0.8	1.0	/
Remaining area	/	/	1

2.3.3.4.2 Transverse positioning of LM1

UDL and TS are positioned longitudinally and transversally on the deck so as to achieve the most unfavourable effect for the studied main girder (girder no. 1 in Figure 2-17) and for the box-girder.

Twin-girder bridge

A straight transverse influence line is used (see Figure 2-20 and Figure 2-22) with the assumption that a vertical load introduced in the web plane of a main girder is entirely resisted by this girder. The unfavourable parts of each longitudinal influence line are then loaded according to the transverse distribution of the traffic vertical loads UDL and TS between the two main girders.

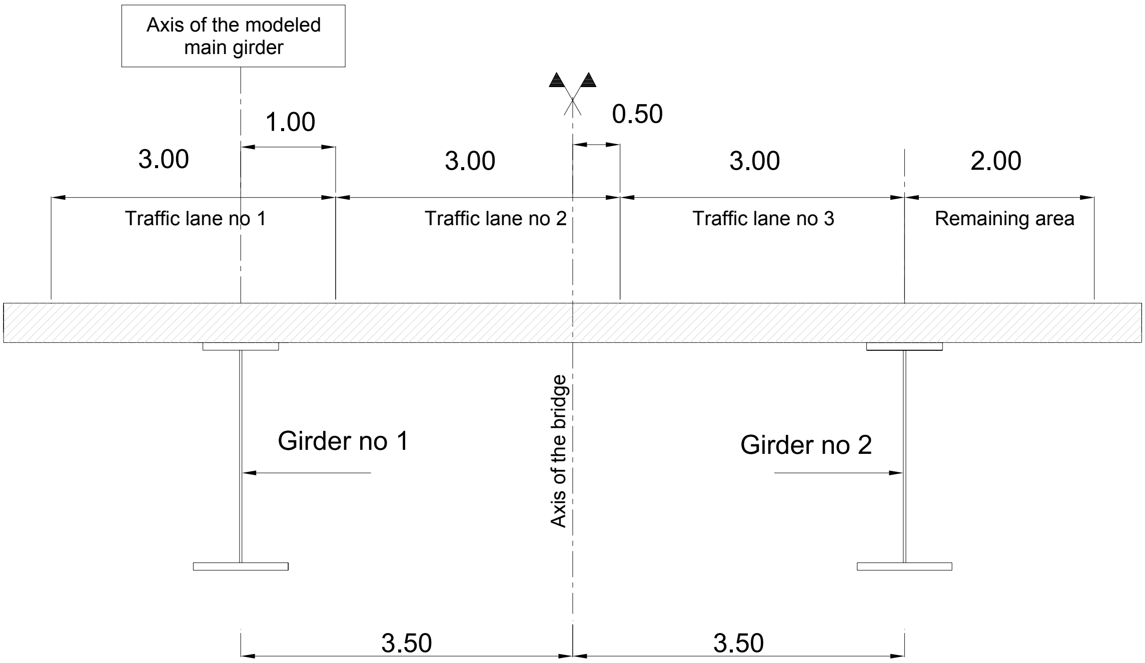

Figure 2-17: Traffic lanes positioning for calculating the girder no.1.

The pavement width between the internal vertical faces of the concrete longitudinal supports of the safety barriers reaches *w* = 11 m, centered on the deck axis. Three traffic lanes each 3 m wide and a 2 m wide remaining area can be placed within this width. The traffic lanes are thus arranged in the most unfavourable way for the studied girder no. 1 according to the diagram in Figure 2-20 (EN 1991-2, 4.2.3).

Box-girder bridge

A horizontal straight transverse influence line is used (see Figure 2-21 and Figure 2-23). It corresponds to the assumption that sufficient stiffening is provided to prevent the deformation of the cross-sections. The eccentric traffic loads *Q (TS)* and *q (UDL)* are modeled by using centered loads with the same values *Q* and *q*, and torque loads (M_Q for the concentrated one and m_q for the distributed one, see Figure 2-18). Torque has been studied and its calculation is explained in Paragraph 2.3.3.5.

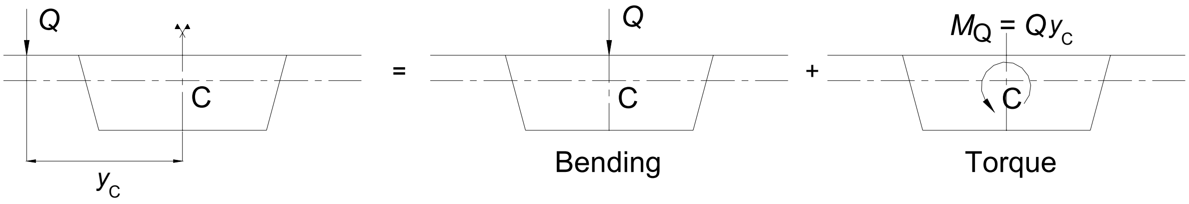

Figure 2-18: Calculation of the box-girder for eccentric concentrated load.

The pavement width between internal vertical faces of the concrete longitudinal supports of the external safety barriers reaches 20.22 m, centered on the deck axis. The safety barrier, which separates the two ways of the road in the middle of the deck, has not been considered when applying the traffic load model 1 on this 20.22 m wide pavement.

Six traffic lanes each 3.00 m wide and a 2.22 m wide remaining area can be placed within this 20.22 m wide pavement. The transverse positioning of traffic lanes doesn't matter for studying the effect of the centered vertical loads Q and q, as each load is resisted equally by the two webs. This latter assumption corresponds to the use of the horizontal transverse influence line in Figure 2-21 and Figure 2-23, with the 0.5 imposed value at each main web location. On the contrary this transverse positioning of the traffic lanes influences the results of the torque global analysis. Figure 2-19 shows the most unfavourable lane distribution when studying torque.

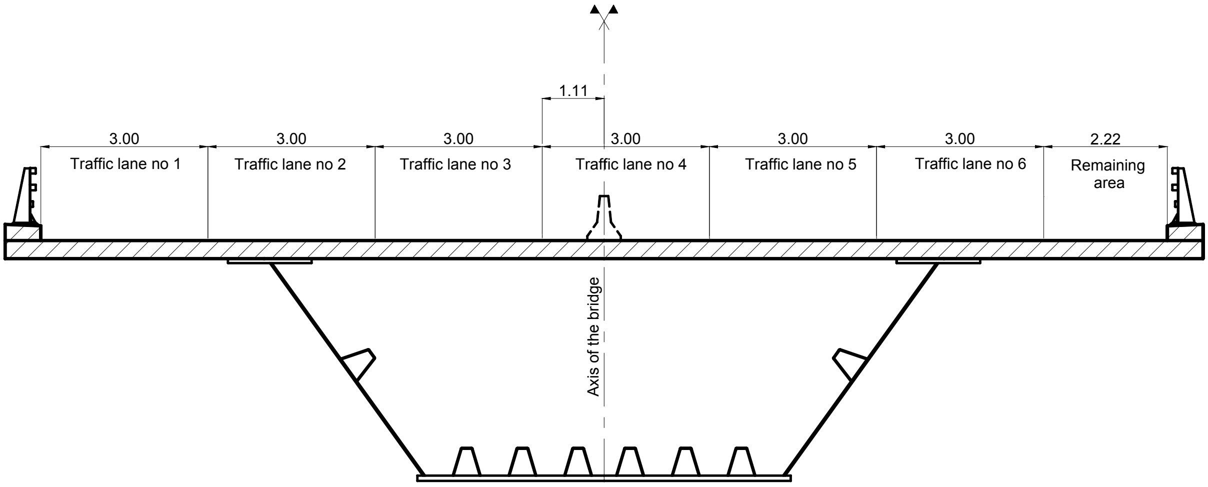

Figure 2-19: Traffic lanes positioning for calculating the box-girder.

EN 1991-2, 4.3.2(1) (a), Load Model 1

(1) Load Model 1 consists of two partial systems:

(a) Double-axle concentrated loads (tandem system: TS), each axle having the following weight:

$$\alpha_q \, Q_k \qquad (4.1)$$

where:

α_q are adjustment factors.

- No more than one tandem system should be taken into account per notional lane.
- Only complete tandem systems should be taken into account.
- For the assessment of general effects, each tandem system should be assumed to travel centrally along the axes of notional lanes (see (5) below for local verifications and Figure 4.2b).
- Each axle of the tandem system should be taken into account with two identical wheels, the load per wheel being therefore equal to $0.5\alpha_q \, Q_k$.
- The contact surface of each wheel should be taken as square and of side 0.40 m (see Figure 4.2b).

(b) Uniformly distributed loads (UDL system), having the following weight per square metre of notional lane:

$$\alpha_q \, q_k \qquad (4.2)$$

where :

α_q are adjustment factors.

The uniformly distributed loads should be applied only in the unfavourable parts of the influence surface, longitudinally and transversally.

NOTE: LM1 is intended to cover flowing, congested or traffic jam situations with a high percentage of heavy lorries. In general, when used with the basic values, it covers the effects of a special vehicle of 600 kN as defined in Annex A.

(4) The characteristic values of ik *Q* and ik *q*, dynamic amplification included, should be taken from Tab 4.2.

Table 4.2: Load model 1: characteristic values

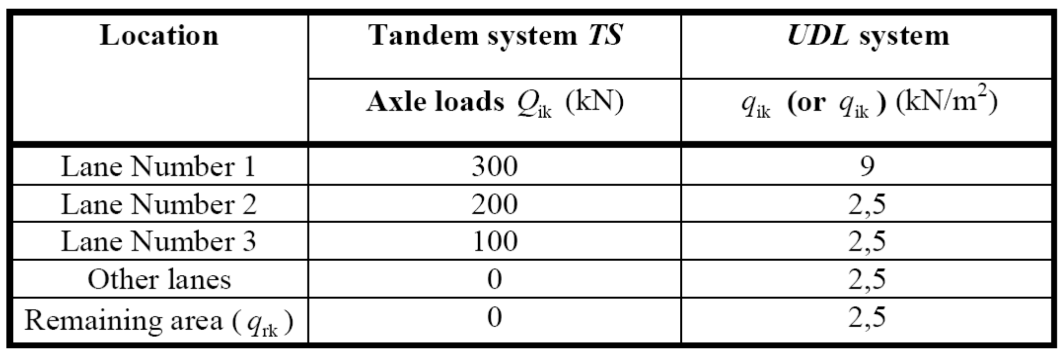

Location	**Tandem system *TS***	***UDL* system**
	Axle loads Q_{ik} (kN)	q_{ik} **(or** q_{ik}**)** (kN/m^2)
Lane Number 1	300	9
Lane Number 2	200	2,5
Lane Number 3	100	2,5
Other lanes	0	2,5
Remaining area (q_{rk})	0	2,5

Tandem System TS

Each axle of the tandem TS has to be centered in its traffic lane. The vertical load magnitudes per axle are given in EN 1991-2, Table 4.2. Figure 2-20 indicates the transverse position of the three tandems considered with respect to the main structural steel girders (EN 1991-2, 4.3.2(1) (a)).

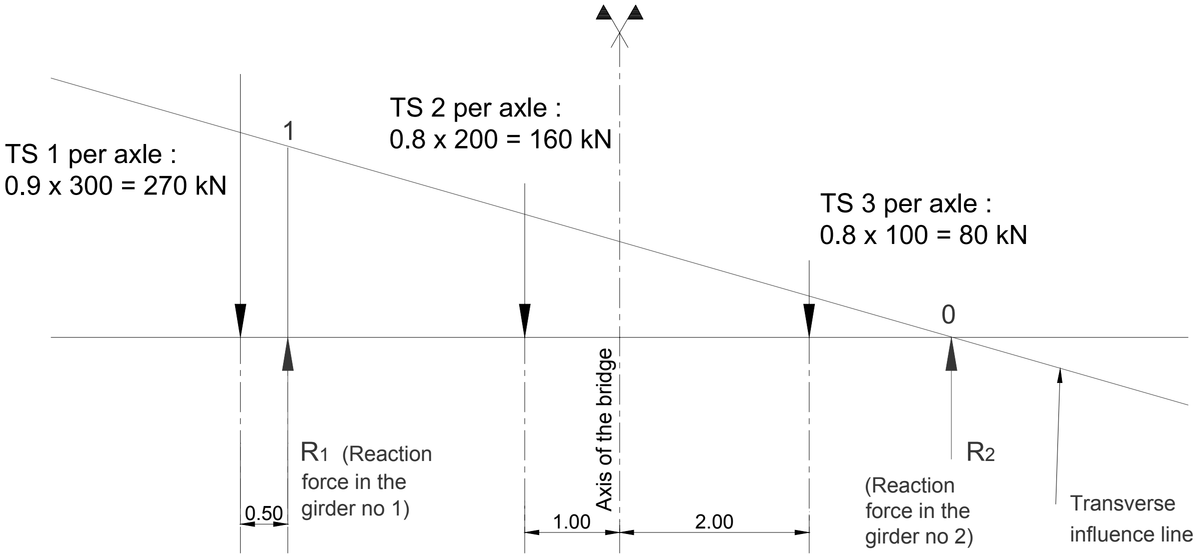
TS 1 per axle :
0.9 x 300 = 270 kN
1
TS 2 per axle :
0.8 x 200 = 160 kN
TS 3 per axle :
0.8 x 100 = 80 kN
0
Axis of the bridge
R1 (Reaction force in the girder no 1)
R2
(Reaction force in the girder no 2)
Transverse influence line
0.50
1.00
2.00

Figure 2-20: Tandem TS loading on the deck for the twin-girder bridge.

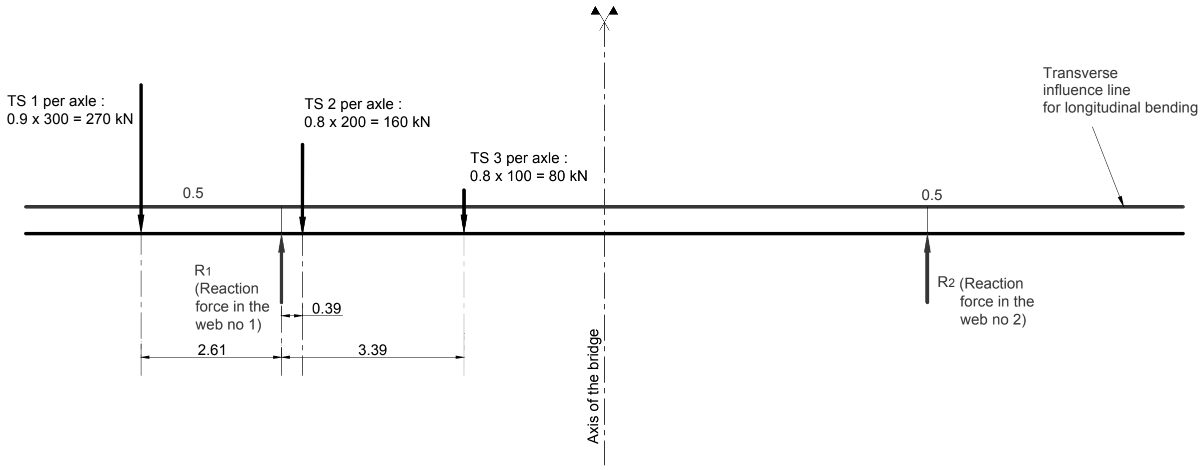
TS 1 per axle :
0.9 x 300 = 270 kN
TS 2 per axle :
0.8 x 200 = 160 kN
TS 3 per axle :
0.8 x 100 = 80 kN
Transverse influence line for longitudinal bending
0.5
0.5
R1 (Reaction force in the web no 1)
0.39
R2 (Reaction force in the web no 2)
2.61
3.39
Axis of the bridge

Figure 2-21: Tandem TS loading on the deck for the box-girder bridge.

Each traffic lane can only support a single tandem TS in the longitudinal direction. The three used tandem TS (one per lane) could not be necessarily located in the same transverse cross-section.

Uniformly Distributed Load UDL

For the twin-girder-bridge, the traffic lanes are loaded with UDL up to the axis of girder no. 2 (see Figure 2-22) i.e. the positive part of the transverse influence line. For the box-girder bridge, given the transverse influence line, the whole pavement width is loaded with UDL The vertical load magnitudes of UDL are given in EN 1991-2, Table 4.2 (EN 1991-2, 4.3.2(1) (b)).

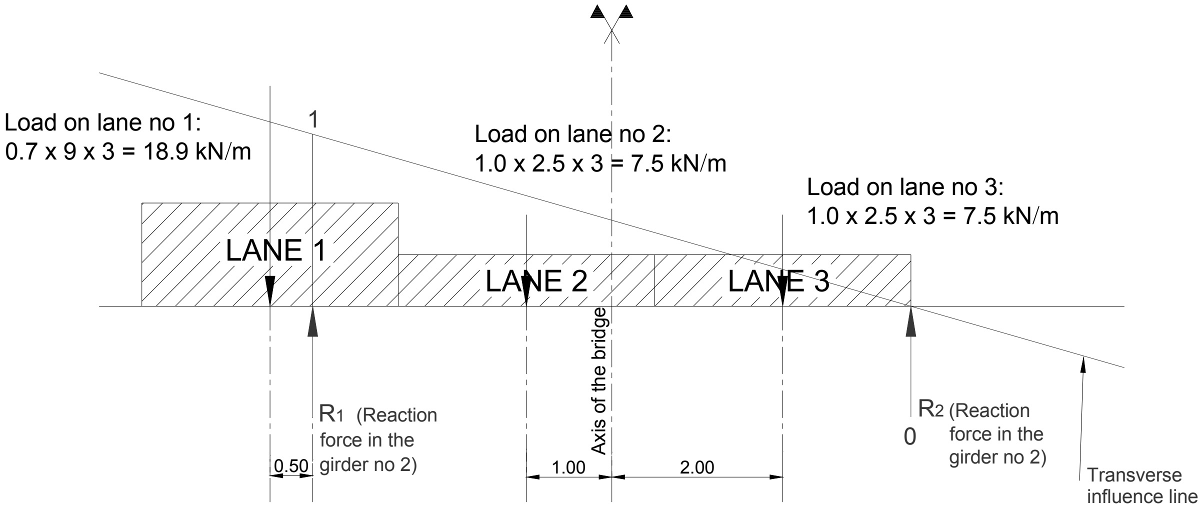
Load on lane no 1:
0.7 x 9 x 3 = 18.9 kN/m
1
Load on lane no 2:
1.0 x 2.5 x 3 = 7.5 kN/m
Load on lane no 3:
1.0 x 2.5 x 3 = 7.5 kN/m
LANE 1
LANE 2
LANE 3
Axis of the bridge
R1 (Reaction force in the girder no 2)
R2 (Reaction force in the girder no 2)
0
0.50
1.00
2.00
Transverse influence line

Figure 2-22: UDL tranverse distribution on the bridge deck for the twin-girder bridge.

NOTE: that if lane no. 3 extended beyond the axis of main girder no. 2 it would only be partly loaded in the positive zone of the transverse influence line.

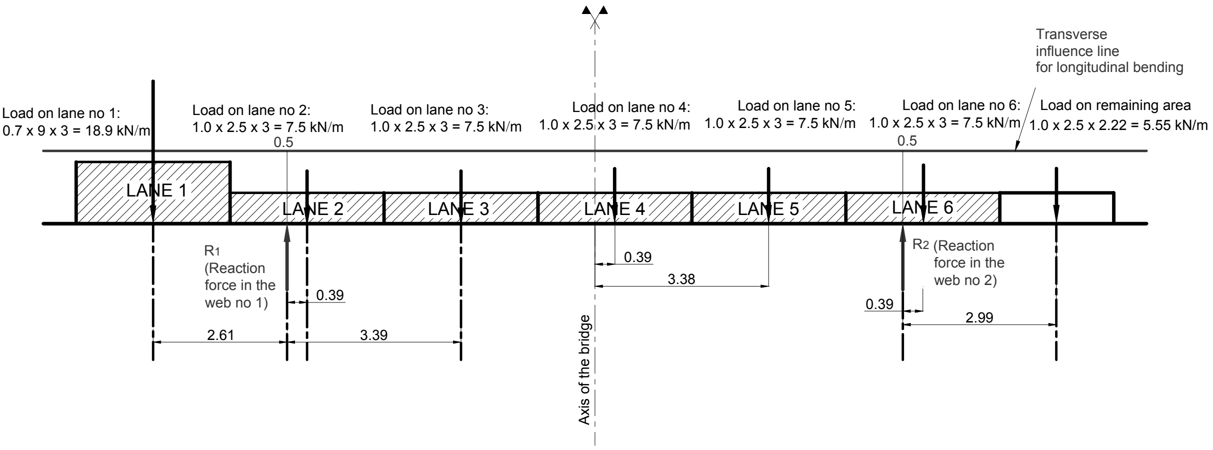
Transverse influence line for longitudinal bending
Load on lane no 1:
0.7 x 9 x 3 = 18.9 kN/m
Load on lane no 2:
1.0 x 2.5 x 3 = 7.5 kN/m
Load on lane no 3:
1.0 x 2.5 x 3 = 7.5 kN/m
Load on lane no 4:
1.0 x 2.5 x 3 = 7.5 kN/m
Load on lane no 5:
1.0 x 2.5 x 3 = 7.5 kN/m
Load on lane no 6:
1.0 x 2.5 x 3 = 7.5 kN/m
Load on remaining area
1.0 x 2.5 x 2.22 = 5.55 kN/m
0.5
0.5
LANE 1
LANE 2
LANE 3
LANE 4
LANE 5
LANE 6
R1 (Reaction force in the web no 1)
R2 (Reaction force in the web no 2)
0.39
0.39
0.39
3.38
2.61
3.39
2.99
Axis of the bridge

Figure 2-23: UDL tranverse distribution on the bridge deck for the box-girder bridge.

2.3.3.4.3 Longitudinal positioning of LM1

The software used to calculate the internal forces and moments automatically moves along the bridge the part of the traffic loads TS and UDL which transversally comes into the modelled girder no. 1 (the most loaded one according to the analysis in the Paragraph 2.3.3.4.2, see Figure 2-30). It directly gives the envelopes of bending moments and shear forces for:

- the characteristic value of LM1 : 1.0·UDL + 1.0·TS
- the frequent value of LM1 : 0.4·UDL + 0.75·TS

EN 1994-2, 5.4.2.2(11), Creep and shrinkage

(11) The St. Venant torsional stiffness of box-girders should be calculated for a transformed cross-section in which the concrete slab thickness is reduced by the modular ratio $n_{0G} = G_a/G_c$ where G_a and G_c are the elastic shear moduli of structural steel and concrete respectively. The effects of creep should be taken into account in accordance with (2) with the modular ratio

$$n_{LG} = n_{0G}\ (1 + \psi_L \varphi_t).$$

EN 1994-2, 5.4.2.3(6), Effects of cracking of concrete

(6) The torsional stiffness of box-girders should be calculated for a transformed cross-section. In areas where the concrete slab is assumed to be cracked due to bending and where membrane shear stresses are so large that shear reinforcement is required, the calculation should be performed considering a slab thickness reduced to one half, unless the effect of cracking is considered in a more precise way.

2.3.3.5 Torque

All the loads applied on the box-girder bridge are transversally symmetrical, except the traffic loads.

So the torque in the sections will be only produced by LM1. Considering the vertical loads applied on the left hand side of the longitudinal axis of the deck:

- for TS, the torque moment (for one axle per tandem) is equal to:

  270 kN x 8.61 m + 160 kN x 5.61 m + 80 kN x 2.61 m = 3431 kN.m

- for UDL, the linear torque moment is equal to:

  18.9 kN/m x 8.61 m + 17.8 kN/m x 3.55 m = 226 kN.m/m.

As already mentioned in Paragraph 2.3.3.4.2 for the longitudinal bending, the software automatically moves along the bridge the traffic loads TS and UDL to calculate the most unfavourable torsional moment in each section. The influence of the thickness variations on the location of the shear centre has been neglected. So every section of the bridge is assumed having the same shear centre.

The St. Venant torsional stiffness of each box section has been calculated by using the following formula:

$$I_t = \frac{4\Omega^2}{\oint \frac{l}{e}}$$

Ω represents the area bordered by the mid-planes of the internal elements of the box cross-section.

For the concrete element, the thickness e is divided by the modular ratio n_{0G} for short-term loading according to EN 1994-2, 5.4.2.2 (11). If the section is located in a cracked zone of the global bending analysis, the slab thickness is reduced to one half to take the effect of cracking into account (EN 1994-2 5.4.2.3 (6)).

For the section located in the middle of the bridge (x = 270 m), it gives:

$$\Omega = \frac{6.5+12}{2}4.15 = 38.4 \text{ m}^2$$

$$n_{0G} = n_0 \frac{1+\nu_c}{1+\nu_a} = 6.1625\frac{1.3}{1.2} = 5.69$$

lower flange: $\frac{l}{e} = \frac{6.5}{0.025} = 260$

each web: $\frac{l}{e} = \frac{4.8}{0.018} = 266$

each upper composite flange: $\frac{l}{e} = \frac{0.75}{0.05 + 0.325/5.69} = 7.0$

upper flange with only concrete: $\frac{l}{e} = \frac{10.5}{0.325/5.69} = 184$

$$\Rightarrow \qquad \sum \frac{l}{e} = 990$$

Thus, this section gives: $I_t = \frac{4\Omega^2}{\oint \frac{l}{e}} = 5.96 \text{ m}^4$.

EN 1990, 4.1.2, Characteristic values of actions

EN 1990, 6.4.3.2(3), Combinations of actions for persistent or transient design situations (fundamental combinations)

(3) The combination of actions in brackets { }, in (6.9b) may either be expressed as:

$$\sum_{j\geq 1}\gamma_{G,j}G_{k,j}\text{"+"}\gamma_P P\text{"+"}\gamma_{Q,1}Q_{k,1}\text{"+"}\sum_{i>1}\gamma_{Q,i}\psi_{0,i}Q_{k,i} \qquad (6.10)$$

or, alternatively for STR and GEO limit states, the less favourable of the two following expressions:

$$\begin{cases}\sum_{j\geq 1}\gamma_{G,j}G_{k,j}\text{"+"}\gamma_P P\text{"+"}\gamma_{Q,1}\psi_{0,1}Q_{k,1}\text{"+"}\sum_{i>1}\gamma_{Q,i}\psi_{0,i}Q_{k,i} & (6.10a)\\ \sum_{j\geq 1}\xi_j\gamma_{G,j}G_{k,j}\text{"+"}\gamma_P P\text{"+"}\gamma_{Q,1}Q_{k,1}\text{"+"}\sum_{i>1}\gamma_{Q,i}\psi_{0,i}Q_{k,i} & (6.10b)\end{cases}$$

where:

"+" implies "to be combined with"

$\sum$ implies "the combined effect of"

ξ is a reduction factor for unfavourable permanent actions *G*

EN 1990, Annex 2, Table A2.4(B), Design values of actions (STR/GEO) (Set B)

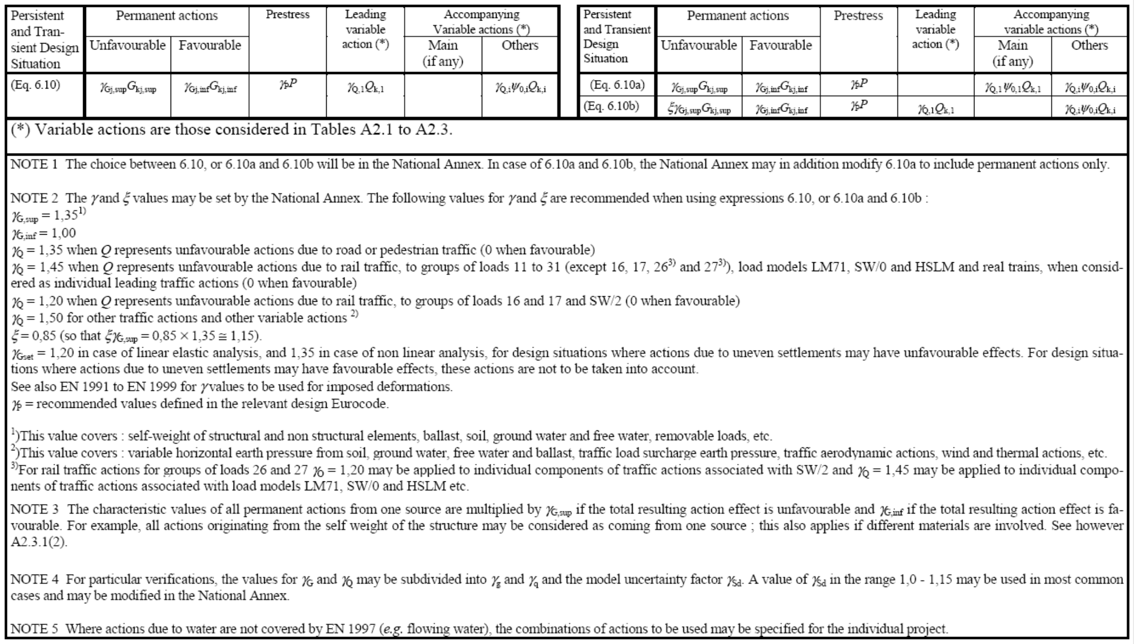

Persistent and Transient Design Situation	Permanent actions		Prestress	Leading variable action (*)	Accompanying Variable actions (*)	
	Unfavourable	Favourable			Main (if any)	Others
(Eq. 6.10)	$\gamma_{Gj,sup}G_{kj,sup}$	$\gamma_{Gj,inf}G_{kj,inf}$	$\gamma_P P$	$\gamma_{Q,1}Q_{k,1}$		$\gamma_{Q,i}\psi_{0,i}Q_{k,i}$

Persistent and Transient Design Situation	Permanent actions		Prestress	Leading variable action (*)	Accompanying variable actions (*)	
	Unfavourable	Favourable			Main (if any)	Others
(Eq. 6.10a)	$\gamma_{Gj,sup}G_{kj,sup}$	$\gamma_{Gj,inf}G_{kj,inf}$	$\gamma_P P$		$\gamma_{Q,1}\psi_{0,1}Q_{k,1}$	$\gamma_{Q,i}\psi_{0,i}Q_{k,i}$
(Eq. 6.10b)	$\xi\gamma_{Gj,sup}G_{kj,sup}$	$\gamma_{Gj,inf}G_{kj,inf}$	$\gamma_P P$	$\gamma_{Q,1}Q_{k,1}$		$\gamma_{Q,i}\psi_{0,i}Q_{k,i}$

(*) Variable actions are those considered in Tables A2.1 to A2.3.

NOTE 1 The choice between 6.10, or 6.10a and 6.10b will be in the National Annex. In case of 6.10a and 6.10b, the National Annex may in addition modify 6.10a to include permanent actions only.

NOTE 2 The γ and ξ values may be set by the National Annex. The following values for γ and ξ are recommended when using expressions 6.10, or 6.10a and 6.10b :
$\gamma_{G,sup} = 1{,}35^{1)}$
$\gamma_{G,inf} = 1{,}00$
$\gamma_Q = 1{,}35$ when Q represents unfavourable actions due to road or pedestrian traffic (0 when favourable)
$\gamma_Q = 1{,}45$ when Q represents unfavourable actions due to rail traffic, to groups of loads 11 to 31 (except 16, 17, $26^{3)}$ and $27^{3)}$), load models LM71, SW/0 and HSLM and real trains, when considered as individual leading traffic actions (0 when favourable)
$\gamma_Q = 1{,}20$ when Q represents unfavourable actions due to rail traffic, to groups of loads 16 and 17 and SW/2 (0 when favourable)
$\gamma_Q = 1{,}50$ for other traffic actions and other variable actions $^{2)}$
$\xi = 0{,}85$ (so that $\xi\gamma_{G,sup} = 0{,}85 \times 1{,}35 \cong 1{,}15$).
$\gamma_{Gset} = 1{,}20$ in case of linear elastic analysis, and 1,35 in case of non linear analysis, for design situations where actions due to uneven settlements may have unfavourable effects. For design situations where actions due to uneven settlements may have favourable effects, these actions are not to be taken into account.
See also EN 1991 to EN 1999 for γ values to be used for imposed deformations.
γ_P = recommended values defined in the relevant design Eurocode.

[1])This value covers : self-weight of structural and non structural elements, ballast, soil, ground water and free water, removable loads, etc.
[2])This value covers : variable horizontal earth pressure from soil, ground water, free water and ballast, traffic load surcharge earth pressure, traffic aerodynamic actions, wind and thermal actions, etc.
[3])For rail traffic actions for groups of loads 26 and 27 $\gamma_Q = 1{,}20$ may be applied to individual components of traffic actions associated with SW/2 and $\gamma_Q = 1{,}45$ may be applied to individual components of traffic actions associated with load models LM71, SW/0 and HSLM etc.

NOTE 3 The characteristic values of all permanent actions from one source are multiplied by $\gamma_{G,sup}$ if the total resulting action effect is unfavourable and $\gamma_{G,inf}$ if the total resulting action effect is favourable. For example, all actions originating from the self weight of the structure may be considered as coming from one source ; this also applies if different materials are involved. See however A2.3.1(2).

NOTE 4 For particular verifications, the values for γ_G and γ_Q may be subdivided into γ_g and γ_q and the model uncertainty factor γ_{Sd}. A value of γ_{Sd} in the range 1,0 - 1,15 may be used in most common cases and may be modified in the National Annex.

NOTE 5 Where actions due to water are not covered by EN 1997 (*e.g.* flowing water), the combinations of actions to be used may be specified for the individual project.

2.3.3.6 Thermal gradient

To simplify the study, the thermal gradient is not addressed in this report. Taken the thermal gradient into account would have had an influence on:

- the value of the stresses at Serviceability Limit State (SLS) due to primary effects of the gradient – but this Design Manual focuses on the ULS buckling phenomena.
- the amplitude of the concrete stress envelope which would have been wider, and consequently the cracked zones of the global analysis, too.

2.3.4 Combinations of actions

2.3.4.1 Design situations

The bridge should be verified for the following design situations:

- Transient design situations:
  - for the structural steel alone under its self-weight (launching steps),
  - during and after concreting of each slab segment (16 or 45 situations for the example following the bridge),
- Permanent design situations:
  - at traffic opening,
  - at infinite time.

The transient design situations, i.e. launching of the structural steel part, are studied in Chapter 4.

Both permanent design situations will be included in the global analysis (through the use of two sets of modular ratios). The verification of the bridge will then be performed once, considering the final envelopes of internal forces and moments.

2.3.4.2 General remarks

The notations used are those of Eurocodes:

- $G_{k,sup}$: characteristic value of an *unfavourable* permanent action (nominal value of self-weight and maximum value of non-structural equipments) taking account of construction phases
- $G_{k,inf}$: characteristic value of a *favourable* permanent action (nominal value of self-weight and minimum value of non-structural equipments) taking account of construction phases
- S : envelope of characteristic values of internal forces and moments (or deformations) due to concrete shrinkage
- UDL_k : envelope of characteristic values of internal forces and moments (or deformations) due to the vertical uniformly distributed loads from Load Model no. 1 in EN 1991-2
- TS_k : envelope of characteristic values of internal forces and moments (or deformations) due to the vertical concentrated loads from Load Model no. 1 in EN 1991-2

An envelope calculation with $G_{k,sup}$ and $G_{k,inf}$ is necessary for the permanent loads, only because of the variability of the deck surfacing load. The nominal value of the self-weight is considered (EN 1990, 4.1.2).

The combinations of actions indicated below have been established using EN 1990 and its normative Annex A2 "Application for bridges”.

The shrinkage is not taken into account if its effect is favourable.

EN 1990 Annex 2, Table A.2.1, Recommended values of ψ factors for road bridges

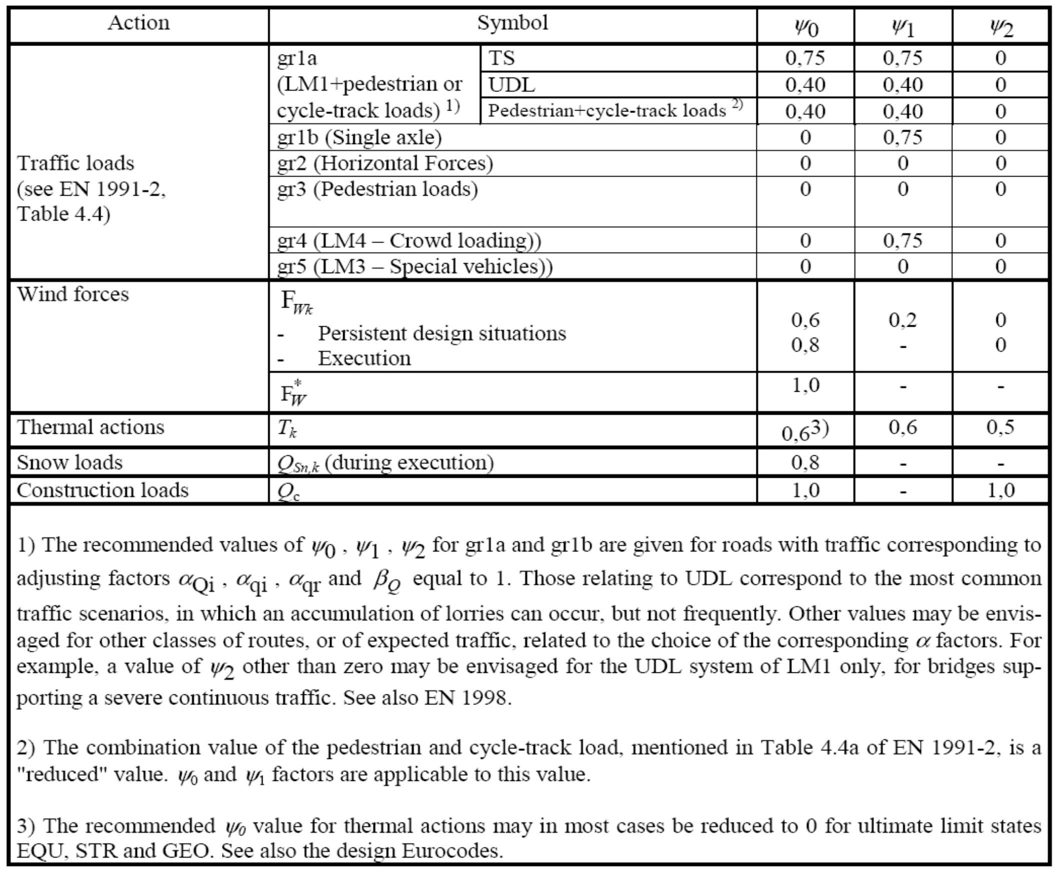

Action	Symbol		ψ_0	ψ_1	ψ_2
Traffic loads (see EN 1991-2, Table 4.4)	gr1a (LM1+pedestrian or cycle-track loads) 1)	TS	0,75	0,75	0
		UDL	0,40	0,40	0
		Pedestrian+cycle-track loads 2)	0,40	0,40	0
	gr1b (Single axle)		0	0,75	0
	gr2 (Horizontal Forces)		0	0	0
	gr3 (Pedestrian loads)		0	0	0
	gr4 (LM4 – Crowd loading))		0	0,75	0
	gr5 (LM3 – Special vehicles))		0	0	0
Wind forces	F_{Wk} - Persistent design situations - Execution		 0,6 0,8	 0,2 -	 0 0
	F_W^*		1,0	-	-
Thermal actions	T_k		0,6 3)	0,6	0,5
Snow loads	$Q_{Sn,k}$ (during execution)		0,8	-	-
Construction loads	Q_c		1,0	-	1,0

1) The recommended values of ψ_0, ψ_1, ψ_2 for gr1a and gr1b are given for roads with traffic corresponding to adjusting factors α_{Qi}, α_{qi}, α_{qr} and β_Q equal to 1. Those relating to UDL correspond to the most common traffic scenarios, in which an accumulation of lorries can occur, but not frequently. Other values may be envisaged for other classes of routes, or of expected traffic, related to the choice of the corresponding α factors. For example, a value of ψ_2 other than zero may be envisaged for the UDL system of LM1 only, for bridges supporting a severe continuous traffic. See also EN 1998.

2) The combination value of the pedestrian and cycle-track load, mentioned in Table 4.4a of EN 1991-2, is a "reduced" value. ψ_0 and ψ_1 factors are applicable to this value.

3) The recommended ψ_0 value for thermal actions may in most cases be reduced to 0 for ultimate limit states EQU, STR and GEO. See also the design Eurocodes.

EN 1990, Annex 2, A2.4.1, General

(1) For serviceability limit states the design values of actions should be taken from Table A2.6 except if differently specified in EN 1991 to EN 1999.

NOTE1: γ factors for traffic and other actions for the serviceability limit state may be defined in the National Annex. The recommended design values are given in Table A2.6, with all γ factors being taken as 1.0.

Table A2.6: Design values of actions for use in the combination of actions

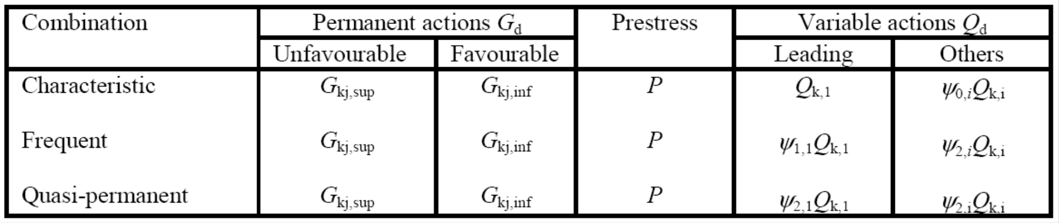

Combination	Permanent actions G_d		Prestress	Variable actions Q_d	
	Unfavourable	Favourable		Leading	Others
Characteristic	$G_{kj,sup}$	$G_{kj,inf}$	P	$Q_{k,1}$	$\psi_{0,i}Q_{k,i}$
Frequent	$G_{kj,sup}$	$G_{kj,inf}$	P	$\psi_{1,1}Q_{k,1}$	$\psi_{2,i}Q_{k,i}$
Quasi-permanent	$G_{kj,sup}$	$G_{kj,inf}$	P	$\psi_{2,1}Q_{k,1}$	$\psi_{2,i}Q_{k,i}$

NOTE 2: The National Annex may also refer to the infrequent combination of actions.

(2) The serviceability criteria should be defined in relation to the serviceability requirements in accordance with 3.4 and EN 1992 to EN 1999. Deformations should be calculated in accordance with EN 1991 to EN 1999, by using the appropriate combinations of actions according to expressions (6.14a) to (6.16b) (see Table A2.6) taking into account the serviceability requirements and the distinction between reversible and irreversible limit states.

NOTE: Serviceability requirements and criteria may be defined as appropriate in the National Annex or for the individual project.

2.3.4.3 ULS combinations other than fatigue

$1.35\ G_{k,sup}$ (or $1.0\ G_{k,inf}$) + (1.0 or 0.0) $S + 1.35\ \{\ UDL_k + TS_k\ \}$

The above-mentioned combination of actions corresponds to Equation (6.10) in EN 1990, 6.4.3.2. Equations (6.10 a) and (6.10 b) have not been used. The γ values have been taken from Table A.2.4 (B) of Annex A2 to EN 1990. The ψ_0 factors used for defining the combination value of a variable action have been taken from Table A.2.1 of Annex A2 to EN 1990.

2.3.4.4 SLS combinations

According to A2.4.1 of Annex A2 to EN 1990, the following combinations should be considered:

- Characteristic SLS combination:

  $G_{k,sup}$ (or $G_{k,inf}$) + (1.0 or 0.0) $S + UDL_k + TS_k$

- Frequent SLS combination:

  $G_{k,sup}$ (or $G_{k,inf}$) + (1.0 or 0.0) $S + 0.4.\ UDL_k + 0.75.\ TS_k$

- Quasi-permanent SLS combination:

  $G_{k,sup}$ (or $G_{k,inf}$) + (1.0 or 0.0) S

EN 1994-2, 5.4.2.3(2), Effects of cracking of concrete

(2) The following method may be used for the determination of the effects of cracking in composite beams with concrete flanges. First the envelope of the internal forces and moments for the characteristic combinations, see EN 1990, 6.5.3, including long-term effects should be calculated using the flexural stiffness $E_a I_1$ of the un-cracked sections. This is defined as “un-cracked analysis”.

In regions where the extreme fibre tensile stress in the concrete due to the envelope of global effectsexceeds twice the strength f_{ctm} or f_{lctm} , see EN 1992-1-1, Table 3.1 or Table 11.3.1, the stiffnessshould be reduced to $E_a I_2$, see 1.5.2.12. This distribution of stiffness may be used for ultimate limit states and for serviceability limit states. A new distribution of internal forces and moments, and deformation if appropriate, is then determined by re-analysis. This is defined as “cracked analysis”.

2.4 Global analysis

2.4.1 General

The global analysis is the calculation of the whole bridge to determine the internal forces and moments and the corresponding stresses in all its cross-sections. This is calculated by respecting the defined construction phases and by considering two particular dates in the bridge life – at traffic opening (short term situation) and at infinite time (long-term situation).

According to Eurocode 4, the global analysis of a two-girder bridge is a first order linear elastic analysis, taking into account the construction phases and the cracking of concrete around intermediate supports.

2.4.1.1 Concrete cracking

For the example, it has been chosen to calculate the cracked lengths around internal supports instead of using the simplified "15%-method". This is achieved by two successive global analysis (EN 1994-2, 5.4.2.3(2)):

- In a first global analysis - called „*uncracked analysis*" - the concrete is considered as uncracked for calculating the cross-sectional properties of all the cross-sections in the modelled main girder;
- In a given cross-section if the longitudinal upper fibre tensile stress σ_c in the concrete slab is higher than $-2 \cdot f_{ctm}$ (= -6.4 MPa in the example) under characteristic SLS combination of actions, then the concrete of this cross-section should be considered as cracked in the second global analysis. This criterion thus defines *cracked zones* on both sides of the intermediate supports;
- In a second global analysis - called „*cracked analysis*" - the concrete slab stiffness in the cracked zones is reduced to the stiffness of its reinforcing steel. The internal forces and moments - as well as the corresponding stress distributions - of this cracked analysis should be used to verify all the transverse cross-sections of the deck.

See also the chart in Figure 2-28.

2.4.1.2 Shear lag in the concrete slab

The shear lag in the concrete slab is taken into account by reducing the actual slab width to an "effective" width. It thus influences the cross sectional properties of the cross-sections which are used in the global analysis (EN 1994-2, 5.4.1.2).

See also Paragraph 2.4.2.2 for the calculation of effective widths in this project.

2.4.2 Internal forces and moments – Stresses

2.4.2.1 Numerical model

2.4.2.1.1 Twin-girder bridge

To analyse the global longitudinal bending, the deck is modelled as a continuous line of bar elements which corresponds to the neutral fiber of the modelled main girder and which is simply supported on piers and abutments. With respect to a fixed reference (which can be attached e.g. to the final longitudinal profile of the pavement) this neutral fiber changes throughout the calculation according to the cross sectional properties (areas and second moments of area) allocated to the bar elements in the model. This is due to the different modular ratios to be considered and to the fact that a given cross-

EN 1994-2, 5.4.1.2(5), Effective width of flanges for shear lag

At mid-span or an internal support, the total effective width b_{eff} , see Figure 5.1, may be determined as:

$$b_{\text{eff}} = b_0 + \sum b_{\text{ei}} \tag{5.3}$$

where:

b_0 is the distance between the centres of the outstand shear connectors;

b_{ei} is the value of the effective width of the concrete flange on each side of the web and taken as $L_{e/8}$ (but not greater than the geometric width b_{i} . The value b_{i} should be taken as the distance from the outstand shear connector to a point mid-way between adjacent webs, measured at mid-depth of the concrete flange, except that at a free edge b_{i} is the distance to the free edge. The length L_{e} should be taken as the approximate distance between points of zero bending moment. For typical continuous composite beams, where a moment envelope from various load arrangements governs the design, and for cantilevers, L_{e} may be assumed to be as shown in Figure 5.1.

section could be composite or not, with a cracked concrete or not, following the phases of the global analysis. In addition to the cross-sections on internal and end supports and at mid-spans, some particular cross-sections are worthy of being at the bar element ends:

- at the quarter and three-quarters of each span (to define the effective widths of the slab to calculate the stress distribution, see also Paragraph 6.2.2),
- at the ends of every slab concreting segment,
- at the thickness changes in the structural steel distribution.
- in order to have a good precision of the cracked zone length, the bar element length is limited to 1.5 m in the central span and to 1.25 m in the end spans.

Every load case is introduced into the numerical model with the corresponding mechanical properties of the cross-sections.

2.4.2.1.2 Box-girder-bridge

Global analysis of the bending moment

The box-girder is modelled as a twin-girder bridge whose bottom flange width is half of the bottom flange of the box-section. A half box-girder is studied (i.e. the equivalent of one girder for a twin-girder bridge).

Major differences are the traffic lane positioning and the transverse influence line, already described in Paragraph 2.3.3.4.

To analyse the global longitudinal bending, the deck is modelled as a continuous line of bar elements which corresponds to the neutral fiber of the modelled half box-girder and which is simply supported on piles and abutments. With respect to a fixed reference (which can be attached, for example, to the final longitudinal profile of the pavement) this neutral fiber changes throughout the calculation according to the mechanical properties (areas and second moments of area) allocated to the bar elements in the model. This is due to the different modular ratios to be considered and to the fact that a given cross-section could be composite or not, with a cracked concrete or not, following the phases of the global analysis.

In addition to the cross-sections on internal and end supports and at mid-spans, some peculiar cross-sections are worthy of being at the bar element ends:

- at the quarter and three-quarters of each span (to define the effective widths of the slab to calculate the stress distribution, see also Paragraph 2.4.2.2),
- at the ends of every slab concreting segment,
- at the thickness changes in the structural steel distribution.

Every load case is introduced into the numerical model with the corresponding mechanical properties of the cross-sections.

Global analysis of the torque

The first model is a 2D model and only represents a half deck. The torque study requires a 3D model with the definition of the torsional stiffness all along the bridge and of the whole box cross-section of the deck.

2.4.2.2 Effective width

2.4.2.2.1 Twin-girder bridge

In a given cross-section of one of the main girder, the effective width of the concrete slab is the sum of 3 terms (see Figure 2-24):

$$b_{eff} = b_0 + \beta_1 b_{e1} + \beta_2 b_{e2} \qquad \text{(EN 1994-2, 5.4.1.2 (5))}$$

EN 1994-2, 5.4.1.2(6), Effective width of flanges for shear lag

The effective width at an end support may be determined as:

$$b_{\mathrm{eff}} = b_0 + \sum \beta_i \, b_{\mathrm{ei}} \tag{5.4}$$

with:

$$\beta_i = (0{,}55 + 0{,}025 \, L_e / b_{\mathrm{ei}}) \leq 1{,}0 \tag{5.5}$$

where:

b_{ei} is the effective width, see (5), of the end span at mid-span and L_e is the equivalent span of the end span according to Figure 5.1.

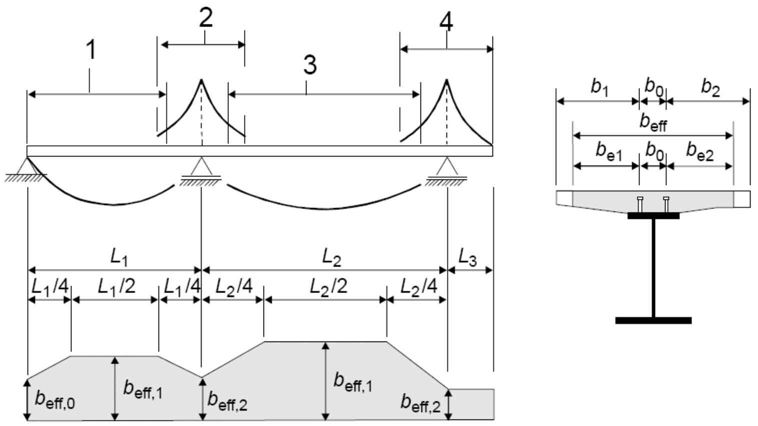
2
4
1
3
b1
b0
b2
beff
be1
b0
be2
L1
L2
L3
L1/4
L1/2
L1/4
L2/4
L2/2
L2/4
beff,0
beff,1
beff,2
beff,1
beff,2

Key:

1 $L_e = 0{,}85 \, L_1$ for $b_{\mathrm{eff},1}$

2 $L_e = 0{,}25(L_1 + L_2)$ for $b_{\mathrm{eff},2}$

3 $L_e = 0{,}70 \, L_2$ for $b_{\mathrm{eff},1}$

4 $L_e = 2 \, L_3$ for $b_{\mathrm{eff},2}$

Figure 5.1: Equivalent spans for effective width of concrete flange

with

b_0 (= 650 mm for the example), the center-to-center distance between the outside stud rows;

$b_{ei} = \min \{L_e/8 \; ; \; b_i\}$ where L_e is the equivalent span length in the considered cross-section and where b_i is the actual geometric width of the slab associated to the main girder;

$\beta_1 = \beta_2 = 1$ except for the cross-sections on end supports C0 and C3 where $\beta_i = 0.55 + 0.025.L_e/b_{ei} < 1.0$ with b_{ei} taken as equal to the effective width at mid-end span (EN 1994-2, 5.4.1.2 (6)).

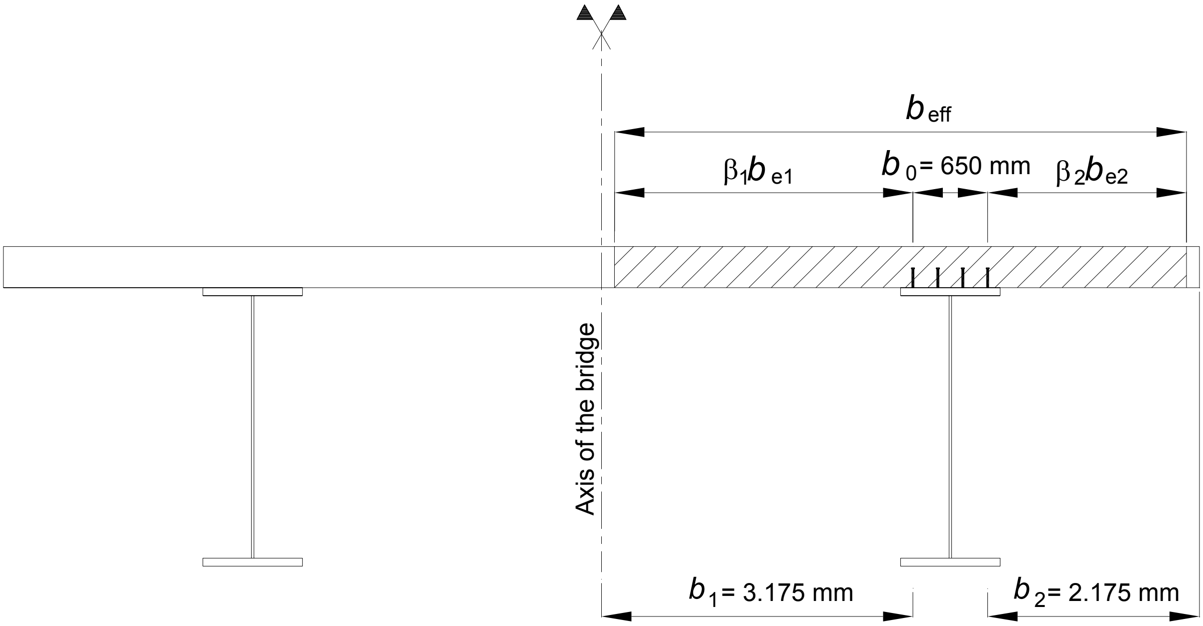

Figure 2-24: Effective slab width for a main girder in a given cross-sectionof the twin-girder bridge.

The equivalent spans are:

$L_{e1} = 0.85 \cdot L_1 = 0.85 \cdot L_1 = 0.85 \cdot 50 = 42.5$ m for the cross-sections located in the end spans C0-P1 and P2-C3 and for the cross-sections located on end supports C0 and C3 (EN 1994-2, Figure 5.1);

$L_{e2} = 0.7 \cdot L_2 = 0.7 \cdot 60 = 42$ m for the cross-sections located in the central span P1-P2;

$L_{e3} = 0.25 \cdot (L_1 + L_2) = 0.25 \cdot (50+60) = 27.5$ m for the cross-sections located on internal supports P1 and P2.

As $L_{ei}/8$ is always greater than b_i for the example it is deduced that the effective width is equal to the actual width except for the cross-sections on end supports C0 and C3 where the factor β_i has an impact:

$\beta_1 = 0.55 + 0.025 \cdot L_{e1}/b_{e1} = 0.55 + 0.025 \cdot 42.5/3.175 = 0.88 < 1.0$,

$\beta_2 = 0.55 + 0.025 \cdot L_{e1}/b_{e2} = 0.55 + 0.025 \cdot 42.5/2.175 = 1.04$ but as $\beta_2 > 1$ $\beta_2 = 1$ is retained

The slab width will therefore vary linearly from 5.634 m on end support C0 to 6.0 m for the abscissa $0.25 \cdot L_1 = 12.5$ m in the span C0-P1 (EN 1994-2, Figure 5.1). Afterwards it will be constant and equal to 6.0 m up to the abscissa $2 \cdot L_1 + L_2 - 0.25 \cdot L_1 = 147.5$ m and then it will vary linearly from 6.0 m to 5.634 m on end support C3.

EN 1994-2, 5.4.1.2(4), Effective width of flanges for shear lag

When elastic global analysis is used, a constant effective width may be assumed over the whole of each span. This value may be taken as the value $b_{\mathrm{eff},1}$ at mid-span for a span supported at both ends, or the value $b_{\mathrm{eff},2}$ at the support for a cantilever.

EN 1994-2, 5.4.1.2(5), Effective width of flanges for shear lag

At mid-span or an internal support, the total effective width b_{eff} , see Figure 5.1, may be determined as:

$$b_{\mathrm{eff}} = b_0 + \sum b_{\mathrm{ei}} \tag{5.3}$$

where:

b_0 is the distance between the centres of the outstand shear connectors;

b_{ei} is the value of the effective width of the concrete flange on each side of the web and taken as $L_{e/8}$ (but not greater than the geometric width b_{i} . The value b_{i} should be taken as the distance from the outstand shear connector to a point mid-way between adjacent webs, measured at mid-depth of the concrete flange, except that at a free edge b_{i} is the distance to the free edge. The length L_{e} should be taken as the approximate distance between points of zero bending moment. For typical continuous composite beams, where a moment envelope from various load arrangements governs the design, and for cantilevers, L_{e} may be assumed to be as shown in Figure 5.1.

EN 1994-2, 5.4.1.2(6), Effective width of flanges for shear lag

The effective width at an end support may be determined as:

$$b_{\mathrm{eff}} = b_0 + \sum \beta_{\mathrm{i}}\, b_{\mathrm{ei}} \tag{5.4}$$

with:

$$\beta_{\mathrm{i}} = (0{,}55 + 0{,}025\, L_{\mathrm{e}} / b_{\mathrm{ei}}) \leq 1{,}0 \tag{5.5}$$

where:

b_{ei} is the effective width, see (5), of the end span at mid-span and L_{e} is the equivalent span of the end span according to Figure 5.1.

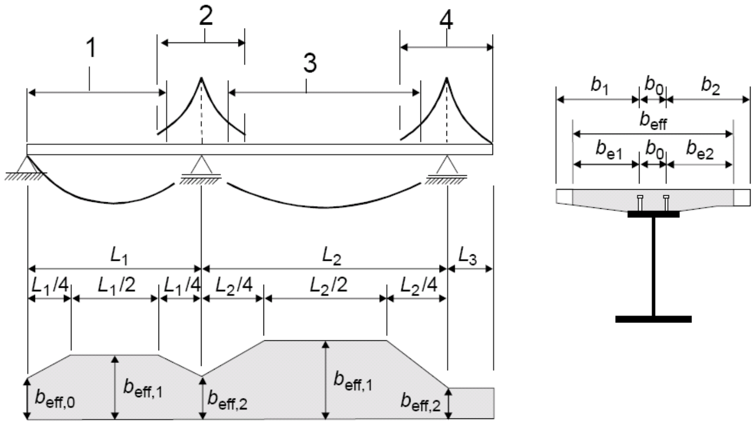

Key:

1 $L_{\mathrm{e}} = 0{,}85\, L_1$ for $b_{\mathrm{eff},1}$

2 $L_{\mathrm{e}} = 0{,}25(L_1 + L_2)$ for $b_{\mathrm{eff},2}$

3 $L_{\mathrm{e}} = 0{,}70\, L_2$ for $b_{\mathrm{eff},1}$

4 $L_{\mathrm{e}} = 2\, L_3$ for $b_{\mathrm{eff},2}$

Figure 5.1: Equivalent spans for effective width of concrete flange

This variable effective width is always taken into account to calculate the longitudinal stress distribution.

To calculate the internal forces and moments with a linear elastic global analysis, constant widths have been used for each span by considering the values at mid-span (EN 1994-2, 5.4.1.2(4)). For the example this means that the calculation can be performed with the actual slab width over the entire bridge length.

$\Rightarrow \quad b_{eff} = 6$ m

2.4.2.2.2 Box-girder bridge

Effective width of the concrete slab

In a given cross-section of one of the main girder, the effective width of the concrete slab is the sum of 3 terms (see Figure 2-25):

$b_{eff} = b_0 + \beta_1 \cdot b_{e1} + \beta_2 \cdot b_{e2}$ (EN 1994-2, 5.4.1.2 (5))

with:

b_0 (= 1250 mm for the example), the center-to-center distance between the outside stud rows;

$b_{ei} = \min \{L_e/8 \, ; \, b_i\}$ where L_e is the equivalent span length in the considered cross-section and where b_i is the actual geometric width of the slab associated to the main girder;

$\beta_1 = \beta_2 = 1$ except for the cross-sections on end supports C0 and C5 where $\beta_i = 0.55 + 0.025 \cdot L_e/b_{ei} < 1.0$ with b_{ei} taken as equal to the effective width at mid-end span (EN 1994-2, 5.4.1.2 (6)).

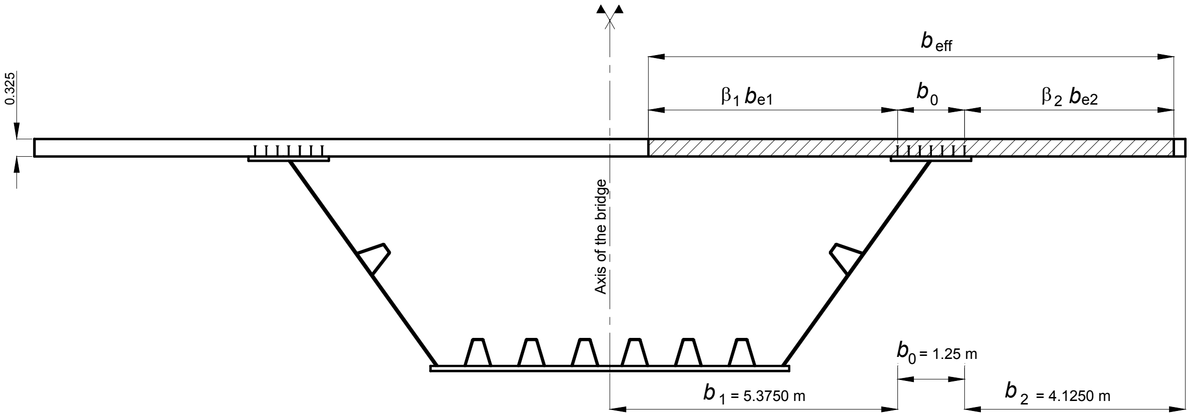

Figure 2-25: Effective slab width for a main girder in a given cross-section of the box-girder bridge.

The equivalent spans are:

$L_{e1} = 0.85 \cdot L_1 = 0.85 \cdot L_1 = 0.85 \cdot 90 = 76.5$ m for the cross-sections located in the end spans C0-P1 and P4-C5 and for the cross-sections located on end supports C0 and C5 (EN 1994-2, Figure 5.1);

$L_{e2} = 0.7 \cdot L_2 = 0.7 \cdot 120 = 84$ m for the cross-sections located in the central spans P1-P2, P2-P3 and P3-P4;

$L_{e3} = 0.25 \cdot (L_1 + L_2) = 0.25 \cdot (90+120) = 52.5$ m for the cross-sections located on internal supports P1 and P4.

$L_{e4} = 0.25 \cdot (L_2 + L_2) = 0.25 \cdot (120+120) = 60$ m for the cross-sections located on internal supports P2 and P3.

EN 1993-1-5, 3.3 (1), Shear lag at the ultimate limit states

(1) At the ultimate limit states shear lag effects may be determined as follows:

a) elastic shear lag effects as determined for serviceability and fatigue limit states,

b) combined effects of shear lag and of plate buckling,

c) elastic-plastic shear lag effects allowing for limited plastic strains.

NOTE1: The National Annex may choose the method to be applied. Unless specified otherwise in EN 1993-2 to EN 1993-6, the method in NOTE: 3 is recommended.

NOTE2: The combined effects of plate buckling and shear lag may be taken into account by using A_{eff} as given by:

$$A_{eff} = A_{c,eff} \cdot \beta_{ult} \qquad (3.3)$$

where $A_{c,eff}$ *is the effective*^{p} *area of the compression flange due to plate buckling (see 4.4 and 4.5);*

β_{ult} *is the effectives width factor for the effect of shear lag at the ultimate limit state, which may be taken as β determined from Table 3.1 with* α_0 *replaced by:*

$$\alpha_0^* = \sqrt{\frac{A_{c,eff}}{b_0 t_f}} \qquad (3.4)$$

t_f *is the flange thickness.*

NOTE3 Elastic-plastic shear lag effects allowing for limited plastic strains may be taken into account using A_{eff} *as follows:*

$$A_{eff} = A_{c,eff} \cdot \beta^{\kappa} \geq A_{c,eff} \cdot \beta \qquad (3.5)$$

where β and κ are taken from Table 3.1.

The expressions in NOTE: 2 and NOTE: 3 may also be applied for flanges in tension in which case $A_{c,eff}$ *should be replaced by the gross area of the tension flange.*

Table 3.1: Effective^{p} width factor β

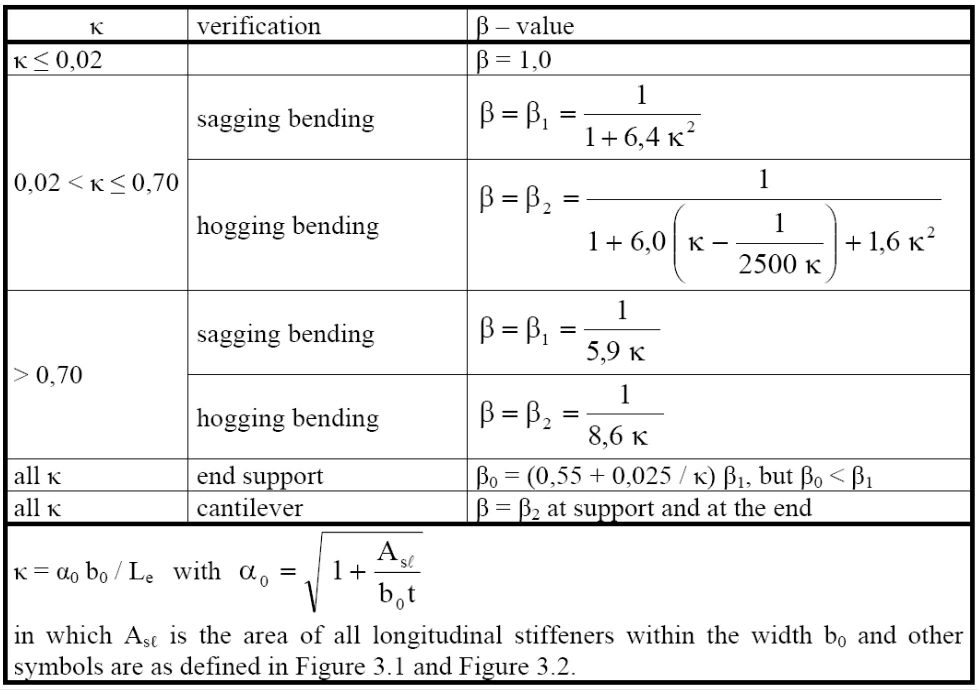

κ	verification	β – value
$\kappa \leq 0{,}02$		$\beta = 1{,}0$
$0{,}02 < \kappa \leq 0{,}70$	sagging bending	$\beta = \beta_1 = \dfrac{1}{1+6{,}4\,\kappa^2}$
	hogging bending	$\beta = \beta_2 = \dfrac{1}{1+6{,}0\left(\kappa - \dfrac{1}{2500\,\kappa}\right)+1{,}6\,\kappa^2}$
$> 0{,}70$	sagging bending	$\beta = \beta_1 = \dfrac{1}{5{,}9\,\kappa}$
	hogging bending	$\beta = \beta_2 = \dfrac{1}{8{,}6\,\kappa}$
all κ	end support	$\beta_0 = (0{,}55 + 0{,}025 / \kappa)\,\beta_1$, but $\beta_0 < \beta_1$
all κ	cantilever	$\beta = \beta_2$ at support and at the end

$\kappa = \alpha_0\, b_0 / L_e$ with $\alpha_0 = \sqrt{1 + \dfrac{A_{s\ell}}{b_0 t}}$

in which $A_{s\ell}$ is the area of all longitudinal stiffeners within the width b_0 and other symbols are as defined in Figure 3.1 and Figure 3.2.

As $L_{ei}/8$ is always greater than b_i for the example it is deduced that the effective width is equal to the actual width except for the cross-sections at end supports C0 and C5 where the factor β_i has an impact:

$\beta_1 = 0.55 + 0.025 \cdot L_{e1}/b_{e1} = 0.55 + 0.025 \cdot 76.5/5.375 = 0.906 < 1.0$,

$\beta_2 = 0.55 + 0.025 \cdot L_{e1}/b_{e2} = 0.55 + 0.025 \cdot 76.5/4.125 = 1.01 > 1.0$ then $\beta_2 = 1$

The slab width will therefore vary linearly from 10.24 m at end support C0 to 10.75 m for the abscissa $0.25 \cdot L_1 = 22.5$ m in the span C0-P1 (EN 1994-2, Figure 5.1). Afterwards it will be constant and equal to 10.75 m up to the abscissa $2 \cdot L_1 + 3 \cdot L_2 - 0.25 \cdot L_1 = 517.5$ m and then it will vary linearly from 10.75 m to 10.24 m at end support C5.

This variable effective width is always taken into account to calculate the longitudinal stress distribution.

To calculate the internal forces and moments with a linear elastic global analysis, constant widths have been used for each span by considering the values at mid-span (EN 1994-2, 5.4.1.2(4)). For the example this means that the calculation can be performed with the actual slab width over the entire bridge length.

$\Rightarrow$ $b_{eff} = 10.75$ m

Effective width of the box-girder bottom flange

Global analysis

For the box-girder bridge global analysis, shear lag is taken into account by an effective width of the steel bottom flange each side of the web which is equal to the smallest of the values between the actual total half width of the steel bottom flange and $L/8$ (on each side of the web), where L is the span length.

In this design example, given the fairly large span lengths, the shear lag effect does not reduce the width at all for the bottom plate.

A bottom flange with a half-width $b_0 = 3250$ mm gives:

- for the end spans, $b_{eff} = \min(b_0 ; L_1/8) = b_0$ with $L_1 = 90$ m,
- for the central spans, $b_{eff} = \min(b_0 ; L_2/8) = b_0$ with $L_2 = 120$ m.

Section analysis

Distinction is made between the shear lag effects for calculating stresses at SLS and at fatigue ULS on one hand, and the shear lag effects for calculating stresses at ULS on the other hand.

ULS stresses are calculated with gross mechanical characteristics (without considering shear lag in the bottom flange and reductions for buckling). Shear lag in the bottom flange is nevertheless described below.

ULS stresses:

At ULS three methods of calculating the effective width for shear lag are proposed in EN 1993-1-5, 3.3, to be chosen by the National Annex. The method recommended in NOTE: 3 of EN 1993-1-5, 3.3(1), is adopted here. The shear lag is then taken into account at ULS via the reduction factor β^{κ}. Factors β and κ are given in EN 1993-1-5 Table 3.1.

This method gives values of β^{κ} nearly equal to 1 (higher than 0.97 in every section).

SLS stresses:

Shear lag is taken into account at SLS via the reduction factor β, which values are around 0.7 for cross-sections located near the intermediate supports. The corresponding SLS stresses have not been systematically calculated as they do not govern the design of the cross-sections and they are not the objective of this Design Manual.

2.4.2.3 Determination of the cracked zones around internal supports

Firstly, a global uncracked analysis is performed for the example. The internal forces and moments as well as the longitudinal stresses σ_c in the concrete slab are calculated by considering the concrete participation in the bending stiffness of all the cross-sections. Figure 2-26 and Figure 2-27 show the stresses thus obtained under SLS characteristic combination of actions as well as the zones where this stress exceeds $2 \cdot f_{ctm}$ in the upper fibre of the concrete slab.

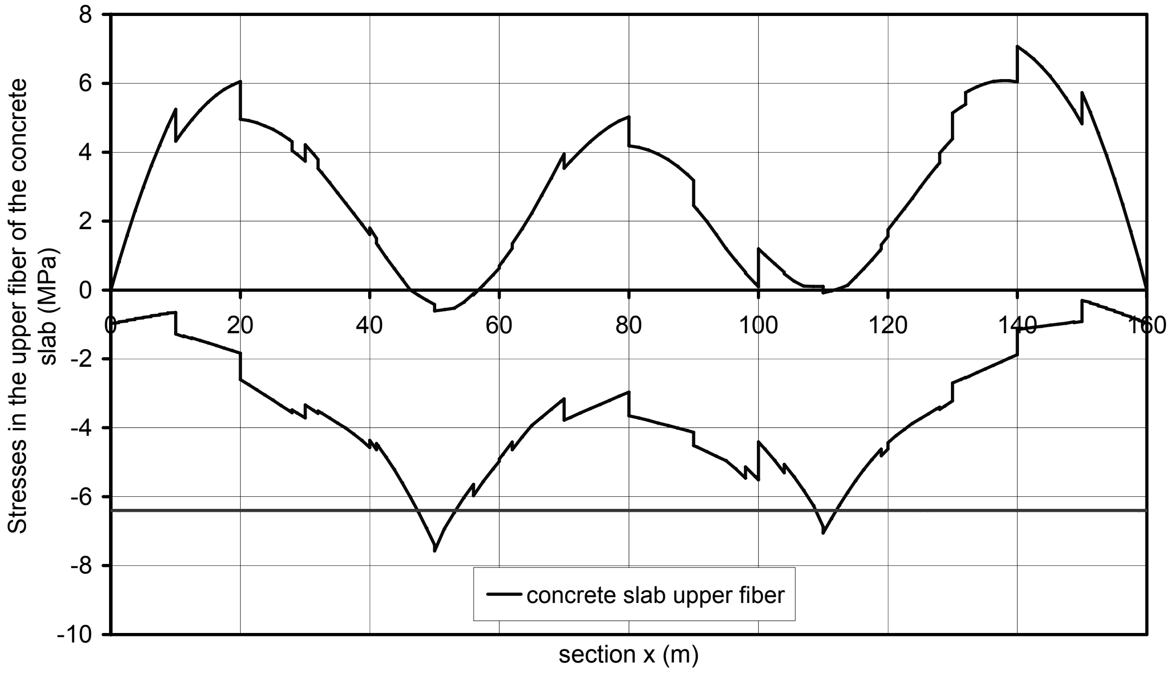

Figure 2-26: Cracked zonesof the twin-girder bridge used in the global analysis.

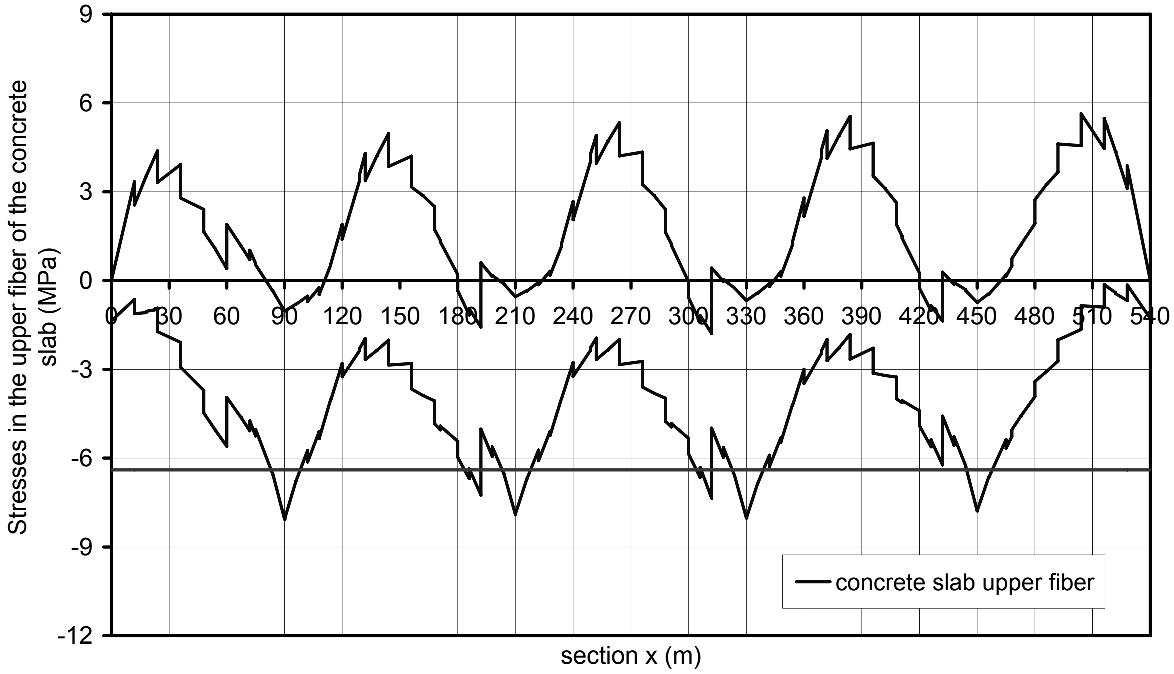

Figure 2-27: Cracked zones of the box-girder bridge used in the global analysis.

EN 1994-2, 5.4.2.2(8)

(8) In regions where the concrete slab is assumed to be cracked, the primary effects due to shrinkage may be neglected in the calculation of secondary effects.

The observed discontinuities in these envelope curves correspond to the end cross-sections of the concreting slab segments and to the cross-sections in which the thicknesses of the structural steel change. Although the bending moment is equal to zero in the cross-sections at the deck ends, the corresponding tensile stresses are not because their values include the self-balancing stresses due to the shrinkage (called "primary effects" or "isostatic effects" in EN 1994-2).

In practical terms, this gives:

Twin-girder bridge

- a cracked zone around P1 which starts at the abscissa x = 47.5 m (i.e. 5.0% for the cracked length in the left end span) and which ends at the abscissa x = 53.0 m (i.e. 5.0% for the cracked length in the central span);
- a cracked zone around P2 which starts at the abscissa x = 109.1 m (i.e. 1.5% for the cracked length in the central span) and which ends at the abscissa x = 112 m (i.e. 4.0% for the cracked length in the right end span).

Box-girder bridge

- a cracked zone around P1 which starts at the abscissa x = 83.1 m (i.e. 7.7 % for the cracked length in the left end span) and which ends at the abscissa x = 98.1 m (i.e 6.7 % for the cracked length in the central span);
- a cracked zone around P2 which starts at the abscissa x = 183.5 m (i.e. 22.1 % for the cracked length in the central span) and which ends at the abscissa x = 217.8 m (i.e. 6.5 % for the cracked length in the central span).
- a cracked zone around P3 which starts at the abscissa x = 304.1 m (i.e. 21.6 % for the cracked length in the central span) and which ends at the abscissa x = 338.8 m (i.e. 7.3 % for the cracked length in the central span).
- a cracked zone around P3 which starts at the abscissa x = 444.4 m (i.e. 4.7 % for the cracked length in the central span) and which ends at the abscissa x = 457.8 m (i.e. 8.7 % for the cracked length in the right end span).

Most of these cracked zones are smaller than 15% of the span lengths, as it would have been directly considered by using the alternative simplified method of EN 1994-2.

They are assymmetric due to the choice made for the order for concreting the slab segments (see Figure 2-5 and Figure 2-11).

2.4.2.4 Shrinkage and cracked zones

During the second step of the global analysis, the cracked zones modify the introduction of the concrete shrinkage in the numerical model.

In fact the isostatic (or "primary") effect of shrinkage ($N_b = E_{cm}.\varepsilon_{cs}.A_b$ which is applied to the center of gravity of the concrete slab) is no longer applied in the cross-sections located in the cracked zones around internal supports (EN 1994-2, 5.4.2.2 (8)).

The « hyperstatic » or « secondary » effect of shrinkage is finally considered as the difference between the internal forces and moments calculated in the continuous girder by the elastic linear analysis under the action of the isostatic effects of shrinkage, and the isostatic effects themselves (see Figure 2-29).

2.4.2.5 Organisation of the global analysis calculations

Figure 2-28 shows the sequence considered for the longitudinal bending calculations in the example. This especially includes the changes of cross sectional properties of the cross-sections following the successive introduction of the load cases into the model with respect to the adopted construction phases.

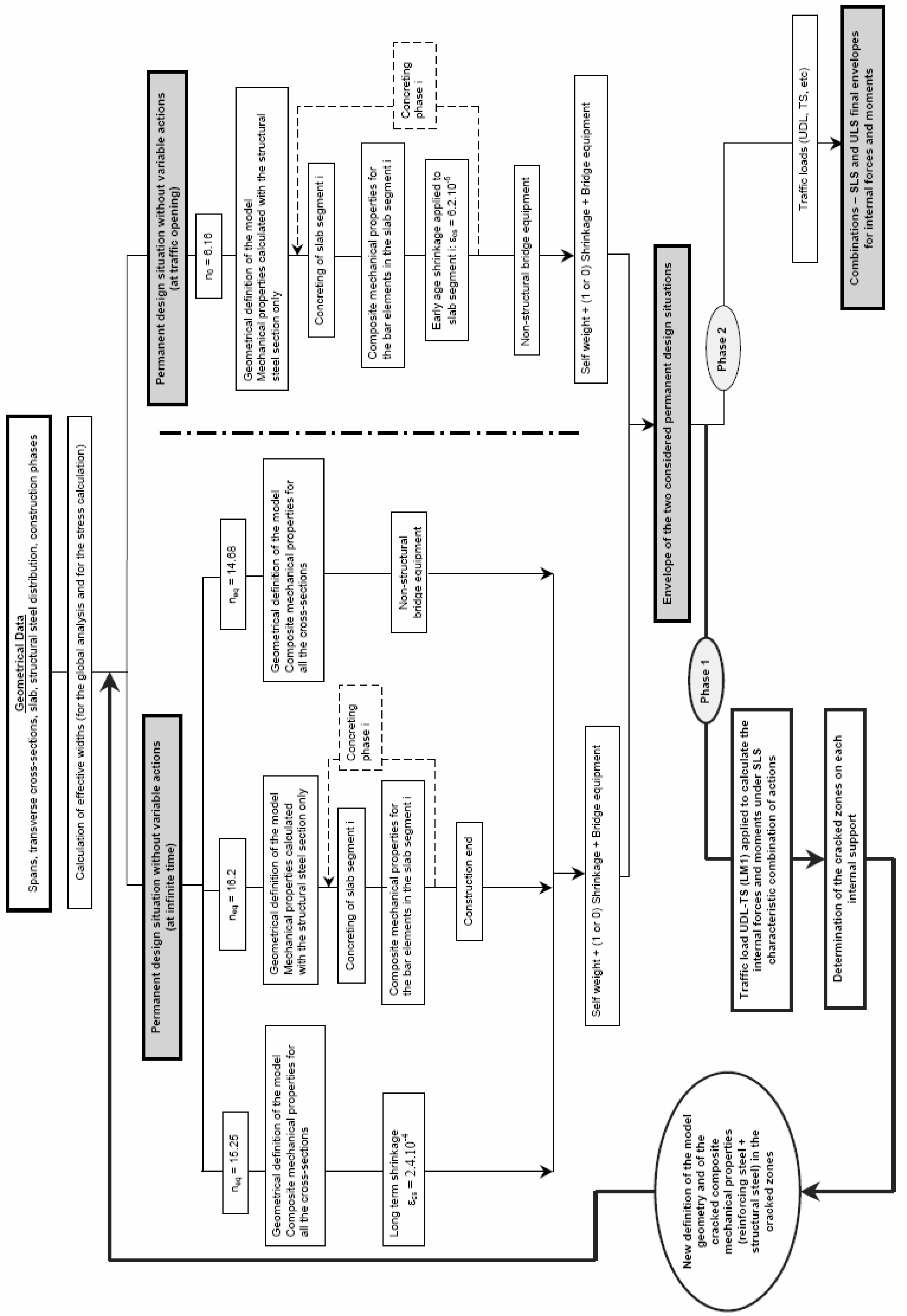
Geometrical Data
Spans, transverse cross-sections, slab, structural steel distribution, construction phases
Calculation of effective widths (for the global analysis and for the stress calculation)
Permanent design situation without variable actions (at infinite time)
n_{eq} = 16.2
Geometrical definition of the model Mechanical properties calculated with the structural steel section only
Concreting phase i
Concreting of slab segment i
Composite mechanical properties for the bar elements in the slab segment i
Construction end
n_{eq} = 14.88
Geometrical definition of the model Composite mechanical properties for all the cross-sections
Non-structural bridge equipment
n_{eq} = 15.25
Geometrical definition of the model Composite mechanical properties for all the cross-sections
Long term shrinkage $\varepsilon_{cs} = 2.4.10^{-4}$
Self weight + (1 or 0) Shrinkage + Bridge equipment
Permanent design situation without variable actions (at traffic opening)
n_0 = 6.16
Geometrical definition of the model Mechanical properties calculated with the structural steel section only
Concreting phase i
Concreting of slab segment i
Composite mechanical properties for the bar elements in the slab segment i
Early age shrinkage applied to slab segment i: $\varepsilon_{cs} = 6.2.10^{-5}$
Non-structural bridge equipment
Self weight + (1 or 0) Shrinkage + Bridge equipment
Envelope of the two considered permanent design situations
Phase 1
Traffic load UDL-TS (LM1) applied to calculate the internal forces and moments under SLS characteristic combination of actions
Determination of the cracked zones on each internal support
New definition of the model geometry and of the cracked composite mechanical properties (reinforcing steel + structural steel) in the cracked zones
Phase 2
Traffic loads (UDL, TS, etc)
Combinations – SLS and ULS final envelopes for internal forces and moments

Figure 2-28: Global analysis organisation chart.

2.4.2.6 Results

2.4.2.6.1 Twin-girder bridge

Figure 2-29 to Figure 2-32 present a few results of internal forces and moments coming from the global analysis of the twin-girder bridge.

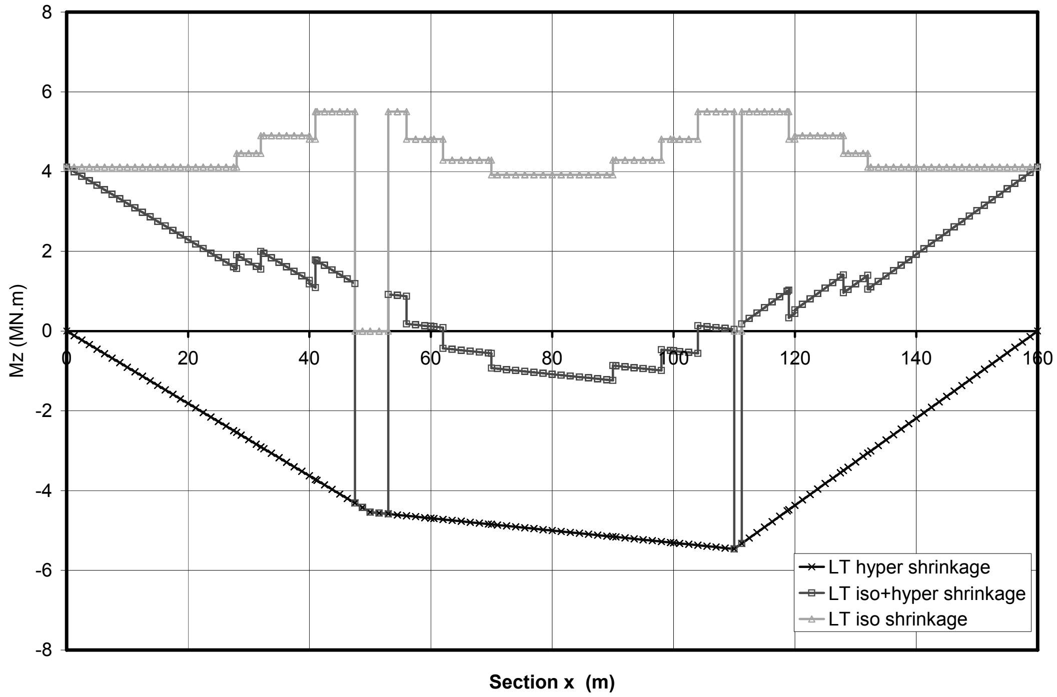

Figure 2-29: Isostatic and hyperstatic bending moments due to the long-term concrete shrinkage for the twin-girder bridge.

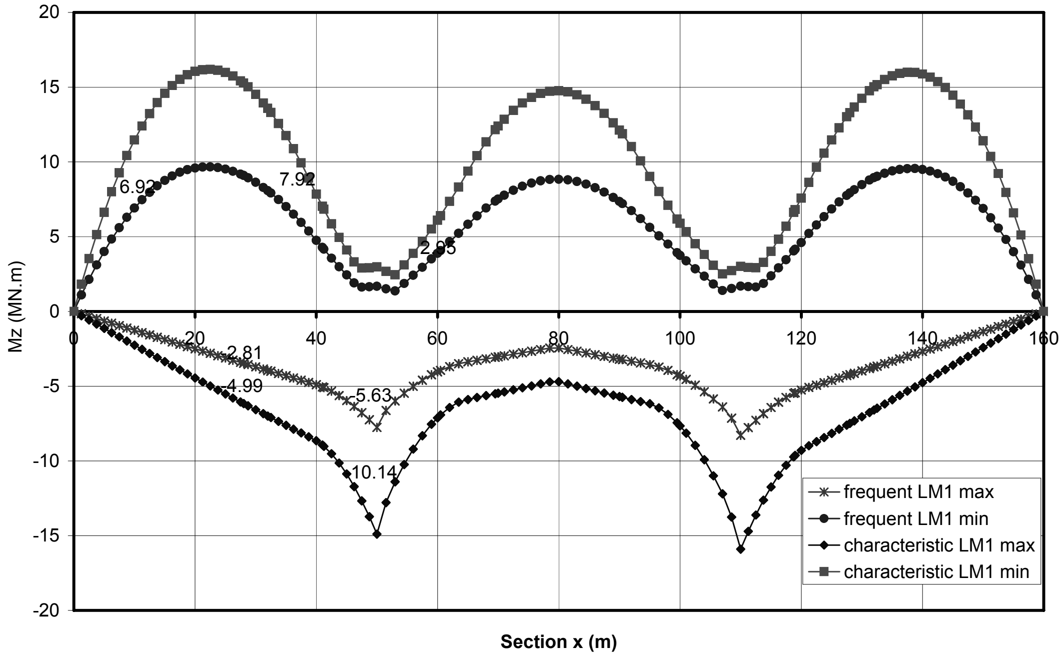

Figure 2-30: Bending moments under the uniformly distributed load and tandem traffic load (frequent and characteristic LM1) for the twin-girder bridge.

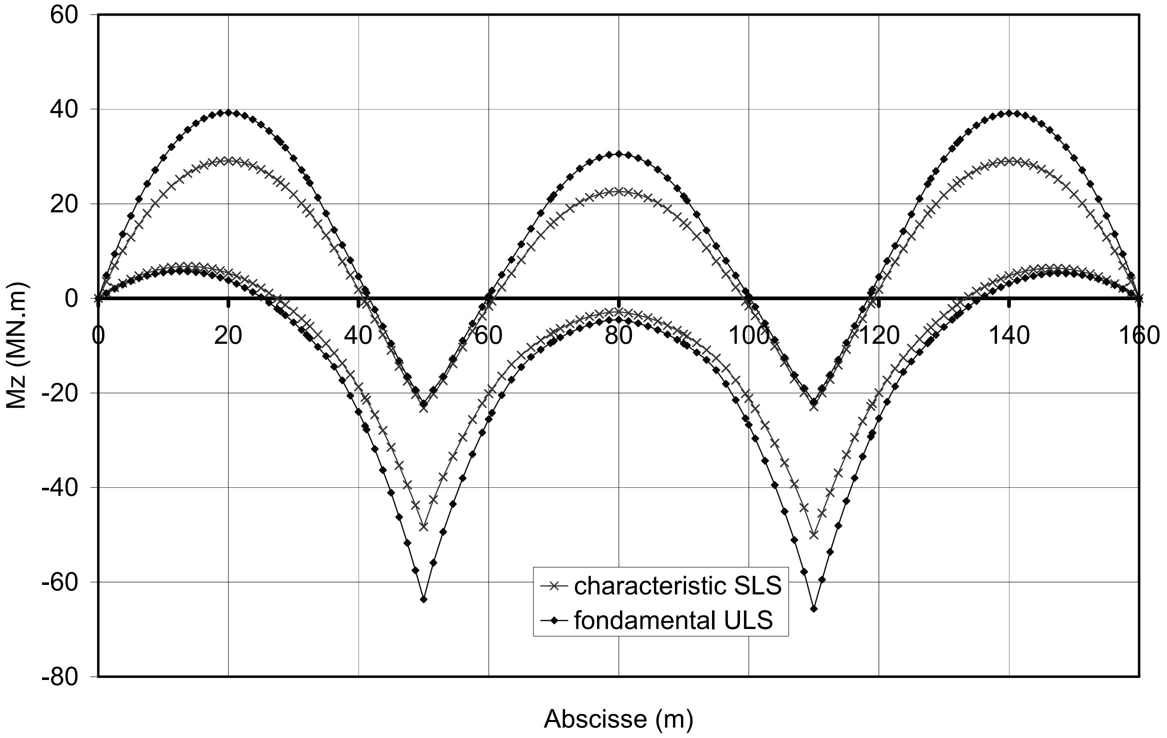

Figure 2-31: Bending moments under the fundamental ULS and characteristic SLS combinations of actions for the twin-girder bridge.

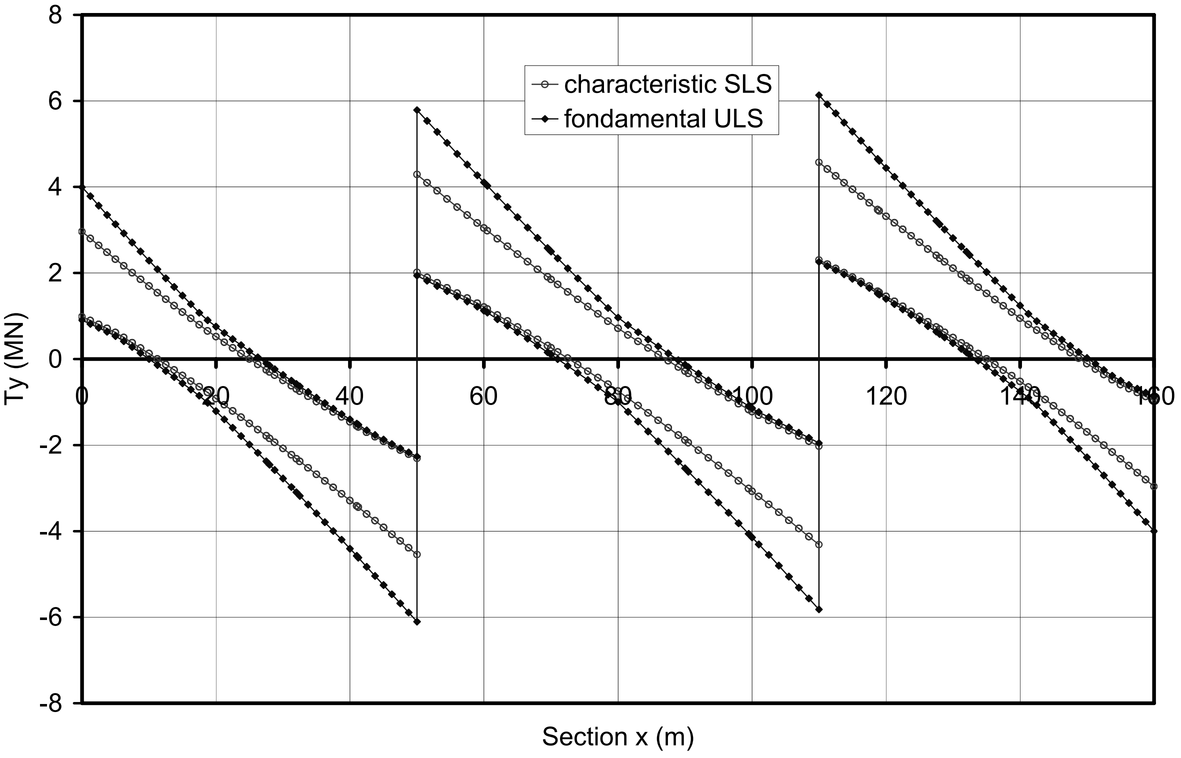

Figure 2-32: Shear forces under the fundamental ULS and characteristic SLS combinations of actions for the twin-girder bridge.

2.4.2.6.2 Box-girder bridge

Figure 2-33 to Figure 2-37 present a few results of internal forces and moments coming from the global analysis of the box-girder bridge.

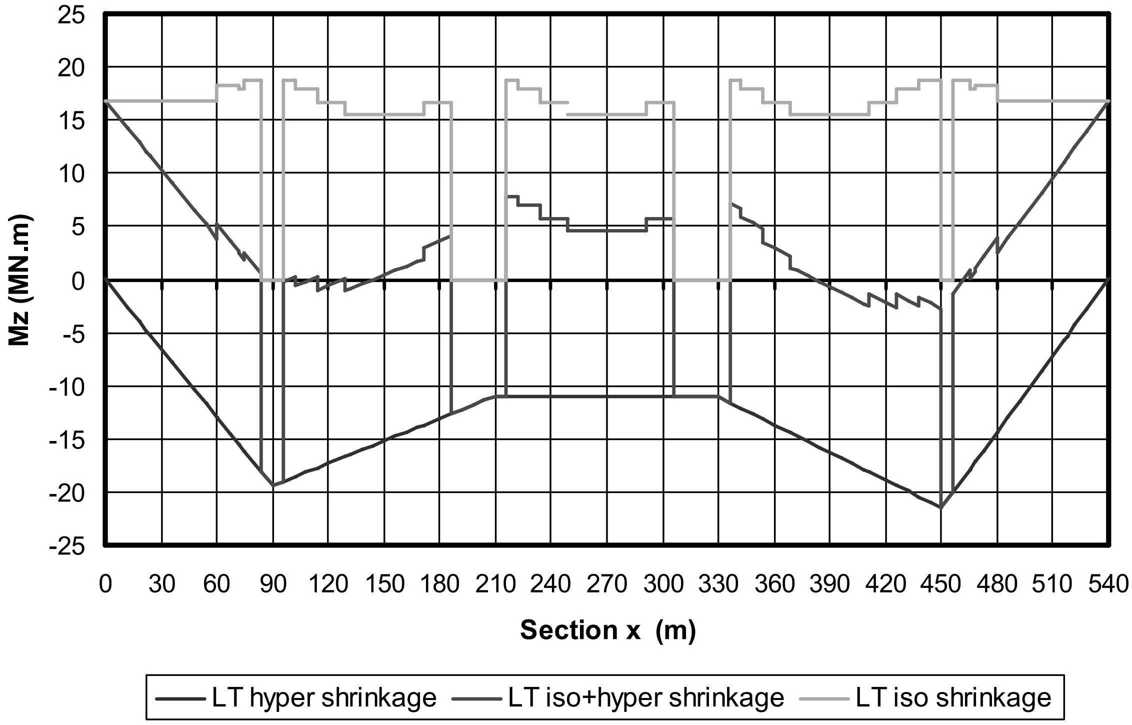

Figure 2-33: Isostatic and hyperstatic bending moments due to the long-term concrete shrinkage for the box-girder bridge.

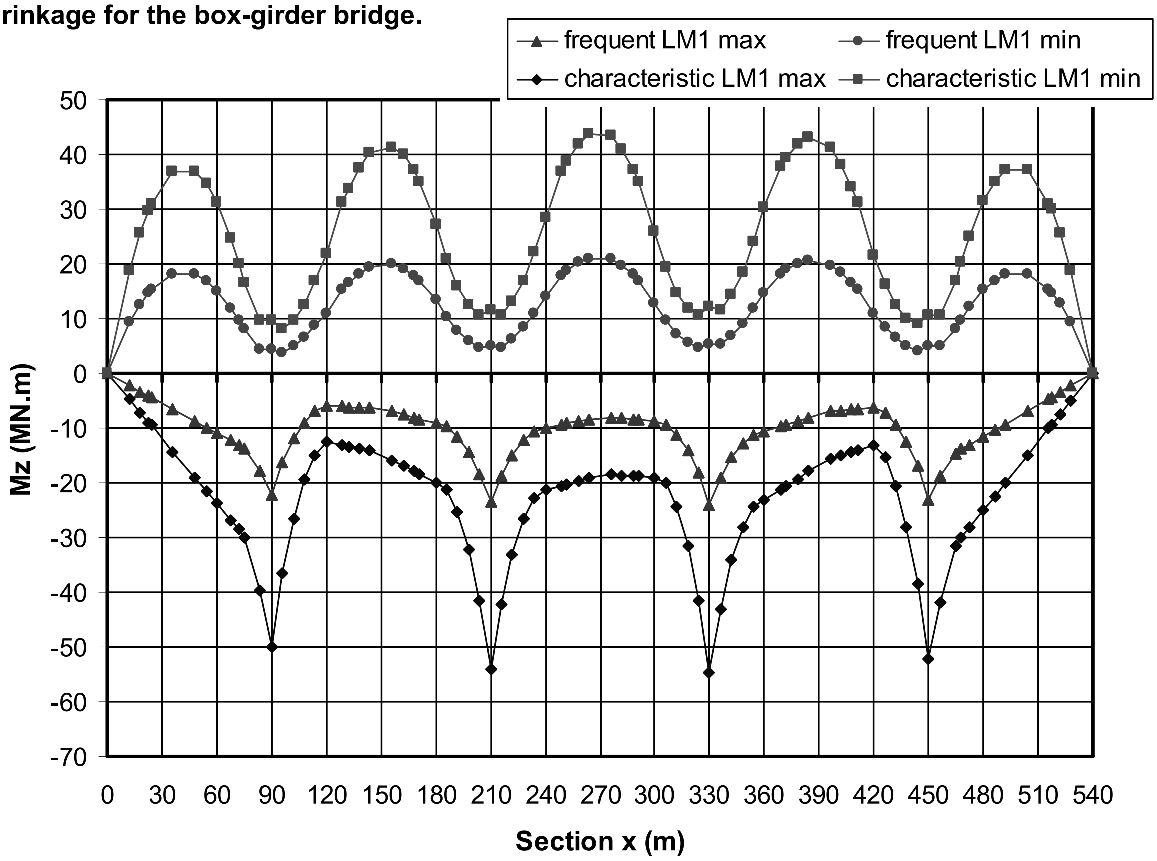

Figure 2-34: Bending moments under the uniformly distributed load and tandem traffic load (frequent and characteristic LM1) for the box-girder bridge

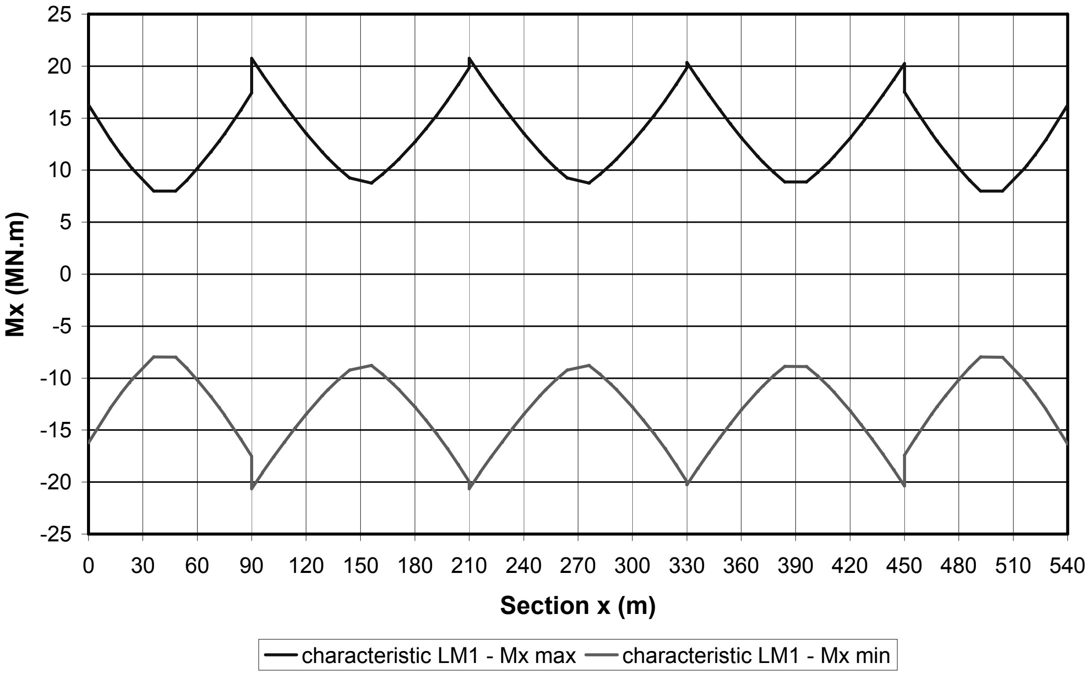

Figure 2-35: Torque under characteristic LM1 for the box-girder bridge.

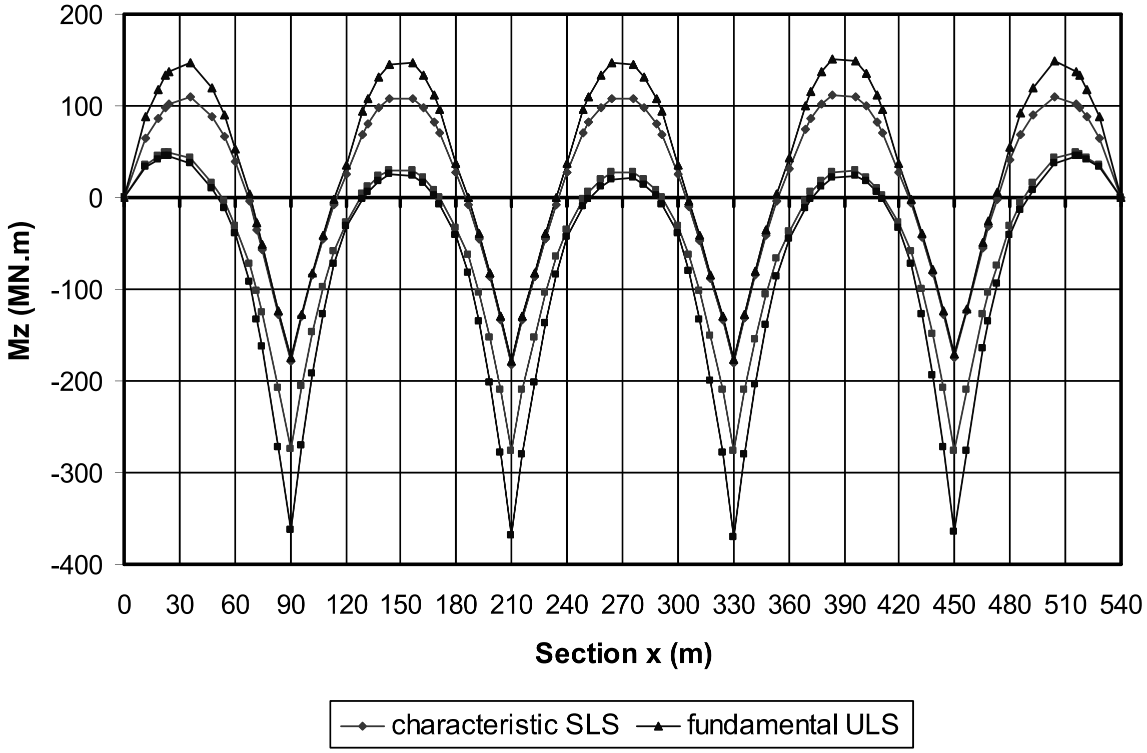

Figure 2-36: Bending moments under the fundamental ULS and characteristic SLS combinations of actions for the box-girder bridge.

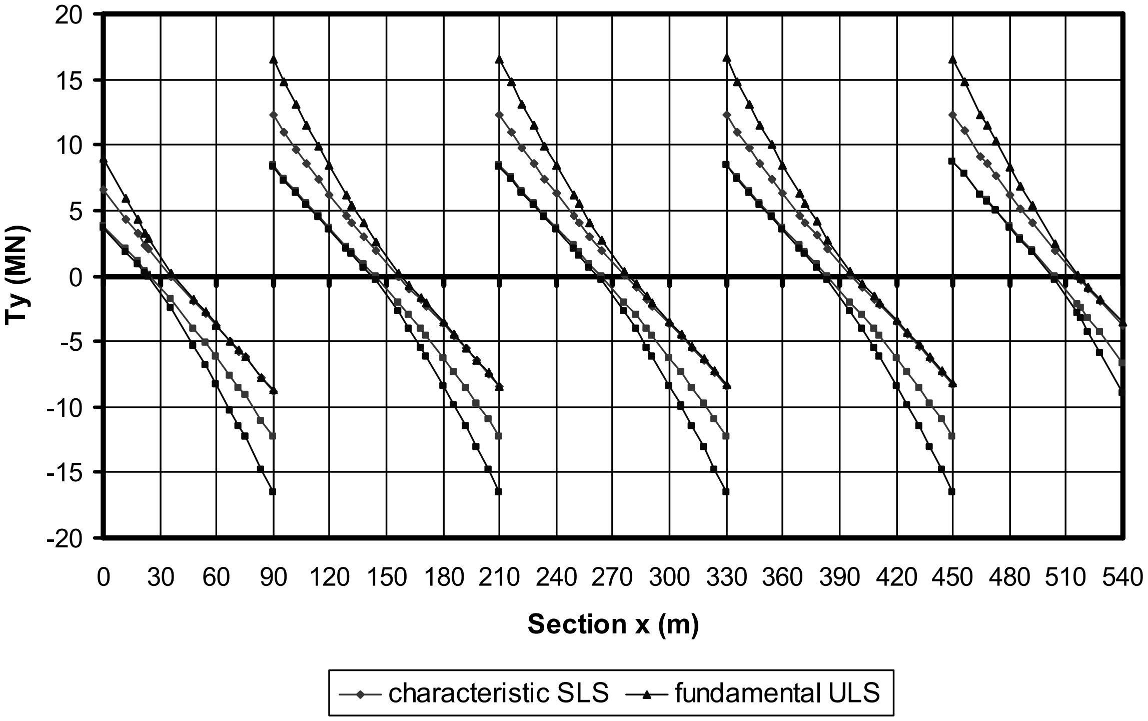

Figure 2-37: Shear forces under the fundamental ULS and characteristic SLS combinations of actions for the box-girder bridge.

3 Cross-section verifications

3.1 Twin-girder bridge

3.1.1 General

According to the location of the vertical stiffeners of the twin-girder bridge (see Figure 3-1) and the shape of the bending moment and shear diagrams at ULS (see Figure 2-31 and Figure 2-32), the different critical sections to check are displayed in Figure 3-2:

- At the end support C0, see Section 3.1.2
- At mid-span C0-P1, see Section 3.1.3
- At mid-span P1-P2, see Section 3.1.4
- At the internal support P2, see Section 3.1.5

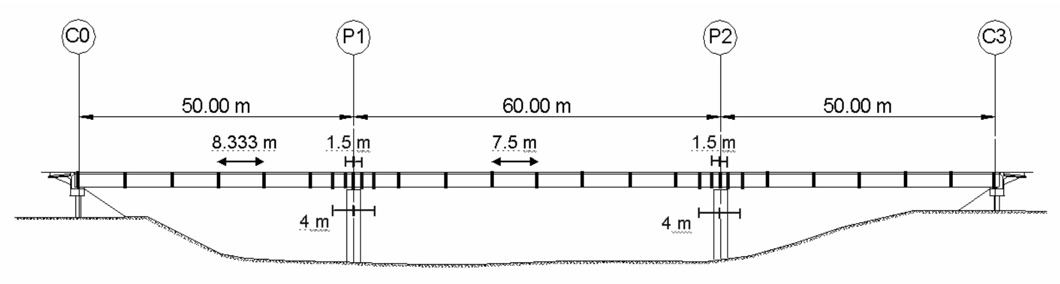
C0
P1
P2
C3
50.00 m
60.00 m
50.00 m
8.333 m
1.5 m
7.5 m
1.5 m
4 m
4 m

Figure 3-1: Position of vertical stiffeners of the twin-girder bridge.

For each critical section, the verification is done on a panel which is located between two vertical stiffeners. For the internal support P2, the three subpanels shown in Figure 3-3 must be checked.

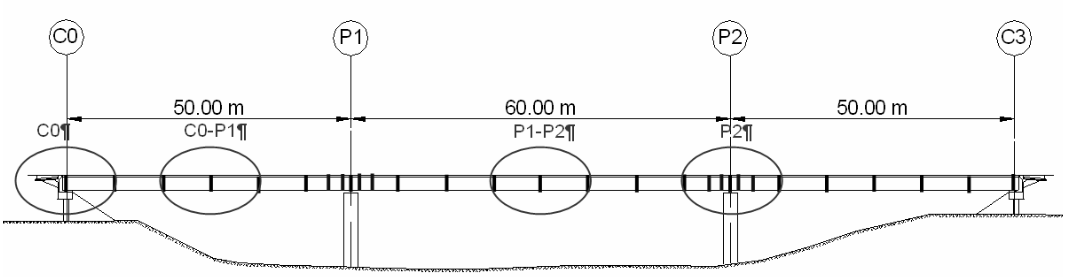
C0
P1
P2
C3
50.00 m
60.00 m
50.00 m
C0¶
C0-P1¶
P1-P2¶
P2¶

Figure 3-2: Checked sections of the twin-girder bridge.

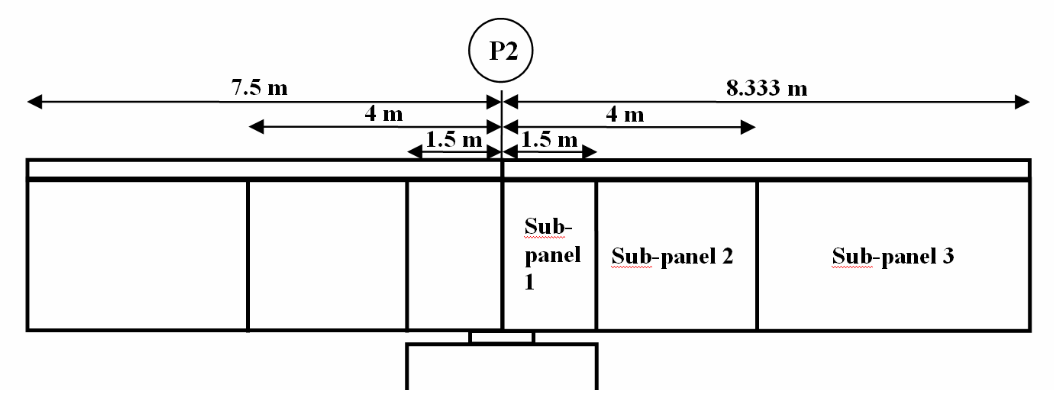
P2
7.5 m
8.333 m
4 m
4 m
1.5 m
1.5 m
Sub-panel 1
Sub-panel 2
Sub-panel 3

Figure 3-3: Different subpanels on the internal support P2.

3.1.2 Check of cross-section at the end support C0

3.1.2.1 Geometry

At end support C0 at ULS the concrete slab is in compression over its whole height. Its contribution is therefore taken into account in the cross-section resistance.

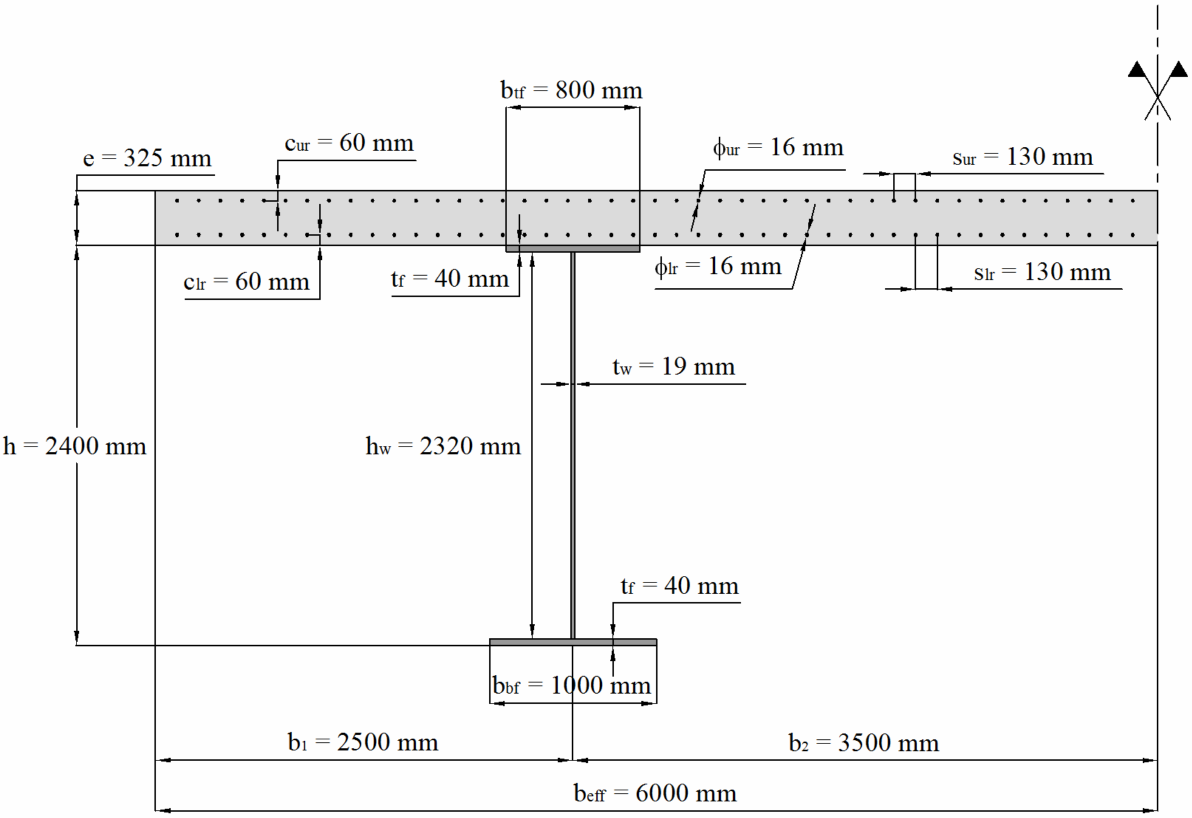
btf = 800 mm
e = 325 mm
cur = 60 mm
φur = 16 mm
sur = 130 mm
clr = 60 mm
tf = 40 mm
φlr = 16 mm
slr = 130 mm
tw = 19 mm
h = 2400 mm
hw = 2320 mm
tf = 40 mm
bbf = 1000 mm
b1 = 2500 mm
b2 = 3500 mm
beff = 6000 mm

Figure 3-4: Cross-section at the end support C0.

General properties of the twin-girder bridge in cross-section C0	**Main areas of the different parts of the composite section**
$L_1 = 50$ m $a = 8.333$ m $h = 2400$ mm $t_w = 19$ mm $b_{tf} = 800$ mm $b_{bf} = 1000$ mm $t_f = 40$ mm $h_w = h - 2t_f = 2.32$ m $e = 32.5$ cm $\phi_{ur} = 16$ mm $\phi_{lr} = 16$ mm $s_{ur} = 130$ mm $s_{lr} = 130$ mm $c_{ur} = 60$ mm $c_{lr} = 60$ mm $b_{eff} = 6$ m $n_{ur} = \frac{b_{eff}}{s_{ur}} = 46.154$ $n_{lr} = \frac{b_{eff}}{s_{lr}} = 46.154$	$A_{atf} = t_{tf} b_{tf} = 0.032$ m² $A_{aw} = t_w h_w = 0.044$ m² $A_{abf} = t_{bf} b_{bf} = 0.04$ m² $A_a = A_{atf} + A_{aw} + A_{abf} = 0.107$ m² $A_{sur} = \frac{\pi d_{ur}^2}{4} = 2.011$ cm² $A_{tsur} = n_{ur} A_{sur} = 92.816$ cm² $A_{slr} = \frac{\pi d_{lr}^2}{4} = 2.011$ cm² $A_{tslr} = n_{lr} A_{slr} = 92.816$ cm² $A_{cur} = c_{ur} b_{eff} = 0.36$ m² $A_{clur} = \left(e - c_{ur} - c_{lr}\right) b_{eff} = 1.23$ m² $A_{clr} = c_{lr} b_{eff} = 0.36$ m² $A_c = e b_{eff} = A_{cur} + A_{clur} + A_{clr} = 1.95$ m² (see notation and Figure 3-4)

3.1.2.2 Material properties

Structural steel

f_{yw} = 345 N/mm² because 16 mm < t_f = 19 mm ≤ 40 mm (see Table 2-4)

$$\varepsilon_w = \sqrt{\frac{235 N/mm^2}{f_{yw}}} = 0.825$$

f_{yf} = 345 N/mm² because 16 mm < t_f = 40 mm ≤ 40 mm (see Table 2-4)

$$\varepsilon_f = \sqrt{\frac{235 N/mm^2}{f_{yf}}} = 0.825$$

$$f_{ydw} = \frac{f_{yw}}{\gamma_{M0}} = 345 \text{ N/mm}^2$$

$$f_{ydf} = \frac{f_{yf}}{\gamma_{M0}} = 345 \text{ N/mm}^2$$

$E_a = 210000$ N/mm²

EN 1994-2, 5.5.2(1), Classification of composite sections without concrete encasement

A steel compression flange that is restrained from buckling by effective attachment to a concrete flange by shear connectors may be assumed to be in Class 1 if the spacing of connectors is in accordance with 6.6.5.5.

EN 1994-2, 6.6

Concrete

f_{ck} = 35 N/mm²

$$f_{cd} = \frac{f_{ck}}{\gamma_c} = 23.333 \text{ N/mm²}$$

E_{cm} = 34077 N/mm²

$$n = \frac{E_a}{E_{cm}} = \frac{210000}{34077} = 6.163$$

Reinforcement

f_{sk} = 500 N/mm²

$$f_{sd} = \frac{f_{sk}}{\gamma_s} = 434.734 \text{ N/mm2}$$

$E_s = E_a$ = 210000 N/mm²

3.1.2.3 Internal forces and moments

The internal forces and moments in this cross-section are (see Figure 2-31 and Figure 2-32):

M_{Ed} = 26.156 MNm (at the end of the panel a = 8.333 m: x = 8.333 m)

V_{Ed} = 3.977 MN (at the support C0: x = 0 m)

3.1.2.4 Determination of the cross-section class

- Bottom flange is in tension: no buckling problem
- Top flange is composite and connected to the slab following the recommendations of EN 1994-2, 6.6: Class 1
- To classify the steel web, the position of the Plastic Neutral Axis (PNA) is determined as:
  - Design plastic resistance of the concrete in compression:

    $$N_c = 0.85.A_c \frac{f_{ck}}{\gamma_c} = 38.675 \text{ MN}$$

  - Design plastic resistance of the structural steel top flange:

    $$N_{atf} = A_{atf} \frac{f_{yf}}{\gamma_{M0}} = 11.04 \text{ MN}$$

  - Design plastic resistance of the structural steel web:

    $$N_{aw} = A_{aw} \frac{f_{yw}}{\gamma_{M0}} = 15.208 \text{ MN}$$

  - Design plastic resistance of the structural steel bottom flange:

    $$N_{abf} = A_{abf} \frac{f_{yf}}{\gamma_{M0}} = 13.8 \text{ MN}$$

  - Design plastic resistance of the structural steel:

    $$N_a = N_{atf} + N_{aw} + N_{abf} = 40.048 \text{ MN}$$

Relations to find the location of the Plastic Neutral Axis (PNA) under positive moment $M_{Pl,Rd}$

RELATIONS	PNA LOCATION
$N_{abf} \geq N_{aw} + N_{atf} + N_c$	PNA in the bottom flange
$N_{abf} + N_{aw} \geq N_{aft} + N_c$ and $N_{abf} < N_{aw} + N_{atf} + N_c$	PNA in the web
$N_a \geq N_c$ and $N_{abf} + N_{aw} < N_{atf} + N_c$	PNA in the top flange
$N_a \geq N_{cur} + N_{clur}$ and $N_a < N_c$	PNA in the slab under lower reinforcements
$N_a + N_{sl} \geq N_{cur}$ and $N_a + N_{sl} < N_{cur} + N_{clur}$	PNA in the slab between reinforcements
$N_a + N_{sl} + N_{su} < N_{cur}$	PNA in the slab above upper reinforcements

EN 1994-2, 6.2.1.2(1), Plastic resistance moment $M_{pl,Rd}$ of a composite cross-section

(1) The following assumptions should be made in the calculation of $M_{pl,Rd}$:

a) there is full interaction between structural steel, reinforcement, and concrete;

b) the effective area of the structural steel member is stressed to its design yield strength f_{yd} in tension or compression;

c) the effective areas of longitudinal reinforcement in tension and in compression are stressed to their design yield strength f_{sd} in tension or compression. Alternatively, reinforcement in compression in a concrete slab may be neglected;

d) the effective area of concrete in compression resists a stress of 0.85 f_{cd}, constant over the whole depth between the plastic neutral axis and the most compressed fibre of the concrete, where f_{cd} is the design cylinder compressive strength of concrete.

Typical plastic stress distributions are shown in Figure 6.2.

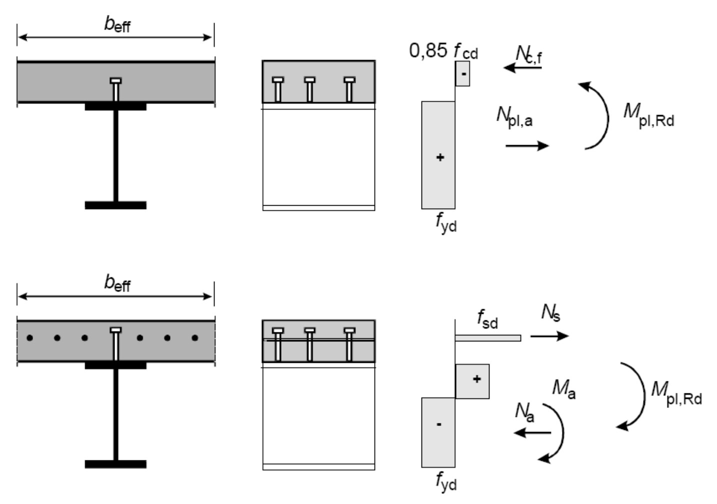

Figure 6.2: Examples of plastic stress distributions for a composite beam with a solid slab and full shear connection in sagging and hogging bending

- Design plastic resistance of the concrete in compression located above upper reinforcements:

$$N_{cur} = 0.85.A_{cur}\frac{f_{ck}}{\gamma_c} = 7.14 \text{ MN}$$

- Design plastic resistance of the concrete in compression located between reinforcements:

$$N_{clur} = 0.85.A_{clur}\frac{f_{ck}}{\gamma_c} = 24.395 \text{ MN}$$

- Design plastic resistance of the concrete in compression located under lower reinforcements:

$$N_{clr} = 0.85.A_{clr}\frac{f_{ck}}{\gamma_c} = 7.14 \text{ MN}$$

- Design plastic resistance of the lower steel reinforcements:

$$N_{sl} = A_{tslr}\frac{f_{sk}}{\gamma_s} = 4.035 \text{ MN}$$

- Design plastic resistance of the upper steel reinforcements:

$$N_{su} = A_{tsur}\frac{f_{sk}}{\gamma_s} = 4.035 \text{ MN}$$

- Location of the Plastic Neutral Axis (PNA):

  $N_a = 40.048$ MN $\geq N_c = 38.675$ MN

  and $N_{abf} + N_{aw} = 29.008$ MN$< N_{atf} + N_c = 49.715$ MN.

  Thus, the PNA is deduced to be located in the top flange at a distance z_{pl} from the extreme lower fibre of the bottom flange. Writing the force equilibrium around the PNA:

$$z_{pl} = h - e - \frac{N_a}{0.85 b_{eff} f_{cd}} = 2.398 \text{ m}$$

  As the PNA is located in the top flange, the whole web is in tension and therefore in Class 1.

Conclusion: the cross-section at the external support C0 and C3 is in class 1 and is checked by a plastic section analysis.

3.1.2.5 Plastic section analysis

3.1.2.5.1 Bending resistance check

The design plastic resistance moment is calculated from the position of the PNA:

$M_{pl,Rd} = 57.597$ MNm

Reinforcement in compression in the concrete slab is neglected according EN 1994-2, 6.2.1.2(1).

$M_{Ed} = 26.156 \text{ MNm} \leq M_{pl,Rd} = 57.597$ MNm

⇒ **Bending resistance is verified!**

EN 1993-1-5, 5.1(2)

Plates with h_w/t greater than $\frac{\eta}{72}\varepsilon$ for an unstiffened web, or $\frac{31}{\eta}\varepsilon\sqrt{k_\tau}$ for a stiffened web, should be checked for resistance to shear buckling and should be provided with transverse stiffeners at the supports, where $\varepsilon = \sqrt{\frac{235}{f_y[N/mm^2]}}$.

EN 1994-2-5, 6.2.2, Resistance to vertical shear

EN 1993-1-5, 6.2.6, Shear

(2) In the absence of torsion the design plastic shear resistance is given by:

$$V_{pl,Rd} = \frac{A_v f_y}{\sqrt{3}\gamma_{M0}}$$

where A_v is the shear area.

(3) The shear area A_v may be taken as follows:

d) for welded I, H and box sections, load parallel to web : $A_V = \eta\sum\left(h_w t_w\right)$

where h_w is the depth of the web; t_w is the web thickness.

EN 1993-1-5, 5.2(1), Design Resistance

For unstiffened or stiffened webs the design resistance for shear should be taken as:

$$V_{b,Rd} = V_{bw,Rd} + V_{bf,Rd} \le \frac{\eta f_{yw}}{\sqrt{3}\gamma_{M1}} h_w t_w \tag{5.1}$$

in which the contribution from the web is given by:

$$V_{bw,Rd} = \frac{\chi_w f_{yw} h_w t_w}{\sqrt{3}\gamma_{M1}} \tag{5.2}$$

and the contribution from the flanges $V_{bf,Rd}$ is according to 5.4.

Comments on the assessment of k_τ: k_τ is the critical coefficient giving the critical shear stress of the plate through the relation:

$$\tau_{cr} = k_\tau\,\sigma_E \qquad \textit{with:} \qquad \sigma_E = \frac{\pi^2\,E}{12\,(1-\nu^2)}\frac{t^2}{b^2}$$

k_τ an be assessed by several ways, assuming the plate supported and free to rotate at its four edges:

- *using Kloppel und Sheer charts*
- *using EBPlate software*
- *using the Annex A of EN 1993-1-5 as follows*

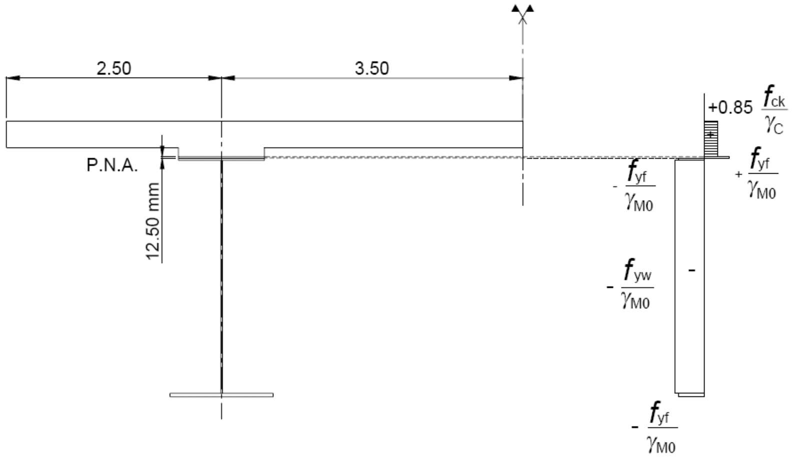

Figure 3-5: Design Plastic resistance moment at external support C0.

3.1.2.5.2 Shear resistance check

The web should be checked in terms of shear buckling if:

- $\frac{h_w}{t_w} > \frac{72}{\eta}\varepsilon_w$ for an unstiffened web
- $\frac{h_w}{t_w} > \frac{31}{\eta}\varepsilon_w\sqrt{k_\tau}$ for a stiffened web

In this example, the web is stiffened by intermediate vertical stiffeners.

Comments: *The stiffening considered here above is provided by intermediate stiffeners. Longitudinal stiffeners are not considered. The web is stiffened at supports.*

A beam stiffened by vertical stiffeners only at its supports should be considered as having an unstiffened web to apply this previous criterion.

The vertical stiffeners at the bracing transverse frames which border the webpanel adjacent to the support C0 and located in span C0-P1, are assumed to be rigid (to be checked by using Section 9 of EN1993-1-5). They are equally spaced by a = 8.333 m.

$k_{\tau st} = 0$ because there is no longitudinal stiffeners

$a/h_w = 3.592 \geq 1$

$$k_\tau = 5.34 + 4\left(\frac{h_w}{a}\right)^2 + k_{\tau st} = 5.65$$

$\frac{h_w}{t_w} = 122.105 > \frac{31}{\eta}\varepsilon_w\sqrt{k_\tau} = 50.679$ then the web should be checked in terms of shear buckling.

The maximum design shear resistance is given by $V_{Rd} = min\ (V_{b,Rd};\ V_{pl,a,Rd})$

$$\text{where } V_{b,Rd} = V_{bw,Rd} + V_{bf,Rd} = \frac{\chi_w f_{yw} h_w t_w}{\sqrt{3}\gamma_{M1}} + \frac{b_f t_f^2 f_{yf}}{c\gamma_{M1}}\left(1 - \left(\frac{M_{Ed}}{M_{f,Rd}}\right)^2\right) \leq \frac{\eta f_{yw} h_w t_w}{\sqrt{3}\gamma_{M1}} = 9.578 \text{ MN}$$

$$V_{pl,a,Rd} = \frac{\eta f_{yw}}{\sqrt{3}\gamma_{M0}} h_w t_w = 10.536 \text{ MN}$$

where η = 1.2 for steel grades up to and including S460

EN 1993-1-5, Annex A3, Shear buckling coefficients

(1) For plates with rigid transverse stiffeners and without longitudinal stiffeners or with more than two longitudinal stiffeners, the shear buckling coefficient k_τ can be obtained as follows:

$$k_\tau = 5.34 + 4\left(\frac{h_w}{a}\right)^2 + k_{\tau st} \text{ when } a/h_w \geq 1$$

$$k_\tau = 4 + 5.34\left(\frac{h_w}{a}\right)^2 + k_{\tau st} \text{ when } a/h_w < 1$$

$$\text{where} \quad k_{\tau st} = 9\left(\frac{h_w}{a}\right)^2 \sqrt[4]{\left(\frac{I_{sl}}{t^3 h_w}\right)^3} \text{ but not less than } k_{\tau st} = \frac{2{,}1}{t}\sqrt[3]{\left(\frac{I_{sl}}{h_w}\right)}$$

a is the distance between transverse stiffeners (see Figure 5.3);

I_{sl} is the second moment of area of the longitudinal stiffener about the z-axis, see Figure 5.3 (b). For webs with two or more longitudinal stiffeners, not necessarily equally spaced, I_{sl} is the sum of the stiffness of the individual stiffeners.

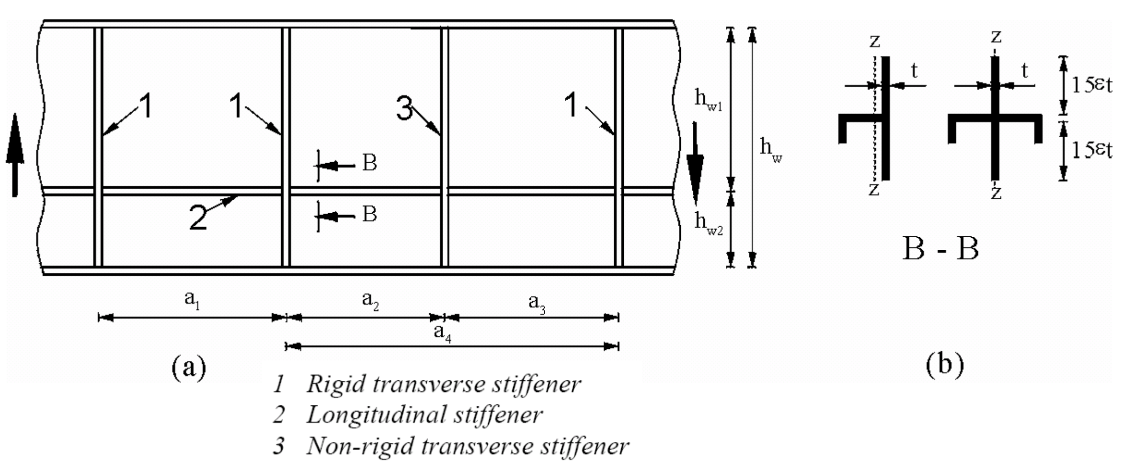

Figure 5.3: Web with transverse and longitudinal stiffeners

EN 1993-1-5, 5.3(3)

(3) The slenderness parameter λ_w may be taken as follows (for transverse stiffeners at supports and intermediate transverse or longitudinal stiffeners or both):

$$\bar{\lambda}_w = \frac{h_w}{37.4 t_w \varepsilon_w \sqrt{k_\tau}}$$

EN 1993-1-5, 5.3(1)

(1) For webs with transverse stiffeners at supports only and for webs with either intermediate transverse stiffeners or longitudinal stiffeners or both, the factor χ_w for the contribution of the web to the shear buckling resistance should be obtained from Table 5.1.

Table 5.1: Contribution from the web χ_w to shear buckling resistance

	Rigid end post	Non-rigid end post
$\bar{\lambda}_w < 0{,}83/\eta$	η	η
$0{,}83/\eta \leq \bar{\lambda}_w < 1{,}08$	$0{,}83/\bar{\lambda}_w$	$0{,}83/\bar{\lambda}_w$
$\bar{\lambda}_w \geq 1{,}08$	$1{,}37/(0{,}7+\bar{\lambda}_w)$	$0{,}83/\bar{\lambda}_w$

Contribution of the web Vbw,Rd

$$V_{bw,Rd} = \frac{\chi_w f_{yw} h_w t_w}{\sqrt{3}\gamma_{M1}}$$

$$\bar{\lambda}_w = \frac{h_w}{37.4 t_w \varepsilon_w \sqrt{k_\tau}} = 1.664 \geq 1.08$$

$$\Rightarrow \qquad \chi_w = \frac{1.37}{\left(0.7 + \bar{\lambda}_w\right)} = 0.579$$

$$V_{bw,Rd} = \frac{\chi_w f_{yw} h_w t_w}{\sqrt{3}\gamma_{M1}} = 4.625 \text{ MN}$$

Contribution from the flanges $V_{bf,Rd}$

$$V_{bf,Rd} = \frac{b_f t_f^2 f_{yf}}{c\gamma_{M1}}\left(1 - \left(\frac{M_{Ed}}{M_{f,Rd}}\right)^2\right)$$

b_f and t_f are taken for the flange which provides the least axial resistance,

b_f being taken as not larger than $15 \cdot \varepsilon \cdot t_f$ on each side of the web,

The lower flange of the cross-section is a structural steel section whereas its upper flange is a composite section (structural steel + concrete slab + eventually reinforcing steel bars). The formulae for calculating $V_{bf,Rd}$ should be used with the lower steel flange properties.

EN 1993-1-5, 5.4(1), Contribution from flanges

(1) When the flange resistance is not completely utilized in resisting the bending moment ($M_{Ed} \leq M_{f,Rd}$), the contribution from the flanges should be obtained as follows:

$$V_{bf,Rd} = \frac{b_f t_f^2 f_{yf}}{c\gamma_{M1}}\left(1 - \left(\frac{M_{Ed}}{M_{f,Rd}}\right)^2\right) \qquad (5.8)$$

b_f and t_f are taken for the flange which provides the least axial resistance,

b_f being taken as not larger than 15εtf on each side of the web,

$M_{f,Rd} = \frac{M_{f,k}}{\gamma_{M0}} =$ is the moment of resistance of the cross-section consisting of the area of the effective composite flanges only,

$$c = a\left(0.25 + \frac{1.6 b_f t_f^2 f_{yf}}{t h_w^2 f_{yw}}\right)$$

EN 1994-2, 6.2.2.5(2)

(2) For the calculation of $M_{f,Rd}$ in EN 1993-1-5, 7.1(1) the design plastic resistance to bending of the effective composite section excluding the steel web should be used.

Relations to find the location of the Plastic Neutral Axis (PNA) under positive moment $M_{Pl,Rd}$

RELATIONS	PNA LOCATION
$N_{abf} \geq N_{aw} + N_{atf} + N_c$	PNA in the bottom flange
$N_{abf} + N_{aw} \geq N_{aft} + N_c$ and $N_{abf} < N_{aw} + N_{atf} + N_c$	PNA in the web
$N_a \geq N_c$ and $N_{abf} + N_{aw} < N_{atf} + N_c$	PNA in the top flange
$N_a \geq N_{cur} + N_{clur}$ and $N_a < N_c$	PNA in the slab under lower reinforcements
$N_a + N_{sl} \geq N_{cur}$ and $N_a + N_{sl} < N_{cur} + N_{clur}$	PNA in the slab between reinforcements
$N_a + N_{sl} + N_{su} < N_{cur}$	PNA in the slab above upper reinforcements

EN 1993-1-5, 7.1(1), Interaction between shear force, bending moment and axial force

(1) Provided that $\bar{\eta}_3$ (see below) does not exceed 0,5, the design resistance to bending moment and axial force need not be reduced to allow for the shear force. If $\bar{\eta}_3$ is more than 0,5 the combined effects of bending and shear in the web of an I or box-girder should satisfy:

$$\bar{\eta}_1 + \left[1 - \frac{M_{f,Rd}}{M_{pl,Rd}}\right]\left[2\bar{\eta}_3 - 1\right]^2 \leq 1 \text{ for } \bar{\eta}_1 \geq \frac{M_{f,Rd}}{M_{Pl,Rd}} \qquad (7.1)$$

where $M_{f,Rd}$ is the design plastic moment of resistance of the section consisting of the effective area of the flanges;

$M_{pl,Rd}$ is the design plastic resistance of the cross-section consisting of the effective area of the flanges and the fully effective web irrespective of its section class.

$$\bar{\eta}_1 = \frac{M_{Ed}}{M_{Pl,Rd}} \; ; \; \bar{\eta}_3 = \frac{V_{Ed}}{V_{bw,Rd}}$$

In addition the requirements in sections 4.6 and 5.5 should be met.

Action effects should include global second order effects of members where relevant.

The design plastic bending resistance $M_{f,Rd}$ of the cross-section consisting of the flanges only (structural steel flange + concrete slab + eventually reinforcing steel bars) should be first calculated. $M_{f,Rd}$ is calculated as $M_{pl,Rd}$ neglecting the web contribution.

To calculate $M_{f,Rd}$, the position of the Plastic Neutral Axis (PNA) is determined (by using the same definition than in Paragraph 3.1.2.4) as:

$$N_{abf} + N_{atf} + N_{sl} = 28.875 \text{ MN} \geq N_{cur} = 7.14 \text{ MN}$$

$$\text{and } N_{abf} + N_{atf} + N_{sl} = 28.875 \text{ MN} < N_{cur} + N_{clur} = 31.535 \text{ MN}$$

Thus the PNA is deduced to be located in the concrete slab between reinforcements at a distance z_{pl} from the extreme lower fiber of the bottom flange. Writing the force equilibrium around the PNA:

$$z_{pl} = h + e - \frac{N_{abf} + N_{atf} + N_{sl}}{0.85.b_{eff}f_{cd}} = 2.482 \text{ m}$$

The design plastic resistance moment of the flanges only is calculated from the position of the PNA: $M_{f,Rd} = 38.704$ MNm.

$$c = a\left(0.25 + \frac{1.6b_f t_f^2 f_{yf}}{t h_w^2 f_{yw}}\right) = 2.25\text{m}$$

$$V_{bf,Rd} = \frac{b_f t_f^2 f_{yf}}{c\gamma_{M1}}\left(1 - \left(\frac{M_{Ed}}{M_{f,Rd}}\right)^2\right) = 0.121 \text{ MN}$$

The contribution of the flanges $V_{bf,Rd}$ is negligible compared to contribution from the web. Then the contribution of the flanges may be neglected.

$$V_{b,Rd} = V_{bw,Rd} + V_{bf,Rd} = 4.625 + 0.121 = 4.746 \text{ MN} \leq \frac{\eta f_{yw} h_w t_w}{\sqrt{3}\gamma_{M1}} = 9.578 \text{ MN}$$

$$V_{Rd} = min\ (V_{b,Rd};\ V_{pl,a,Rd}) = min(4.746;\ 10.536) = 4.746 \text{ MN}$$

Cross section verification

The verification should be performed as follows:

$$V_{Ed} = 3.977 \text{ MN} \leq V_{Rd} = 4.746 \text{ MN}$$

$$\eta_3 = \frac{V_{Ed}}{V_{Rd}} = 0.838 \leq 1$$

⇒ **Shear resistance is verified!**

3.1.2.5.3 M-V-interaction

$$V_{Ed} = 3.977 \text{ MN} \geq 0.5\ V_{Rd} = 2.373 \text{ MN}$$

Therefore the M-V-interaction should be checked.

$$\frac{M_{Ed}}{M_{f,Rd}} = 0.676 \leq 1;\ \frac{V_{Ed}}{V_{bw,Rd}} = 0.86 \leq 1$$

$M_{Ed} < M_{f,Rd}$ so that according to EN 1993-1-5, 7.1(1), there is no interaction. It means that the flanges are enough to resist alone the bending moment so that the entire web can be used for the resistance to the shear force.

Then flanges of the steel girder take the bending moment and web of the steel beam takes shear force.

⇒ **There is no interaction.**

Further explanations on the determination of the cross-section class

See Paragraph 3.1.2.4, page 85f.

Further explanations on the bending resistance check

See Paragraph 3.1.2.5.1, page 87f.

Further explanations on the shear resistance check

See Paragraph 3.1.2.5.2, page 89ff.

3.1.3 Check of cross-section at mid-span C0-P1

3.1.3.1 Geometry

The geometry is the same as for the check of cross-section at external support C0 (see Paragraph 3.1.2.1.)

At mid-span C0-P1 at ULS the concrete slab is in compression over its whole height. Its contribution is therefore taken into account in the cross-section resistance.

The effective width of the slab is the same as for the check of cross-section at external support C0 (see Paragraph 3.1.2.1).

⇒ $b_{eff} = 6$ m

3.1.3.2 Material properties

See Paragraph 3.1.2.2.

3.1.3.3 Internal forces and moments

The bending moment and shear force in this cross-section are (see Figure 2-31 and Figure 2-32):

$M_{Ed} =$ 39.314 MNm (at a distance of 25 m of the external support C0: x = 25 m)

$V_{Ed} =$ 1.952 MN (at a distance of 20 m of the external support C0: x = 20 m)

The check is realised on the third panel located at mid-span CO-P1 (see Figure 3-2). In a safe way, maximum values of internal forces acting on this panel are used to check it.

3.1.3.4 Determination of the cross-section class

The Class of section is the same as for the check of cross-section at external support C0 (see Paragraph 3.1.2.1.)

Conclusion: the cross-section at mid-span C0-P1 and P2-C3 is in class 1 and is checked by a plastic section analysis.

3.1.3.5 Plastic section analysis

3.1.3.5.1 Bending resistance check

As the geometry of the section at mid-span C0-P1 is the same as in C0, $M_{pl,Rd}$ does not change:

$M_{pl,Rd} = 57.597$ MNm

Reinforcement in compression in the concrete slab is neglected according to EN 1994-2, 6.2.1.2(1).

$M_{Ed} = 39.314 \text{ MNm} \leq M_{pl,Rd} = 57.597 \text{ MNm}$

⇒ **Bending resistance is verified!**

3.1.3.5.2 Shear resistance check

As the geometry of the section at mid-span C0-P1 is the same as in C0, $V_{bw,\,Rd}$ does not change:

$V_{bw,\,Rd} = 4.625$ MN

On the contrary, as $V_{bf,\,Rd}$ is a function of M_{Ed} and because M_{Ed} changes:

Further explanations on the M-V-interaction

See Paragraph 3.1.2.5.3, page 93.

$$M_{f,\,Rd} = 38.704 \text{ MN} \Rightarrow \frac{M_{Ed}}{M_{f,Rd}} = 1.016 \geq 1 \Rightarrow V_{bf,\,Rd} = 0 \text{ MN} \leq \frac{\eta f_{yw} h_w t_w}{\sqrt{3}\gamma_{M1}} = 9.578 \text{ MN}$$

Then:

$$V_{Rd} = V_{bw,\,Rd} = 4.625 \text{ MN}$$

Cross-section verification

The verification should be performed as follows:

$V_{Ed} = 1.952$ MN ≤ $V_{Rd} = min\ (4.625;\ 10.536) = 4.625$ MN is verified.

$$\eta_3 = \frac{V_{Ed}}{V_{Rd}} = 0.422 \leq 1$$

⇒ **Shear resistance is verified!**

3.1.3.5.3 M-V-interaction

$V_{Ed} = 1.952 \text{ MN} \leq 0.5 \cdot V_{Rd} = 2.318 \text{ MN}$

⇒ **There is no need to check the M-V-interaction.**

3.1.4 Check of cross-section at mid-span P1-P2

3.1.4.1 Geometry

At mid-span P1-P2 at ULS the concrete slab is almost in compression over its whole height. Its contribution is therefore taken into account in the cross-section resistance. The values in **bold** are the values which only change compared to the check of the cross-section at external support C0, see Section 3.1.2.

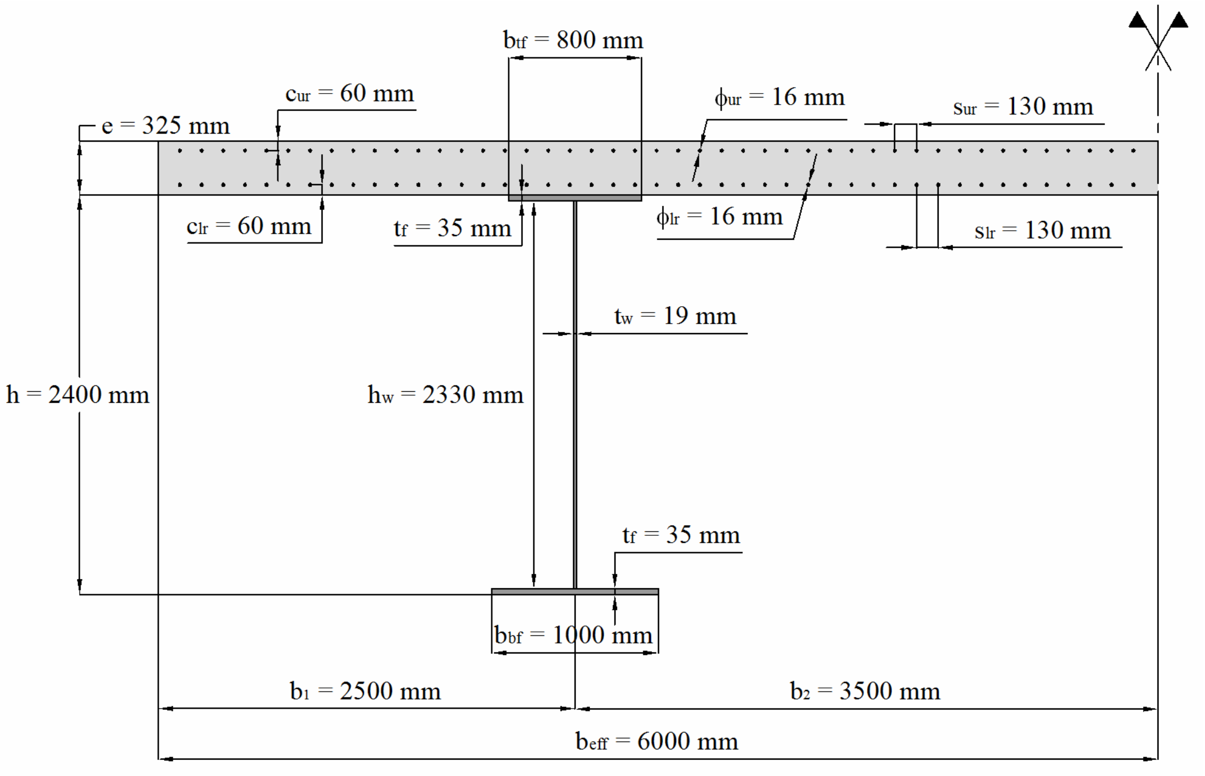
btf = 800 mm
cur = 60 mm
e = 325 mm
ϕur = 16 mm
sur = 130 mm
clr = 60 mm
tf = 35 mm
ϕlr = 16 mm
slr = 130 mm
tw = 19 mm
h = 2400 mm
hw = 2330 mm
tf = 35 mm
bbf = 1000 mm
b1 = 2500 mm
b2 = 3500 mm
beff = 6000 mm

Figure 3-6: Cross-section at mid-span P1-P2.

General properties of the twin-girder bridge in cross-section P1-P2	**Principle areas of the different part of the composite section**
L_2 = 60 m **a = 7.5 m** h = 2400 mm t_w = 19 mm b_{tf} = 800 mm b_{bf} = 1000 mm **t_f = 35 mm** **$h_w = h - 2t_f$ = 2.33 m** e = 32.5 cm ϕ_{ur} = 16 mm ϕ_{lr} = 16 mm s_{ur} = 130 mm s_{lr} = 130 mm c_{ur} = 60 mm c_{lr} = 60 mm b_{eff} = 6 m $n_{ur} = \frac{b_{eff}}{s_{ur}} = 46.154$ $n_{lr} = \frac{b_{eff}}{s_{lr}} = 46.154$	$A_{atf} = t_{tf} b_{tf} = 0.028 \text{ m}^2$ $A_{aw} = t_w h_w = 0.044 \text{ m}^2$ $A_{abf} = t_{bf} b_{bf} = 0.035 \text{ m}^2$ $A_a = A_{atf} + A_{aw} + A_{abf} = 0.107 \text{ m}^2$ $A_{sur} = \frac{\pi d_{ur}^2}{4} = 2.011 \text{ cm}^2$ $A_{tsur} = n_{ur} A_{sur} = 92.816 \text{ cm}^2$ $A_{slr} = \frac{\pi d_{lr}^2}{4} = 2.011 \text{ cm}^2$ $A_{tslr} = n_{lr} A_{slr} = 92.816 \text{ cm}^2$ $A_{cur} = c_{ur} b_{eff} = 0.36 \text{ m}^2$ $A_{clur} = \left(e - c_{ur} - c_{lr}\right) b_{eff} = 1.23 \text{ m}^2$ $A_{clr} = c_{lr} b_{eff} = 0.36 \text{ m}^2$ $A_c = e b_{eff} = A_{cur} + A_{clur} + A_{clr} = 1.95 \text{ cm}^2$ (see notation and Figure 3-6)

3.1.4.2 Material properties

Structural steel

f_{yw} = 345 N/mm² because 16 mm < t_f = 19 mm ≤ 40 mm (see Table 2-4)

$$\varepsilon_w = \sqrt{\frac{235 N/mm^2}{f_{yw}}} = 0.825$$

f_{yf} = 345 N/mm² because 16 mm < **t_f = 35 mm** ≤ 40 mm (see Table 2-4)

$$\varepsilon_f = \sqrt{\frac{235 N/mm^2}{f_{yf}}} = 0.825$$

$$f_{ydw} = \frac{f_{yw}}{\gamma_{M0}} = 345 \text{ N/mm}^2$$

$$f_{ydf} = \frac{f_{yf}}{\gamma_{M0}} = 345 \text{ N/mm}^2$$

E_a = 210000 N/mm²

Further explanations on the determination of the cross-section class

See Paragraph 3.1.2.4, page 91f.

Concrete

See Paragraph 3.1.2.2.

Reinforcement

See Paragraph 3.1.2.2.

3.1.4.3 Internal forces and moments

The internal forces and moments in this cross-section are (see Figure 2-31 and Figure 2-32):

M_{Ed} = **30.17 MNm** (at mid-span of the second span L_2 panel: x = 80 m)
V_{Ed} = **2.152 MN** (at a distance a = 7.5 m of the mid-span of the second span L_2: x = 87.5 m)

3.1.4.4 Determination of the cross-section class

- Bottom flange is in tension: Class 1
- Top flange is composite and connected to the slab following the recommendations of EN 1994-2, 6.6: Class 1
- To classify the steel web, the position of the Plastic Neutral Axis (PNA) is determined as:
  - Design plastic resistance of the concrete in compression located above upper reinforcements of the slab:

    $$N_{cur} = 0.85.A_{cur}\frac{f_{ck}}{\gamma_c} = 7.14 \text{ MN}$$

  - Design plastic resistance of the concrete in compression located between upper and lower reinforcements of the slab:

    $$N_{clur} = 0.85.A_{clur}\frac{f_{ck}}{\gamma_c} = 24.395 \text{ MN}$$

  - Design plastic resistance of the concrete in compression located under lower reinforcements of the slab:

    $$N_{clr} = 0.85.A_{clr}\frac{f_{ck}}{\gamma_c} = 7.4 \text{ MN}$$

  - Design plastic resistance of the concrete in compression:

    $$N_c = N_{cur} + N_{clur} + N_{clr} = 38.675 \text{ MN}$$

  - Design plastic resistance of the total upper reinforcements:

    $$N_{sur} = A_{tsur} f_{sd} = 4.035 \text{ MN}$$

  - Design plastic resistance of the total lower reinforcements:

    $$N_{slr} = A_{tslr} f_{sd} = 4.035 \text{ MN}$$

  - Design plastic resistance of the structural steel top flange:

    $$N_{atf} = A_{atf}\frac{f_{yf}}{\gamma_{M0}} = \mathbf{9.66\ MN}$$

  - Design plastic resistance of the structural steel web:

    $$N_{aw} = A_{aw}\frac{f_{yw}}{\gamma_{M0}} = \mathbf{15.273\ MN}$$

Relations to find the location of the Plastic Neutral Axis (PNA) under positive moment $M_{Pl,Rd}$

RELATIONS	PNA LOCATION
$N_{abf} \geq N_{aw} + N_{atf} + N_c$	PNA in the bottom flange
$N_{abf} + N_{aw} \geq N_{aft} + N_c$ and $N_{abf} < N_{aw} + N_{atf} + N_c$	PNA in the web
$N_a \geq N_c$ and $N_{abf} + N_{aw} < N_{atf} + N_c$	PNA in the top flange
$N_a \geq N_{cur} + N_{clur}$ and $N_a < N_c$	PNA in the slab under lower reinforcements
$N_a + N_{sl} \geq N_{cur}$ and $N_a + N_{sl} < N_{cur} + N_{clur}$	PNA in the slab between reinforcements
$N_a + N_{sl} + N_{su} < N_{cur}$	PNA in the slab above upper reinforcements

Further explanations on the bending resistance check

See Paragraph 3.1.2.5.1, page 87f.

Further explanations on the shear resistance check

See Paragraph 3.1.2.5.2, page 89ff.

- Design plastic resistance of the structural steel bottom flange:

  $$N_{abf} = A_{abf}\frac{f_{yf}}{\gamma_{M0}} = \mathbf{12.075\ MN}$$

- Design plastic resistance of the structural steel :

  $$N_a = N_{atf} + N_{aw} + N_{abf} = \mathbf{37.008\ MN}$$

- Location of the Plastic Neutral Axis (PNA):

  N_a **= 37.008 MN** $\geq N_{cur} + N_{clur} = 31.535$ MN

  and N_a = **37.008 MN** $< N_c = 38.675$ MN

  Thus, the PNA is deduced to be located in the slab in the lower reinforcements at a distance z_{pl} from the extreme lower fiber of the bottom flange. Writing the force equilibrium around the PNA:

  $$z_{pl} = h + e - \frac{N_a}{0.85 b_{eff} f_{cd}} = 2.414 \text{ m}$$

  As the PNA is located in the slab below lower reinforcement, the whole web is in tension and therefore in Class 1.

Conclusion: the cross-section at the mid-span P_1-P_2 is in class 1 and is checked by a plastic section analysis.

3.1.4.5 Plastic section analysis

3.1.4.5.1 Bending resistance check

The design plastic resistance moment is calculated from the position of the PNA:

$M_{pl,Rd}$ = **53.532 MNm**

Reinforcement in compression in the concrete slab is neglected according EN 1994-2, 6.2.1.2(1).

$M_{Ed} = 30.17$ MNm $\leq M_{pl,Rd} = 53.532$ MNm

⇒ **Bending resistance is verified!**

3.1.4.5.2 Shear resistance check

The web should be checked in terms of shear buckling if:

- $\frac{h_w}{t_w} > \frac{72}{\eta}\varepsilon_w$ for unstiffened web
- $\frac{h_w}{t_w} > \frac{31}{\eta}\varepsilon_w\sqrt{k_\tau}$ for stiffened web

In this case, the web is stiffened by vertical stiffeners.

$\frac{h_w}{t_w} = 122.632 > \frac{31}{\eta}\varepsilon_w\sqrt{k_t} = 51.019$ then the web should be checked in terms of shear buckling.

The maximum design shear resistance is given by:

$V_{Rd} = min\ (V_{b,Rd};\ V_{pl,a,Rd})$

where $V_{b,Rd} = V_{bw,Rd} + V_{bf,Rd} = \dfrac{\chi_w f_{yw} h_w t_w}{\sqrt{3}\gamma_{M1}} + \dfrac{b_f t_f f_{yf}}{c\gamma_{M1}}\left(1-\left(\dfrac{M_{Ed}}{M_{f,Rd}}\right)^2\right) \le \dfrac{\eta f_{yw} h_w t_w}{\sqrt{3}\gamma_{M1}} = 9.62$ MN

$$V_{pl,a,Rd} = \frac{\eta f_{yw}}{\sqrt{3}\gamma_{M0}} h_w t_w = 10.582 \text{ MN}$$

where η = 1.2 for steel grades up to and including S460

Contribution of the web $V_{bw,Rd}$

$$V_{bw,Rd} = \frac{\chi_w f_{yw} h_w t_w}{\sqrt{3}\gamma_{M1}}$$

The vertical stiffeners at the bracing transverse frames which border the webpanel located in span P1–P2, are assumed to be rigid (to be checked by using Section 9 of EN 1993-1-5). They are equally spaced by a = 8.333 m.

$k_{\tau st} = 0$ because there is no longitudinal stiffeners

$a/h_w = 3.219 \geq 1$

$$k_\tau = 5.34 + 4\left(\frac{h_w}{a}\right)^2 + k_{\tau st} = 5.726$$

$$\bar{\lambda}_w = \frac{h_w}{37.4 t_w \varepsilon_w \sqrt{k_\tau}} = 1.66 \geq 1.08$$

$$\Rightarrow \quad \chi_w = \frac{1.37}{\left(0.7+\bar{\lambda}_w\right)} = 0.58$$

$$V_{bw,Rd} = \frac{\chi_w f_{yw} h_w t_w}{\sqrt{3}\gamma_{M1}} = 4.653 \text{ MN}$$

Contribution from the flanges $V_{bf,Rd}$

$$V_{bf,Rd} = \frac{b_f t_f^2 f_{yf}}{c\gamma_{M1}}\left(1-\left(\frac{M_{Ed}}{M_{f,Rd}}\right)^2\right)$$

b_f and t_f are taken for the flange which provides the least axial resistance,

b_f being taken as not larger than $15\varepsilon t_f$ on each side of the web,

The lower flange of the cross-section is a structural steel section whereas its upper flange is a composite section (structural steel + concrete). The formulae for calculating $V_{bf,Rd}$ should be used with the lower steel flange properties.

The design plastic bending resistance $M_{f,Rd}$ of the cross-section consisting of the flanges only should be first calculated. $M_{f,Rd}$ is calculated as $M_{pl,Rd}$ but neglecting the web contribution.

To calculate $M_{f,Rd}$, the position of the Plastic Neutral Axis (PNA) is determined (by using the same definition than in Paragraph 3.1.2.4) as:

$N_{abf} + N_{atf} + N_{sl} = 25.77 \text{ MN} \geq N_{cur} = 7.14$ MN

and $N_{abf} + N_{atf} + N_{sl} = 25.77 \text{ MN} < N_{cur} + N_{clur} = 31.535$ MN

Thus, the PNA is deduced to be located in the concrete slab between reinforcements at a distance z_{pl} from the extreme lower fiber of the bottom flange. Writing the force equilibrium around the PNA:

Further explanations on the M-V-interaction

See Paragraph 3.1.2.5.3, page 93.

$$z_{pl} = h + e - \frac{N_{abf} + N_{atf} + N_{sl}}{0.85.b_{eff}f_{cd}} = 2.508 \text{ m}$$

The design plastic resistance moment of the flanges only is calculated from the position of the PNA: $M_{f,Rd} = 34.281$ MNm

$$c = a\left(0.25 + \frac{1.6b_f t_f^2 f_{yf}}{th_w^2 f_{yw}}\right) = 1.989 \text{ m}$$

$$V_{bf,Rd} = \frac{b_f t_f^2 f_{yf}}{c\gamma_{M1}}\left(1 - \left(\frac{M_{Ed}}{M_{f,Rd}}\right)^2\right) = 0.035\text{MN}$$

The contribution $V_{bf,Rd}$ of the flanges is negligible.

$$V_{b,Rd} = V_{bw,Rd} + V_{f,Rd} = 4.667 + 0.035 = 4.688 \text{ MN}$$

$$V_{Rd} = min\ (V_{b,Rd};\ V_{pl,a,Rd}) = min(4.688;\ 10.582) = 4.688 \text{ MN}$$

Cross-section verification

The verification should be performed as follows:

$$V_{Ed} = 2.152 \text{ MN} \leq V_{Rd} = 4.688 \text{ MN}$$

$$\eta_3 = \frac{V_{Ed}}{V_{Rd}} = 0.459 \leq 1$$

⇒ **Shear resistance is verified!**

3.1.4.5.3 M-V-interaction

$$V_{Ed} = 2.152 \text{ MN} \leq 0.5\ V_{Rd} = 2.344 \text{ MN}$$

⇒ **There is no need to check the M-V-interaction.**

3.1.5 Check of cross-section at the internal support P2

Two vertical stiffeners are added to reduce the length *a* of each webpanel located at each side of the interal support P2. According to Figure 3-3, at each side of the internal support P2, these two vertical stiffeners divide the panel in three parts: denoted subpanel 1, 2 and 3.

NOTE: Here a subpanel denotes a longitudinally unstiffened webpanel which is only bordered by flanges and transverse stiffeners on each side.

3.1.5.1 Subpanel 1 - Geometry

At internal support P2 at ULS the concrete slab is in tension over its whole height. Its contribution is therefore neglected in the cross-section resistance.

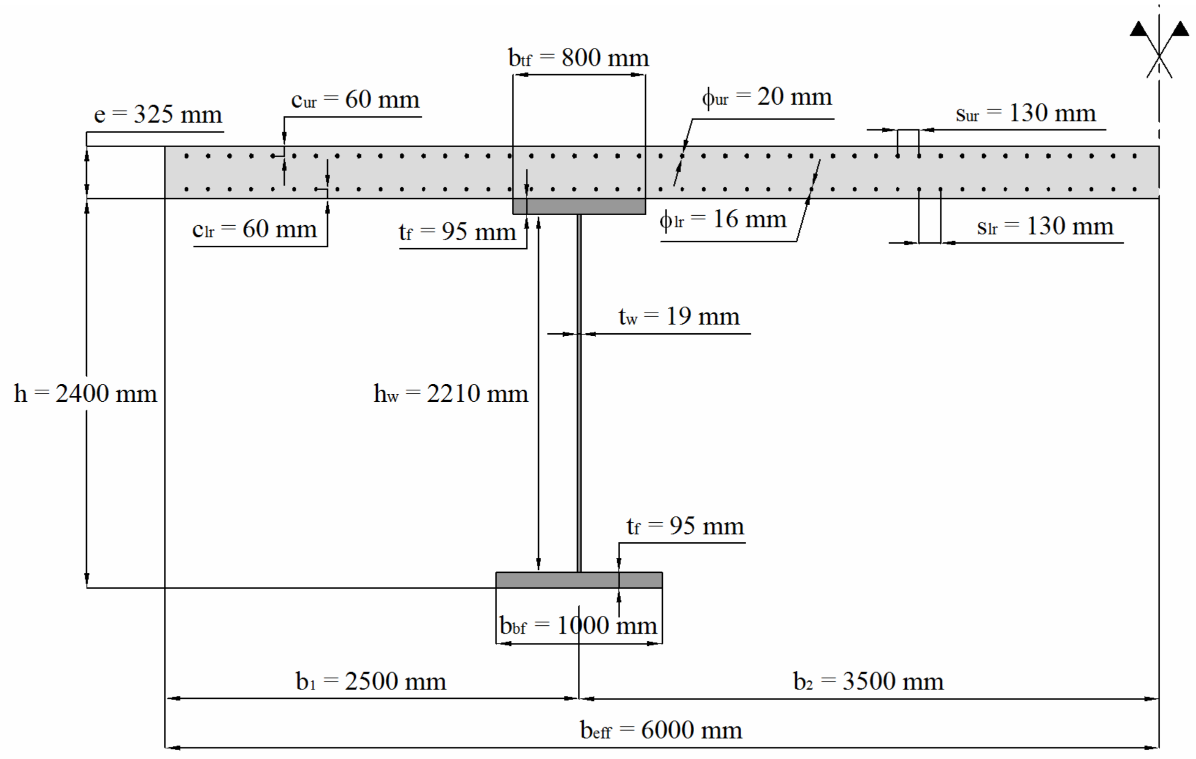
b_tf = 800 mm
e = 325 mm
c_ur = 60 mm
ϕ_ur = 20 mm
s_ur = 130 mm
c_lr = 60 mm
t_f = 95 mm
ϕ_lr = 16 mm
s_lr = 130 mm
t_w = 19 mm
h = 2400 mm
h_w = 2210 mm
t_f = 95 mm
b_bf = 1000 mm
b_1 = 2500 mm
b_2 = 3500 mm
b_eff = 6000 mm

Figure 3-7: Cross-section at the internal support P2.

General properties of the twin-girder bridge in cross-section P2	Main areas of the different parts of the composite section
$L_1 = L_3 = 50$ m, $L_2 = 60$ m $a = 1.5$ m $h = 2400$ mm $t_w = 19$ mm $b_{tf} = 800$ mm $b_{bf} = 1000$ mm $t_f = 95$ mm $h_w = h - 2t_f = 2.21$ m $e = 32.5$ cm $\phi_{ur} = 20$ mm $\phi_{lr} = 16$ mm $s_{ur} = 130$ mm $s_{lr} = 130$ mm $c_{ur} = 60$ mm $c_{lr} = 60$ mm $b_{eff} = 6$ m $n_{ur} = \frac{b_{eff}}{s_{ur}} = 46.154$ $n_{lr} = \frac{b_{eff}}{s_{lr}} = 46.154$	$A_{atf} = t_{tf} b_{tf} = 0.076$ m² $A_{aw} = t_w h_w = 0.042$ m² $A_{abf} = t_{bf} b_{bf} = 0.095$ m² $A_a = A_{atf} + A_{aw} + A_{abf} = 0.213$ m² $A_{sur} = \frac{\pi d_{ur}^2}{4} = 3.142$ cm² $A_{tsur} = n_{ur} A_{sur} = 144.997$ cm² $A_{slr} = \frac{\pi d_{lr}^2}{4} = 2.011$ cm² $A_{tslr} = n_{lr} A_{slr} = 92.816$ cm² $A_{cur} = c_{ur} b_{eff} = 0.36$ m² $A_{clur} = (e - c_{ur} - c_{lr}) b_{eff} = 1.23$ m² $A_{clr} = c_{lr} b_{eff} = 0.36$ m² $A_c = e b_{eff} = A_{cur} + A_{clur} + A_{clr} = 1.95$ cm² (see notation and Figure 3-7)

EN 1993-1-1, Table 5.2 (sheet 2 of 3), Maximum width-to-thickness ratios for compression parts

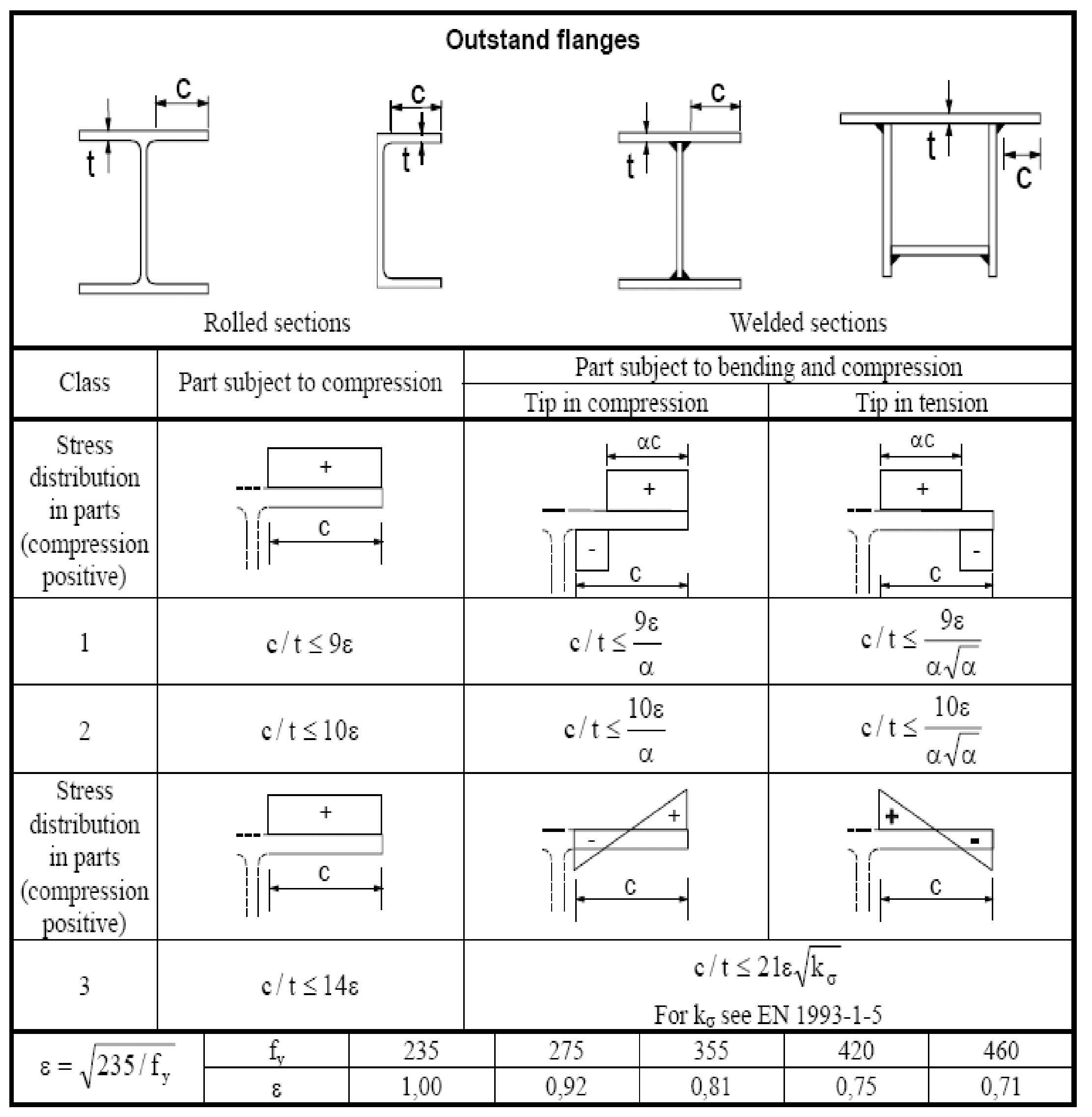

Outstand flanges

Rolled sections

Welded sections

Class	Part subject to compression	Part subject to bending and compression	
		Tip in compression	Tip in tension
Stress distribution in parts (compression positive)	+ c	αc + - c	αc + - c
1	$c/t \le 9\varepsilon$	$c/t \le \dfrac{9\varepsilon}{\alpha}$	$c/t \le \dfrac{9\varepsilon}{\alpha\sqrt{\alpha}}$
2	$c/t \le 10\varepsilon$	$c/t \le \dfrac{10\varepsilon}{\alpha}$	$c/t \le \dfrac{10\varepsilon}{\alpha\sqrt{\alpha}}$
Stress distribution in parts (compression positive)	+ c	+ - c	+ - c
3	$c/t \le 14\varepsilon$	$c/t \le 21\varepsilon\sqrt{k_\sigma}$ For k_σ see EN 1993-1-5	

$\varepsilon = \sqrt{235/f_y}$	f_y	235	275	355	420	460
	ε	1,00	0,92	0,81	0,75	0,71

3.1.5.2 Subpanel 1 - Material properties

Structural steel

f_{yw} = 345 N/mm² because 16 mm < t_f = 19 mm ≤ 40 mm (see Table 2-4)

$$\varepsilon_w = \sqrt{\frac{235 N/mm^2}{f_{yw}}} = 0.825$$

f_{yf} = 315 N/mm² because 80 mm < t_f = 95 mm ≤ 100 mm (see Table 2-4)

$$\varepsilon_f = \sqrt{\frac{235 N/mm^2}{f_{yf}}} = 0.825$$

$$f_{ydw} = \frac{f_{yw}}{\gamma_{M0}} = 345 \text{ N/mm}^2$$

$$f_{ydf} = \frac{f_{yf}}{\gamma_{M0}} = 315 \text{ N/mm}^2$$

E_a = 210000 N/mm²

Concrete

See Paragraph 3.1.2.2.

Reinforcement

See Paragraph 3.1.2.2.

3.1.5.3 Subpanel 1 - Internal forces and moments

The internal forces and moments in this cross-section are (see Figure 2-31 and Figure 2-32):

M_{Ed} = 65.44 MNm (at the internal support P2: x = 110 m)

V_{Ed} = 6.087 MN (at the internal support P2: x = 110 m)

The maximum value of bending moment and shear force is in the internal support P_2 (see Figure 2-31 and Figure 2-32). Figure 2-31 and Figure 2-32 are not perfectly symmetric.

3.1.5.4 Subpanel 1 - Determination of the cross-section class

- The top flange is in tension: Class 1
- The bottom flange is in compression :

  $\frac{c_{bf}}{t_f} = \frac{b_{bf} - t_w}{2t_f}$ = 5.163 ≤ 9ε = 7.774 therefore in Class 1

- The web is in tension in its upper part and in compression in its lower part. To classify the steel web, the position of the Plastic Neutral Axis (PNA) is determined as follows:
  - Design plastic resistance of total reinforcements of the slab:

    $$N_{su} + N_{sl} = \left(A_{tsur} + A_{tslr}\right)\frac{f_{sk}}{\gamma_s} = 10.339 \text{ MN}$$

  - Design plastic resistance of the structural steel top flange:

Relations to find the location of the Plastic Neutral Axis (PNA) under negative moment $M_{Pl,Rd}$

RELATIONS	PNA LOCATION
$N_{abf} \geq N_{aw} + N_{atf} + N_{sl} + N_{su}$	PNA in the bottom flange
$N_{abf} + N_{aw} \geq N_{atf} + N_{sl} + N_{su}$ and $N_{abf} < N_{aw} + N_{atf} + N_{sl} + N_{su}$	PNA in the web
$N_a \geq N_{sl} + N_{su}$ and $N_{abf} + N_{aw} < N_{atf} + N_{sl} + N_{su}$	PNA in the top flange
$N_{sl} + N_{su} > N_a$	PNA in the slab

EN 1993-1-1, Table 5.2 (sheet 1 of 3), Maximum width-to-thickness ratios for compression parts

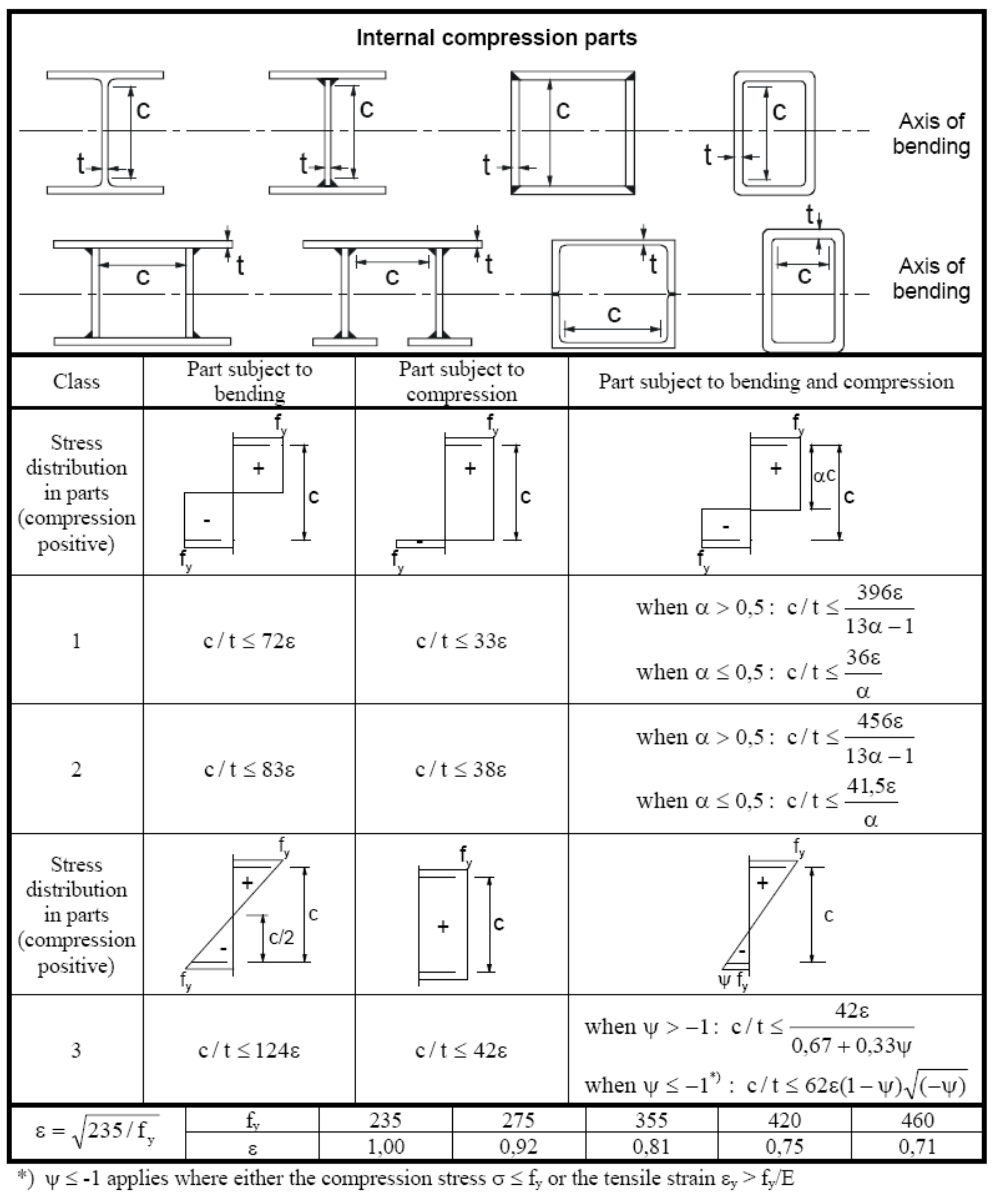
Internal compression parts
c
t
Axis of bending
c
t
Axis of bending
f_y
+
-
c
αc
c/2
ψf_y

Class	Part subject to bending	Part subject to compression	Part subject to bending and compression
Stress distribution in parts (compression positive)			
1	$c/t \leq 72\varepsilon$	$c/t \leq 33\varepsilon$	when $\alpha > 0{,}5$: $c/t \leq \frac{396\varepsilon}{13\alpha - 1}$ when $\alpha \leq 0{,}5$: $c/t \leq \frac{36\varepsilon}{\alpha}$
2	$c/t \leq 83\varepsilon$	$c/t \leq 38\varepsilon$	when $\alpha > 0{,}5$: $c/t \leq \frac{456\varepsilon}{13\alpha - 1}$ when $\alpha \leq 0{,}5$: $c/t \leq \frac{41{,}5\varepsilon}{\alpha}$
Stress distribution in parts (compression positive)			
3	$c/t \leq 124\varepsilon$	$c/t \leq 42\varepsilon$	when $\psi > -1$: $c/t \leq \frac{42\varepsilon}{0{,}67 + 0{,}33\psi}$ when $\psi \leq -1^{*)}$: $c/t \leq 62\varepsilon(1-\psi)\sqrt{(-\psi)}$

$\varepsilon = \sqrt{235/f_y}$	f_y	235	275	355	420	460
	ε	1,00	0,92	0,81	0,75	0,71

*) $\psi \leq -1$ applies where either the compression stress $\sigma \leq f_y$ or the tensile strain $\varepsilon_y > f_y/E$

$$N_{atf} = A_{atf} \frac{f_{yf}}{\gamma_{M0}} = 23.94 \text{ MN}$$

- Design plastic resistance of the structural steel webassumed to be entirely in compression:

$$N_{aw} = A_{aw} \frac{f_{yw}}{\gamma_{M0}} = 14.487 \text{ MN}$$

- Design plastic resistance of the structural steel bottom flange:

$$N_{abf} = A_{abf} \frac{f_{yf}}{\gamma_{M0}} = 29.925 \text{ MN}$$

- Design plastic resistance of the structural steel :

$$N_a = N_{atf} + N_{aw} + N_{abf} = 68.352 \text{ MN}$$

- Location of the Plastic Neutral Axis (PNA) :

$N_{abf} + N_{aw} = 44.412$ MN $\geq N_{atf} + N_{sl} + N_{su} = 34.279$ MN

and $N_{abf} = 29.925$ MN $< N_{aw} + N_{atf} + N_{sl} + N_{su} = 48.766$ MN

Thus, the PNA is deduced to be located in the steel web at a distance z_{pl} from the extreme lower fiber of the bottom flange. Writing the force equilibrium around the PNA:

$$z_{pl} = \frac{2hb_{tf} f_{yf} + N_{su} + N_{sl} - N_a}{2b_{tf} f_{yf}} = 1.532 \text{ m}$$

More than half the web height is in compression:

$$\alpha = \frac{(z_{pl} - t_f)}{h_w} = 0.65 > 0.5$$

Therefore the limiting slenderness between Class 2 and Class 3 is given by:

$$\frac{c_w}{t_w} = \frac{h_w}{t_w} = 116.316 >> \frac{456\varepsilon_w}{13\alpha - 1} = 50.492$$

The steel web is at least in Class 3 and reasoning is now based on the elastic stress distribution at ULS given by the global analysis which taken into account the history of the construction (erection phasing: see Paragraph 2.1.4):

$$\sigma_{abfu} = \text{-}276.93 \text{ N/mm}^2$$

$$\sigma_{atfl} = 265.58 \text{ N/mm}^2$$

And the elastic stress disrtibution at ULS:

$$\psi_w = \frac{\sigma_{atfl}}{\sigma_{abfu}} = \frac{-266.71}{265.58} = \text{-}1.043 \leq 1$$

Therefore the limiting slenderness between Class 3 and Class 4 is given by:

$$\frac{c_w}{t_w} = \frac{h_w}{t_w} = 116.316 > 62\varepsilon(1 - \psi_w)\sqrt{-\psi_w} = 106.737$$

It is deduced that the steel web is in Class 4.

Conclusion: the cross-section at the internal support P1 and P2 is in Class 4 and is checked by a elastic section analysis.

EN 1993-1-5, 4.6(3)

(3) The plate buckling verification of the panel should be carried out for the stress resultants at a distance 0.4a or 0.5b, whichever is the smallest, from the panel end where the stresses are the greater. In this case the gross sectional resistance needs to be checked at the end of the panel.

EN 1993-1-5, 4.4, Plate elements without longitudinal stiffeners

(1) The effective^p areas of flat compression elements should be obtained using Table 4.1 for internal elements and Table 4.2 for outstand elements. The effective^p area of the compression zone of a plate with the gross cross-sectional area Ac should be obtained from:

$$A_{c,eff} = \rho\, A_c \qquad (4.1)$$

where ρ is the reduction factor for plate buckling.

(2) The reduction factor ρ may be taken as follows:

- internal compression elements:

$\rho = 1{,}0$ for $\bar{\lambda}_p \leq 0{,}673$

$\rho = \dfrac{\bar{\lambda}_p - 0{,}055(3+\psi)}{\bar{\lambda}_p^2} \leq 1$ for $\bar{\lambda}_p > 0{,}673$, where $(3 + \psi) \geq 0$

- outstand compression elements:

$\rho = 1{,}0$ for $\bar{\lambda}_p \leq 0{,}748$

$\rho = \dfrac{\bar{\lambda}_p - 0{,}188}{\bar{\lambda}_p^2} \leq 1$ for $\bar{\lambda}_p > 0{,}748$

where $\bar{\lambda}_p = \sqrt{\dfrac{f_y}{\sigma_{cr}}} = \dfrac{\bar{b}/t}{28{,}4\varepsilon\sqrt{k_\sigma}}$

ψ is the stress ratio determined in accordance with 4.4(3) and 4.4(4)

$\bar{b}$ is the appropriate width to be taken as follows (for definitions, see Table 5.2 of EN 1993-1-1)

b_w for webs;

b for internal flange elements (except RHS);

b - 3 t for flanges of RHS;

c for outstand flanges;

h for equal-leg angles;

h for unequal-leg angles;

k_σ is the buckling factor corresponding to the stress ratio ψ and boundary conditions. For long plates k_σ is given in Table 4.1 or Table 4.2 as appropriate;

3.1.5.5 Subpanel 1 - Elastic section analysis

3.1.5.5.1 Bending resistance check

The section is in Class 4 so that its effective cross-section under bending moment has to be calculated according to section EN 1993-1-5, 4.4.

Bottom flange in compression

$k_{\sigma bf} = 0.43$ (see Table 4.2 of EN 1993-1-5, 4.4: outstand elements)

$$\bar{\lambda}_{pbf} = \frac{\bar{b}/t}{28,4\varepsilon\sqrt{k_\sigma}} = \frac{\frac{b_{bf}-t_w}{2t_f}}{28,4\varepsilon_f\sqrt{k_{\sigma bf}}} = 0.321 \leq 0.748$$

⇒ $\rho_{bf} = 1$ there is no reduction of the width of the bottom flange. The full bottom flange is effective.

Web in bending

Stresses at the end of the web are given by global analysis:

$\sigma_{atfl} = \text{-}276.93$ MPa

$\sigma_{abfu} = 265.58$ MPa

$$\psi_w = \frac{\sigma_{atfl}}{\sigma_{abfu}} = \text{-}1.043 \leq 1$$

$k_{\sigma w} = 5.98(1-\psi)^2 = 24.953$ (see Table 4.1 of EN 1993-1-5, 4.4: internal compression elements)

$$\bar{\lambda}_{pw} = \frac{\bar{b}/t}{28,4\varepsilon\sqrt{k_\sigma}} = \frac{\frac{h_w}{t_w}}{28,4\varepsilon_w\sqrt{k_{\sigma w}}} = 0.993 \ > 0.673$$

⇒ $\rho_w = \dfrac{\bar{\lambda}_p - 0,055(3+\psi_w)}{\bar{\lambda}_p^2} =$ 0.898; there is a reduction of the height of the steel web

Then the effective height of the web in compression can be calculated:

$$h_{weff} = \frac{\rho_w h_w}{(1-\psi_w)} = 0.971 \text{ m}$$

And this effective height of the web can be distributed as show in Table 4.1 of EN 1993-1-5:

$h_{we1} = 0.4h_{weff} = 0.388$ m

$h_{we2} = 0.6h_{weff} = 0.583$ m

Final mechanical properties of the effective structural steel twin-girder section (only flanges and web)

The effective cross-sectional properties can be calculated:

$$A_{a.eff} = A_{atf} + A_{abf} + \left(h_{weff} + h_w - h_s + t_f\right)t_w = 0.21 \text{ m}^2$$

EN 1993-1-5, 4.4, Table 4.2, Outstand compression elements

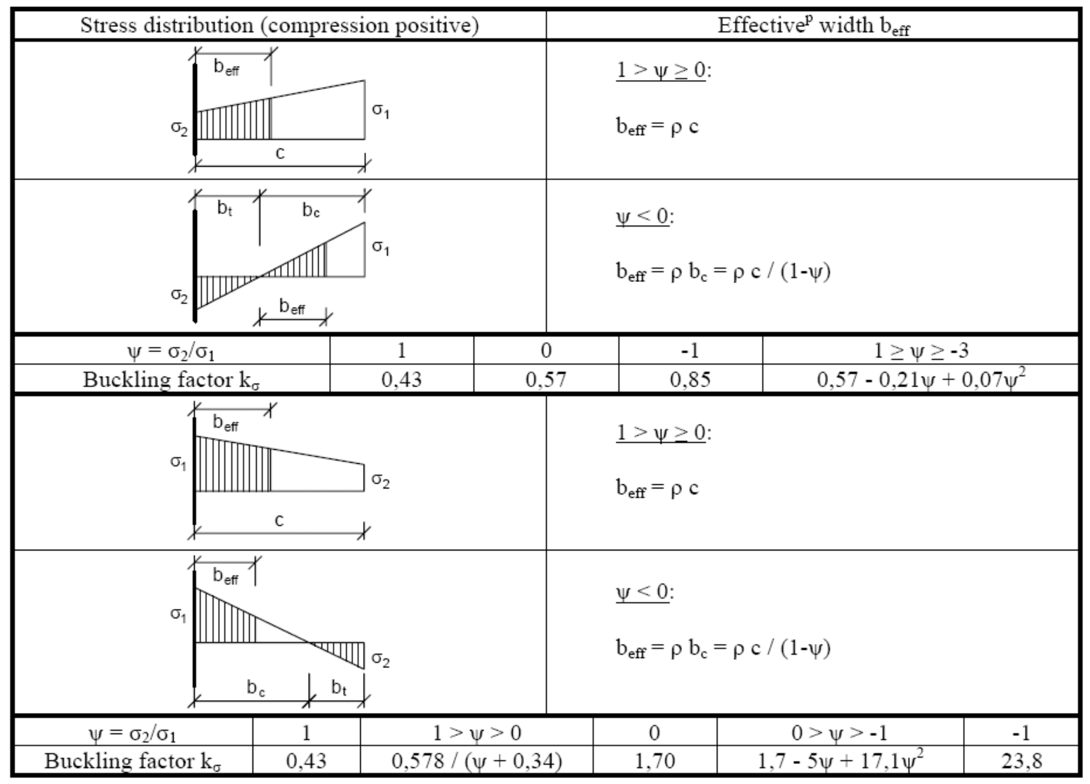

Stress distribution (compression positive)	Effective^p width b_{eff}
b_{eff} σ_2 σ_1 c	$1 > \psi \geq 0$: $b_{eff} = \rho\, c$
b_t b_c σ_1 σ_2 b_{eff}	$\psi < 0$: $b_{eff} = \rho\, b_c = \rho\, c\,/\,(1-\psi)$

$\psi = \sigma_2/\sigma_1$	1	0	-1	$1 \geq \psi \geq -3$
Buckling factor k_σ	0,43	0,57	0,85	$0{,}57 - 0{,}21\psi + 0{,}07\psi^2$

Stress distribution (compression positive)	Effective^p width b_{eff}
b_{eff} σ_1 σ_2 c	$1 > \psi \geq 0$: $b_{eff} = \rho\, c$
b_{eff} σ_1 σ_2 b_c b_t	$\psi < 0$: $b_{eff} = \rho\, b_c = \rho\, c\,/\,(1-\psi)$

$\psi = \sigma_2/\sigma_1$	1	$1 > \psi > 0$	0	$0 > \psi > -1$	-1
Buckling factor k_σ	0,43	$0{,}578\,/\,(\psi + 0{,}34)$	1,70	$1{,}7 - 5\psi + 17{,}1\psi^2$	23,8

EN 1993-1-5, 4.4, Table 4.1, Internal compression elements

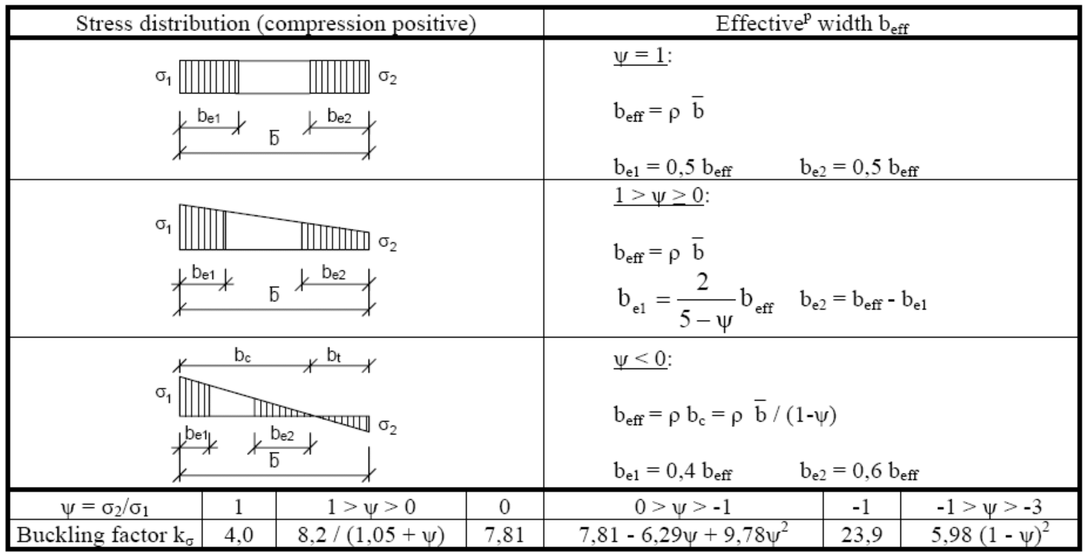

Stress distribution (compression positive)	Effective^p width b_{eff}
σ_1 σ_2 b_{e1} b_{e2} $\bar{b}$	$\psi = 1$: $b_{eff} = \rho\, \bar{b}$ $b_{e1} = 0{,}5\, b_{eff}$ $\quad b_{e2} = 0{,}5\, b_{eff}$
σ_1 σ_2 b_{e1} b_{e2} $\bar{b}$	$1 > \psi \geq 0$: $b_{eff} = \rho\, \bar{b}$ $b_{e1} = \frac{2}{5-\psi} b_{eff}$ $\quad b_{e2} = b_{eff} - b_{e1}$
b_c b_t σ_1 σ_2 b_{e1} b_{e2} $\bar{b}$	$\psi < 0$: $b_{eff} = \rho\, b_c = \rho\, \bar{b}\,/\,(1-\psi)$ $b_{e1} = 0{,}4\, b_{eff}$ $\quad b_{e2} = 0{,}6\, b_{eff}$

$\psi = \sigma_2/\sigma_1$	1	$1 > \psi > 0$	0	$0 > \psi > -1$	-1	$-1 > \psi > -3$
Buckling factor k_σ	4,0	$8{,}2\,/\,(1{,}05 + \psi)$	7,81	$7{,}81 - 6{,}29\psi + 9{,}78\psi^2$	23,9	$5{,}98\,(1 - \psi)^2$

The effective elastic neutral axis (ENA) must be determinated from the extreme lower fiber of the bottom flange:

$$h_{a.seff} = \frac{A_{abf}\frac{t_f}{2} + A_{atf}\left(h - \frac{t_f}{2}\right) + h_{we1}t_w\left(t_f + \frac{h_{we1}}{2}\right) + \left(h_{we2} + h_w - h_s + t_f\right)t_w\left(h - t_f - \frac{h_{we2} + h_w - h_s + t_f}{2}\right)}{A_{a.eff}} = 1.106 \text{ m}$$

And it can be deduced, the effective second moment of area of the cross-section:

$$I_{a.eff} = \frac{b_{bf}t_f^3}{12} + A_{abf}\left(h_{a.seff} - \frac{t_f}{2}\right)^2 + \frac{b_{tf}t_f^3}{12} + A_{atf}\left(h - \frac{t_f}{2} - h_{a.seff}\right)^2$$

$$+\frac{t_w h_{we1}^3}{12} + h_{we1}t_w\left(h_{a.seff} - \frac{h_{we1}}{2} - t_f\right)^2$$

$$+\left(h_{we2} + h_w - h_s + t_f\right)t_w\left(h - \frac{h_{we2} + h_w - h_s + 3t_f}{2} - h_{a.seff}\right)^2 = 0.241 \text{ m}^4$$

Final mechanical properties of the effective composite twin-girder section (structural steel and reinforcements)

The effective cross-sectional properties can be calculated:

$$A_{eff} = A_{tsur} + A_{tslr} + A_{atf} + A_{abf} + \left(h_{weff} + h_w - h_s + t_f\right)t_w = 0.233 \text{ m}^2$$

The effective elastic neutral axis (ENA) must be determinated from the extreme lower fiber of the bottom flange:

$$h_{seff} = \frac{A_{abf}\frac{t_f}{2} + A_{atf}\left(h - \frac{t_f}{2}\right) + A_{tslr}\left(h + c_{lr}\right) + A_{tsur}\left(h + e - c_{ur}\right) + h_{we1}t_w\left(t_f + \frac{h_{we1}}{2}\right) + \left(h_{we2} + h_w - h_s + t_f\right)t_w\left(h - t_f - \frac{h_{we2} + h_w - h_s + t_f}{2}\right)}{A_{eff}} = 1.257 \text{ m}$$

And it can be deduced, the effective second moment of area of the cross-section:

$$I_{eff} = \frac{b_{bf}t_f^3}{12} + A_{abf}\left(h_{seff} - \frac{t_f}{2}\right)^2 + \frac{b_{tf}t_f^3}{12} + A_{atf}\left(h - \frac{t_f}{2} - h_{seff}\right)^2$$

$$+\frac{t_w h_{we1}^3}{12} + h_{we1}t_w\left(h_{seff} - \frac{h_{we1}}{2} - t_f\right)^2$$

$$+\left(h_{we2} + h_w - h_s + t_f\right)t_w\left(h - \frac{h_{we2} + h_w - h_s + 3t_f}{2} - h_{seff}\right)^2$$

$$+A_{tslr}\left(h + c_{lr} - h_{seff}\right)^2 + A_{tsur}\left(h + e - c_{ur} - h_{seff}\right)^2 = 0.288 \text{ m}^4$$

The stress in the upper reinforcement of the concrete slab is given by the global analysis:

$$\sigma_{tsur} = \text{-}185.85 \text{ MPa}$$

EN1993-1-1, 6.2.1(9)

(9) Where all the compression parts of a cross-section are Class 3, its resistance should be based on an elastic distribution of strains across the cross-section. Compressive stresses should be limited to the yield strength at the extreme fibres.

NOTE: The extreme fibres may be assumed at the midplane of the flanges for ULS checks. For fatigue see EN 1993-1-9.

Final mechanical properties of the gross composite twin-girder cross section (structural steel and reinforcement)

The cross-sectional properties can be calculated:

$$A = A_{tsur} + A_{tslr} + A_{atf} + A_{abf} + A_{aw} = 0.237 \text{ m}^2$$

The elastic neutral axis (ENA) must be determinated from the extreme lower fiber of the bottom flange:

$$h_s = \frac{A_{abf}\frac{t_f}{2} + A_{atf}\left(h - \frac{t_f}{2}\right) + A_{aw}\left(t_f + \frac{h_w}{2}\right) + A_{tslr}\left(h + c_{lr}\right) + A_{tsur}\left(h + e - c_{ur}\right)}{A} = 1.247 \text{ m}$$

And it can be deduced, the effective second moment of area of the cross-section:

$$I = \frac{b_{bf}t_f^3}{12} + A_{abf}\left(h_s - \frac{t_f}{2}\right)^2 + \frac{b_{tf}t_f^3}{12} + A_{atf}\left(h - \frac{t_f}{2} - h_s\right)^2 + \frac{t_w h_w^3}{12} + A_{aw}\left(h_s - \frac{h}{2}\right)^2$$

$$+A_{tslr}\left(h + c_{lr} - h_s\right)^2 + A_{tsur}\left(h + e - c_{ur} - h_s\right)^2 = 0.29 \text{ m}^4$$

The bending moment taken by the composite twin-girder section (structural steel and reinforcements):

$$M_{c,Ed} = \frac{\sigma_{tsur} I}{h + e - c_{ur} - h_s} = \text{-38.224 MNm}$$

The bending moment taken by the structural steel twin-girder section (only flanges and web):

$$M_{a,Ed} = M_{Ed} - M_{c,Ed} = \text{-65.44 + 38.224 = -27.216 MNm}$$

Then, the stress on each level of the cross-section can be easily determinated:

$$\sigma_{abfleff} = \frac{-M_{a,Ed}h_{a.seff}}{I_{a.eff}} + \frac{-M_{c,Ed}h_{seff}}{I_{eff}} = 291.511 \text{ N/mm}^2 \leq f_{ydf} = 315 \text{ N/mm}^2$$

$$\sigma_{abfueff} = \frac{-M_{a,Ed}(h_{a.seff} - t_f)}{I_{a.eff}} + \frac{-M_{c,Ed}(h_{seff} - t_f)}{I_{eff}} = 268.184 \text{ N/mm}^2$$

$$\leq \min\left(f_{ydf}; f_{ydw}\right) = 315 \text{ N/mm}^2$$

$$\sigma_{atfleff} = \frac{M_{a,Ed}(h - t_f - h_{a.seff})}{I_{a.eff}} + \frac{M_{c,Ed}(h - t_f - h_{seff})}{I_{eff}} = \text{-274.462 N/mm}^2$$

$$\leq \min\left(f_{ydf}; f_{ydw}\right) = 315 \text{ N/mm}^2$$

$$\sigma_{atfueff} = \frac{M_{a,Ed}(h - h_{a.seff})}{I_{a.eff}} + \frac{M_{c,Ed}(h - h_{seff})}{I_{eff}} = |\text{-297.788}| \text{ N/mm}^2 \leq f_{ydf} = 315 \text{ N/mm}^2$$

$$\sigma_{tslreff} = \frac{M_{c,Ed}(h + c_{lr} - h_{seff})}{I_{eff}} = |\text{-159.674}| \text{ N/mm}^2 \leq f_{sd} = 434.783 \text{ N/mm}^2$$

$$\sigma_{tsureff} = \frac{M_{c,Ed}(h + e - c_{ur} - h_{seff})}{I_{eff}} = |\text{-186.873}| \text{ N/mm}^2 \leq f_{sd} = 434.783 \text{ N/mm}^2$$

The bending moment resistance is governed by the resistance of the top flange:

$$\eta_1 = \frac{\left|\sigma_{atfueff}\right|}{f_{ydf}} = 0.945 \leq 1$$

The cross-section at subpanel 1 on the internal support P2 is therefore checked for bending at ULS.

Further explanations on the shear resistance check

See Paragraph 3.1.2.5.2, page 89ff.

The verifications are here performed with the stresses in the extreme fibres of the structural steel flanges. Remember that the use of the stresses in the mid-plan of the flanges is also allowable.

⇒ **Bending resistance is verified!**

3.1.5.5.2 Shear resistance check

The web should be checked in terms of shear buckling if:

- $\frac{h_w}{t_w} > \frac{72}{\eta}\varepsilon_w$ for unstiffened web
- $\frac{h_w}{t_w} > \frac{31}{\eta}\varepsilon_w\sqrt{k_t}$ for stiffened web

In this case, the web is stiffened by vertical stiffeners.

$\frac{h_w}{t_w} = 116.316 > \frac{31}{\eta}\varepsilon_w\sqrt{k_t} = 84.188$ then the web should be checked in terms of shear buckling.

The maximum design shear resistance is given by $V_{Rd} = min\ (V_{b,Rd};\ V_{pl,a,Rd})$

where $$V_{b,Rd} = V_{bw,Rd} + V_{bf,Rd} = \frac{\chi_w f_{yw} h_w t_w}{\sqrt{3}\gamma_{M1}} + \frac{b_f t_f^2 f_{yf}}{c\gamma_{M1}}\left(1-\left(\frac{M_{Ed}}{M_{f,Rd}}\right)^2\right) \le \frac{\eta f_{yw} h_w t_w}{\sqrt{3}\gamma_{M1}} = 9.124 \text{ MN}$$

$$V_{pl,a,Rd} = \frac{\eta f_{yw}}{\sqrt{3}\gamma_{M0}} h_w t_w = 10.037 \text{ MN}$$

where η = 1.2 for steel grades up to and including S460

Contribution of the web $V_{bw,Rd}$

$$V_{bw,Rd} = \frac{\chi_w f_{yw} h_w t_w}{\sqrt{3}\gamma_{M1}}$$

The vertical stiffeners at the bracing transverse frames which border the webpanel adjacent to the support P1 and located in span P1-P2, are assumed to be rigid (to be checked by using Section 9 of EN 1993-1-5). They are equally spaced by a = 7.5 m or 8.33 m, depending on the span. Near the support P2, the first subpanel has a length a = 1.5 m.

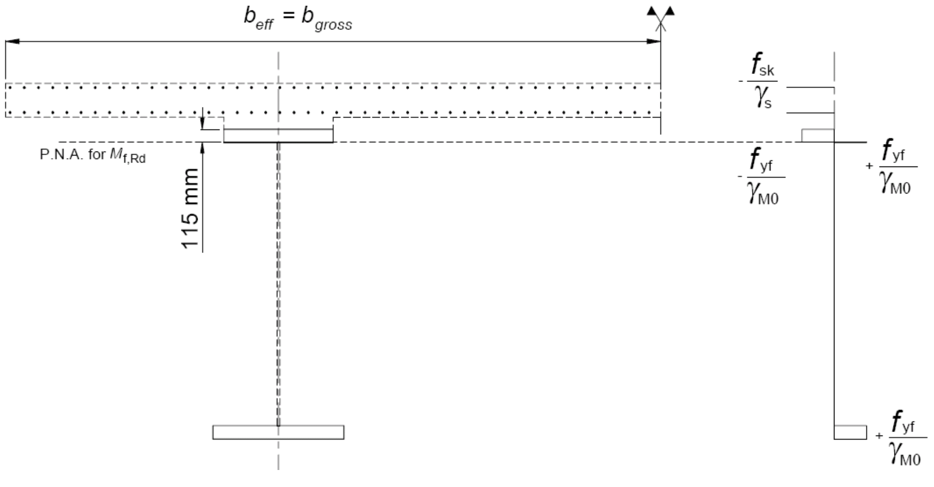
$b_{eff} = b_{gross}$
P.N.A. for $M_{f,Rd}$
115 mm
$-\frac{f_{sk}}{\gamma_s}$
$-\frac{f_{yf}}{\gamma_{M0}}$
$+\frac{f_{yf}}{\gamma_{M0}}$
$+\frac{f_{yf}}{\gamma_{M0}}$

Figure 3-8: Design Plastic resistance moment $M_{f,Rd}$ of the flanges only at internal support support P2.

$k_{\tau st} = 0$ because there is no longitudinal stiffeners

$a/h_w = 0.679 \leq 1$

$$k_\tau = 4 + 5.34\left(\frac{h_w}{a}\right)^2 + k_{\tau st} = 15.592$$

$$\frac{0.83}{\eta} = 0.692 \leq \bar{\lambda}_w = \frac{h_w}{37.4 t_w \varepsilon_w \sqrt{k_\tau}} = 0.954 < 1.08$$

$$\Rightarrow \qquad \chi_w = \frac{0.83}{\bar{\lambda}_w} = 0.87$$

$$V_{bw,Rd} = \frac{\chi_w f_{yw} h_w t_w}{\sqrt{3}\gamma_{M1}} = 6.613 \text{ MN}$$

Contribution from the flanges $V_{bf,Rd}$

$$V_{bf,Rd} = \frac{b_f t_f^2 f_{yf}}{c\gamma_{M1}}\left(1 - \left(\frac{M_{Ed}}{M_{f,Rd}}\right)^2\right)$$

b_f and t_f are taken for the flange which provides the least axial resistance,

b_f being taken as not larger than $15 \cdot \varepsilon \cdot t_f$ on each side of the web,

The lower flange of the cross-section is a structural steel section whereas its upper flange is a composite section (structural steel + reinforcing steel). The formulae for calculating $V_{bf,Rd}$ should be used with the lower steel flange properties.

The design plastic bending resistance $M_{f,Rd}$ of the cross-section consisting of the flanges and the reinforcing steel should be first calculated. $M_{f,Rd}$ is calculated as $M_{pl,Rd}$ neglecting the web contribution.

To calculate $M_{f,Rd}$, the position of the Plastic Neutral Axis (PNA) is determined as:

- Design plastic resistance of total reinforcements of the slab:

$$N_{su} + N_{sl} = \left(A_{tsur} + A_{tslr}\right)\frac{f_{sk}}{\gamma_s} = 10.339 \text{ MN}$$

- Design plastic resistance of the structural steel top flange:

$$N_{atf} = A_{atf}\frac{f_{yf}}{\gamma_{M0}} = 23.94 \text{ MN}$$

- Design plastic resistance of the structural steel bottom flange:

$$N_{abf} = A_{abf}\frac{f_{yf}}{\gamma_{M0}} = 29.925 \text{ MN}$$

- Location of the Plastic Neutral Axis (PNA):

  $N_{abf} + N_{atf} = 53.865 \text{ MN} \geq N_{su} + N_{sl}, = 10.339 \text{ MN}$

  and $N_{abf} = 29.925 \text{ MN} < N_{atf} + N_{su} + N_{sl}, = 34.279 \text{ MN}$

  Thus, the PNA is deduced to be located in the top flange at a distance z_{pl} from the extreme lower fiber of the bottom flange. Writing the force equilibrium around the PNA deduced:

$$z_{pl} = \frac{2hb_{tf} f_{yf} N_{su} + N_{sl} - N_{abf} - N_{atf}}{2b_{tf} f_{yf}} = 2.314 \text{ m}$$

The design plastic resistance moment of the flanges only is calculated from the position of the PNA: $M_{f,Rd}$ = 71.569 MNm

EN 1993-1-5, 9.3.5, Welds

(1) The web to flange welds may be designed for the nominal shear flow V_{Ed} / h_w if V_{Ed} does not exceed $\chi_w f_{yw} h_w t \big/ \left(\sqrt{3}\gamma_{M1}\right)$. For larger values V_{Ed} the weld between flanges and webs should be designed for the shear flow $\eta f_{yw} t \big/ \left(\sqrt{3}\gamma_{M1}\right)$.

(2) In all other cases welds should be designed to transfer forces along and across welds making up.

EN 1993-1-5, 9.3, Shear

EN 1993-1-5, 5.5, Verification

(1) The verification should be performed as follows:

$$\eta_3 = \frac{V_{Ed}}{V_{b,Rd}} \leq 1$$

where V_{Ed} is the design shear force including shear from torque.

EN 1994-2, 6.2.2.4(1)

(1) Where the vertical shear force V_{Ed} exceeds half the shear resistance V_{Rd} given by $V_{pl,Rd}$ in 6.2.2.2 or $V_{b,Rd}$ in 6.2.2.3, whichever is the smaller, allowance should be made for its effect on the resistance moment.

Further explanations on the M-V-interaction

See Paragraph 3.1.2.5.3, page 93.

EN 1994-2, 6.2.2.4(3)

(3) For cross-sections in Class 3 and 4, EN 1993-1-5, 7.1 is applicable using the calculated stresses of the composite section.

EN 1993-1-5, 7.1(2)

(2) The criterion given in (1) should be verified at all sections other than those located at a distance less than $h_w/2$ from a support with vertical stiffeners.

$$c = a\left(0.25 + \frac{1.6 b_f t_f^2 f_{yf}}{t h_w^2 f_{yw}}\right) = 0.545 \text{ m}$$

$$V_{bf,Rd} = \frac{b_f t_f^2 f_{yf}}{c \gamma_{M1}}\left(1 - \left(\frac{M_{Ed}}{M_{f,Rd}}\right)^2\right) = 0.621 \text{ MN}$$

In this case, the contribution of the flanges $V_{bf,Rd}$ is not negligible compared to contribution from the web and represents 8.6 % of the design shear buckling resistance.

$$V_{b,Rd} = V_{bw,Rd} + V_{bf,Rd} = 6.613 + 0.621 = 7.234 \text{ MN} \leq \frac{\eta f_{yw} h_w t_w}{\sqrt{3}\gamma_{M1}} = 9.124 \text{ MN}$$

$$V_{Rd} = min\ (V_{b,Rd};\ V_{pl,a,Rd}) = min(7.234;\ 10.037) = 7.234 \text{ MN}$$

The following checks should also be performed:

- The web to flange weld should be designed for the shear stress per unit length of $\frac{\eta f_{yw}}{\gamma_{M1}\sqrt{3}} t_w$;
- The tranverse stiffeners along the webpanel edges (and possibly the longitudinal stiffeners) should act as rigid end post;

The flanges are not completely used for resisting to bending moment (i.e. $M_{Ed} \leq M_{f,\ Rd}$ which is verified in the example: $M_{Ed} = 65.44$ MNm $\leq M_{f,\ Rd} = 71.569$ MNm

Cross-section verification

The verification should be performed as follows:

$$V_{Ed} = 6.087 \text{ MN} \leq V_{Rd} = min\ (7.234;\ 10.037) = 7.234 \text{ MN}$$

$$\eta_3 = \frac{V_{Ed}}{V_{Rd}} = 0.841 \leq 1$$

⇒ **Shear resistance is verified!**

3.1.5.5.3 M-V-interaction

$$V_{Ed} = 6.087 \text{ MN} \geq 0.5\ V_{Rd} = 3.617 \text{ MN}$$

Therefore the M-V-interaction should be checked.

$$\frac{M_{Ed}}{M_{f,Rd}} = 0.914 \leq 1$$

$$\frac{V_{Ed}}{V_{bw,Rd}} = 0.893 \leq 1$$

$M_{Ed} < M_{f,Rd}$ so that according to EN 1993-1-5, 7.1 (1), there is no interaction. It means that the flanges are enough to resist alone the bending moment so that the entire web can be used for the resistance to the shear force.

Then flanges of the steel girder take the bending moment and web of the steel beam takes shear force.

⇒ **There is no interaction.**

Further explanations on the determination of the cross-section class

See Paragraph 3.1.5.4, page 117ff.

Further explanations on the bending resistance check

See Paragraph 3.1.2.5.1, page 87f. and Paragraph 3.1.5.5.1, page 121ff.

3.1.5.6 Subpanel 2 - Geometry

Follow the same procedure as for subpanel 1 (see Paragraph 3.1.5.1)

At internal support P2 at ULS the concrete slab is in tension over its whole height. Its contribution is therefore neglected in the cross-section resistance.

The geometry of the cross-section of the subpanel 2 is totaly the same as the geometry of the cross-section of the subpanel 1. Only the length of the panel change (a = 2,5 m)

3.1.5.7 Subpanel 2 - Material properties

See Paragraph 3.1.5.2.

The material properties of the cross-section of the subpanel 2 are identical to the material properties of the cross-section of the subpanel 1.

3.1.5.8 Subpanel 2 - Internal forces and moments

The internal forces and moments in this cross-section are (see Figure 2-31 and Figure 2-32):

$M_{Ed} =$ 58.222 MNm (at the internal support P2: x = 111.5 m)

$V_{Ed} =$ 5.843 MN (at the internal support P2: x = 111.5 m)

3.1.5.9 Subpanel 2 - Determination of the cross-section class

See Paragraph 3.1.5.4.

As the geometry of the cross-section does not change compared to subpanel 1, the cross-section class is the same for subpanel 2.

3.1.5.10 Subpanel 2 - Elastic section analysis

3.1.5.10.1 Bending resistance check

The plate buckling verification of the panel should be carried out for the stress resultants at a distance 0.4·a or 0.5·b: *min(0.4·a ; 0.5·b) = min(1 ; 1.105)* = 1 m

Then the value of the bending moment becomes: M_{Ed} *(min(0.4a ; 0.5b))* = 53.659 MNm

The stress on each level of the cross-section can be easily determined:

$$\sigma_{abfleff} = \frac{-M_{a,Ed} h_{a.seff}}{I_{a.eff}} + \frac{-M_{c,Ed} h_{seff}}{I_{eff}} = 259.181 \text{ N/mm}^2 \leq f_{ydf} = 315 \text{ N/mm}^2$$

$$\sigma_{abfueff} = \frac{-M_{a,Ed}(h_{a.seff} - t_f)}{I_{a.eff}} + \frac{-M_{c,Ed}(h_{seff} - t_f)}{I_{eff}} = 238.478 \text{ N/mm}^2$$

$$\leq \min\left(f_{ydf}; f_{ydw}\right) = 315 \text{ N/mm}^2$$

$$\sigma_{atfleff} = \frac{M_{a,Ed}(h - t_f - h_{a.seff})}{I_{a.eff}} + \frac{M_{c,Ed}(h - t_f - h_{seff})}{I_{eff}} = |-243.132| \text{ N/mm}^2$$

$$\leq \min\left(f_{ydf}; f_{ydw}\right) = 315 \text{ N/mm}^2$$

$$\sigma_{atfueff} = \frac{M_{a,Ed}(h - h_{a.seff})}{I_{a.eff}} + \frac{M_{c,Ed}(h - h_{seff})}{I_{eff}} = |-263.835| \text{ N/mm}^2 \leq f_{ydf} = 315 \text{ N/mm}^2$$

Further explanations on the shear resistance check

See Paragraph 3.1.2.5.2, page 89ff.

$$\sigma_{tslreff} = \frac{M_{c,Ed}(h + c_{lr} - h_{seff})}{I_{eff}} = |\text{-}145.378| \text{ N/mm}^2 \leq f_{sd} = 434.783 \text{ N/mm}^2$$

$$\sigma_{tsureff} = \frac{M_{c,Ed}(h + e - c_{ur} - h_{seff})}{I_{eff}} = |\text{-}170.141| \text{ N/mm}^2 \leq f_{sd} = 434.783 \text{ N/mm}^2$$

The bending moment resistance is governed by the resistance of the top flange:

$$\eta_1 = \frac{|\sigma_{atfueff}|}{f_{ydf}} = 0.838 \leq 1$$

⇒ **Bending resistance is verified!**

3.1.5.10.2 Shear resistance check

The web should be checked in terms of shear buckling if:

$\frac{h_w}{t_w} = 116.316 > \frac{31}{\eta}\varepsilon_w\sqrt{k_t} = 62.035$ so that the check is necessary.

The maximum design shear resistance is given by#

$V_{Rd} = min\ (V_{b,Rd};\ V_{pl,a,Rd})$

where $V_{b,Rd} = V_{bw,Rd} + V_{bf,Rd} \leq \frac{\eta f_{yw} h_w t_w}{\sqrt{3}\gamma_{M1}} = 9.124$ MN

$V_{pl,a,Rd} = 10.037$ MN

where η = 1.2 for steel grades up to and including S460

Contribution of the web $V_{bw,Rd}$

$$V_{bw,Rd} = \frac{\chi_w f_{yw} h_w t_w}{\sqrt{3}\gamma_{M1}}$$

The vertical stiffeners at the bracing transverse frames which border the webpanel adjacent to the support P2 and located in span P1-P2, are assumed to be rigid (to be checked by using Section 9 of EN 1993-1-5). They are equally spaced by *a* = 7;5 m. Near the support P2, the second subpanel has a length a = 2.5 m.

$k_{\tau st} = 0$ because there is no longitudinal stiffeners

$a/h_w = 1.131 \geq 1$

$$k_\tau = 5.34 + 4\left(\frac{h_w}{a}\right)^2 + k_{\tau st} = 8.466$$

$$\bar{\lambda}_w = \frac{h_w}{37.4 t_w \varepsilon_w \sqrt{k_\tau}} = 1.295 \geq 1.08$$

$$\Rightarrow \chi_w = \frac{1.37}{\left(0.7 + \bar{\lambda}_w\right)} = 0.687$$

$V_{bw,Rd} == 5.221$ MN

Further explanations on the M-V-interaction

See Paragraph 3.1.2.5.3, page 93 and Paragraph 3.1.5.5.3, page 131.

Contribution from the flanges $V_{bf,Rd}$

The design plastic resistance moment of the flanges only is calculated from the position of the PNA (see Paragraph 3.1.5.5.2): $M_{f,\,Rd} = 71.569$ MNm

$$c = a\left(0.25 + \frac{1.6 b_f t_f^2 f_{yf}}{t h_w^2 f_{yw}}\right) = 0.909 \text{ m}$$

$$V_{bf,Rd} = \frac{b_f t_f^2 f_{yf}}{c\gamma_{M1}}\left(1 - \left(\frac{M_{Ed}}{M_{f,Rd}}\right)^2\right) = 0.769 \text{ MN}$$

In this case, the contribution of the flanges $V_{bf,Rd}$ is not negligible compared to the contribution from the web and represents 12.8 % of the design shear buckling resistance.

$$V_{b,Rd} = V_{bw,Rd} + V_{bf,Rd} = 5.221 + 0.769 = 5.99 \text{ MN} \leq \frac{\eta f_{yw} h_w t_w}{\sqrt{3}\gamma_{M1}} = 9.124 \text{ MN}$$

$$V_{Rd} = min\ (V_{b,Rd};\ V_{pl,a,Rd}) = min(5.99;\ 9.124) = 5.99 \text{ MN}$$

The flanges are not completely used to resist the bending moment (i.e. $M_{Ed} \leq M_{f,\,Rd}$ which is verified in the example: $M_{Ed} = 58.222$ MNm $\leq M_{f,\,Rd} = 71.569$ MNm

Cross-section verification

The verification should be performed as follows:

$$V_{Ed} = 5.843 \text{ MN} \leq V_{Rd} = min\ (5.99;\ 10.037) = 5.99 \text{ MN}$$

$$\eta_3 = \frac{V_{Ed}}{V_{Rd}} = 0.975 \leq 1$$

⇒ **Shear resistance is verified!**

3.1.5.10.3 M-V-interaction

$$V_{Ed} = 5.843 \text{ MN} \geq 0.5\ V_{Rd} = 2.995 \text{ MN}$$

Therefore the M-V-interaction should be checked.

$$\frac{M_{Ed}}{M_{f,Rd}} = 0.814 \leq 1\ ;\quad \frac{V_{Ed}}{V_{bw,Rd}} = 0.975 \leq 1$$

$M_{Ed} < M_{f,Rd}$ so that according to EN 1993-1-5, 7.1 (1), there is no interaction. It means that the flanges are enough to resist alone the bending moment so that the entire web can be used for the resistance to the shear force.

Then flanges of the steel girder take the bending moment and web of the steel beam takes shear force.

⇒ **There is no interaction.**

3.1.5.11 Subpanel 3 - Geometry

Follow the same procedure as for sup-panel 1 (see Paragraph 3.1.5.1)

At internal support P2 at ULS the concrete slab is in tension over its whole height. Its contribution is therefore neglected in the cross-section resistance.

The geometry of the cross-section of the subpanel 3 is totaly the same as the geometry of the cross-section of the subpanel 1. Only the length of the panel change (a = 4.333 m)

Further explanations on the determination of the cross-section class

See Paragraph 3.1.5.4, page 117ff.

Further explanations on the bending resistance check

See Paragraph 3.1.2.5.1, page 87f. and Paragraph 3.1.5.5.1, page 121ff.

3.1.5.12 Subpanel 3 - Material properties

See Paragraph 3.1.5.2.

The material properties of the cross-section of the subpanel 3 are identical to the material properties of the cross-section of the subpanel 1.

3.1.5.13 Subpanel 3 - Internal forces and moments

The internal forces and moments in this cross-section are (see Figure 2-31 and Figure 2-32):

M_{Ed} = 47.188 MNm (at the internal support P2: x = 114 m)

V_{Ed} = 5.435 MN (at the internal support P2: x = 114 m)

3.1.5.14 Subpanel 3 - Determination of the cross-section class

See Paragraph 3.1.5.4.

As the geometry of the cross-section does not change compared to subpanel 1, the cross-section class is the same for subpanel 3.

3.1.5.15 Subpanel 3 - Elastic section analysis

3.1.5.15.1 Bending resistance check

The plate buckling verification of the panel should be carried out for the stress resultants at a distance 0.4·a or 0.5·b: *min(0.4·a ; 0.5·b) = min(1.733 ; 1.105)* = 1.105 m

Then the value of the bending moment becomes: M_{Ed} *(min(0.4a ; 0.5b))* = 42.707 MNm

The stress on each level of the cross-section can be easily determinated:

$$\sigma_{abfleff} = \frac{-M_{a,Ed} h_{a.seff}}{I_{a.eff}} + \frac{-M_{c,Ed} h_{seff}}{I_{eff}} = 209.739 \text{ N/mm}^2 \leq f_{ydf} = 315 \text{ N/mm}^2$$

$$\sigma_{abfueff} = \frac{-M_{a,Ed}(h_{a.seff} - t_f)}{I_{a.eff}} + \frac{-M_{c,Ed}(h_{seff} - t_f)}{I_{eff}} = 193.052 \text{ N/mm}^2$$

$$\leq \min\left(f_{ydf}; f_{ydw}\right) = 315 \text{ N/mm}^2$$

$$\sigma_{atfleff} = \frac{M_{a,Ed}(h - t_f - h_{a.seff})}{I_{a.eff}} + \frac{M_{c,Ed}(h - t_f - h_{seff})}{I_{eff}} = |-195.141| \text{ N/mm}^2$$

$$\leq \min\left(f_{ydf}; f_{ydw}\right) = 315 \text{ N/mm}^2$$

$$\sigma_{atfueff} = \frac{M_{a,Ed}(h - h_{a.seff})}{I_{a.eff}} + \frac{M_{c,Ed}(h - h_{seff})}{I_{eff}} = |-211.828| \text{ N/mm}^2 \leq f_{ydf} = 315 \text{ N/mm}^2$$

$$\sigma_{tslreff} = \frac{M_{c,Ed}(h + c_{lr} - h_{seff})}{I_{eff}} = |-123.815| \text{ N/mm}^2 \leq f_{sd} = 434.783 \text{ N/mm}^2$$

$$\sigma_{tsureff} = \frac{M_{c,Ed}(h + e - c_{ur} - h_{seff})}{I_{eff}} = |-144.905| \text{ N/mm}^2 \leq f_{sd} = 434.783 \text{ N/mm}^2$$

The bending moment resistance is governed by the resistance of the top flange:

$$\eta_1 = \frac{\left|\sigma_{atfueff}\right|}{f_{ydf}} = 0.672 \leq 1$$

⇒ **Bending resistance is verified!**

Further explanations on the shear resistance check

See Paragraph 3.1.2.5.2, page 89ff.

3.1.5.15.2 Shear resistance check

The web should be checked in terms of shear buckling if:

$\frac{h_w}{t_w} = 116.316 > \frac{31}{\eta}\varepsilon_w\sqrt{k_t} = 53.856$ then the web should be checked in terms of shear buckling.

The maximum design shear resistance is given by

$$V_{Rd} = min\ (V_{b,Rd};\ V_{pl,a,Rd})$$

where $V_{b,Rd} = V_{bw,Rd} + V_{bf,Rd} \leq \frac{\eta f_{yw} h_w t_w}{\sqrt{3}\gamma_{M1}} = 9.124$ MN

$$V_{pl,a,Rd} = \frac{\eta f_{yw}}{\sqrt{3}\gamma_{M0}} h_w t_w = 10.037 \text{ MN}$$

where η = 1.2 for steel grades up to and including S460

Contribution of the web $V_{bw,Rd}$

$k_{\tau st} = 0$ because there is no longitudinal stiffeners

$$a/h_w = 1.961 \geq 1$$

$$k_\tau = 5.34 + 4\left(\frac{h_w}{a}\right)^2 + k_{\tau st} = 6.381$$

$$\bar{\lambda}_w = \frac{h_w}{37.4 t_w \varepsilon_w \sqrt{k_\tau}} = 1.492 \geq 1.08$$

$$\Rightarrow \chi_w = \frac{1.37}{\left(0.7 + \bar{\lambda}_w\right)} = 0.625$$

$$V_{bw,Rd} == 4.753 \text{ MN}$$

Contribution from the flanges $V_{bf,Rd}$

The design plastic resistance moment of the flanges only is calculated from the position of the PNA (see Paragraph 3.1.5.5.2): $M_{f,Rd} = 71.569$ MNm

$$c = a\left(0.25 + \frac{1.6 b_f t_f^2 f_{yf}}{t h_w^2 f_{yw}}\right) = 1.576 \text{ m}$$

$$V_{bf,Rd} = \frac{b_f t_f^2 f_{yf}}{c\gamma_{M1}}\left(1 - \left(\frac{M_{Ed}}{M_{f,Rd}}\right)^2\right) = 0.742 \text{ MN}$$

The design plastic resistance moment of the flanges only is calculated from the position of the PNA: $M_{f,Rd} = 71.569$ MNm

In this case, the contribution of the flanges $V_{bf,Rd}$ is not negligible compared to contribution from the web and represent 13.5 % of the design shear buckling resistance.

$$V_{b,Rd} = V_{bw,Rd} + V_{bf,Rd} = 4.753 + 0.742 = 5.494 \text{ MN} \leq \frac{\eta f_{yw} h_w t_w}{\sqrt{3}\gamma_{M1}} = 9.124 \text{ MN}$$

$$V_{Rd} = min\ (V_{b,Rd};\ V_{pl,a,Rd}) = min(5.494;\ 10.037) = 5.494 \text{ MN}$$

Further explanations on the M-V-interaction

See Paragraph 3.1.2.5.3, page 93 and Paragraph 3.1.5.5.3, page 131.

The flanges are not completely used for resisting to bending moment (i.e. $M_{Ed} \leq M_{f,Rd}$ which is verified in the example: $M_{Ed} = 47.188$ MNm $\leq M_{f,Rd} = 71.569$ MNm

Cross-section verification

The verification should be performed as follows:

$$V_{Ed} = 5.435 \text{ MN} \leq V_{Rd} = min\,(5.494;\ 10.037) = 5.494 \text{ MN}$$

$$\eta_3 = \frac{V_{Ed}}{V_{Rd}} = 0.989 \leq 1$$

Therefore the cross-section at support P2 is checked under shear force.

3.1.5.15.3 M-V-interaction

$$V_{Ed} = 5.435 \text{ MN} \geq 0.5\ V_{Rd} = 2.747 \text{ MN}$$

Therefore the M-V-interaction should be checked.

$$\frac{M_{Ed}}{M_{f,Rd}} = 0.659 \leq 1\ ;\ \frac{V_{Ed}}{V_{bw,Rd}} = 1.106 \geq 1\ ;\ \frac{V_{Ed}}{V_{b.Rd}} = 0.989 \leq 1$$

$M_{Ed} < M_{f,Rd}$ so that according to EN 1993-1-5, 7.1 (1), there is no interaction. It means that the flanges are enough to resist alone the bending moment so that the entire web can be used for the resistance to the shear force.

Thus, the flanges of the steel girder take the bending moment and web of the steel beam takes shear force.

⇒ There is no interaction.

3.2 Box-girder bridge

3.2.1 General

According to the shape of the bending moment and shear force diagrams at ULS (see Figure 2-36 and Figure 2-37), the two different critical sections to check are displayed in Figure 3-9:

- At mid-span P1-P2, see Section 3.2.2
- At the internal support P3, see Section 3.2.3

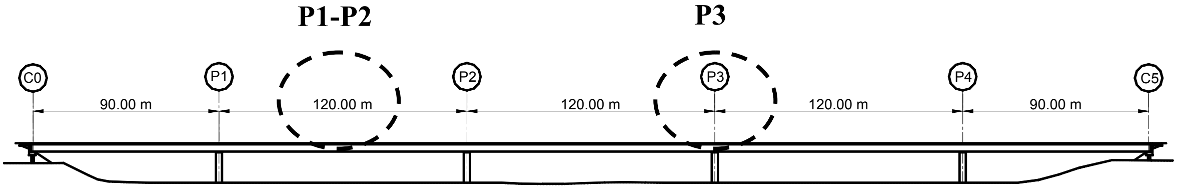

Figure 3-9: Checked sections of the box-girder bridge.

For each critical section, the verification is done on a panel which is located between two vertical stiffeners.

3.2.2 Check of cross-section at mid-span P1-P2

3.2.2.1 Geometry

At mid-span P1-P2, at ULS the concrete slab is almost in compression over its whole height. Its contribution is therefore taken into account in the cross-section resistance.

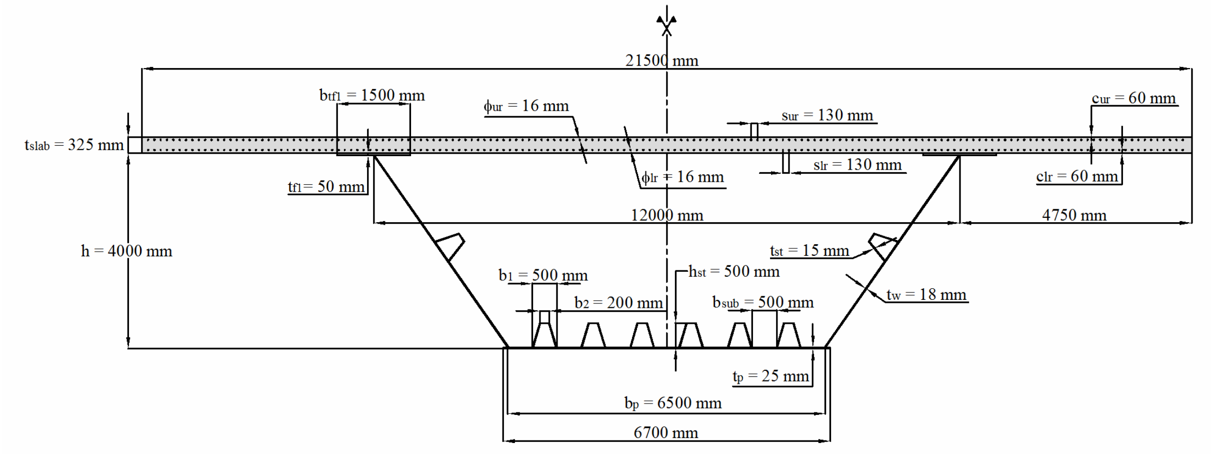
21500 mm
btfl = 1500 mm
ϕur = 16 mm
sur = 130 mm
cur = 60 mm
tslab = 325 mm
tfl = 50 mm
ϕlr = 16 mm
slr = 130 mm
clr = 60 mm
12000 mm
4750 mm
h = 4000 mm
tst = 15 mm
b1 = 500 mm
hst = 500 mm
b2 = 200 mm
bsub = 500 mm
tw = 18 mm
tp = 25 mm
bp = 6500 mm
6700 mm

Figure 3-10: Cross-section of the box-girder bridge at mid-span P1-P2.

General properties of the box-girder bridge in cross-section P1-P2	**Main areas of the different parts of the composite section**
$L_1 = L_2 = 120$ m $a = 4$ m $h = 4$ m $h_w = \dfrac{(h - t_{t.tf} - t_p)}{\cos(\theta_w)} = 4.763$ m $t_w = 18$ mm $b_p = 6500$ mm $t_p = 25$ mm $t_{slab} = 32.5$ cm $\phi_{ur} = 16$ mm $\phi_{lr} = 16$ mm $s_{ur} = 130$ mm $s_{lr} = 130$ mm $c_{ur} = 60$ mm $c_{lr} = 60$ mm $b_{slab} = 21.5$ m	$A_{atf} = t_{tf} b_{tf} = 0.075\ \mathrm{m^2}$ $A_{aw} = t_w h_w = 0.086\ \mathrm{m^2}$ $A_{st.w} = 2h_{st.w} t_{st.v.w} + b_{2.st.w} t_{st.w} = 184.451\ \mathrm{cm^2}$ $A_{abf} = t_p b_p = 0.163\ \mathrm{m^2}$ $A_{sur} = \dfrac{\pi d_{ur}^2}{4} = 2.011\ \mathrm{cm^2}$ $A_{tsur} = n_{ur} A_{sur} = 332.525\ \mathrm{cm^2}$ $A_{slr} = \dfrac{\pi d_{lr}^2}{4} = 2.011\ \mathrm{cm^2}$ $A_{tslr} = n_{lr} A_{slr} = 332.525\ \mathrm{cm^2}$ $A_c = t_{slab} b_{slab} = 6.987\ \mathrm{m^2}$ (see notation and Figure 3-10)

3.2.2.2 Material properties

Structural steel

$f_y(t_w) = 345$ N/mm² because 16 mm < t_w = 18 mm ≤ 40 mm (see Table 2-4)

$$\varepsilon(t_w) = \sqrt{\frac{235 N/mm^2}{f_y(t_w)}} = 0.825$$

$f_y(t_p) = 345$ N/mm² because 16 mm < t_p = 25 mm ≤ 40 mm (see Table 2-4)

$$\varepsilon(t_p) = \sqrt{\frac{235 N/mm^2}{f_y(t_p)}} = 0.825$$

$f_y(t_{tf}) = 335$ N/mm² because 40 mm < t_{tf} = 50 mm ≤ 63 mm (see Table 2-4)

$$\varepsilon(t_{tf}) = \sqrt{\frac{235 N/mm^2}{f_y(t_{tf})}} = 0.838$$

$f_y(t_{st.w}) = 315$ N/mm² because $t_{st.w}$ = 15 mm ≤ 16 mm (see Table 2-4)

$$\varepsilon(t_{st.w}) = \sqrt{\frac{235 N/mm^2}{f_y(t_{st.w})}} = 0.814$$

$$f_{yd}(t_w) = \frac{f_y(t_w)}{\gamma_{M0}} = 345 \text{ N/mm}^2,\ f_{yd}(t_p) = \frac{f_y(t_p)}{\gamma_{M0}} = 345 \text{ N/mm}^2,$$

$$f_{yd}(t_{tf}) = \frac{f_y(t_{tf})}{\gamma_{M0}} = 335 \text{ N/mm}^2,\ f_{yd}(t_{st.w}) = \frac{f_y(t_{st.w})}{\gamma_{M0}} = 355 \text{ N/mm}^2$$

$E_a = 210000$ N/mm²

Concrete

$f_{ck} = 35$ N/mm²

$$f_{cd} = \frac{f_{ck}}{\gamma_c} = 23.333 \text{ N/mm}^2$$

$E_{cm} = 34077$ N/mm²

$$n = \frac{E_a}{E_{cm}} = \frac{210000}{34077} = 6.163$$

Reinforcement

$f_{sk} = 500$ N/mm²

$$f_{sd} = \frac{f_{sk}}{\gamma_s} = 434.734 \text{ N/mm2}$$

$E_s = E_a = 210000$ N/mm²

3.2.2.3 Internal forces and moments

The internal forces and moments are obtained from the design model at ULS based on the cracked global analysis (see Section 2.4.2.6.2) and, considering the construction steps, they are as follows for the whole box section (see Figure 2-36 and Figure 2-37):

Further explanations on the determination of the cross-section class

See Paragraph 3.1.5.4, page 117ff.

M_{Ed} = 2·150.411 MNm = 300.822 MNm for the whole cross-section

V_{Ed} = 2·2.697 MN = 5.394 MN

i.e. $V_{\frac{Ed.proj}{2}} = \dfrac{V_{Ed}}{2\cos(\theta_w)}$ = 3.273 MN in each steel web by taking its inclination into account

where $\theta_w = a\tan(\dfrac{12-b_p}{2h}) = 0.602$ =34.509°

3.2.2.4 Reduction due to shear lag effect

Verification if shear lag effect has to be taken into account:

Bridge span:	L_1 = 120 m and L_2 = 120 m
Effective length:	L_e = 0.7 L_2= 84 m
Considered width:	$b_0 = b_p/2$ = 3.25 m

⇒ $b_0 < L_e/50$ requirement not fulfilled! Shear lag effect has to be taken into account.

Shear lag parameters:

$$\alpha^\circ_0 := \sqrt{1 + \frac{\frac{A_{sl}}{2}}{b_0 \cdot t_p}} = 1.297$$

$$\kappa := \alpha^\circ_0 \cdot \frac{b_0}{L_e} = 0.05$$

$$\beta_{ult} := \left| \begin{array}{ll} 1 \quad \text{if} \ \kappa \le 0.02 & \\ \dfrac{1}{1 + 6 \cdot \left(\kappa - \dfrac{1}{2500 \cdot \kappa} \right) + 1.6 \cdot \kappa^2} & \text{if} \ 0.02 < \kappa \le 0.7 \\ \dfrac{1}{8.6 \cdot \kappa} \quad \text{otherwise} & \end{array} \right.$$

$$\beta_{ult} = 0.795$$

$$\beta_{ult}^{\ \kappa} = 0.989$$

3.2.2.5 Determination of the cross-section class

The web is in tension in its upper part and in tension in its lower part. As the upper flange is perfectly connected to the slab, it is a Class 1 element. To classify the steel web, the position of the Plastic Neutral Axis (PNA) is determined as follows:

- Design plastic resistance of the bottom flange

$$N_{a.bf} = \left(n_{st}\left[t_{st} f_{yd}(t_{st.w})(b_2 + 2b_3) + t_p f_{yd}(t_p)(b_1 + b_{sub})\right] + t_p f_{yd}(t_p)(0.2m + b_{sub})\right)\beta_{ult}^{\kappa} = 95.967 \text{ MN}$$

- Design plastic resistance of the 2 webs

$$N_{a.w} = 2\left[(h - t_{tf} - t_p)t_{w.h} f_{yd}(t_w)\right] = 59.158 \text{ MN}$$

Relations to find the location of the Plastic Neutral Axis (PNA) under positive moment $M_{Pl,Rd}$

RELATIONS	PNA LOCATION
$N_{abf} \geq N_{aw} + N_{atf} + N_c$	PNA in the bottom flange
$N_{abf} + N_{aw} \geq N_{aft} + N_c$ and $N_{abf} < N_{aw} + N_{atf} + N_c$	PNA in the web
$N_a \geq N_c$ and $N_{abf} + N_{aw} < N_{atf} + N_c$	PNA in the top flange
$N_c > N_{abf} + N_{aw} + N_{atf}$	PNA in the slab

Further explanations on the bending resistance check

See Paragraph 3.1.2.5.1, page 87f.

Further explanations on the shear resistance check

See Paragraph 3.1.2.5.2, page 89ff.

- Design plastic resistance of the 2 structural steel top flange 1

$$N_{a.tf} = 2b_{tf}t_{tf}f_{yd}(t_{tf}) = 59.158 \text{ MN}$$

- Design plastic resistance of the concrete slab in compression

$$N_{a.tf} = 0.85t_{slab}b_{slab}f_{cd} = 138.585 \text{ MN}$$

- Location of the Plastic Neutral Axis (PNA)

$N_{abf} + N_{aw} + N_{atf} = 206.484$ MN $\geq N_c = 138.585$ MN

and $N_{abf} + N_{aw} = 156.234$ MN $< N_c + N_{atf} = 188.835$ MN

Thus, the PNA is deduced to be located in the top flange at a distance z_{pl} from the extreme lower fiber of the bottom flange. Writing the force equilibrium around the PNA gives:

$$z_{pl} = \frac{4hb_{tf}f_{yd}(t_{tf}) + N_c - N_{a.bf} - N_{a.w} - N_{a.tf}}{4b_{tf}f_{yd}(t_{tf})} = 3.967 \text{ m}$$

Thus, the whole web is in tension.

Conclusion: the cross-section at mid-span P1-P2 is in Class 1 and is checked by a plastic section analysis.

3.2.2.6 Bending resistance verification

The design plastic resistance moment is calculated from the position of the PNA
(see Paragraph 3.2.2.5):

$$M_{pl,Rd} = N_{a.bf}\left(z_{pl} - \frac{t_p}{2}\right) + N_{a.w}\left(z_{pl} - \frac{\left(h - t_{tf} + t_p\right)}{2}\right) + N_c\left(h + \frac{t_{slab}}{2} - z_{pl}\right) + \frac{\left(h - z_{pl}\right)^2}{2}b_{tf}f_{yd}(t_{tf}) + \frac{\left(h - t_f - z_{pl}\right)^2}{2}b_{tf}f_{yd}(t_{tf}) = 524.044 \text{ MNm}$$

Reinforcement in compression in the concrete slab is neglected according EN 1994-2, 6.2.1.2(1).

$M_{Ed} = 300.822$ MNm $< M_{pl,Rd} = 524.044$ MNm

Bending resistance is verified!

3.2.2.7 Shear resistance verification

3.2.2.7.1 Shear in the box-girder webs

The box-girder web is transversally stiffened on both sides at mid-span P1-P2 ($a_w = 4$ m).

Stiffened webpanel

To evaluate the shear buckling coefficient of the stiffened webpanel, the second moment of area of the longitudinal stiffener must be calculated according to EN 1993-1-5, Figure 5.3:

$$15\varepsilon\left(t_w\right)t_w = 0.223 \text{ m} \leq \frac{b_{1.st.w}}{2} = 0.25 \text{ m}$$

The elastic neutral axis of the web stiffener with the width $15\varepsilon\left(t_w\right)t_w$ on both sides of the stiffener is:

$$z_{st.w} = \frac{2h_{st.w}t_{st.v.w}\left(\frac{h_{st.w}+t_w}{2}\right) + b_{2.st.w}t_{st.w}\left(h_{st.w}+\frac{t_w}{2}\right)}{2h_{st.w}t_{st.v.w} + b_{2.st.w}t_{st.w} + 4\cdot 15\varepsilon\left(t_w\right)t_w^2} = 0.158\text{m}$$

The second moment of area of the web stiffener is:

$$I_{st.w} = I_{sl.w} = b_{2.st.w}t_{st.w}(h_{st.w} - z_{st.w})^2 + 2\left[\frac{t_{st.v.w}h_{st.w}^3}{12} + t_{st.w}h_{st.w}\left(\frac{h_{st.w}}{2} - z_{st.w}\right)^2\right] + 4\cdot 15\varepsilon(t_w)t_w t_w z_{st.w}^2$$

$$= 9.829\cdot 10^{-4}\ \text{m}^4$$

According to EN 1993-1-5, Annex 3(2), as there is only one stiffener in the web and the aspect ratio is $\alpha_w = \frac{a_w}{h_w} = 0.84 \leq 3$, the shear buckling coefficient is:

$$k_{\tau.w} = 4{,}1 + \frac{6{,}3 + 0{,}18\frac{I_{sl.w}}{t_w^3 h_w}}{\alpha_w^2} + 2{,}2\sqrt[3]{\frac{I_{sl,w}}{t_w^3 h_w}} = 29.287$$

The transverse stiffeners of the bracings frames bordering the webpanel close to mid-span P1-P2 are assumed to be rigid.

$$\frac{h_w}{t_w} = \frac{4763}{18} = 264.617 > \frac{31}{\eta}\varepsilon(t_w)\sqrt{k_{\tau.w}} = 115.383$$

Thus, the stiffened webpanel must be checked against shear buckling.

The reduced slenderness of the stiffened webpanel:

$$\bar{\lambda}_w = \frac{h_w}{37.4t_w\varepsilon(t_w)\sqrt{k_{\tau.w}}} = 1.584$$

NOTE: Alternatively, the reduced slenderness can be calculated by another way which gives the same results.

The elastic critical shear buckling stress is given by:

$$\tau_{cr} = k_{\tau.w}\sigma_E = 79.384\ \text{MPa}$$

$$\text{with } \sigma_E = \frac{\pi^2 E_a t_w^2}{12\left(1-\nu^2\right)h_w^2} = 2.711\ \text{MPa}$$

$$\Rightarrow \qquad \bar{\lambda}_w = \sqrt{\frac{f_y(t_w)}{\tau_{cr}\sqrt{3}}} = 1.584$$

Web subpanels

It is possible that one or both of the two web subpanels are more critical than the stiffened webpanel. Thus, the two web subpanels must be also checked. As the longitudinal stiffeners is located at the middle of the height of the web, the two webs subpanels have the same width and the same reduced slenderness.

According to EN 1993-1-5, Annex 3(1), as the aspect ratio is $\alpha_w = \frac{a_w}{b_{spw}} = \frac{4}{2.016} = 1.984 \geq 1$, the shear buckling coefficient is:

$$k_{\tau.w.sp} = 5.34 + 4\left(\frac{b_{w.sp}}{a_w}\right)^2 = 6.356$$

EN 1993-1-1, 6.2.6, Shear

(1) The design value of the shear force V_{Ed} at each cross-section should satisfy:

$$\frac{V_{Ed}}{V_{c,Rd}} \leq 1,0 \qquad (6.17)$$

where $V_{c,Rd}$ is the design shear resistance. For plastic design $V_{c,Rd}$ is the design plastic shear resistance $V_{pl,Rd}$ as given in (2). For elastic design $V_{c,Rd}$ is the design elastic shear resistance calculated using (4) and (5).

(2) In the absence of torsion the design plastic shear resistance is given by:

$$V_{pl,Rd} = \frac{A_v\left(f_y / \sqrt{3}\right)}{\gamma_{M0}} \qquad (6.18)$$

where A_v is the shear area.

EN 1993-1-5, 5.5, Verification

(1) The verification should be performed as follows:

$$\eta_3 = \frac{V_{Ed}}{V_{b,Rd}} \leq 1$$

where V_{Ed} is the design shear force including shear from torque.

$$\frac{b_{w.sp}}{t_w} = \frac{2016}{18} = 112.015 > \frac{31}{\eta}\varepsilon(t_w)\sqrt{k_{\tau.w}} = 53.754$$

Thus, the web subpanels must be checked against shear buckling.

The reduced slenderness of the web subpanel:

$$\bar{\lambda}_{w.sp} = \frac{b_{w.sp}}{37.4 t_w \varepsilon(t_w)\sqrt{k_{\tau.w.sp}}} = 1.439$$

Shear resistance verification

Thus, it is the stiffened webpanel which is critical: $\bar{\lambda}_w = \max(\bar{\lambda}_w, \bar{\lambda}_{w.sp}) = 1.584$

As the webpanel close to mid-span P1-P2 is assumed to be rigid and $1.08 \le \bar{\lambda}_w$, the reduction factor is:

$$\chi_w = \frac{1.37}{\left(0.7 + \bar{\lambda}_w\right)} = 0.6$$

The maximum design value of the shear resistance is given by

$V_{Rd} = \min(V_{b,Rd}; V_{pl,a,Rd})$ with $V_{b,Rd} = V_{bw,Rd}$

neglecting the flange contribution to the resistance:

$$V_{bw,Rd} = \min\left(\frac{\chi_w f_y(t_w) h_w t_w}{\sqrt{3}\gamma_{M1}}; \frac{\eta f_y(t_w) h_w t_w}{\sqrt{3}\gamma_{M1}}\right) = 9.312 \text{ MN}$$

$$V_{pl,a,Rd} = \frac{\eta f_y(t_w) h_w t_w}{\sqrt{3}\gamma_{M0}} = 20.493\text{MN}$$

so that $\eta_3 = \frac{V_{Ed}}{V_{Rd}} = \frac{3.273}{9.312} = 0.351 < 1$

Shear resistance is verified!

Addition of torsional effect

The maximum torque on the box-girder bridge at mid-span P1-P2 is equal to M_T = 1.35.8.774 MNm = 11.845 MNm (see Figure 2-35).

The area inside the median line of the cross-section of the box-girder bridge is:

$$S = \frac{\left(b_t + b_p\right)\left(h + \frac{t_{slab}}{2}\right)}{2} = \frac{\left(12 + 6.5\right)\left(4 + \frac{0.325}{2}\right)}{2} = 38.503 \text{ m}^2$$

The shear stress in the web is given by the Bredt formula:

$$\tau_{Ed,T,web} = \frac{M_T}{2St_w} = 8.545\text{MPa}$$

The shear force in the web due to torque is:

$$V_{Ed,T,web} = \tau_{Ed,T,web} t_w h_w = 0.733 \text{ MN}$$

Thus, the verification of shear including torsional effects gives:

Further explanations on the M-V-interaction

See Paragraph 3.1.2.5.3, page 93.

$$\eta_3 = \frac{V_{Ed} + V_{T,web}}{V_{Rd}} = \frac{3.273 + 0.733}{9.312} = 0.43 < 1$$

Shear resistance inluding shear from torque is verified!

3.2.2.8 Interaction between bending moment and shear force

$$\bar{\eta}_3 = \frac{V_{Ed}}{V_{bw,Rd}} = 0.43 \leq 0.5$$

⇒ **There is no need to check the M-V-interaction.**

3.2.3 Check of cross-section at the internal support P3

3.2.3.1 Geometry

As the concrete slab is in tension around the internal support P3, the strength is not taken into account for checking the cross-section. Only the longitudinal slab reinforcement is considered.

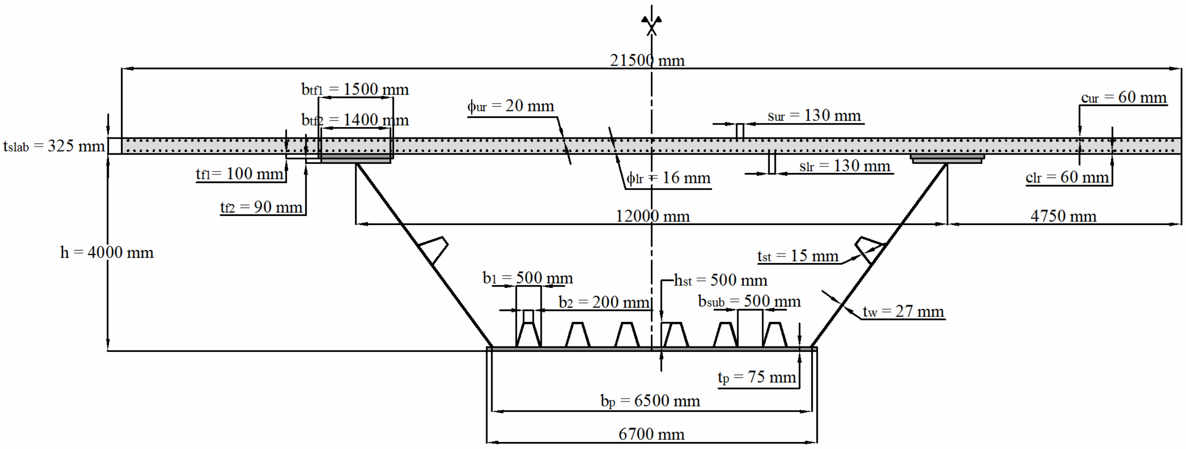
21500 mm
btf1 = 1500 mm
btf2 = 1400 mm
ϕur = 20 mm
sur = 130 mm
cur = 60 mm
tslab = 325 mm
tf1= 100 mm
tf2 = 90 mm
ϕlr = 16 mm
slr = 130 mm
clr = 60 mm
12000 mm
4750 mm
h = 4000 mm
tst = 15 mm
b1 = 500 mm
b2 = 200 mm
hst = 500 mm
bsub = 500 mm
tw = 27 mm
tp = 75 mm
bp = 6500 mm
6700 mm

Figure 3-11: Cross-section of the box-girder bridge at the internal support P3.

General properties of the box-girder bridge in cross-section P3	Main areas of the different parts of the composite section
$L_1 = L_2 = 120$ m $a = 2.5$ m $h = 4$ m $h_w = \frac{(h - t_{t.tf.1} - t_{t.tf.2} - t_p)}{\cos(\theta_w)} = 4.533$ m $t_w = 27$ mm $b_p = 6500$ mm $t_p = 75$ mm $t_{slab} = 32.5$ cm	$A_{atf.1} = t_{tf.1} b_{tf.1} = 0.15$ m² $A_{atf.2} = t_{tf.2} b_{tf.2} = 0.126$ m² $A_{aw} = t_w h_w = 0.122$ m² $A_{st.w} = 2h_{st.w} t_{st.v.w} + b_{2.st.w} t_{st.w} = 184.451$ cm^2 $A_{abf} = t_p b_p = 0.488$ m² $A_{sur} = \frac{\pi d_{ur}^2}{4} = 3.142$ cm²

General properties of the box-girder bridge in cross-section P3	**Main areas of the different parts of the composite section**
$\phi_{ur} = 20$ mm $\phi_{lr} = 16$ mm $s_{ur} = 130$ mm $s_{lr} = 130$ mm $c_{ur} = 60$ mm $c_{lr} = 60$ mm $b_{slab} = 21.5$ m	$A_{tsur} = n_{ur} A_{sur} = 519.571$ cm² $A_{slr} = \frac{\pi d_{lr}^2}{4} = 2.011$ cm² $A_{tslr} = n_{lr} A_{slr} = 332.525$ cm² $A_c = t_{slab} b_{slab} = 6.987$ m^2 (see notation and Figure 3-11)

3.2.3.2 Material properties

Structural steel

$f_y(t_w) = 345$ N/mm² because 16 mm < t_w = 27 mm ≤ 40 mm (see Table 2-4)

$$\varepsilon(t_w) = \sqrt{\frac{235 N/mm^2}{f_y(t_w)}} = 0.825$$

$f_y(t_p) = 325$ N/mm² because 63 mm < t_p = 75 mm ≤ 80 mm (see Table 2-4)

$$\varepsilon(t_p) = \sqrt{\frac{235 N/mm^2}{f_y(t_p)}} = 0.85$$

$f_y(t_{tf.1}) = 315$ N/mm² because 80 mm < $t_{tf.1}$ = 100 mm ≤ 100 mm (see Table 2-4)

$$\varepsilon(t_{tf.1}) = \sqrt{\frac{235 N/mm^2}{f_y(t_{tf.1})}} = 0.864$$

$f_y(t_{tf.2}) = 315$ N/mm² because 80 mm < $t_{tf.2}$ = 90 mm ≤ 100 mm (see Table 2-4)

$$\varepsilon(t_{tf.2}) = \sqrt{\frac{235 N/mm^2}{f_y(t_{tf.2})}} = 0.864$$

$f_y(t_{st.w}) = 355$ N/mm² because $t_{st.w}$ = 15 mm ≤ 16 mm (see Table 2-4)

$$\varepsilon(t_{st.w}) = \sqrt{\frac{235 N/mm^2}{f_y(t_{st.w})}} = 0.814$$

$$f_{yd}(t_w) = \frac{f_y(t_w)}{\gamma_{M0}} = 345 \text{ N/mm}^2,\ f_{yd}(t_p) = \frac{f_y(t_p)}{\gamma_{M0}} = 325 \text{ N/mm}^2,\ f_{yd}(t_{tf.1}) = \frac{f_y(t_{tf.1})}{\gamma_{M0}} = 315 \text{ N/mm}^2$$

$$f_{yd}(t_{tf.2}) = \frac{f_y(t_{tf.2})}{\gamma_{M0}} = 315 \text{ N/mm}^2,\ f_{yd}(t_{st.w}) = \frac{f_y(t_{st.w})}{\gamma_{M0}} = 355 \text{ N/mm}^2$$

$E_a = 210000$ N/mm²

Concrete

See Paragraph 3.2.2.2

Reinforcement

See Paragraph 3.2.2.2

3.2.3.3 Internal forces and moments

The internal forces and moments are obtained from the design model at ULS based on the cracked global analysis (see Section 2.4.2.6.2) and, considering the construction steps, they are as follows for the whole box section (see Figure 2-36 and Figure 2-37):

$M_{Ed} = 2 \cdot -369.889$ MNm = -739.778 MNm for the cross-section

$V_{Ed} = 2 \cdot 16.617$ MN = 33.234 MN for the whole cross-section

i.e. $V_{\frac{Ed.proj}{2}} = \dfrac{V_{Ed}}{2\cos(\theta_w)} = 20.165$ MN in each steel web by taking its inclination into account

where $\theta_w = a\tan(\dfrac{12 - b_p}{2h}) = 0.602 = 34.509°$

The maximal ULS stress in the upper reinforcement in cracked behaviour (hogging moment) given by the global analysis is:

$\sigma_{\sup.re\inf} = -144.598$ MPa

The bending moment $M_{c,\,Ed}$ applied to the composite box section (structural steel part + reinforcement) is:

$$M_{c,Ed} = \frac{\sigma_{\sup.re\inf} I_{tot}}{h + t_{slab} - c_{ur} - z_{na}} = -321.654 \text{ MNm}$$

The bending moment M_a applied to the structural steel is:

$$M_{a,Ed} = M_{Ed} - M_{c,Ed} = -739.778 \text{ MNm} - (-321.654 \text{ MNm}) = -418.124 \text{ MNm}$$

Thus, the bending moment M_{Ed} is the sum of the moment $M_{a,Ed}$ = -418.124 MNm applied to the box section (structural steel part only) as long as it behaves as a pure structural steel structure (before the concreting step of the slab segment which includes the studied box section) and of the bending moment $M_{c,Ed}$ = -321.654 MNm applied to the composite box section (structural steel part + reinforcement).

3.2.3.4 Mechanical properties of the gross cross-section

The mechanical properties of the composite box section (structural steel part and reinforcement) are:

- Area

$$\begin{aligned} A_{tot} := {} & A_{tsur} + A_{tslr} + 2\cdot\left(b_{tf.1}\cdot t_{tf.1} + b_{tf.2}\cdot t_{tf.2}\right) + 2\cdot\left[\left(h - t_{tf.1} - t_{tf.2} - t_p\right)\cdot t_{w.h} + A_{st.w}\right] \cdots \\ & + n_{st}\cdot\left[t_{st}\cdot\left(b_2 + 2\cdot b_3\right) + t_p\cdot\left(b_1 + b_{sub}\right)\right] + \left(b_{sub} + 0.2\text{m}\right)\cdot t_p \end{aligned}$$

$$A_{tot} = 1.532\,\text{m}^2$$

- First moment of area

$$\begin{aligned} S_{na} := {} & A_{tsur}\cdot\left(h + t_{slab} - c_{ur}\right) + A_{tslr}\cdot\left(h + c_{lr}\right) \cdots \\ & + 2\cdot\left[b_{tf.1}\cdot t_{tf.1}\cdot\left(h - \frac{t_{tf.1}}{2}\right) + b_{tf.2}\cdot t_{tf.2}\cdot\left(h - t_{tf.1} - \frac{t_{tf.2}}{2}\right)\right] \cdots \\ & + 2\cdot\left[\left(h - t_{tf.1} - t_{tf.2} - t_p\right)\cdot t_{w.h}\cdot\frac{\left(h - t_{tf.1} - t_{tf.2} - t_p\right)}{2} + A_{st.w}\cdot\frac{h - t_{tf.1} - t_{tf.2} + t_p}{2}\right] \cdots \\ & + \left[n_{st}\cdot\left[t_{st}\cdot\left(b_2 + 2\cdot b_3\right) + t_p\cdot\left(b_1 + b_{sub}\right)\right] + \left(b_{sub} + 0.2\text{m}\right)\cdot t_p\right]\cdot z_{sl.1} \end{aligned}$$

$$S_{na} = 3.081\cdot\text{m}^3$$

- Distance between the center of gravity and the lower face of the bottom flange

$$z_{na} := \frac{S_{na}}{A_{tot}} = 2.011\,\text{m}$$

- Second moment of area

$$\begin{aligned}
I_{tot} := {} & A_{tsur}\cdot\left(h + t_{slab} - c_{ur} - z_{na}\right)^2 + A_{tslr}\cdot\left(h + c_{lr} - z_{na}\right)^2 \ldots \\
& + 2\cdot\left[\frac{b_{tf.1}\cdot t_{tf.1}{}^3}{12} + \left(b_{tf.1}\cdot t_{tf.1}\right)\cdot\left(h - \frac{t_{tf.1}}{2} - z_{na}\right)^2\right] \ldots \\
& + 2\cdot\left[\frac{b_{tf.2}\cdot t_{tf.2}{}^3}{12} + \left(b_{tf.2}\cdot t_{tf.2}\right)\cdot\left(h - t_{tf.1} - \frac{t_{tf.2}}{2} - z_{na}\right)^2\right] \ldots \\
& + 2\cdot\left[\frac{t_{w.h}\cdot\left(h - t_{tf.1} - t_{tf.2} - t_p\right)^3}{12} + t_{w.h}\cdot\left(h - t_{tf.1} - t_{tf.2} - t_p\right)\cdot\left(\frac{h - t_{tf.1} - t_{tf.2} - t_p}{2} - z_{na}\right)^2\right] \ldots \\
& + 2\cdot A_{st.w}\cdot\left(\frac{h - t_{tf.1} - t_{tf.2} + t_p}{2} - z_{na}\right)^2 \ldots \\
& + \left[n_{st}\cdot\left[t_{st}\cdot\left(b_2 + 2\cdot b_3\right) + t_p\cdot\left(b_1 + b_{sub}\right)\right] + \left(b_{sub} + 0.2\text{m}\right)\cdot t_p\right]\cdot\left(z_{na} - z_{sl.1}\right)^2 + n_{st}\cdot I_{sl.1}
\end{aligned}$$

$$I_{tot} = 5.014\text{m}^4$$

3.2.3.5 Effective area of the bottom flange

3.2.3.5.1 General

In the following, the ultimate resistance of the longitudinal stiffened bottom plate is determined according to EN 1993-1-5, Section 3, Section 4 and Annex A.

3.2.3.5.2 Plate parameters

Geometry of the panel

Number of stiffeners (equally spaced):	$n_{st} = 6$ (≥ 3!)
Length of panel:	$a_p = 4.0$ m
Width of panel:	$b_p = 6.5$ m
Thickness of panel:	$t_p = 75$ mm

Geometry of the trapezoidal stiffeners

Distance between webs of stiffener:	$b_1 = 0.5$ m
Width of stiffener flange:	$b_2 = 0.2$ m
Height of stiffener:	$h_{st} = 0.4925$ m
Thickness of stiffener:	$t_{st} = 15$ mm

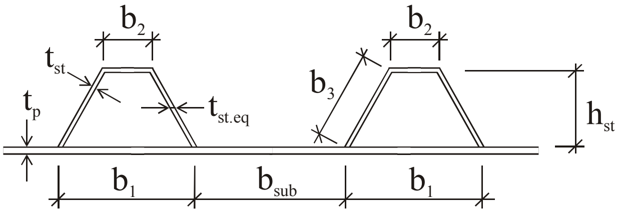

Figure 3-12: Geometry of the trapezoidal stiffeners.

EN 1993-1-5, 4.5.1, General

(1) For plates with longitudinal stiffeners the effective^p areas from local buckling of the various subpanels between the stiffeners and the effective^p areas from the global buckling of the stiffened panel should be accounted for.

(2) The effective^p section area of each subpanel should be determined by a reduction factor in accordance with 4.4 to account for local plate buckling. The stiffened plate with effective^p section areas for the stiffeners should be checked for global plate buckling (by modelling it as an equivalent orthotropic plate) and a reduction factor ρ should be determined for overall plate buckling.

(3) The effective^p area of the compression zone of the stiffened plate should be taken as:

$$A_{c,eff} = \rho_c \cdot A_{c,eff,loc} + \sum b_{edge,eff} \cdot t \qquad (4.5)$$

where $A_{c,eff,loc}$ is the effective^p section areas of all the stiffeners and subpanels that are fully or partially in the compression zone except the effective parts supported by an adjacent plate element with the width $b_{edge,eff}$, see example in Figure 4.4.

(4) The area $A_{c,eff,loc}$ should be obtained from:

$$A_{c,eff,loc} = A_{s\ell,eff} + \sum_c \rho_{loc} \cdot b_{c.eff} \cdot t \qquad (4.6)$$

where $\sum_c$ applies to the part of the stiffened panel width that is in compression except the parts $b_{edge,eff}$, see Figure 4.4;

$A_{s\ell,eff}$ is the sum of the effective^p sections according to 4.4 of all longitudinal stiffeners with gross area $A_{s\ell}$ located in the compression zone;

$b_{c,loc}$ is the width of the compressed part of each subpanel;

ρ_{loc} is the reduction factor from 4.4(2) for each subpanel.

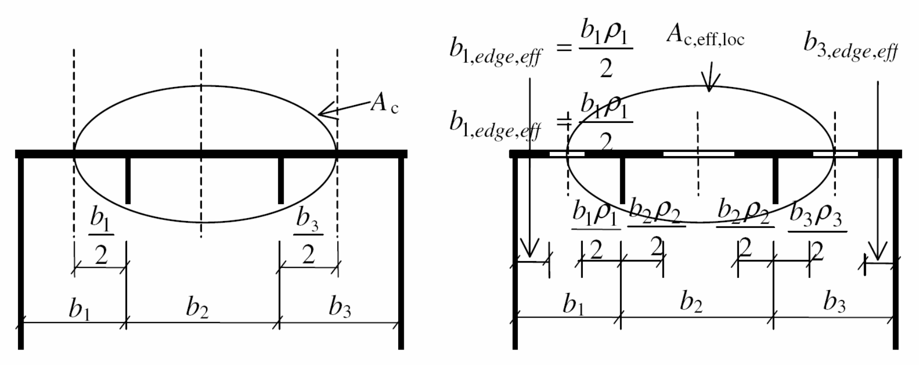

Figure 4.4: Stiffened plate under uniform compression

NOTE: For non-uniform compression see Figure A.1.

Resulting parameters

Width of each subpanel:

$$b_{sub} := \frac{b_p - n_{st} \cdot b_1}{\left(n_{st} + 1\right)} = 0.5\,m$$

Width of each stiffener web:

$$b_3 := \sqrt{h_{st}^2 + \left(\frac{b_1 - b_2}{2}\right)^2} = 0.515\,m$$

Equivalent thickness of stiffener web:

$$t_{st.eq} := t_{st} \cdot \frac{b_3}{h_{st}} = 15.68 \cdot mm$$

3.2.3.5.3 Effective^p cross-section of subpanels and stiffeners

Stress distribution:

$\psi = 1$

Buckling factor for internal compression elements:

$k_\sigma = 4$

Slenderness of analysed plate:

$$\bar{\lambda}_{local}(b, t) := \frac{b}{t \cdot 28.4 \cdot \varepsilon \cdot \sqrt{k_\sigma}}$$

Reduction factor for internal compression elements:

$$\rho_{local}(b, t) := \begin{cases} 1 & \text{if } \lambda_{local}(b, t) < 0.673 \\ \dfrac{\lambda_{local}(b, t) - 0.22}{\lambda_{local}(b, t)^2} & \text{otherwise} \end{cases}$$

Geometry of local panels and resulting effective^p width due to local buckling:

Table 3-1: Resulting effective^p width of subpanels and stiffener plates.

Panel	b	t	$\bar{\lambda}_{local}$	ρ_{local}	b_{eff}
1	0.5 m	75 mm	0.138	1.000	0.5
2	0.2 m	15 mm	0.289	1.000	0.2
3	0.515 m	15 mm	0.743	0.948	0.488
sub	0.5 m	75 mm	0.138	1.000	0.5

Effective local area (without edges):

$$A_{c.eff.loc} := n_{st} \cdot \left[t_{st} \cdot \left(b_{2.eff} + 2 \cdot b_{3.eff}\right) + t_p \cdot \left(b_{1.eff} + b_{sub.eff}\right)\right] = 0.556\,m^2$$

EN 1993-1-5, Annex A, Calculation of critical stresses for stiffened plates

A.1 Equivalent orthotropic plate

(1) Plates with at least three longitudinal stiffeners may be treated as equivalent orthotropic plates.

(2) The elastic critical plate buckling stress of the equivalent orthotropic plate may be taken as:

$$\sigma_{cr,p} = k_{\sigma,p} \cdot \sigma_E \tag{A.1}$$

where $\sigma_E = \dfrac{\pi^2 \cdot E \cdot t^2}{12(1-\nu^2)\cdot b^2} = 190000\left(\dfrac{t}{b}\right)^2$ in [MPa]

$k_{\sigma,p}$ is the buckling coefficient according to orthotropic plate theory with the stiffeners smeared over the plate;

b is defined in Figure A.1;

t is the thickness of the plate.

NOTE1: The buckling coefficient $k_{\sigma,p}$ is obtained either from appropriate charts for smeared stiffeners or relevant computer simulations; alternatively charts for discretely located stiffeners may be used provided local buckling in the subpanels can be ignored and treated separately.

NOTE2: $\sigma_{cr,p}$ is the elastic critical plate buckling stress at the edge of the panel where the maximum compression stress occurs, see Figure A.1.

NOTE3: Where a web is of concern, the width b in equations (A.1) and (A.2) should be replaced by h_w.

NOTE4: For stiffened plates with at least three equally spaced longitudinal stiffeners the plate buckling coefficient $k_{\sigma,p}$ (global buckling of the stiffened panel) may be approximated by:

$$k_{\sigma,p} = \frac{2\left(\left(1+\alpha^2\right)^2+\gamma-1\right)}{\alpha^2(\psi+1)(1+\delta)} \quad \text{if } \alpha \le \sqrt[4]{\gamma} \tag{A.2}$$

$$k_{\sigma,p} = \frac{4(1+\gamma)}{(\psi+1)(1+\delta)} \quad \text{if } \alpha > \sqrt[4]{\gamma}$$

with $\psi = \dfrac{\sigma_2}{\sigma_1} \ge 0,5$; $\gamma = \dfrac{I_{s\ell}}{I_p}$; $\delta = \dfrac{\Sigma A_{s\ell}}{A_p}$; $\alpha = \dfrac{a}{b} \ge 0,5$

where: $I_{s\ell}$ is the second moment of area of the whole stiffened plate;

I_p is the second moment of area for bending of the plate $= \dfrac{bt^3}{12(1-\nu^2)} = \dfrac{bt^3}{10,92}$;

$\Sigma A_{s\ell}$ is the sum of the gross areas of the individual longitudinal stiffeners;

A_p is the gross area of the plate = bt;

σ_1 is the larger edge stress;

σ_2 is the smaller edge stress.

Gross area (without edges):

$$A_c := n_{st}\cdot\left[t_{st}\cdot\left(b_2 + 2\cdot b_3\right) + t_p\cdot\left(b_1 + b_{sub}\right)\right] = 0.561\,\mathrm{m}^2$$

3.2.3.5.4 Effective^p cross-section of the whole bottom flange

Determination of the elastic critical plate buckling stress (global buckling)

Plate parameters:

$$z_{sl} := \frac{n_{st}\cdot\left[\left(h_{st} + t_p\right)t_{st.eq}\cdot h_{st} + \left(h_{st} + \frac{t_p - t_{st}}{2}\right)\cdot t_{st}\cdot b_2\right]}{A_c} = 63.674\cdot\mathrm{mm}$$

$$I_{sl} := n_{st}\cdot\left[2\cdot\left[\frac{h_{st}^{\,3}\cdot t_{st.eq}}{12} + h_{st}\cdot t_{st.eq}\cdot\left(\frac{h_{st}}{2} - z_{sl}\right)^2\right] + \frac{t_{st}^{\,3}\cdot b_2}{12} + b_2\cdot t_{st}\cdot\left(h_{st} - z_{sl}\right)^2\right]\ldots$$

$$+\frac{b_p\cdot t_p^{\,3}}{12} + b_p\cdot t_p\cdot z_{sl}^{\,2} \qquad\qquad I_{sl} = 1.048\times 10^6\cdot\mathrm{cm}^4$$

$$I_p := \frac{b_p\cdot t_p^{\,3}}{12\cdot\left(1 - \nu^2\right)} = 2.511\times 10^4\cdot\mathrm{cm}^4$$

$$A_{sl} := n_{st}\,t_{st}\cdot\left(b_2 + 2\cdot b_3\right) = 1.107\times 10^5\cdot\mathrm{mm}^2$$

$$A_p := b_p\cdot t_p = 4.875\times 10^5\cdot\mathrm{mm}^2$$

$$\gamma := \frac{I_{sl}}{I_p} = 41.724$$

$$\delta := \frac{A_{sl}}{A_p} = 0.227$$

$$\alpha := \frac{a_p}{b_p} = 0.615 \quad = 0.5$$

$$k_{\sigma.p} := \left|\begin{array}{ll} \dfrac{2\cdot\left[\left(1 + \alpha^2\right)^2 + \gamma - 1\right]}{\alpha^2\cdot(\psi + 1)\cdot(1 + \delta)} & \text{if } \alpha \le \sqrt[4]{\gamma} \\ \dfrac{4\cdot\left(1 + \sqrt{\gamma}\right)}{(\psi + 1)\cdot(1 + \delta)} & \text{otherwise} \end{array}\right.$$

$$k_{\sigma.p} = 91.732$$

Euler stress:

$$\sigma_E := \frac{\pi^2\cdot E\cdot t_p^{\,2}}{12\cdot\left(1 - \nu^2\right)\cdot b_p^{\,2}} = 25.269\cdot\mathrm{N}\cdot\mathrm{mm}^{-2}$$

EN 1993-1-5, 4.5.2, Plate type behaviour

(1) The relative plate slenderness p l of the equivalent plate is defined as:

$$\bar{\lambda}_p = \sqrt{\frac{\beta_{A,c} \cdot f_y}{\sigma_{cr,p}}} \quad \text{with } \beta_{A,c} = \frac{A_{c,eff,loc}}{A_c} \qquad (4.7)$$

where A_c is the gross area of the compression zone of the stiffened plate except the parts of the subpanels supported by an adjacent plate, see Figure 4.4 (to be multiplied by the shear lag factor if shear lag is relevant, see 3.3);

$A_{c,eff,loc}$ is the effective area of the same part of the plate (including shear lag effect, if relevant) with due allowance made for possible plate buckling of subpanels and/or stiffeners.

(2) The reduction factor ρ for the equivalent orthotropic plate is obtained from 4.4(2) provided $\bar{\lambda}_p$ is calculated from equation (4.7).

NOTE: For calculation of $\sigma_{cr,p}$ see Annex A.

EN 1993-1-5, 4.5.3, Column type buckling behaviour

(1) The elastic critical column buckling stress $\sigma_{cr,c}$ of an unstiffened (see 4.4) or stiffened (see 4.5) plate should be taken as the buckling stress with the supports along the longitudinal edges removed.

(2) For an unstiffened plate the elastic critical column buckling stress $\sigma_{cr,c}$ may be obtained from

$$\sigma_{cr,c} = \frac{\pi^2 \cdot E \cdot t^2}{12\left(1-\nu^2\right) \cdot a^2} \qquad (4.8)$$

(3) For a stiffened plate $\sigma_{cr,c}$ may be determined from the elastic critical column buckling stress $\sigma_{cr,s\ell}$ of the stiffener closest to the panel edge with the highest compressive stress as follows:

$$\sigma_{cr,c} = \frac{\pi^2 \cdot E \cdot I_{s\ell,1}}{A_{s\ell,1} \cdot a^2} \qquad (4.9)$$

where $I_{s\ell,1}$ is the second moment of area of the gross cross-section of the stiffener and the adjacent parts of the plate, relative to the out-of-plane bending of the plate;

$A_{s\ell,1}$ is the gross cross-sectional area of the stiffener and the adjacent parts of the plate according to Figure A.1.

NOTE: $\sigma_{cr,c}$ may be obtained from $\sigma_{cr,c} = \sigma_{cr,s\ell} \cdot b_c / b_{sl,1}$, where $\sigma_{cr,c}$ is related to the compressed edge of the plate, and $b_{s\ell,1}$ and b_c are geometric values from the stress distribution used for the extrapolation, see Figure A.1.

(4) The relative column slenderness $\bar{\lambda}_c$ is defined as follows: […]

$$\bar{\lambda}_c = \sqrt{\frac{\beta_{A,c} f_y}{\sigma_{cr,c}}} \qquad \text{for stiffened plates} \qquad (4.11)$$

with $\beta_{A,c} = \dfrac{A_{s\ell,1,eff}}{A_{s\ell,1}}$; $A_{s\ell,1}$ is defined in 4.5.3(3);

$A_{s\ell,1,eff}$ is the effective cross-sectional area of the stiffener and the adjacent parts of the plate with due allowance for plate buckling, see Figure A.1.

Elastic critical plate buckling stress of equivalent orthotropic plate:

$$\sigma_{cr.p} := k_{\sigma.p} \cdot \sigma_E = 2.318 \times 10^3 \cdot N \cdot mm^{-2}$$

Plate type behaviour

Reduction factor $\beta_{A.c}$:

$$\beta_{A.c} := \frac{A_{c.eff.loc}}{A_c} = 0.991$$

Relative slenderness of the equivalent plate:

$$\lambda_p := \sqrt{\frac{\beta_{A.c} \cdot f_y(t_p)}{\sigma_{cr.p}}} = 0.373$$

Reduction factor for internal compression elements:

$$\rho_p := \begin{vmatrix} 1 \ \text{ if } \ \lambda_p < 0.673 \\ \dfrac{\lambda_p - 0.22}{\lambda_p^{\,2}} \ \text{ otherwise} \end{vmatrix} = 1$$

Column type buckling behaviour

Effective gross-section of stiffener:

$$b_{1.sl} := (b_{sub} + b_1) = 1\,m$$

$$A_{sl.1} := t_{st} \cdot (b_2 + 2 \cdot b_3) + t_p \cdot b_{1.sl} = 9.345 \times 10^4 \cdot mm^2$$

$$z_{sl.1} := \frac{(h_{st} + t_p) t_{st.eq} \cdot h_{st} + \left(h_{st} + \dfrac{t_p - t_{st}}{2}\right) \cdot t_{st} \cdot b_2}{A_{sl.1}} = 63.674 \cdot mm$$

$$I_{sl.1} := \left[2 \cdot \left[\frac{h_{st}^{\,3} \cdot t_{st.eq}}{12} + h_{st} \cdot t_{st.eq} \cdot \left(\frac{h_{st}}{2} - z_{sl.1}\right)^2\right] + \frac{t_{st}^{\,3} \cdot b_2}{12} + b_2 \cdot t_{st} \cdot (h_{st} - z_{sl.1})^2\right] \ldots$$
$$+ \frac{b_{1.sl} \cdot t_p^{\,3}}{12} + b_{1.sl} \cdot t_p \cdot z_{sl.1}^{\,2} \qquad I_{sl.1} = 1.718 \times 10^9 \cdot mm^4$$

Effective net cross-section of stiffener:

$$b_{1.sl.eff} := (b_{sub.eff} + b_{1.eff}) = 1\,m$$

$$A_{sl.1.eff} := t_{st} \cdot (b_{2.eff} + 2 \cdot b_{3.eff}) + t_p \cdot b_{1.sl.eff} = 9.264 \times 10^4 \cdot mm^2$$

Elastic critical bucking stress for an equivalent column:

$$\sigma_{cr.sl} := \frac{\pi^2 \cdot E \cdot I_{sl.1}}{A_{sl.1} \cdot a_p^{\,2}} = 2.382 \times 10^3 \cdot N \cdot mm^{-2}$$

EN 1993-1-5, 4.5.3, Column type behaviour

(5) The reduction factor χ_c should be obtained from 6.3.1.2 of EN 1993-1-1. For unstiffened plates α = 0,21 corresponding to buckling curve a should be used. For stiffened plates its value should be increased to:

$$\alpha_e = \alpha + \frac{0{,}09}{i/e} \qquad (4.12)$$

with $i = \sqrt{\frac{I_{s\ell,1}}{A_{s\ell,1}}}$

e = max (e_1, e_2) is the largest distance from the respective centroids of the plating and the one-sided stiffener (or of the centroids of either set of stiffeners when present on both sides) to the neutral axis of the effective column, see Figure A.1;

α = 0.34 (curve b) for closed section stiffeners;

= 0.49 (curve c) for open section stiffeners.

EN 1993-1-5, 4.5.4, Interaction between plate and column buckling

(1) The final reduction factor ρ_c should be obtained by interpolation between χ_c and ρ as follows:

$$\rho_c = (\rho - \chi_c)\,\xi\,(1-\xi) + \chi_c \qquad (4.13)$$

where $\xi = \frac{\sigma_{cr,p}}{\sigma_{cr,c}} - 1$ but $0 \leq \xi \leq 1$

$\sigma_{cr,p}$ is the elastic critical plate buckling stress, see Annex A.1(2);

$\sigma_{cr,c}$ is the elastic critical column buckling stress according to 4.5.3(2) and (3), respectively;

χ_c is the reduction factor due to column buckling.

ρ is the reduction factor due to plate buckling, see 4.4(1).

Reduction factor $\beta_{A.c}$:

$$\beta_{A.c.} := \frac{A_{sl.1.eff}}{A_{sl.1}} = 0.991$$

Relative column slenderness:

$$\lambda_c := \sqrt{\frac{\beta_{A.c.} \cdot f_y(t_p)}{\sigma_{cr.sl}}} = 0.368$$

$$i := \sqrt{\frac{I_{sl.1}}{A_{sl.1}}} = 0.136\,m$$

$$e_1 := \frac{t_p}{2} + \frac{h_{st}\left(t_{st.eq} \cdot h_{st} + t_{st} \cdot b_2\right)}{\left(2t_{st.eq} \cdot h_{st} + t_{st} \cdot b_2\right)} - z_{sl.1} = 260.127 \cdot mm$$

$$e_2 := z_{sl.1} = 63.674 \cdot mm$$

$$e := \left| \begin{array}{ll} e_1 & \text{if } e_1 \geq e_2 \\ e_2 & \text{otherwise} \end{array} \right.$$

Imperfection factor α_e:

$$\alpha_e := \alpha_0 + \frac{0.09}{\frac{i}{e}} = 0.513$$

Reduction factor for column buckling:

$$\chi_c(\phi) := \left| \begin{array}{ll} 1 & \text{if } \lambda_c < 0.2 \\ \dfrac{1}{\phi + \sqrt{\phi^2 - \lambda_c^2}} & \text{otherwise} \end{array} \right.$$

$$\phi := 0.5 \cdot \left[1 + \alpha_e \cdot \left(\lambda_c - 0.2\right) + \lambda_c^2\right] = 0.611$$

$$\chi_c := \chi_c(\phi) = 0.911$$

Interaction between plate and column buckling

Weighting factor ξ:

$$\xi := \frac{\sigma_{cr.p}}{\sigma_{cr.sl}} - 1$$

$$\xi = 0$$

Final reduction factor ρ_c:

$$\rho_c := \left(\rho_p - \chi_c\right) \cdot \xi \cdot (2 - \xi) + \chi_c = 0.911$$

Effective^p area of compression zone:

$$A_{c.eff} := \rho_c \cdot A_{c.eff.loc} + b_{sub.eff} \cdot t_p = 5.437 \times 10^5 \cdot mm^2$$

3.2.3.5.5 Parameter study

Figure 3-13 summarises the results of the above performed design calculation for a variation of number of stiffeners n_{st} and thickness of bottom plate t_p. From the diagram the following conclusions can be drawn:

1. With increasing bottom plate thickness t_p, the critical buckling stress σ_p and thus the reduction factor ρ_c decreases. This is due to the fact that with increasing plate thickness and with constant stiffener-geometry the stiffening effect of the stiffeners decreases. → Decreasing of the continous lines (utilisation level η).

   NOTE: The parameter study has been performed with the hand-calculation formulae of EN 1993-1-5, Annex A. This effect can be minimized by using EBPlate with discrete stiffeners.

2. With increasing bottom plate thickness t_p, the characteristic value of the yield strength f_y decreases. In conclusion the slenderness $\bar{\lambda}$ increases. → slight non-linearity of the behaviour described in 2. (continous lines are not straight).
3. With increasing plate thickness t_p the effective area $A_{c.eff}$ and thus the maximum axial force in the bottom plate increases (broken lines).
4. Apart from case [$t_p = 35$; $n_{st} = 3$] there is no reduction due to local buckling of the bottom plate.
5. From the $A_{c.eff}$-function it can be seen that by increasing the thickness t_p about 8 mm the number of stiffeners can be decreased down to four stiffeners. This would mean a benefit with regard to number of welds and amount of labour.

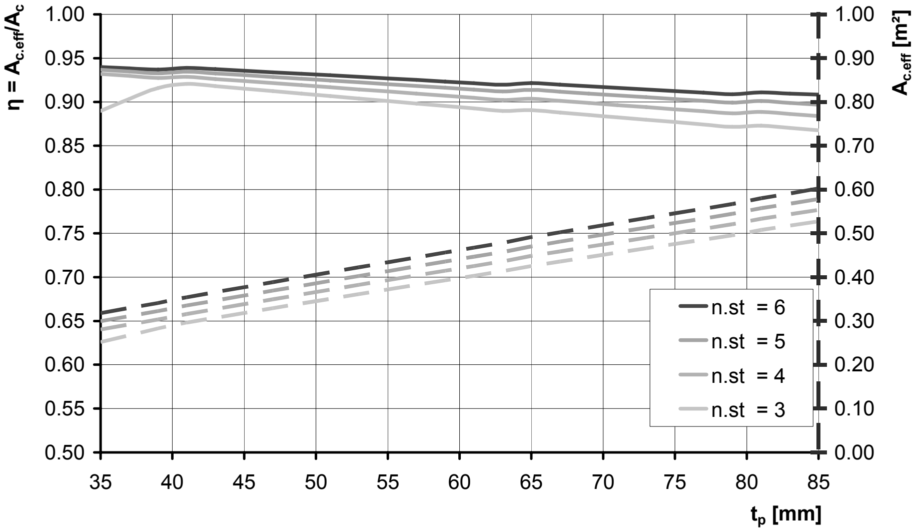

Figure 3-13: Utilisation level (left ordinate) and effective^p area (right ordinate) of bottom plate in function of bottom plate thickness t_p; curve parameter = number of stiffeners n_{st}.

EN 1993-1-5, 3.1, General

(1) Shear lag in flanges may be neglected if $b_0 < L_e/50$ where b_0 is taken as the flange outstand or half the width of an internal element and L_e is the length between points of zero bending moment, see 3.2.1(2).

EN 1993-1-5, 3.2.1, Effective width

(1) The effectives width b_{eff} for shear lag under elastic conditions should be determined from:

$$b_{eff} = \beta\, b_0 \qquad (3.1)$$

where the effectives factor β is given in Table 3.1.

This effective width may be relevant for serviceability and fatigue limit states.

(2) Provided adjacent spans do not differ more than 50% and any cantilever span is not larger than half theadjacent span the effective lengths L_e may be determined from Figure 3.1. For all other cases L_e should betaken as the distance between adjacent points of zero bending moment.

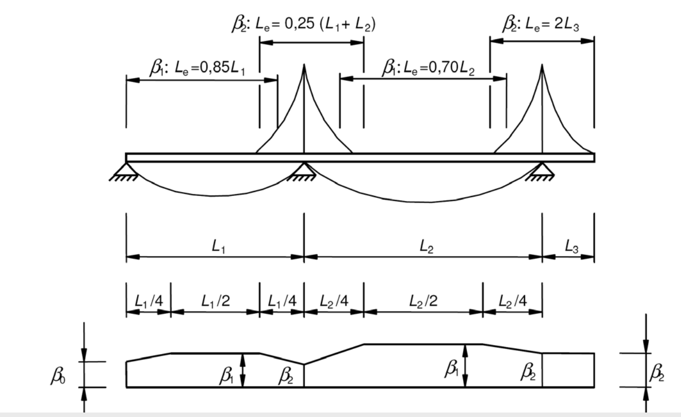

Figure 3.1: Effective length L_e for continuous beam and distribution of effective^{s} width

Table 3.1: Effective^{s} width factor β

κ	Verification	β – value
$\kappa \le 0{,}02$		$\beta = 1{,}0$
$0{,}02 < \kappa \le 0{,}70$	sagging bending	$\beta = \beta_1 = \dfrac{1}{1 + 6{,}4\,\kappa^2}$
	hogging bending	$\beta = \beta_2 = \dfrac{1}{1 + 6{,}0\left(\kappa - \dfrac{1}{2500\,\kappa}\right) + 1{,}6\,\kappa^2}$
$> 0{,}70$	sagging bending	$\beta = \beta_1 = \dfrac{1}{5{,}9\,\kappa}$
	hogging bending	$\beta = \beta_2 = \dfrac{1}{8{,}6\,\kappa}$
all κ	end support	$\beta_0 = (0{,}55 + 0{,}025 / \kappa)\,\beta_1$, but $\beta_0 < \beta_1$
all κ	Cantilever	$\beta = \beta_2$ at support and at the end

$\kappa = \alpha_0\, b_0 / L_e$ with $\alpha_0 = \sqrt{1 + \dfrac{A_{s\ell}}{b_0 t}}$

in which $A_{s\ell}$ is the area of all longitudinal stiffeners within the width b_0 and other symbols are as defined in Figure 3.1 and Figure 3.2.

EN 1993-1-5, 3.3, Shear lag at the ultimate limit state

NOTE3: Elastic-plastic shear lag effects allowing for limited plastic strains may be taken into account using A_{eff} as follows

$$A_{eff} = A_{c.eff}\,\beta^{\kappa} \ge A_{c.eff}\,\beta \qquad (3.1)$$

where β and κ are taken from Table 3.1.

3.2.3.5.6 Reduction due to shear lag effect

Verification if shear lag effect has to be taken into account:

Bridge span: $L_1 = 120$ m and $L_2 = 120$ m

Effective length: $L_e = 0.25\ (L_1 + L_2)\cdot 120\ \text{m} = 60$ m

Considered width: $b_0 = b_p/2 = 3.25$ m

⇒ $b_0 < L_e/50$ requirement not fulfilled! Shear lag effect has to be taken into account.

Shear lag parameters:

$$\alpha^\circ_0 := \sqrt{1 + \frac{\frac{A_{sl}}{2}}{b_0 \cdot t_p}} = 1.108$$

$$\kappa := \alpha^\circ_0 \cdot \frac{b_0}{L_e} = 0.06$$

$$\beta_{ult} := \left| \begin{array}{ll} 1 \quad \text{if } \kappa \le 0.02 & \\ \dfrac{1}{1 + 6\cdot\left(\kappa - \dfrac{1}{2500\cdot\kappa}\right) + 1.6\cdot\kappa^2} & \text{if } 0.02 < \kappa \le 0.7 \\ \dfrac{1}{8.6\cdot\kappa} \quad \text{otherwise} & \end{array} \right.$$

$$\beta_{ult} = 0.754$$

3.2.3.5.7 Effective area of the stiffened plate

Effective area of compression zone taking into account effects of plate buckling and shear lag:

$$A_{effEP} := A_{c.eff} \cdot b_{ult}^{k} = 0.535\ \text{m}^2$$

3.2.3.5.8 New mechanical properties of the cross-section

The new mechanical properties of the cross-section are then calculated by replacing the gross area of the bottom flange by its effective area.

The web has been stiffened by a longitudinal closed stiffener located at mid-depth due to shear verifications. For simplification reasons, this stiffener is not considered in the bending verification.

New mechanical properties of the steel part of the box-section

The new mechanical properties of the steel part (structural steel only) of the box section are:

- Area:

$$A_{tot.a.eff} := A_{effEP} + 2.\left(h - t_{tf.1} - t_{tf.2} - t_p\right)\cdot t_{w.h} + 2\left(b_{tf.1}\cdot t_{tf.1} + b_{tf.2}\cdot t_{tf.2}\right)$$

$$A_{tot.a.eff} = 1.331\ \text{m}^2$$

- First moment of area:

$$S_{a.na} := 2\cdot\left[b_{tf.1}\cdot t_{tf.1}\cdot\left(h-\frac{t_{tf.1}}{2}\right)+b_{tf.2}\cdot t_{tf.2}\cdot\left(h-t_{tf.1}-\frac{t_{tf.2}}{2}\right)\right]\ ...$$
$$+\ 2\cdot t_{w.h}\cdot\left(h-t_{tf.1}-t_{tf.2}-t_p\right)\cdot\left(\frac{h-t_{tf.1}-t_{tf.2}+t_p}{2}\right)+A_{effEP}\cdot z_{sl.1}$$

$$S_{a.na} = 2.666\cdot m^3$$

- Distance between the center of gravity and the lower face of the bottom flange:

$$z_{tot.a.na} := \frac{S_{a.na}}{A_{tot.a.eff}} = 2.003\ m$$

- Second moment of area:

$$I_{tot.a.eff} := 2\cdot\left[\frac{b_{tf.1}\cdot t_{tf.1}{}^3}{12}+\left(b_{tf.1}\cdot t_{tf.1}\right)\cdot\left(h-\frac{t_{tf.1}}{2}-z_{tot.a.na}\right)^2\right]\ ...$$
$$+\ 2\cdot\left[\frac{b_{tf.2}\cdot t_{tf.2}{}^3}{12}+\left(b_{tf.2}\cdot t_{tf.2}\right)\cdot\left(h-t_{tf.1}-\frac{t_{tf.2}}{2}-z_{tot.a.na}\right)^2\right]\ ...$$
$$+\ 2\cdot\left[t_{w.h}\cdot\left(h-t_{tf.1}-t_{tf.2}-t_p\right)\cdot\left(\frac{h-t_{tf.1}-t_{tf.2}+t_p}{2}-z_{tot.a.na}\right)^2\ ...\atop +\ \frac{t_{w.h}\cdot\left(h-t_{tf.1}-t_{tf.2}-t_p\right)^3}{12}\right]\ ...$$
$$+\ A_{effEP}\cdot\left(z_{tot.a.na}-z_{sl.1}\right)^2+n_{st}\cdot I_{sl.1}$$

$$I_{tot.a.eff} = 4.308\ m^4$$

New mechanical properties of the composite box-section

The mechanical properties of the composite box section (structural steel part and reinforcement) are:

- Area:

$$A_{tot.eff} := A_{tot.a.eff}+A_{tsur}+A_{tslr} = 1.416\ m^2$$

- First moment of area:

$$S_{na} := S_{a.na}+A_{tsur}\cdot\left(h+t_{slab}-c_{ur}\right)+A_{tslr}\cdot\left(h+c_{lr}\right) = 3.023\cdot m^3$$

- Distance between the center of gravity and the lower face of the bottom flange:

$$z_{tot.na} := \frac{S_{na}}{A_{tot.eff}} = 2.134\ m$$

EN 1993-1-1, Table 5.2 (sheet 1 of 3), Maximum width-to-thickness ratios for compression parts

Internal compression parts

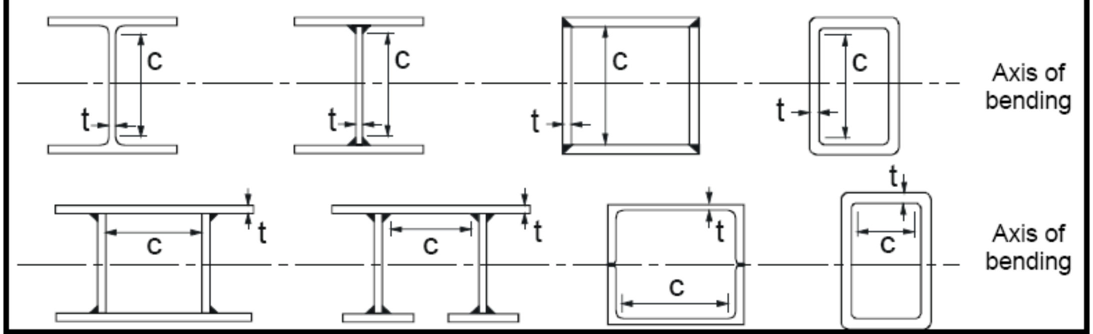

Class	Part subject to bending	Part subject to compression	Part subject to bending and compression
Stress distribution in parts (compression positive)	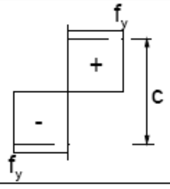	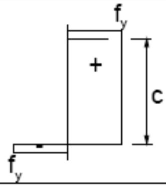	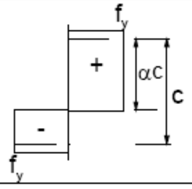
1	$c/t \le 72\varepsilon$	$c/t \le 33\varepsilon$	when $\alpha > 0{,}5$: $c/t \le \frac{396\varepsilon}{13\alpha - 1}$ when $\alpha \le 0{,}5$: $c/t \le \frac{36\varepsilon}{\alpha}$
2	$c/t \le 83\varepsilon$	$c/t \le 38\varepsilon$	when $\alpha > 0{,}5$: $c/t \le \frac{456\varepsilon}{13\alpha - 1}$ when $\alpha \le 0{,}5$: $c/t \le \frac{41{,}5\varepsilon}{\alpha}$
Stress distribution in parts (compression positive)	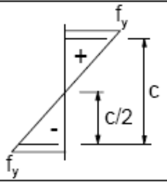	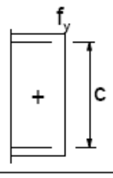	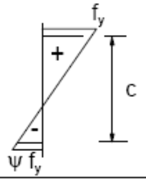
3	$c/t \le 124\varepsilon$	$c/t \le 42\varepsilon$	when $\psi > -1$: $c/t \le \frac{42\varepsilon}{0{,}67 + 0{,}33\psi}$ when $\psi \le -1^{*)}$: $c/t \le 62\varepsilon(1-\psi)\sqrt{(-\psi)}$

$\varepsilon = \sqrt{235/f_y}$	f_y	235	275	355	420	460
	ε	1,00	0,92	0,81	0,75	0,71

*) $\psi \le -1$ applies where either the compression stress $\sigma \le f_y$ or the tensile strain $\varepsilon_y > f_y/E$

- Second moment of area:

$$
\begin{aligned}
I_{tot.eff} := {} & A_{tsur}\cdot\left(h + t_{slab} - c_{ur} - z_{tot.na}\right)^2 + A_{tslr}\cdot\left(h + c_{lr} - z_{tot.na}\right)^2 \cdots \\
& + 2\cdot\left[\frac{b_{tf.1}\cdot t_{tf.1}^{\,3}}{12} + \left(b_{tf.1}\cdot t_{tf.1}\right)\cdot\left(h - \frac{t_{tf.1}}{2} - z_{tot.na}\right)^2\right] \cdots \\
& + 2\cdot\left[\frac{b_{tf.2}\cdot t_{tf.2}^{\,3}}{12} + \left(b_{tf.2}\cdot t_{tf.2}\right)\cdot\left(h - t_{tf.1} - \frac{t_{tf.2}}{2} - z_{tot.na}\right)^2\right] \cdots \\
& + 2\cdot\left[\begin{array}{l} t_{w.h}\cdot\left(h - t_{tf.1} - t_{tf.2} - t_p\right)\cdot\left(\dfrac{h - t_{tf.1} - t_{tf.2} + t_p}{2} - z_{tot.na}\right)^2 \cdots \\ + \dfrac{t_{w.h}\cdot\left(h - t_{tf.1} - t_{tf.2} - t_p\right)^3}{12} \end{array}\right] \cdots \\
& + A_{effEP}\cdot\left(z_{tot.na} - z_{sl.1}\right)^2 + n_{st}\cdot I_{sl.1}
\end{aligned}
$$

$$I_{tot.eff} = 4.69\,\mathrm{m}^4$$

3.2.3.6 Effective area of the web

3.2.3.6.1 General

From the values of the bending moments M_a and M_c (see Paragraph 3.2.3.3) and of the mechanical properties in Paragraph 3.2.3.5, the normal extreme stresses in the web at ULS are as follows:

$$\sigma_{abfu} = \frac{-M_a\left(z_{tota.na} - t_p\right)}{I_{tot.a.eff}} + \frac{-M_c\left(z_{tot.na} - t_p\right)}{I_{tot.eff}} = 328.263 \text{ MPa}$$

$$\sigma_{atfl} = \frac{M_a\left(h - t_{tf.1} - t_{tf.2} - z_{tot.a.na}\right)}{I_{tot.a.eff}} + \frac{M_c\left(h - t_{tf.1} - t_{tf.2} - z_{tot.na}\right)}{I_{tot.eff}} = \text{-}290.373 \text{ MPa}$$

3.2.3.6.2 Determination of the cross-section class

The bottom flange is already a class 4 element due to the webs of the stiffeners, so that the whole section is already classified (elastic analysis should be performed). Thus, it has to be only determined if the web is a Class 3 or Class 4 panel in order to eventually reduce it.

Reasoning is based on the elastic stress distribution at ULS given by Paragraph 3.2.3.6 which takes into account the effects of plate buckling and shear lag:

$$\sigma_{abfu} = 328.263 \text{ N/mm}^2$$

$$\sigma_{atfl} = \text{-}290.373 \text{ N/mm}^2$$

And the elastic stress distribution at ULS:

$$\psi_w = \frac{\sigma_{atfl}}{\sigma_{abfu}} = \text{-}0.885 > \text{-}1$$

Thus, the limiting slenderness between Class 3 and Class 4 is given by:

$$\frac{c_w}{t_w} = \frac{h_w}{t_w} = 167.872 > \frac{42\varepsilon}{0.67 + 0.33\cdot\psi_w} = 91.681$$

It is deduced that the steel web is in Class 4.

EN 1993-1-5, 4.4 Table 4.1, Internal compression elements

Stress distribution (compression positive)	Effective^p width b_{eff}
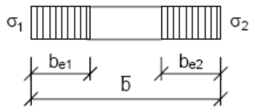	$\psi = 1$: $b_{eff} = \rho\ \bar{b}$ $b_{e1} = 0,5\ b_{eff}$ $b_{e2} = 0,5\ b_{eff}$
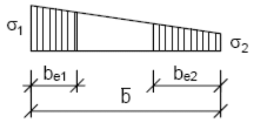	$1 > \psi \geq 0$: $b_{eff} = \rho\ \bar{b}$ $b_{e1} = \frac{2}{5-\psi} b_{eff}$ $b_{e2} = b_{eff} - b_{e1}$
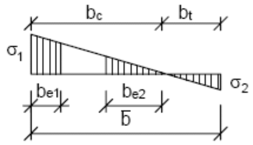	$\psi < 0$: $b_{eff} = \rho\ b_c = \rho\ \bar{b} / (1-\psi)$ $b_{e1} = 0,4\ b_{eff}$ $b_{e2} = 0,6\ b_{eff}$

$\psi = \sigma_2/\sigma_1$	1	$1 > \psi > 0$	0	$0 > \psi > -1$	-1	$-1 > \psi > -3$
Buckling factor k_σ	4,0	$8,2 / (1,05 + \psi)$	7,81	$7,81 - 6,29\psi + 9,78\psi^2$	23,9	$5,98\ (1 - \psi)^2$

EN 1993-1-5, 4.4 Table 4.2, Outstand compression elements

Stress distribution (compression positive)	Effective^p width b_{eff}
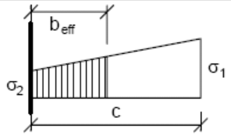	$1 > \psi \geq 0$: $b_{eff} = \rho\ c$
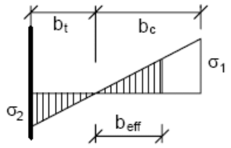	$\psi < 0$: $b_{eff} = \rho\ b_c = \rho\ c / (1-\psi)$

$\psi = \sigma_2/\sigma_1$	1	0	-1	$1 \geq \psi \geq -3$
Buckling factor k_σ	0,43	0,57	0,85	$0,57 - 0,21\psi + 0,07\psi^2$

Stress distribution (compression positive)	Effective^p width b_{eff}
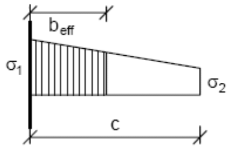	$1 > \psi \geq 0$: $b_{eff} = \rho\ c$
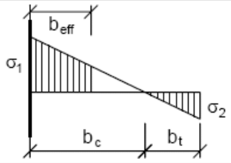	$\psi < 0$: $b_{eff} = \rho\ b_c = \rho\ c / (1-\psi)$

$\psi = \sigma_2/\sigma_1$	1	$1 > \psi > 0$	0	$0 > \psi > -1$	-1
Buckling factor k_σ	0,43	$0,578 / (\psi + 0,34)$	1,70	$1,7 - 5\psi + 17,1\psi^2$	23,8

EN 1993-1-5, 4.4(3)

(3) For flange elements of I-sections and box-girders the stress ratio ϕ used in Table 4.1 and Table 4.2 should be based on the properties of the gross cross-sectional area, due allowance being made for shear lag in the flanges if relevant. For web elements the stress ratio ψ used in Table 4.1 should be obtained using a stress distribution based on the effective area of the compression flange and the gross area of the web.

Conclusion: the cross-section at the internal support P1, P2 and P3 is in Class 4 and is checked by a elastic section analysis.

The web is in Class 4, so that its effective cross-section under bending moment has to be calculated according to EN 1993-1-5, 4.4.

Web in bending

$k_{\sigma w} = 5.98\left(1-\psi\right)^2 = 21.027$ (see EN1993-1-5, 4.4, Table 4.1, Internal compression elements)

$$\bar{\lambda}_{pw} = \frac{\bar{b}/t}{28,4\varepsilon\sqrt{k_\sigma}} = \frac{\frac{h_w}{t_w}}{28,4\varepsilon_w\sqrt{k_{\sigma w}}} = 1.562 > 0.673$$

$\Rightarrow \quad \rho_w = \dfrac{\bar{\lambda}_{pw} - 0,055(3+\psi_w)}{\bar{\lambda}_{pw}^2} = 0.593$; There is a reduction of the height of the steel web

Thus, the effective height of the web in compression can be calculated:

$$h_{weff} = \frac{\rho_w h_w}{\left(1-\psi_w\right)} = 1.425 \text{ m}$$

And this effective height of the web can be distributed as shown in EN1993-1-5, Table 4.1:

$$h_{we1} = \left(\frac{-\psi_w}{1-\psi_w}\right)\cdot h_w + 0.6h_{weff} = 2.127 + 0.855 = 2.983 \text{ m}$$

$$h_{we2} = 0.4h_{weff} = 0.57 \text{ m}$$

NOTE:The effective area of the box section webs is determined after that of its stiffened bottom flange. The reverse calculation would not lead to the same effective area of the cross-section at P3 and it would not comply with EN 1993-1-5.

3.2.3.6.3 Effective mechanical properties of the box section

The final effective mechanical properties of the cross-section are calculated by replacing the gross area of the bottom flange and web by their effective areas.

Final mechanical properties of the steel part of the box-section

The final mechanical properties of the effective steel box section (structural steel only) of the box section are:

- Area:

$$A_{eff.w} := \left(h_{w.e1} + h_{w.e2}\right)\cdot t_w = 0.096\,\text{m}^2$$

$$A_{tot.a.eff} := A_{effEP} + 2.A_{eff.w} + 2\left(b_{tf.1}\cdot t_{tf.1} + b_{tf.2}\cdot t_{tf.2}\right) = 1.278\,\text{m}^2$$

- First moment of area:

$$S_{a.na} := 2\cdot\left[b_{tf.1}\cdot t_{tf.1}\cdot\left(h - \frac{t_{tf.1}}{2}\right) + b_{tf.2}\cdot t_{tf.2}\cdot\left(h - t_{tf.1} - \frac{t_{tf.2}}{2}\right)\right] + A_{effEP}\cdot z_{sl.1}\,\cdots$$
$$+ 2\cdot t_w\cdot h_{w.e1}\cdot\left(h - t_{tf.1} - t_{tf.2} - \frac{h_{w.e1}\cdot\cos\left(q_w\right)}{2}\right) + 2\cdot t_w\cdot h_{w.e2}\cdot\frac{h_{w.e2}\cdot\cos\left(q_w\right)}{2}$$

$$S_{a.na} = 2.613\cdot\text{m}^3$$

- Distance between the center of gravity and the lower face of the bottom flange:

$$z_{tot.a.na} := \frac{S_{a.na}}{A_{tot.a.eff}} = 2.044\,\mathrm{m}$$

- Second moment of area:

$$\begin{aligned} I_{tot.a.eff} := {} & 2\cdot\left[\frac{b_{tf.1}\cdot t_{tf.1}^{\,3}}{12} + \left(b_{tf.1}\cdot t_{tf.1}\right)\cdot\left(h - \frac{t_{tf.1}}{2} - z_{tot.a.na}\right)^2\right] \ldots \\ & + 2\cdot\left[\frac{b_{tf.2}\cdot t_{tf.2}^{\,3}}{12} + \left(b_{tf.2}\cdot t_{tf.2}\right)\cdot\left(h - t_{tf.1} - \frac{t_{tf.2}}{2} - z_{tot.a.na}\right)^2\right] \ldots \\ & + 2\cdot\left[\begin{aligned} & \frac{t_{w.h}\cdot\left(h_{w.e1}\cdot\cos\left(q_w\right)\right)^3}{12} + t_w\cdot h_{w.e1}\cdot\left(h - t_{tf.1} - t_{tf.2} - \frac{h_{w.e1}\cdot\cos\left(q_w\right)}{2} - z_{tot.a.na}\right)^2 \ldots \\ & + \frac{t_{w.h}\cdot\left(h_{w.e2}\cdot\cos\left(q_w\right)\right)^3}{12} + t_w\cdot h_{w.e2}\cdot\left(z_{tot.a.na} - t_p - \frac{h_{w.e2}\cdot\cos\left(q_w\right)}{2}\right)^2 \end{aligned}\right] \ldots \\ & + A_{effEP}\cdot\left(z_{tot.a.na} - z_{sl.1}\right)^2 + n_{st}\cdot I_{sl.1} \end{aligned}$$

$$I_{tot.a.eff} = 4.244\,\mathrm{m}^4$$

Final mechanical properties of the composite box-section

The final mechanical properties of the composite box section (structural steel part and reinforcement) are:

- Area:

$$A_{tot.eff} := A_{tot.a.eff} + A_{tsur} + A_{tslr} = 1.364\,\mathrm{m}^2$$

- First moment of area:

$$S_{na} := S_{a.na} + A_{tsur}\cdot\left(h + t_{slab} - c_{ur}\right) + A_{tslr}\cdot\left(h + c_{lr}\right) = 2.97\cdot\mathrm{m}^3$$

- Distance between the center of gravity and the lower face of the bottom flange:

$$z_{tot.na} := \frac{S_{na}}{A_{tot.eff}} = 2.178\,\mathrm{m}$$

- Second moment of area:

$$\begin{aligned} I_{tot.eff} := {} & A_{tsur}\cdot\left(h + t_{slab} - c_{ur} - z_{tot.na}\right)^2 + A_{tslr}\cdot\left(h + c_{lr} - z_{tot.na}\right)^2 \ldots \\ & + 2\cdot\left[\frac{b_{tf.1}\cdot t_{tf.1}^{\,3}}{12} + \left(b_{tf.1}\cdot t_{tf.1}\right)\cdot\left(h - \frac{t_{tf.1}}{2} - z_{tot.na}\right)^2\right] \ldots \\ & + 2\cdot\left[\frac{b_{tf.2}\cdot t_{tf.2}^{\,3}}{12} + \left(b_{tf.2}\cdot t_{tf.2}\right)\cdot\left(h - t_{tf.1} - \frac{t_{tf.2}}{2} - z_{tot.na}\right)^2\right] \ldots \\ & + 2\cdot\left[\begin{aligned} & \frac{t_{w.h}\cdot\left(h_{w.e1}\cdot\cos\left(q_w\right)\right)^3}{12} + t_w\cdot h_{w.e1}\cdot\left(h - t_{tf.1} - t_{tf.2} - \frac{h_{w.e1}\cdot\cos\left(q_w\right)}{2} - z_{tot.na}\right)^2 \ldots \\ & + \frac{t_{w.h}\cdot\left(h_{w.e2}\cdot\cos\left(q_w\right)\right)^3}{12} + t_w\cdot h_{w.e2}\cdot\left(z_{tot.na} - t_p - \frac{h_{w.e2}\cdot\cos\left(q_w\right)}{2}\right)^2 \end{aligned}\right] \ldots \\ & + A_{effEP}\cdot\left(z_{tot.na} - z_{sl.1}\right)^2 + n_{st}\cdot I_{sl.1} \end{aligned}$$

$$I_{tot.eff} = 4.61\,\mathrm{m}^4$$

EN 1993-1-5, 4.6(1)

Member verification for uniaxial bending should be performed as follows:

$$\eta_1 = \frac{N_{Ed}}{\frac{f_y A_{eff}}{\gamma_{M0}}} + \frac{M_{Ed} + N_{Ed} e_N}{\frac{f_y W_{eff}}{\gamma_{M0}}} \leq 1{,}0 \qquad (4.14)$$

Where A_{ef} is the effective cross-section area in accordance with 4.3(3);

e_N is the shift in the position of neutral axis, see 4.3(3);

M_{Ed} is the design bending moment;

N_{Ed} is the design bending moment;

W_{eff} is the effective elastic section modulus, see 4.3(4);

γ_{M0} is the partial safety factor, see application parts EN 1993-2 to 6.

NOTE: For members subject to compression and biaxaial bending the above equation 4.14 may be modified as follows:

$$\eta_1 = \frac{N_{Ed}}{\frac{f_y A_{eff}}{\gamma_{M0}}} + \frac{M_{y,Ed} + N_{Ed} e_{y,N}}{\frac{f_y W_{y,eff}}{\gamma_{M0}}} + \frac{M_{z,Ed} + N_{Ed} e_{z,N}}{\frac{f_y W_{z,eff}}{\gamma_{M0}}} \leq 1{,}0 \qquad (4.15)$$

$M_{y,Ed}$, $M_{z,Ed}$ *are the design bending moments with respect to y and z axes respectively;*e_{yN}, e_{zN} *are the eccentricitieswith respect to the neutral axis.*

Further explanations on the shear resistance check

See Paragraph 3.1.2.5.2, page 89ff.

3.2.3.7 Bending resistance verification

From the values of the bending moments M_a and M_c (see Paragraph 3.2.3.3) and of the mechanical properties in Paragraph 3.2.3.6, the normal extreme stress at ULS are:

$$\sigma_{abfl} = \frac{-M_a(z_{tot.a.na})}{I_{tot.a.eff}} + \frac{-M_c(z_{tot.na})}{I_{tot.eff}} = 353.374 \text{ MPa}$$

$$\sigma_{atf2l} = \frac{M_a(h - t_{tf.1} - t_{tf.2} - z_{tot.a.na})}{I_{tot.a.eff}} + \frac{-M_c(h - t_{tf.1} - t_{tf.2} - z_{tot.na})}{I_{tot.eff}} = \text{-}287.808 \text{ MPa}$$

$$\sigma_{atf1l} = \frac{M_a(h - t_{tf.1} - z_{tot.a.na})}{I_{tot.a.eff}} + \frac{-M_c(h - t_{tf.1} - z_{tot.na})}{I_{tot.eff}} = \text{-}302.954 \text{ MPa}$$

$$\sigma_{atfu} = \frac{M_a(h - z_{tot.a.na})}{I_{tot.a.eff}} + \frac{-M_c(h - z_{tot.na})}{I_{tot.eff}} = \text{-}319.783 \text{ MPa}$$

$$\sigma_{s.reinf} = \frac{-M_c(h + t_{slab} - c_{ur} - z_{tot.na})}{I_{tot.eff}} = \text{-}145.599 \text{ MPa}$$

It is then clearly verified that:

$$\sigma_{abfl} \leq f_{yd}(t_p) = \frac{f_y(t_p)}{\gamma_{M0}} = 325 \text{ MPa} \qquad \Rightarrow \eta_{1,\,abfl} = 1.087 > 1.0$$

$$\sigma_{atf2l} \geq f_{yd}(t_{tf.2}) = \frac{f_y(t_{tf.2})}{\gamma_{M0}} = 315 \text{ MPa} \qquad \Rightarrow \eta_{1,\,atfl} = 0.914 < 1.0$$

$$\sigma_{atf1l} \geq f_{yd}(t_{tf.1}) = \frac{f_y(t_{tf.1})}{\gamma_{M0}} = 315 \text{ MPa} \qquad \Rightarrow \eta_{1,\,atfl} = 0.962 < 1.0$$

$$\sigma_{atfu} \geq f_{yd}(t_{tf.1}) = \frac{f_y(t_{tf.1})}{\gamma_{M0}} = 315 \text{ MPa} \qquad \Rightarrow \eta_{1,\,atfl} = 1.015 > 1.0$$

$$\sigma_{sreinf} \geq f_{sd} = \frac{f_{sk}}{\gamma_s} = 434.783 \text{ MPa} \qquad \Rightarrow \eta_{1,\,s.reinf} = 0.335 < 1.0$$

The effective box section has been checked here with the calculated bending moment in the cross-section at support P3. The stress in the lower flange and in the upper flange is too high ($\eta_1 > 1.0$). The calculation should normally be carried out with a lower value calculated in the cross-section located at the distance min $[0.4 \cdot a;\ 0.5 \cdot h_w]$ from the support P3. Moreover, the stresses can be checked at mid-depth of the flanges. By doing this, the stresses should decrease under the limit value ($\eta_1 = 1.0$).

NOTE: The bending moment resistance does not take into account in the calculation the presence of the web stiffener.

3.2.3.8 Shear resistance verification

3.2.3.8.1 Shear in the box section webs

The box section web is transversally stiffened on both sides at the internal support P3 (a_w = 2.5 m).

Stiffened webpanel

To evaluate the shear buckling coefficient of the stiffened webpanel, the second moment of area of the longitudinal stiffener must be calculated according to EN 1993-1-5, Figure 5.3:

EN 1993-1-5, 4.6(3)

The plate buckling verification of the panel should be carried out for the stress resultants at a distance 0.4·a or 0.5·b, whichever is the smallest, from the panel end where the stresses are the greater. In this case the gross sectional resistance needs to be checked at the end of the panel.

EN 1993-1-5, Annex A3, Shear buckling coefficients

(1) For plates with rigid transverse stiffeners and without longitudinal stiffeners or with more than two longitudinal stiffeners, the shear buckling coefficient k_τ can be obtained as follows:

$$\begin{aligned} k_\tau &= 5.34 + 4\left(\frac{h_w}{a}\right)^2 + k_{\tau st} \text{ when } a/h_w \geq 1 \\ k_\tau &= 4 + 5.34\left(\frac{h_w}{a}\right)^2 + k_{\tau st} \text{ when } a/h_w < 1 \end{aligned} \qquad \text{(A.5)}$$

where $k_{\tau st} = 9\left(\frac{h_w}{a}\right)^2 \sqrt[4]{\left(\frac{I_{sl}}{t^3 h_w}\right)^3}$ but not less than $k_{\tau st} = \frac{2{,}1}{t}\sqrt[3]{\left(\frac{I_{sl}}{h_w}\right)}$

a	is the distance between transverse stiffeners (see Figure 5.3);
I_{sl}	is the second moment of area of the longitudinal stiffener about the z-axis, see Figure 5.3 (b).

For webs with two or more longitudinal stiffeners, not necessarily equally spaced, I_{sl} is the sum of the stiffness of the individual stiffeners.

NOTE: No intermediate non-rigid transverse stiffeners are allowed for in equation (A.5)

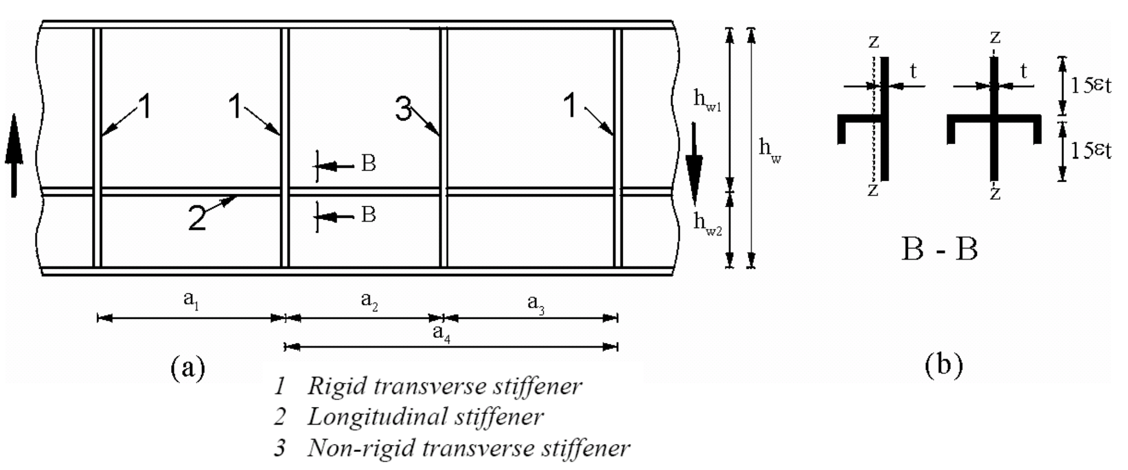

Figure **5.3: Web with transverse and longitudinal stiffeners**

(2) The equation (A.5) also applies to plates with one ort wo logitudinal stiffeners, if the aspect ratio $\alpha = \frac{a}{h_w}$ satisfies α ≥ 3. For plates with one ort wo longitudinal stiffeners and an aspect ratio α < 3 the shear buckling coefficient should be taken from:

$$k_\tau = 4{,}1 + \frac{6{,}3 + 0{,}18\frac{I_{sl}}{t^3 h_w}}{\alpha^2} + 2{,}2\sqrt[3]{\frac{I_{sl}}{t^3 h_w}} \qquad \text{(A.6)}$$

$$15\varepsilon\left(t_w\right)t_w = 0.334\text{m} \geq \frac{b_{1.st.w}}{2} = 0.25\text{ m}$$

The elastic neutral axis of the web stiffener with the width $15\varepsilon\left(t_w\right)t_w$ on both sides of the stiffener is:

$$z_{st.w} = \frac{2h_{st.w}t_{st.v.w}\frac{t_w + h_{st.w}}{2} + b_{2.st.w}t_{st.w}\left(h_{st.w} + \frac{t_w}{2}\right)}{2h_{st.w}t_{st.v.w} + b_{2.st.w}t_{st.w} + \left(2\cdot 15\varepsilon\left(t_w\right)t_w + b_{1.st.w}\right)t_w} = 0.111\text{ m}$$

The second moment of area of the web stiffener is:

$$I_{st.w} = I_{sl.w} = b_{2.st.w}t_{st.w}(h_{st.w} - z_{st.w})^2 + 2\left[\frac{t_{st.v.w}h_{st.w}^3}{12} + t_{st.w}h_{st.w}(\frac{h_{st.w}}{2} - z_{st.w})^2\right] + \left[2\cdot 15\varepsilon(t_w)t_w + b_{1.st.w}\right]t_w z_{st.w}^2$$

$= 1.215.10^{-3}$ m^4

According to EN1993-1-5, Annex A3(2), as there is only one stiffener in the web and the aspect ratio is $\alpha_w = \frac{a_w}{h_w} = 0.552 \leq 3$, the shear buckling coefficient is:

$$k_{\tau.w} = 4,1 + \frac{6,3 + 0,18\frac{I_{sl.w}}{t_w^3 h_w}}{\alpha_w^2} + 2,2\sqrt[3]{\frac{I_{sl,w}}{t_w^3 h_w}} = 38.119$$

The transverse stiffeners of the bracings frames bordering the webpanel close to support P3 are assumed to be rigid.

$$\frac{h_w}{t_w} = \frac{4533}{27} = 167.872 > \frac{31}{\eta}\varepsilon(t_w)\sqrt{k_{\tau.w}} = 131.636$$

Thus, the stiffened webpanel must be checked against shear buckling.

The reduced slenderness of the stiffened webpanel:

$$\bar{\lambda}_w = \frac{h_w}{37.4t_w\varepsilon(t_w)\sqrt{k_{\tau.w}}} = 0.881$$

Web subpanels

It is possible that one or both of the two web subpanels are more critical than the stiffened webpanel. Thus, the two web subpanels must be also checked. As the longitudinal stiffeners is located at the middle of the height of the web, the two webs subpanels have the same width and the same reduced slenderness.

According to EN 1993-1-5, Annex A3(1), as the aspect ratio is $\alpha_w = \frac{a_w}{b_{spw}} = \frac{2.5}{2.016} = 1.24 \geq 1$, the shear buckling coefficient is:

$$k_{\tau.w.sp} = 5.34 + 4\left(\frac{b_{w.sp}}{a_w}\right)^2 = 7.942$$

$$\frac{b_{w.sp}}{t_w} = \frac{2016}{27} = 74.677 > \frac{31}{\eta}\varepsilon(t_w)\sqrt{k_{\tau.w}} = 60.085$$

Thus, the web subpanels must be checked against shear buckling.

The reduced slenderness of the web subpanel:

$$\bar{\lambda}_{w.sp} = \frac{b_{w.sp}}{37.4t_w\varepsilon(t_w)\sqrt{k_{\tau.w.sp}}} = 0.858$$

EN 1993-1-1, 6.2.6, Shear

(1) The design value of the shear force V_{Ed} at each cross-section should satisfy:

$$\frac{V_{Ed}}{V_{c,Rd}} \leq 1,0 \qquad (6.17)$$

where $V_{c,Rd}$ is the design shear resistance. For plastic design $V_{c,Rd}$ is the design plastic shear resistance $V_{pl,Rd}$ as given in (2). For elastic design $V_{c,Rd}$ is the design elastic shear resistance calculated using (4) and (5).

(2) In the absence of torsion the design plastic shear resistance is given by:

$$V_{pl,Rd} = \frac{A_v\left(f_y / \sqrt{3}\right)}{\gamma_{M0}} \qquad (6.18)$$

where A_v is the shear area.

EN 1993-1-5, 5.5, Verification

(1) The verification should be performed as follows:

$$\eta_3 = \frac{V_{Ed}}{V_{b,Rd}} \leq 1$$

where V_{Ed} is the design shear force including shear from torque.

EN 1993-1-1, 6.2.7(9), Torsion

(9) For combined shear force and torsional moment the plastic shear resistance accounting for torsional effects should be reduced from $V_{pl,Rd}$ to $V_{pl,T,Rd}$ and the design shear force should satisfy:

$$\frac{V_{Ed}}{V_{pl,T,Rd}} \leq 1 \qquad (6.25)$$

in which $V_{pl,T,Rd}$ may be derived as follows:

- for a structural hollow section:

$$V_{pl,T,Rd} = \left[1 - \frac{\tau_{t.Ed}}{\left(f_y \big/ \sqrt{3}\right) \big/ \gamma_{M0}}\right] V_{pl,Rd} \qquad (6.28)$$

where $V_{pl,Rd}$ is given in 6.2.6.

Shear resistance verification

Thus, it is the stiffened webpanel which is critical: $\bar{\lambda}_w = \max(\bar{\lambda}_w, \bar{\lambda}_{w.sp}) = 0.881$

As the webpanel close to support P3 is assumed to be rigid and $0.8 \leq \bar{\lambda}_w \leq 1.08$, the reduction factor is:

$$\chi_w = \frac{0.83}{\bar{\lambda}_w} = 0.942$$

The maximum design value of the shear resistance is given by

$V_{Rd} = \min\,(V_{b,Rd};\ V_{pl,a,Rd})$ with $V_{b,Rd} = V_{bw,Rd}$

neglecting the flange contribution to the resistance:

$$V_{bw,Rd} = \frac{\chi_w f_y(t_w) h_w t_w}{\sqrt{3}\gamma_{M1}} = 20.881 \text{ MN}$$

$$V_{b,Rd} = \min\left(V_{bw,Rd}; \frac{\eta f_y(t_w) h_w t_w}{\sqrt{3}\gamma_{M1}} \right) = 20.881 \text{ MN}$$

$$V_{pl,a,Rd} = \frac{\eta f_y(t_w) h_w t_w}{\sqrt{3}\gamma_{M0}} = 29.251 \text{MN}$$

so that $\eta_3 = \dfrac{V_{Ed}}{V_{Rd}} = \dfrac{20.165}{20.881} = 0.966 \leq 1$

Shear resistance is verified!

Addition of torsional effect

The maximum torque on the box-girder bridge at the internal support P3 is equal to M_T = 1.35·20.761 MNm = 28.027 MNm (see Figure 2-35).

The area inside the median line of the box-girder bridge:

$$S = \frac{\left(b_t + b_p\right)\left(h + \frac{t_{slab}}{2}\right)}{2} = \frac{\left(12 + 6.5\right)\left(4 + \frac{0.325}{2}\right)}{2} = 38.503 \text{ m}^2$$

The shear stress in the web is given by the Bredt formula:

$$\tau_{Ed,T,web} = \frac{M_T}{2St_w} = 13.48 \text{MPa}$$

The shear force in the web due to torque is:

$$V_{Ed,T,web} = \tau_{Ed,T,web} t_w h_w = 1.65 \text{ MN}$$

Thus, the verification of shear including the torsional effect gives:

$$\eta_3 = \frac{V_{Ed} + V_{T,web}}{V_{Rd}} = \frac{20.165 + 1.65}{20.881} = 1.045 > 1$$

η_3 > 1, but the maximum torque value is combined with the maximum design value of the shear resistance which do usually not appear at the same time.

EN 1993-1-5, Annex A3, Shear buckling coefficients

(1) For plates with rigid transverse stiffeners and without longitudinal stiffeners or with more than two longitudinal stiffeners, the shear buckling coefficient k_τ can be obtained as follows:

$$\begin{aligned} k_\tau &= 5.34 + 4\left(\frac{h_w}{a}\right)^2 + k_{\tau st} \text{ when } a/h_w \geq 1 \\ k_\tau &= 4 + 5.34\left(\frac{h_w}{a}\right)^2 + k_{\tau st} \text{ when } a/h_w < 1 \end{aligned} \qquad \text{(A.5)}$$

where $k_{\tau st} = 9\left(\frac{h_w}{a}\right)^2 \sqrt[4]{\left(\frac{I_{sl}}{t^3 h_w}\right)^3}$ but not less than $k_{\tau st} = \frac{2,1}{t}\sqrt[3]{\left(\frac{I_{sl}}{h_w}\right)}$

a is the distance between transverse stiffeners (see Figure 5.3);

I_{sl} is the second moment of area of the longitudinal stiffener about the z-axis, see Figure 5.3 (b).

For webs with two or more longitudinal stiffeners, not necessarily equally spaced, I_{sl} is the sum of the stiffness of the individual stiffeners.

NOTE: No intermediate non-rigid transverse stiffeners are allowed for in equation (A.5)

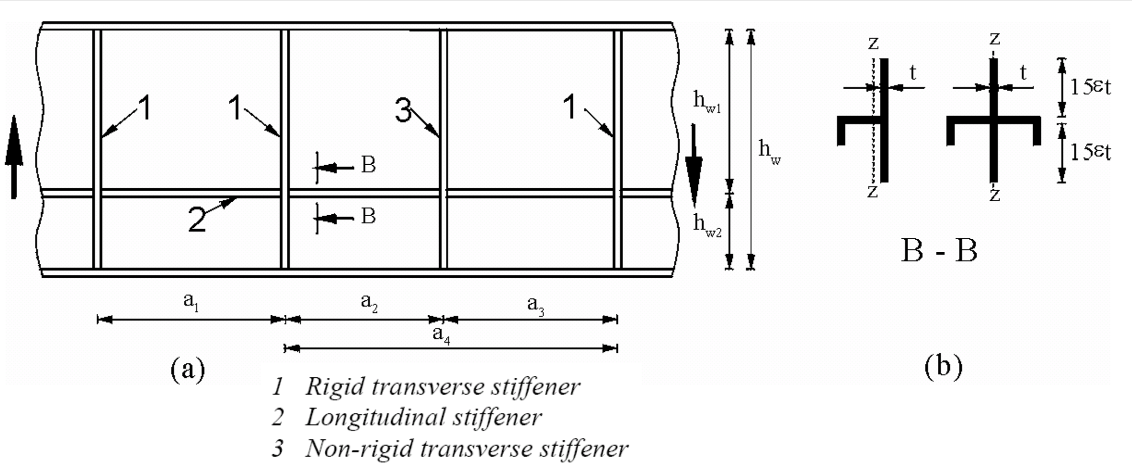

Figure **5.3: Web with transverse and longitudinal stiffeners**

(2) The equation (A.5) also applies to plates with one ort wo logitudinal stiffeners, if the aspect ratio $\alpha = \frac{a}{h_w}$ satisfies α ≥ 3. For plates with one ort wo longitudinal stiffeners and an aspect ratio α < 3 the shear buckling coefficient should be taken from:

$$k_\tau = 4,1 + \frac{6,3 + 0,18\frac{I_{sl}}{t^3 h_w}}{\alpha^2} + 2,2\sqrt[3]{\frac{I_{sl}}{t^3 h_w}} \qquad \text{(A.6)}$$

Shear verification including torsional effect

The shear area of the box section:

$$A_v = h_w t_w = 0.122 \text{ m}^2$$

The design plastic shear resistance:

$$V_{pl.Rd} = \frac{\eta A_v (f_y / \sqrt{3})}{\gamma_{M0}} = 29.251 \text{ MN}$$

The reduced design plastic shear resistance:

$$V_{pl.T.Rd} = \left[1 - \frac{\tau_{t.Ed}}{\left(f_y / \sqrt{3} \right) / \gamma_{M0}} \right] V_{pl.Rd} = 27.272 \text{ MN}$$

Thus, the verification in shear including torsional effect gives:

$$\frac{V_{Ed}}{V_{pl.T.Rd}} = \frac{20.165}{27.272} = 0.739 \leq 1$$

Shear resistance inluding shear from torque is verified!

3.2.3.8.2 Shear in the stiffened bottom flange of the box section

Calculation of the shear stress in the bottom flange

The shear stress in the bottom flange varies from $\tau_{Ed,min} = 0$ in the vertical symmetry axis of the cross-section to $\tau_{Ed,max}$ at the junction of the bottom flange with the main web. $\tau_{Ed,max}$ is calculated considering the construction phases and using the initial gross cross-section.

The shear force $V_{Ed} = 33.234$ MN at support P3 is broken down into:

- $V_{Ed,a} = 19.675$ MN applied to the structural steel box section only ($I_{tot.a} = 4.588$ m^4, $z_{na.a} = 1.882$ m) and which corresponds to a shear stress in the bottom flange equal to:

  $$\tau_{Ed,a} = \frac{V_{Ed.a}}{I_{tot.a}} \frac{\mu_{t.a}}{t_p} = 26.25 \text{ MPa}$$

  where $\mu_{t,a}$ is the moment of area of the botton flange with respect to the elastic neutral axis of the cross-section:

  $$\mu_{t.a} = \frac{b_p}{2} t_p z_{na.a} = 0.459 \text{ m}^3$$

- $V_{Ed,c} = 13.559$ MN applied to the composite box section ($I_{tot} = 5.015$ m^4, $z_{na.a} = 2.01$ m) and which corresponds to a shear stress in the bottom flange equal to:

  $$\tau_{Ed,c} = \frac{V_{Ed.c}}{I_{tot}} \frac{\mu_{t.c}}{t_p} = 17.674 \text{ MPa}$$

  where $\mu_{t.c} = \frac{b_p}{2} t_p z_{na} = 0.49 \text{ m}^3$

$$\Rightarrow \qquad \tau_{Ed,\max} = \tau_{Ed,a} + \tau_{Ed,c} = 43.924 \text{ MPa}$$

The shear stress due to torsion should be added to this value by using the same way than in previous Paragraph 3.2.3.8.1.

The shear stress in the web is given by the Bredt formula:

$$\tau_{Ed,T,bf} = \frac{M_T}{2St_p} = 4.853\text{MPa}$$

$$\Rightarrow \qquad \tau_{Ed,\max} = \tau_{Ed,a} + \tau_{Ed,c} + \tau_{Ed,T,bf} = 48.776 \text{ MPa}$$

Shear stress check in the global stiffened bottom flange

The bottom flange is transversally stiffened on both sides at the internal support P3 (a_w = 2.5 m) and longitudinally stiffened every b_{sub} = 0.5 m by six closed-section stiffeners equally spaced.

To evaluate the shear buckling coefficient of the stiffened bottom flange panel, the second moment of area of the bottom flange stiffener must be calculated according to EN 1993-1-5, Figure 5.3:

$$15\varepsilon\left(t_p\right)t_p = 0.957 \text{ m} \geq \frac{b_{1.st.w}}{2} = 0.25 \text{ m and } 15\varepsilon\left(t_p\right)t_p = 0.957 \text{ m} \geq \frac{b_{sub}}{2} = 0.25 \text{ m}$$

Then the elastic neutral axis of the web stiffener with the width $15\varepsilon\left(t_p\right)t_p$ (with the upper limit $b_{sub}/2$ or $b_{1.st1w}/2$) on both sides of the stiffener is:

$$z_{st.p} = \frac{2h_{st.w}t_{st.v.w}\dfrac{t_p + h_{st.w}}{2} + b_{2.st.w}t_{st.w}\left(h_{st.w} + \dfrac{t_p - t_{st.w}}{2}\right)}{2h_{st.w}t_{st.v.w} + b_{2.st.w}t_{st.w} + \left(b_{sub} + b_{1.st.w}\right)t_p} = 63.674 \text{ mm}$$

The second moment of area of one bottom flange stiffener is:

$$I_{st.p} = b_{2.st.w}t_{st.w}(h_{st.w} - z_{st.w})^2 + 2\left[\frac{t_{st.v.w}h_{st.w}^3}{12} + t_{st.w}h_{st.w}(\frac{h_{st.w}}{2} - z_{st.p})^2\right] + \left[b_{sub} + b_{1.st.w}\right]t_w z_{st.p}^2 + \frac{\left[b_{sub} + b_{1.st.w}\right]t_p^3}{12}$$

$$I_{st.p} = 1.718.10^{-3} \text{ m}^4$$

The second moment of area of the six bottom flange stiffeners is:

$$I_{sl.p} = 6I_{st.p} = 0.01 \text{ m}^4$$

According to EN 1993-1-5, Annex A3 (2), as there are six stiffeners in the bottom flange and the aspect ratio $\alpha_p = \frac{a_w}{b_p} = 0.385 \leq 1$, the shear buckling coefficient is:

$$k_{\tau.p} = 4 + 5.34\left(\frac{b_p}{a_w}\right)^2 + k_{\tau st.p} = 204.342$$

where $k_{\tau st.p} = 9\left(\dfrac{b_p}{a_W}\right)^2 \sqrt[4]{\left(\dfrac{I_{sl.p}}{t_p^3 b_p}\right)^3} = 164.243 \geq \dfrac{2.1}{t_p}\sqrt[3]{\dfrac{I_{sl.p}}{b_p}} = 3.265$

The tranverse stiffeners of the bracings frames bordering the bottom flange panel close to support P3 are assumed to be rigid.

$$\frac{b_p}{t_p} = \frac{6500}{75} = 86.667 < \frac{31}{\eta}\varepsilon(t_p)\sqrt{k_{\tau.p}} = 314.015$$

Thus, the bottom flange must not be checked against shear buckling. It is therefore deduced that no global plate buckling occurs due to shear stress in the bottom flange.

$$\Rightarrow \qquad \tau_{Ed,\max}/2 = 48.776 \text{ MPa}/2 = 24.388 \text{ MPa} \leq \tau_{Rd} = \frac{\eta f_y(t_p)}{\gamma_{M1}\sqrt{3}} = 204.697 \text{ MPa (with } \eta = 1.2\text{)}$$

$$\Rightarrow \qquad \eta_3 = \frac{\tau_{Ed,\max}/2}{\tau_{Rd}} = 0.119 < 1$$

EN 1993-1-1, 6.2.6 (4)

(4) For verifying the design elastic shear resistance $V_{c,Rd}$ the following criterion for a critical point of the cross-section may be used unless the buckling verification in EN 1993-1-5, Section 5 applies:

$$\frac{\tau_{Ed}}{f_y / \sqrt{3}\gamma_{M0}} \leq 1,0 \qquad (6.19)$$

where τ_{Ed} may be obtained from: $\tau_{Ed} = \frac{V_{Ed} S}{It}$ (6.20)

where V_{Ed} is the design value of the shear force

S is the first moment of area about the centroidal axis of that portion of the cross-section between the point at which the shear is required and the boundary of the cross-section

I is second moment of area of the whole cross-section

t is the thickness at the examined point

NOTE: The verification according to (4) is conservative as it excludes partial plastic shear distribution, which is permitted in elastic design, see (5). Therefore it should only be carried out where the verification on the basis of $V_{c,Rd}$ according to equation (6.17) cannot be performed.

Further explanations on the M-V-interaction

See Paragraph 3.1.2.5.3, page 93.

EN 1993-1-5, 7.1(2)

(2) The criterion given in (1) should be verified at all sections other than those located at a distance less than $h_w/2$ from a support with vertical stiffeners.

EN 1993-1-5, 7.1(5)

(5) A flange in a box-girder should be verified using 7.1(1) taking $M_{f,Rd} = 0$ and τ_{Ed} taken as the average shear stress in the flange which should not be less than half the maximum shear stress in the flange and η_1 is taken as η_1 according to 4.6(1). In addition the subpanels should be checked using the average shear stress within the subpanel and χ_w determined for shear buckling of the subpanel according to 5.3, assuming the longitudinal stiffeners to be rigid.

Shear stress check in each subpanel of the bottom flange

The longitudinal stiffeners are assumed to be rigid. In the bottom flange they define subpanels of the size a_w = 2500 mm and b_{sub} = 500 mm. These subpanels should be individually checked for shear resistance. The verification is only performed in the most loaded subpanel, namely the one bordering the main steel web of the box section where the average shear stress reaches.

$$\tau_{Ed} = \tau_{Ed,\max} + \frac{\left(\tau_{Ed.t.bf} - \tau_{Ed,\max}\right) b_{sub}/2}{b_p/2} = 48.776 + \frac{(4.853 - 48.776)500/2}{6500/2} = 45.398 \text{ MPa}$$

According to EN 1993-1-5, Annex 3(2), as the aspect ratio $\alpha_{sub} = \frac{a_w}{b_{sub}} = 5 \geq 1$, the shear buckling coefficient is:

$$k_{\tau.p} = 5.34 + 4\left(\frac{b_{sub}}{a_w}\right)^2 + k_{\tau st.sub} = 5.5$$

where $k_{\tau st.sub} = 0$

The transverse stiffeners of the bracings frames bordering the bottom flange panel close to support P3 are assumed to be rigid.

$$\frac{b_{sub}}{t_p} = \frac{500}{75} = 6.667 < \frac{31}{\eta}\varepsilon(t_p)\sqrt{k_{\tau.sub}} = 51.517$$

Thus, the subpanels of the bottom flange must not be checked against shear buckling. It is therefore deduced that no local buckling occurs in the bottom flange due to shear.

$\Rightarrow$ $\tau_{Ed} = 45.398$ MPa $\leq \tau_{b,Rd} = \frac{\eta f_y(t_p)}{\gamma_{M1}\sqrt{3}} = 204.697$ MPa (with $\eta = 1.2$)

$\Rightarrow$ $\eta_3 = \frac{\tau_{Ed}}{\tau_{b,Rd}} = 0.22 \leq 1$

Shear resistance is verified!

3.2.3.9 Interaction between bending moment and shear force

3.2.3.9.1 M-V-interaction in the box-girder webs

The section to be verified is located at a distance $h_w/2$ = 2.266 m from support P3. In this section M_{Ed} = -670.487 MNm and V_{Ed} = 18.932 MN (considering the inclination of the web).

$$\overline{\eta}_3 = \frac{V_{Ed}}{V_{bw,Rd}} = 0.914 \geq 0.5$$

The M-V-interaction should be checked by justifying the following criterion in the box section webs:

$$\overline{\eta}_1 + \left[1 - \frac{M_{f,Rd}}{M_{pl,Rd}}\right]\left[2\overline{\eta}_3 - 1\right]^2 \leq 1 \text{ if } \overline{\eta}_1 = \frac{M_{Ed}}{M_{Pl,Rd}} \geq \frac{M_{f,Rd}}{M_{Pl,Rd}}$$

The plastic bending moment resistance of the section, as well as the plastic bending moment resistance of the flanges only, is calculated with the effective cross-sections of the flanges (taking into acccount the shear lag effect and the possibility of plate buckling).

The web is in tension in its upper part and in compression in its lower part. To calculate $M_{f,Rd}$ the position of the Plastic Neutral Axis (PNA) is determined as follows:

Relations to find the location of the Plastic Neutral Axis (PNA) under negative moment $M_{Pl,Rd}$

RELATIONS	PNA LOCATION
$N_{abf} \geq N_{atf.1} + N_{atf.2} + N_{sl} + N_{su}$	PNA in the bottom flange
$N_{abf} + N_{atf.2} \geq N_{atf.1} + N_{sl} + N_{su}$ and $N_{abf} < N_{atf.1} + N_{atf.2} + N_{sl} + N_{su}$	PNA in the top flange 2
$N_{abf} + N_{atf.2} + N_{atf.1} \geq N_{sl} + N_{su}$ and $N_{abf} + N_{atf.2} < N_{atf.1} + N_{sl} + N_{su}$	PNA in the top flange 1
$N_{sl} + N_{su} > N_{abf} + N_{atf.1} + N_{atf.2}$	PNA in the slab

- Design plastic resistance of the bottom flange:

$$N_{a.bf} = \left[n_{st} \left[t_{st} f_{yd}(t_{st.w})(b_{2.eff} + 2b_{3.eff}) + t_p f_{yd}(t_p)(b_{1.eff} + b_{sub.eff}) \right] \rho_c + t_p f_{yd}(t_p)(0.2m + b_{sub.eff}) \right] \beta_{ult}^{\kappa} =$$

$= 181.359$ MN

- Design plastic resistance of the two structural steel top flanges 1:

$$N_{a.tf.1} := 2 \cdot b_{tf.1} \cdot t_{tf.1} \cdot f_{yd}(t_{tf.1}) = 94.5\,\mathrm{MN}$$

- Design plastic resistance of the two structural steel top flanges 2:

$$N_{a.tf.2} := 2 \cdot b_{tf.2} \cdot t_{tf.2} \cdot f_{yd}(t_{tf.2}) = 79.38\,\mathrm{MN}$$

- Design plastic resistance of the upper steel reinforcement:

$$N_{su} := A_{s.ur} \cdot f_{sd} = 22.59\,\mathrm{MN}$$

- Design plastic resistance of the lower steel reinforcement:

$$N_{sl} := A_{s.lr} \cdot f_{sd} = 14.458\,\mathrm{MN}$$

- Location of the Plastic Neutral Axis (PNA)

  $N_{abf} + N_{atf.2} = 275.857$ MN $\geq N_{atf.1} + N_{sl} + N_{su} = 131.548$ MN

  and $N_{abf} = 181.357$ MN $< N_{atf.1} + N_{atf.2} + N_{sl} + N_{su} = 210.928$ MN

  Thus the PNA is deduced to be located in the top flange 2 at a distance z_{pl} from the extreme lower fiber of the bottom flange. Writing the force equilibrium around the PNA deduced:

$$z_{pl} = \frac{4\left(h - t_{tf.1}\right) b_{tf.2} f_{yd}(t_{tf.2}) + N_{a.tf.1} + N_{su} + N_{sl} - N_{a.bf} - N_{a.tf.2}}{4 b_{tf.2} f_{yd}(t_{tf.2})} = 3.827\ \mathrm{m}$$

The design plastic resistance moment of the flanges only is calculated from the position of the PNA:

$$\begin{aligned} M_{f,Rd} &= N_{su}(h + t_{slab} - c_{ur} - z_{pl}) + N_{sl}(h + c_{lr} - z_{pl}) \\ &+ \frac{\left(h - t_{tf.1} - z_{pl}\right)^2}{2} 2b_{tf.2} f_{yd}(t_{tf.2}) + \frac{\left(h - t_{tf.1} - t_{tf.2} - z_{pl}\right)^2}{2} 2b_{tf.2} f_{yd}(t_{tf.2}) = 714.623\ \mathrm{MNm} \\ &+ N_{a.tf.1}\left(h - \frac{t_{tf.1}}{2} - z_{pl}\right) + N_{a.bf}\left(z_{pl} - \frac{t_p}{2}\right) \end{aligned}$$

As $|M_{Ed}| = 709.513$ MNm $< M_{f.Rd} = 714.623$ MNm, there is finally no need to verify the interaction criteria.

3.2.3.9.2 Interaction M-V in the bottom flange of the box section

The value $\eta_3 = 0.119$ has already been calculated in Paragraph 3.2.3.8.2. Thus, $\eta_3 < 0.5$.

⇒ **There is no need to check the M-V-interaction.**

4 Verifications during erection

4.1 Twin-girder bridge

4.1.1 General

The construction phasing of the twin-girder bridge is done according to the following scheme: firstly, the steel superstructure of the twin-girder bridge is erected by the incremental launching technique. Secondly, the concrete slab is cast in-situ according to the order already described in Section 2.1.4. Finally, the non-structural equipment is installed. During erection, usually each cross-section has to be verified at every construction stage which cannot all be part of this section. Thus, in the following, the verifications during erection focus on the patch loading resistance of the steel girders during launching.

The bridge is launched from one side (abutment C0) only. In order to recover and to reduce the deflection of the cantilever part when approaching a support, a launching nose is used. The launching nose has a length of 11.75 m and its total weight decreases from 18 kN/m at the cross-section connected to the bridge girders to 12 kN/m at its free end. A provisional wind bracing is added between the two steel girders for the launching process. At the supports, sliding skates with a loading length of s_s = 1.5 m are used.

The determination of the patch loading resistance is done both according to Section 6, EN 1993-1-5 in Section 4.1.2 and according to Section 10, EN 1993-1-5 in Section 4.1.3. However, initially the most unfavourable launching situation has been determined as shown in Figure 4-1 which corresponds to a location of the steel girders at a position of x = 111.75 m.

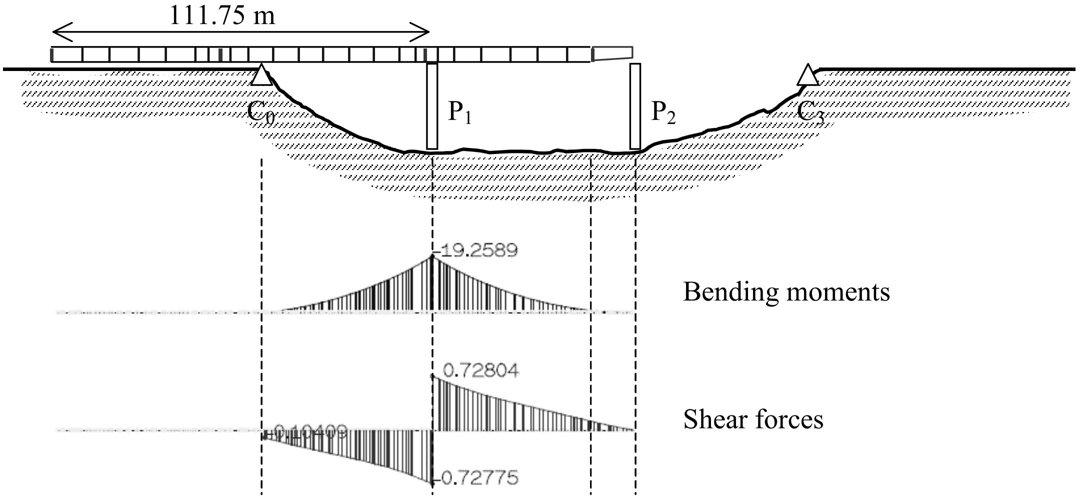

Figure 4-1: Most unfavourable launching situation.

The dimensions of the studied panel at the decisive cross-section are given in Figure 4-2. The web is longitudinally unstiffened and the spacing of the vertical stiffeners is based on the verifications against lateral torsional buckling, i.e. 3.5 m here. On the safe side, additional stiffeners which may have been added for shear verification are not considered.

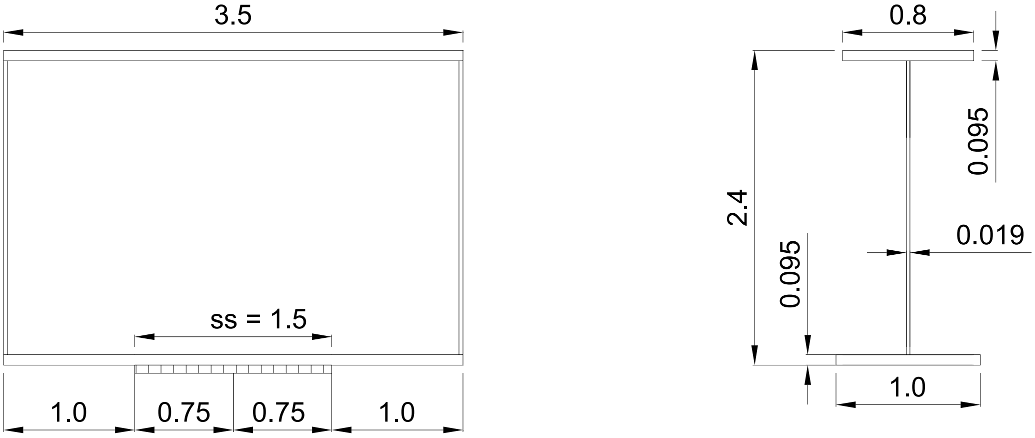
3.5
ss = 1.5
1.0
0.75
0.75
1.0
0.8
2.4
0.095
0.019
0.095
1.0

Figure 4-2: Dimensions of the studied panel in [m].

From the global analysis, the internal design forces (for use with Section 6, EN 1993-1-5) are given below for one main steel girder.

M_{Ed} = -19.26 MNm

$V_{Ed,max}$ = 0.73 MN

$V_{Ed,applied} = V_{Ed,max} - F_{Ed}/2 = 0$ MN

F_{Ed} = 1.46 MN

The resulting stress field (for use with Section 10, EN 1993-1-5) acting at the studied panel is shown in Figure 4-3.

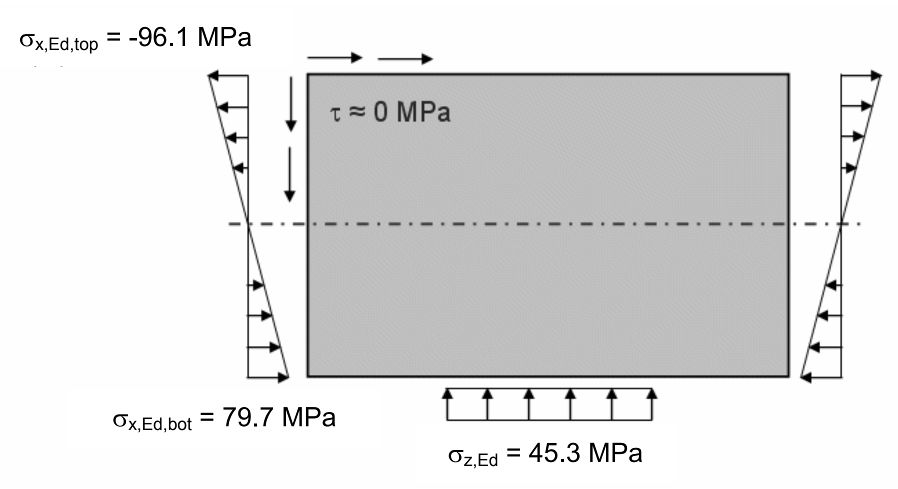
$\sigma_{x,Ed,top}$ = -96.1 MPa
$\tau \approx 0$ MPa
$\sigma_{x,Ed,bot}$ = 79.7 MPa
$\sigma_{z,Ed}$ = 45.3 MPa

Figure 4-3: Stress field acting at the studied panel.

Buckling value k_F

The formula given for the buckling value k_F must be exclusively used for the determination of the critical load F_{cr} because the reduction curve $\chi_F(\bar{\lambda}_F)$ has been calibrated based on this formula for k_F.

4.1.2 Verifications according to Sections 6 and 7, EN 1993-1-5

In the following, the patch loading resistance according to Section 6, EN 1993-1-5 is determined. The interaction between transverse force and bending moment is checked according to Section 7, EN 1993-1-5.

Determination of the critical load F_{cr}

$k_F := 6 + 2 \cdot \left(\frac{h_w}{a} \right)^2$ $\qquad$ $k_F = 6.80$

$F_{cr} := 0.9 \cdot k_F \cdot 210000\text{MPa} \cdot \frac{t_w^{\ 3}}{h_w}$ $\qquad$ $F_{cr} = 3.99\,\text{MN}$

Determination of the yield load F_y

$m_1 := \frac{f_{yf} \cdot b_f}{f_{yw} \cdot t_w}$ $\qquad$ $m_1 = 48.05$

$m_2 := 0.02 \cdot \left(\frac{h_w}{t_f} \right)^2$ $\qquad$ $m_2 = 10.82$

$l_y := s_s + 2 \cdot t_f \cdot \left(1 + \sqrt{m_1 + m_2} \right)$

$l_{y.} := \begin{vmatrix} l_y & \text{if } l_y \le a \\ a & \text{if } l_y > a \end{vmatrix}$ $\qquad$ $l_y = 3148\,\text{mm}$

$F_y := l_y \cdot t_w \cdot f_{yw}$ $\qquad$ $F_y = 20.63\,\text{MN}$

Determination of the slenderness parameter $\bar{\lambda}_F$

$\lambda_F := \sqrt{\frac{F_y}{F_{cr}}}$ $\qquad$ $\lambda_F = 2.27$

Here, the slenderness parameter is larger than $\bar{\lambda}_F = 0.5$ which is a precondition to use the above formula for m_2. For $\lambda_F \le 0.5$, m_2 should be set to zero according to Paragraph 6.5(1), EN 1993-1-5.

Determination of the reduction factor χ_F

$\chi_F := \begin{vmatrix} 1.0 & \text{if } \lambda_F \le 0.5 \\ \frac{0.5}{\lambda_F} & \text{if } \lambda_F > 0.5 \end{vmatrix}$ $\qquad$ $\chi_F = 0.22$

Improved resistance to transverse forces

In the COMBRI research project and in [31] it has been shown that in case the value m_2 is set to zero and, due to the changed definition of the yield load, the reduction curve is recalibrated, not only the resistance to transverse forces can be improved but also the scatter of the resistance model becomes smaller. For details, see the COMBRI Final report [7].

Interaction between transverse force and bending moment

In Section 7.2(1), EN 1993-1-5, the interaction should be determined as follows:

$$\eta_2 + 0.8 \cdot \eta_1 \leq 1.4$$

If $\eta_2 = 1.0$ is assumed, it can be shown that the influence of bending moment must be taken into account only for $\eta_1 > 0.5$.

Determination of the patch loading resistance

$$L_{eff} := \chi_F \cdot l_y \qquad L_{eff} = 691.9\,\text{mm}$$

$$F_{Rd} := \frac{f_{yw} \cdot L_{eff} \cdot t_w}{\gamma_{M1}} \qquad F_{Rd} = 4.12\,\text{MN}$$

$$\eta_2 := \frac{F_{Ed}}{F_{Rd}} \qquad \eta_2 = 0.353$$

Interaction between transverse force and bending moment

Here, $\eta_1 = 0.265 < 0.5$ so that the interaction with bending moment is not decisive.

However, in the following the calculation according Section 7, EN 1993-1-5 is shown:

$$\eta_2 + 0.8 \cdot \eta_1 \quad \leq \quad 1.4$$

Here $\eta_1 = 0.270$ and $\eta_2 = 0.353$, so that the interaction verification becomes

$$0.353 + 0.8 \cdot 0.270 = 0.569 \quad < \quad 1.4$$

4.1.3 Verifications according to Section 10, EN 1993-1-5

In the following, the patch loading resistance according to Section 10, EN 1993-1-5 is determined.

Determination of α_{cr}

The determination of the minimum load amplifier α_{cr} for the design loads to reach the elastic critical load of the plate under the complete stress field can be either determined

- **for each component of the stress field (e.g. by a hand-calculation)**

$$\sigma_E := 189800\text{MPa} \cdot \left(\frac{t_w}{h_w}\right)^2 \qquad \sigma_E = 14.03\,\text{MPa}$$

Elastic critical longitudinal stress acc. to Table 4.1, Section 4.4, EN 1993-1-5

$$k_{\sigma.x} := \left| \begin{array}{l} \dfrac{8.2}{1.05 + \psi} \quad \text{if } 1 \geq \psi > 0 \\ 7.81 - 6.29\psi + 9.78\psi^2 \quad \text{if } 0 \geq \psi > -1 \\ 5.98 \cdot (1 - \psi)^2 \quad \text{if } -1 \geq \psi > -3 \end{array} \right. \qquad k_{\sigma.x} = 29.08$$

$$\sigma_{cr.x} := k_{\sigma.x} \cdot \sigma_E \qquad \sigma_{cr.x} = 407.95\,\text{MPa}$$

$$\alpha_{cr.x} := \frac{\sigma_{cr.x}}{\sigma_{x.Ed.bot}} \qquad \alpha_{cr.x} = 5.12$$

Elastic critical transverse stress with k = 2.08 acc. to Table 8.12 [38]

$$\sigma_{cr.z} := k \cdot \sigma_E \cdot a \cdot \frac{1}{s_s + 2 \cdot t_f} \qquad \sigma_{cr.z} = 60.43\,\text{MPa}$$

$$\alpha_{cr.z} := \frac{\sigma_{cr.z}}{\sigma_{z.Ed}} \qquad \alpha_{cr.z} = 1.33$$

Elastic critical shear stress acc. to Eq. (A.5), Annex A.3, EN 1993-1-5

$$k_\tau := \left| \begin{array}{ll} 5.34 + 4.00 \cdot \left(\frac{h_w}{a}\right)^2 & \text{if } \frac{a}{h_w} \ge 1 \\ 4.00 + 5.34 \cdot \left(\frac{h_w}{a}\right)^2 & \text{if } \frac{a}{h_w} < 1 \end{array} \right. \qquad k_\tau = 6.93$$

$$\tau_{cr} := k_\tau \cdot \sigma_E \qquad \tau_{cr} = 97.29\,\text{MPa}$$

$$\alpha_{cr.\tau} := \frac{\tau_{cr}}{\tau_{Ed}} \qquad \alpha_{cr.\tau.} := \infty$$

Minimum load amplifier acc. to Eq. (10.6), Section 10, EN 1993-1-5

$$\alpha_{cr} := \frac{1}{\frac{1+\psi}{4\alpha_{cr.x}} + \frac{1}{2\alpha_{cr.z}} + \sqrt{\left(\frac{1+\psi}{4\alpha_{cr.x}} + \frac{1}{2\alpha_{cr.z}}\right)^2 + \frac{1-\psi}{2 \cdot \alpha_{cr.x}^2} + \frac{1}{\alpha_{cr.\tau}^2}}}$$

$$\alpha_{cr} = 1.276$$

- **for the complete stress field (e.g. by using appropriate software)**

  In case e.g. software EBPlate is used, the minimum load amplifier can be determined in a single step as $\alpha_{cr} = 1.259$.

In the following calculations, the value $\alpha_{cr} = 1.276$ is further used.

Determination of $\alpha_{ult,k}$

$$\sigma_{eq} := \sqrt{\sigma_{x.Ed.bot}^2 + \sigma_{z.Ed}^2 - \sigma_{x.Ed.bot} \cdot \sigma_{z.Ed} + 3 \cdot \tau_{Ed}^2} \qquad \sigma_{eq} = 69.26\,\text{MPa}$$

$$\alpha_{ult.k} := \frac{f_{yw}}{\sqrt{\sigma_{x.Ed.bot}^2 + \sigma_{z.Ed}^2 - \sigma_{x.Ed.bot} \cdot \sigma_{z.Ed} + 3 \cdot \tau_{Ed}^2}} \qquad \alpha_{ult.k} = 4.98$$

Elastic critical column-buckling stress $\sigma_{cr,c}$

The determination of $\sigma_{cr,c}$ in the transverse direction should take into account the nonlinear stress distribution in the web for which no hand-calculation method exists at the moment. Instead, a common approach is to assume a linearly varying stress distribution for a pin-ended strut which is zero at one end and which can be calculated acc. to DIN 4114 as follows: $\sigma_{cr,c} = 1.88 \cdot \sigma_E$.

It should be noted that this simplification may lead to unsafe results because $\sigma_{cr,c}$ is underestimated and in turn the ratio $\sigma_{cr,p}/\sigma_{cr,c}$, is overestimated so that column-like behaviour is not detected correctly. The shorter the loading lengths is, the larger this deviation is.

Reduction curve for transverse stresses, column-like behaviour and interpolation function

In the COMBRI project it has been shown that the interpolation function acc. to Eq. (4.13), Section 4.5.4, EN 1993-1-5, which takes into account column-like buckling, is not appropriate for patch loading stresses in the transverse direction. Moreover, the ratio of $\sigma_{cr,p}/\sigma_{cr,c}$, for which column-like buckling needs to be considered, should be 2.7 (and not 2.0 as given in Eq. (4.13)).

Basically, either a new interpolation function is required or a reduction curve should be used which can be used with the existing interpolation function. A new interpolation function has been derived e.g. by Seitz [40] and this method is introduced in the COMBRI Final report [7]. However, e.g. for the new German DIN-Fachbericht 103 [12], it has been decided to use the reduction curve of Annex B, EN 1993-1-5, for transverse stresses because this approach complies well with current Eurocode rules and could be easier implemented. Thus, for a welded girder Table B.1, Annex B.1, EN 1993-1-5 gives:

$$\bar{\lambda}_{p0} := 0.80 \qquad \alpha_p := 0.34 \qquad \phi_{p.} := 0.5 \cdot \left[1 + \alpha_p \cdot \left(\lambda_p - \lambda_{p0}\right) + \lambda_p\right]$$

which is to be used in

$$\rho := \frac{1}{\phi_{p.} + \sqrt{\phi_{p.}^{2} - \lambda_p}}$$

This reduction curve is used on the right hand-side instead of Eq. (4.13), Section 4.5.4,
EN 1993-1-5.

Determination of the slenderness parameter $\bar{\lambda}_p$

$$\lambda_p := \sqrt{\frac{\alpha_{ult.k}}{\alpha_{cr}}} \qquad \lambda_p = 1.976$$

Determination of the reduction factors

The determination of the reduction factors for the design loads to reach the elastic critical load of the plate under the complete stress field can be either determined

- **using different buckling curves**

  Longitudinal stress acc. to Eq. (4.2), Section 4.4, EN 1993-1-5

$$\rho_x := \frac{\lambda_p - 0.055\cdot(3+\psi)}{\lambda_p^{\ 2}} \qquad \rho_x = 0.481$$

  Check of column-like behaviour in the longitudinal direction

  Column-like buckling in the longitudinal direction for plates should be checked according to Section 4.4(6), EN 1993-1-5, for panel aspect ratios a < 1.0. Therefore column-like behaviour is not calculated in detail here.

  Transverse stress acc. to Annex B.1, EN 1993-1-5

$$\rho_{z.} := \frac{1}{\phi_{p..} + \sqrt{\phi_{p..}^{\ 2} - \lambda_p}} \quad \text{with} \quad \phi_{p..} = 1.688 \qquad \rho_{z.} = 0.381$$

  Check of column-like behaviour in the transverse direction

  Due to the nonlinear distribution of transverse stresses in the web, the determination of the critical column-buckling stress has been done here most accurately based on the energy method which takes into account the nonlinear stress distribution.

$$\sigma_{cr.c} := 28.55\text{MPa}$$

$$\frac{\sigma_{cr.z}}{\sigma_{cr.c}} = 2.12 \qquad \xi := \frac{\sigma_{cr.z}}{\sigma_{cr.c}} - 1 \qquad \xi = 1.12$$

  Because $\xi > 1.0$, column-like behaviour does not have to be considered acc. to the definition in the existing Section 4.5.4, EN 1993-1-5.

  Shear stress acc. to Table 5.1, Section 5.3, EN 1993-1-5 with $\eta = 1.2$.

$$\chi_w := \left| \begin{array}{l} 1.0 \quad \text{if } \lambda_p < \dfrac{\eta}{0.83} \\ \dfrac{0.83}{\lambda_p} \quad \text{if } \lambda_p \geq \dfrac{\eta}{0.83} \end{array} \right. \qquad \chi_w = 0.420$$

Use of a corrected interpolation function instead of the reduction curve acc. to Annex B.1, EN 1993-1-5

For comparison, the use of the newly derived interpolation function acc. to Seitz [40] would give:

$$\eta_{Seitz} = 0.477$$

For comparison with Section 4.1.2 “Application of Section 6, EN 1993-1-5”, the pure patch loading resistance leads to F_{Rd} = 3.13 MN. This also shows that the application of existing Section 10, EN 1993-1-5 [23] in combination with Section 4, EN 1993-1-5 overestimates the patch loading resistance by 22.4% (F_{Rd} = 3.83 MN). In contrast to this, results from the newly derived interpolation function (F_{Rd} = 3.13 MN) and from the buckling curve based on Annex B.1, EN 1993-1-5 (F_{Rd} = 3.17 MN) correspond well with a difference of about 1.3 %.

- **using a single buckling curve**

According to Table B.1, Annex B.1, EN 1993-1-5

$\lambda_{p0} := 0.80 \qquad \alpha_p := 0.34$

$\phi_{p.} := 0.5 \cdot \left[1 + \alpha_p \cdot \left(\lambda_p - \lambda_{p0}\right) + \lambda_p\right]$

$\phi_{p.} = 1.688$

$$\rho := \frac{1}{\phi_{p.} + \sqrt{\phi_{p.}^2 - \lambda_p}}$$

$\rho = 0.381$

Determination of the patch loading resistance

- **using different buckling curves**

$$\eta_{diff} := \sqrt{\left(\frac{\sigma_{x.Ed.bot}}{\rho_x \cdot \frac{f_{yw}}{\gamma_{M1}}}\right)^2 + \left(\frac{\sigma_{z.Ed}}{\rho_z \cdot \frac{f_{yw}}{\gamma_{M1}}}\right)^2 - \left(\frac{\sigma_{x.Ed.bot}}{\rho_x \cdot \frac{f_{yw}}{\gamma_{M1}}}\right) \cdot \left(\frac{\sigma_{z.Ed}}{\rho_z \cdot \frac{f_{yw}}{\gamma_{M1}}}\right) + 3 \cdot \left(\frac{\tau_{Ed}}{\chi_w \cdot \frac{f_{yw}}{\gamma_{M1}}}\right)^2}$$

$\eta_{diff} = 0.472$

For comparison with Section 4.1.2 “Application of Section 6, EN 1993-1-5”, the pure patch loading resistance leads to $F_{Rd} = 3.17$ MN.

- **using a single buckling curve**

$\alpha_{Rd} = \frac{\rho \cdot \alpha_{ult,k}}{\gamma_{M1}} \qquad \alpha_{Rd} = 1.727 \qquad \eta_{single} = \frac{1}{\alpha_{Rd}} = 0.579$

For comparison with Section 4.1.2 “Application of Section 6, EN 1993-1-5”, the pure patch loading resistance leads to $F_{Rd} = 3.17$ MN.

4.1.4 Results

In Figure 4-4 the distribution of the patch loading resistances is summarised along the whole bridge length. It can be shown that the most unfavourable launching situation (F_{Ed} = 1.456 MN) can be easily verified not only with the cross-section near the support P2 (x = 111.75) but also with other cross-sections in the span region.

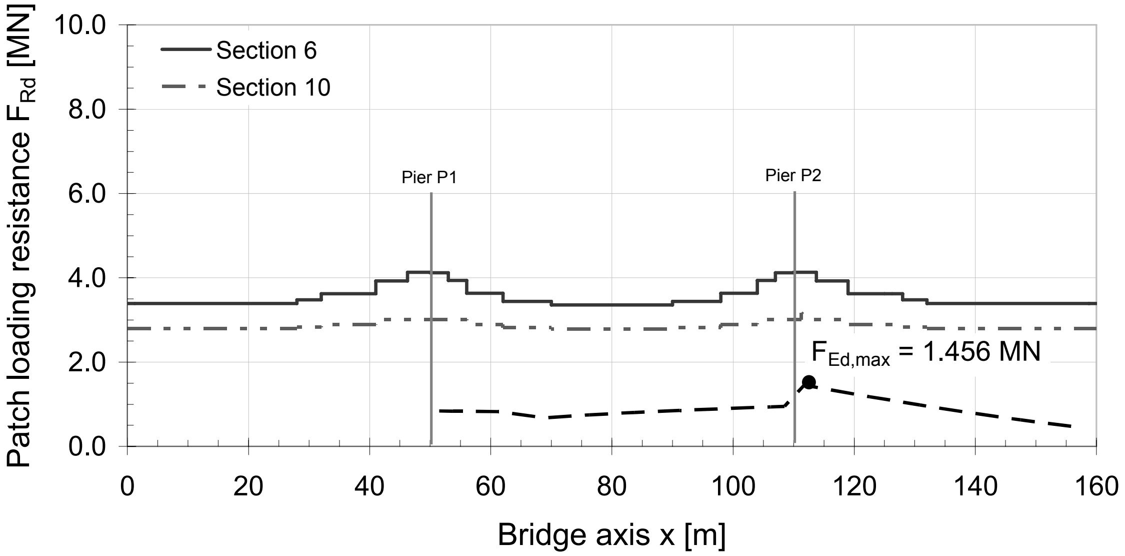

Figure 4-4: Distribution of patch loading resistances according to EN 1993-1-5 along the bridge length.

4.2 Box-girder bridge

4.2.1 General

The construction phasing of the box-girder bridge is done according to the following scheme: firstly, the steel superstructure of the box-girder bridge is erected by the incremental launching technique. Secondly, the concrete slab is cast in-situ according to the order already described in Section 2.2.4. Finally, the non-structural equipment is installed. During erection, usually each cross-section has to be verified at every construction stage which cannot all be part of this section. Thus, in the following, the verifications during erection focus on the patch loading resistance of the steel girders during launching.

The bridge is launched from one side (abutment C0) only. In order to recover and to reduce the deflection of the cantilever part when approaching a support, a launching nose is used. The launching nose has a length of 28 m and its total weight decreases from 57 kN/m at the cross-section connected to the bridge girder to 28 kN/m at its free end. A provisional wind bracing is added between the upper flanges for the launching process. At the supports, sliding skates with a loading length of s_s = 3.0 m are used.

The determination of the patch loading resistance is done both according to Section 6, EN 1993-1-5, in Section 4.2.2 and according to Section 10, EN 1993-1-5, in Section 4.2.3. In the following, the different launching situations which will be checked are introduced. In all diagrams the internal forces and support reactions are given for one half of the box-girder.

The most unfavourable launching situation for maximum bending has been determined as shown in Figure 4-1 which corresponds to a location of the steel girder at a position of x = 448 m.

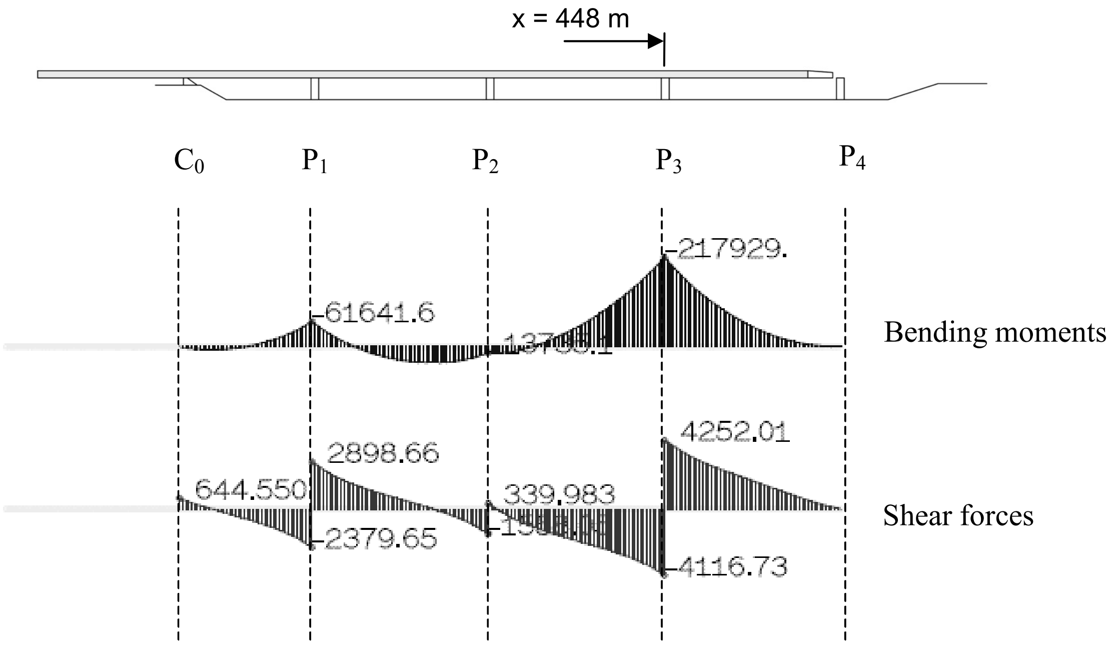

Figure 4-5: Launching situation "1" (most unfavourable both for maximum bending and pier cross-section).

The most unfavourable launching situation for the weakest cross-section has been determined as shown in Figure 4-6 which corresponds to a location of the steel girder at a position of x = 484 m.

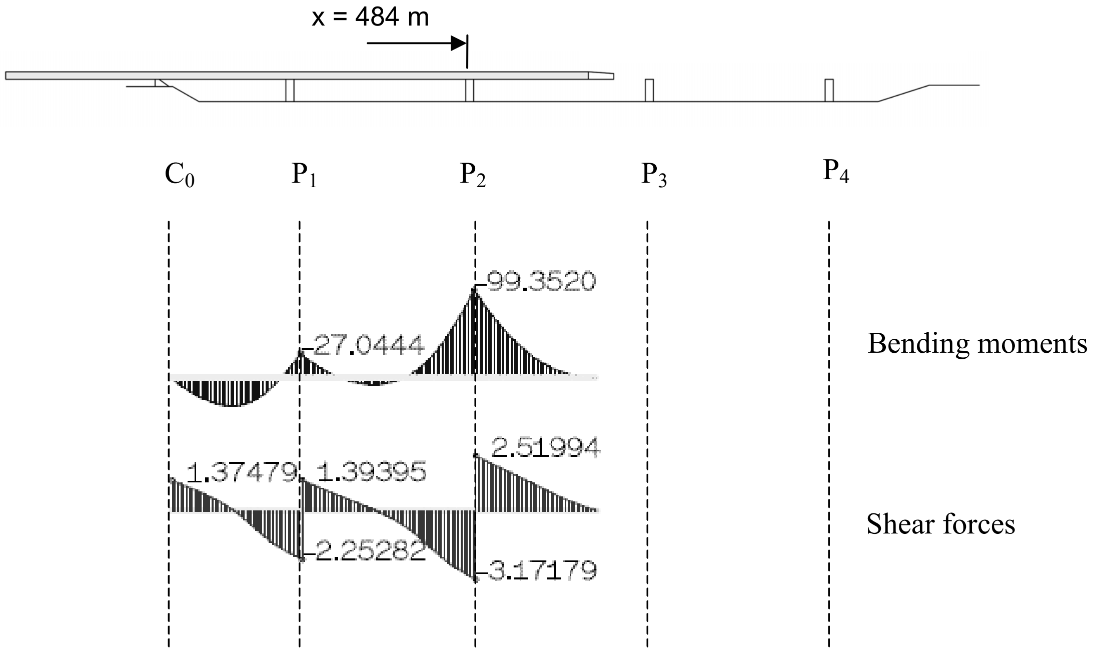
x = 484 m
C0
P1
P2
P3
P4
99.3520
27.0444
Bending moments
2.51994
1.37479
1.39395
-2.25282
-3.17179
Shear forces

Figure 4-6: Launching situation "2" (most unfavourable for weakest end-span cross-section).

The most unfavourable launching situation for unequal shear distribution has been determined as shown in Figure 4-7 which corresponds to a location of the steel girder at a position of x = 408 m.

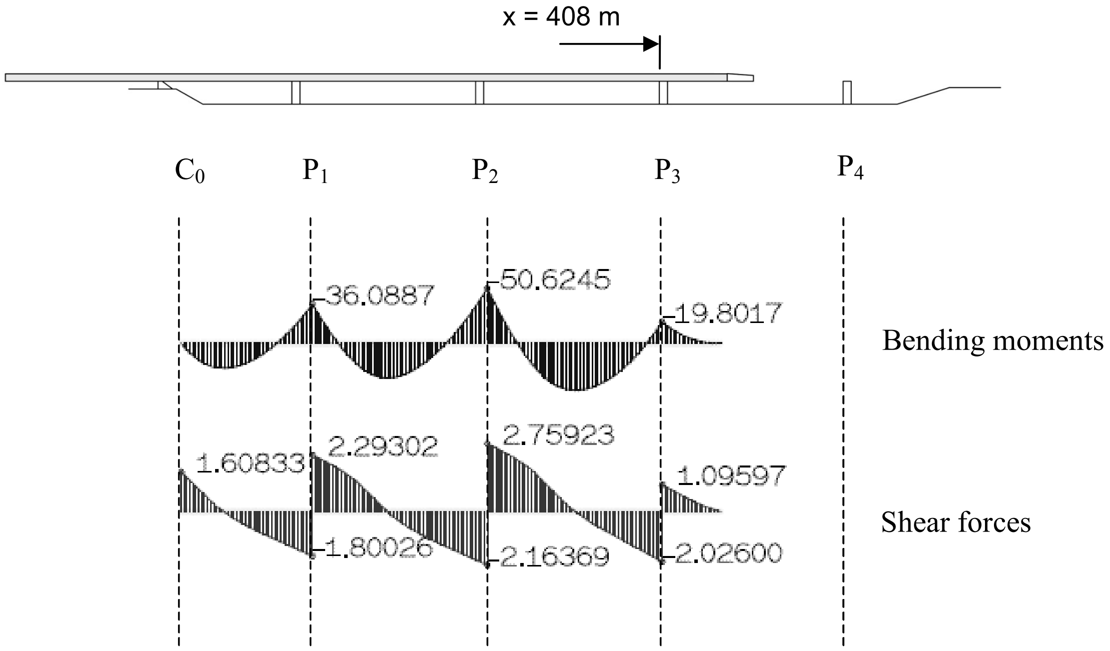
x = 408 m
C0
P1
P2
P3
P4
36.0887
50.6245
19.8017
Bending moments
1.60833
2.29302
2.75923
1.09597
-1.80026
-2.16369
-2.02600
Shear forces

Figure 4-7: Launching situation "3" (most unfavourable for weakest mid-span cross-section).

The dimensions of the studied panel at the decisive cross-sections are given in Table 4-1 and Figure 4-2. The web is longitudinally stiffened at $0.2 \cdot h_w$ with reference to the neutral axis of the stiffener, which is an efficient stiffener position in case of patch loading and might not necessarily be in accordance with the choice of stiffener position in the other sections of this document, and the spacing of the vertical stiffeners is based on the verifications against lateral torsional buckling, i.e. 4.0 m here.

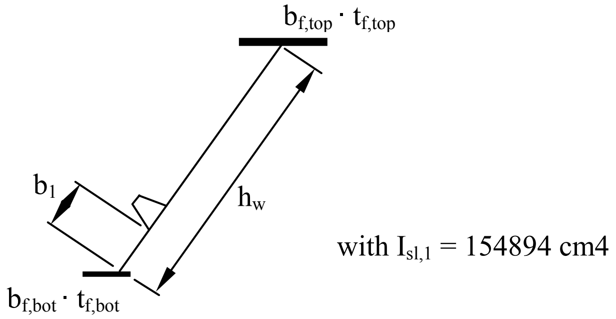
$b_{f,top} \cdot t_{f,top}$
b_l
h_w
with $I_{sl,1}$ = 154894 cm4
$b_{f,bot} \cdot t_{f,bot}$

Figure 4-8: Notations of the studied panel in [mm].

Table 4-1: Dimensions of the studied panels in [mm].

		Launching situation		
		"1"	"2"	"3"
$b_{f,top}$	[mm]	1500	1500	1500
$t_{f,top}$	[mm]	184	70	50
h_w	[mm]	4539.4	4726.2	4762.6
t_w	[mm]	27	20	18
$b_{f,bot}$	[mm]	1015.3	527.1	405.1
$t_{f,bot}$	[mm]	75	35	25
b_l	[mm]	657.9	695.2	702.5

From the global analysis, the internal design forces (for use with Section 6, EN 1993-1-5) are given below. In case of internal forces and support reactions the values are given for each web.

Table 4-2: Internal design forces.

		Launching situation		
		"1"	"2"	"3"
M_{Ed}	[MNm]	-217.93	-99.35	-50.62
$V_{Ed,max}$	[MN]	4.25	3.17	2.16
$V_{Ed,applied} = V_{Ed,max} - F_{Ed}/2$	[MN]	-0.83	-0.29	-0.83
F_{Ed}	[MN]	8.37	5.69	4.92
$F_{Ed,web}$	[MN]	10.15	6.91	5.97
$F_{Ed,bottom\ plate}$	[MN]	5.75	3.91	3.38

The calculations in Section 4.2.2 showed that the negative bending moment has an influence on the patch loading resistance only for launching position "1". In all cases, the additional shear force is almost negligible. For these reasons, the calculation for launching situation "1" is given in detail in Section 4.2.2.1 whereas for launching situations "2" and "3", which are relevant for the mid- and end-span verifications, only results are presented in Sections 4.2.2.2 and 4.2.2.3.

Determination of the critical load F_{cr}

In EN 1993-1-5 the determination of the critical load of a longitudinally stiffened web is based on the lowest buckling value k_F. In the diagram below buckling values for different panel aspect ratios and stiffener positions are given. Based on that, the formula in EN 1993-1-5 describes only the increasing branch and is therefore limited to a range of application $b_1/h_w \leq 0.3$.

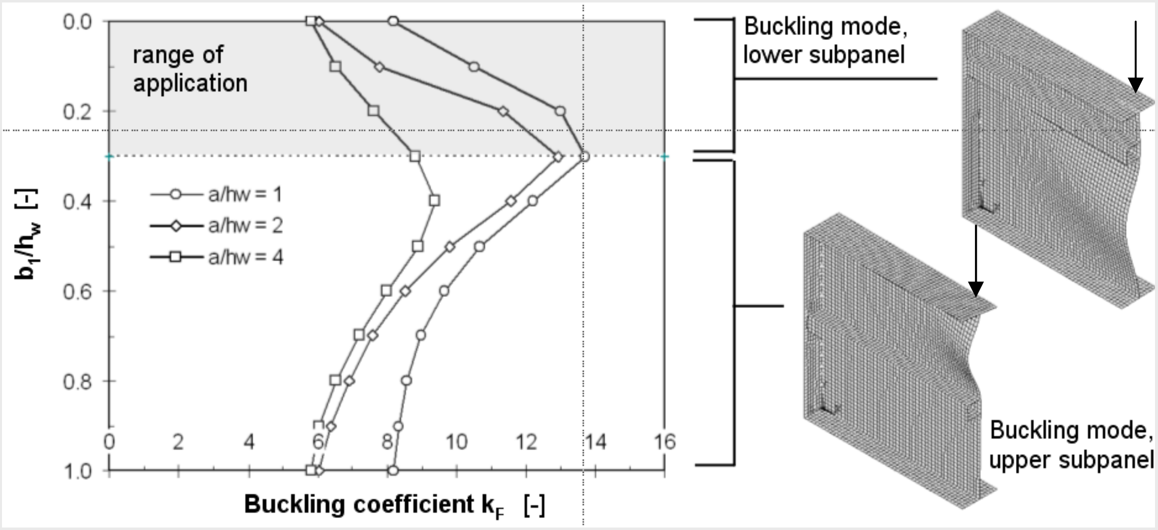

Thus, according to a EN 1993-1-5 calculation, the most advantageous stiffener position is at $b_1/h_w = 0.3$ although this might be not true in reality. In general, the patch loading resistance increases with decreasing distance between stiffener and loaded flange. In the COMBRI project, this paradox has been solved within the COMBRI project, see [7] as well as [5] and [9].

Improved resistance to transverse forces

In the COMBRI research project and in [5], [9] it has been shown that in case the value m_2 is set to zero and, due to the changed definition of the yield load, the reduction curve is recalibrated, not only the resistance to transverse forces can be improved but also the scatter of the resistance model becomes smaller. Whereas the work in [5] is related to the improved resistance model for longitudinally unstiffened girder according to [31], the work of [9] can be used with current Eurocode rules. For this reason, in the German National Annex to EN 1993-1-5 [11] the proposal of [9] has been adopted for the national choice of the patch loading resistance model for longitudinally stiffened girders. For details, see also the COMBRI Final Report [7].

On the following page, the example calculation according to [9] is shown.

4.2.2 Verifications according to Section 6, EN 1993-1-5

4.2.2.1 Launching situation "1"

In the following, the patch loading resistance according to Section 6, EN 1993-1-5 is determined. The interaction between transverse force and bending moment is checked according to Section 7, EN 1993-1-5.

Determination of the critical load F_{cr}

$$\gamma_{s.} := 10.9 \cdot \frac{I_{sl.1}}{h_w \cdot t_w^{\;3}} \qquad \gamma_{s.} = 188.96$$

$$\gamma_{s.min} := 13 \cdot \left(\frac{a}{h_w}\right)^3 + 210 \cdot \left(0.3 - \frac{b_1}{a}\right) \qquad \gamma_{s.min} = 37.36$$

$$\gamma_s := \left| \begin{array}{ll} 10.9 \cdot \dfrac{I_{sl.1}}{h_w \cdot t_w^{\;3}} & \text{if } \gamma_{s.} \le \gamma_{s.min} \\ 13 \cdot \left(\dfrac{a}{h_w}\right)^3 + 210 \cdot \left(0.3 - \dfrac{b_1}{a}\right) & \text{if } \gamma_{s.} > \gamma_{s.min} \end{array} \right.$$

$$\gamma_s = 37.36$$

$$k_F := 6 + 2 \cdot \left(\frac{h_w}{a}\right)^2 + \left(5.44 \cdot \frac{b_1}{a} - 0.21\right) \cdot \sqrt{\gamma_s} \qquad k_F = 12.76$$

$$F_{cr} := 0.9 \cdot k_F \cdot 210000\text{MPa} \cdot \frac{t_w^{\;3}}{h_w} \qquad F_{cr} = 10.46\,\text{MN}$$

Determination of the yield load F_y

$$m_1 := \frac{f_{yf} \cdot b_f}{f_{yw} \cdot t_w} \qquad m_1 = 35.42$$

$$m_2 := 0.02 \cdot \left(\frac{h_w}{t_f}\right)^2 \qquad m_2 = 73.26$$

$$l_y := s_s + 2 \cdot t_f \cdot \left(1 + \sqrt{m_1 + m_2}\right)$$

$$l_y := \left| \begin{array}{ll} l_y & \text{if } l_y \le a \\ a & \text{if } l_y > a \end{array} \right. \qquad l_y = 4000\,\text{mm}$$

$$F_y := l_y \cdot t_w \cdot f_{yw} \qquad F_y = 37.26\,\text{MN}$$

Example calculation based on the procedure according to Davaine [9]

Determination of the critical load F_{cr}

$$F_{cr.1} := F_{cr} \qquad F_{cr.1} = 10.46\,\mathrm{MN}$$

$$k_{F.2} := \left[0.8\cdot\left(\frac{s_s + 2\cdot t_f}{a}\right) + 0.6\right]\cdot\left(\frac{a}{b_1}\right)^{0.6\cdot\left(\frac{s_s+2\cdot t_f}{a}\right)+0.5} \qquad k_{F.2} = 7.12$$

$$F_{cr.2} := k_{F.2}\cdot 189800\mathrm{MPa}\cdot\frac{t_w^{\;3}}{b_1} \qquad F_{cr.2} = 40.41\,\mathrm{MN}$$

$$F_{cr.} := \frac{F_{cr.1}\cdot F_{cr.2}}{F_{cr.1} + F_{cr.2}} \qquad F_{cr.} = 8.31\,\mathrm{MN}$$

Determination of the yield load F_y

The factor m_2 has to be set to zero in this procedure.

$$m_{2.} := 0$$

$$l_{y.} := s_s + 2\cdot t_f\cdot\left(1 + \sqrt{m_1}\right)$$

$$l_{y.} := \begin{cases} l_y & \text{if } l_y \le a \\ a & \text{if } l_y > a \end{cases} \qquad l_{y.} = 4000\,\mathrm{mm}$$

$$F_{y.} := l_{y.}\cdot t_w\cdot f_{yw} \qquad F_{y.} = 37.26\,\mathrm{MN}$$

Determination of the slenderness parameter $\bar{\lambda}_F$

$$\lambda_{F.} := \sqrt{\frac{F_{y.}}{F_{cr.}}} \qquad \lambda_{F.} = 2.12$$

Determination of the reduction factor χ_F

$$\phi := 0.5\cdot\left[1 + 0.21\cdot\left(\lambda_F - 0.80\right) + \lambda_F\right] \qquad \phi = 1.56$$

$$\rho := \frac{1}{\phi + \sqrt{\phi^2 - \lambda_F}} \qquad \rho = 0.436$$

Determination of the patch loading resistance

$$L_{eff.} := \rho\cdot l_{y.} \qquad L_{eff.} = 1744.7\,\mathrm{mm}$$

$$F_{Rd.} := \frac{f_{yw}\cdot L_{eff.}\cdot t_w}{\gamma_{M1}} \qquad F_{Rd.} = 14.77\,\mathrm{MN}$$

$$\eta_2 := \frac{F_{Ed.web}}{F_{Rd.}} \qquad \eta_2 = 0.687$$

Determination of the slenderness parameter $\overline{\lambda}_F$

$$\lambda_F := \sqrt{\frac{F_y}{F_{cr}}} \qquad \lambda_F = 1.89$$

Here, the slenderness parameter is larger than $\overline{\lambda}_F = 0.5$ which is a precondition to use the above formula for m_2. For $\lambda_F \leq 0.5$, m_2 should be set to zero according to Paragraph 6.5(1), EN 1993-1-5.

Determination of the reduction factor χ_F

$$\chi_F := \begin{vmatrix} 1.0 \quad \text{if } \lambda_F \leq 0.5 \\ \dfrac{0.5}{\lambda_F} \quad \text{if } \lambda_F > 0.5 \end{vmatrix} \qquad \chi_F = 0.26$$

Determination of the patch loading resistance

$$L_{eff} := \chi_F \cdot l_y \qquad L_{eff} = 1059.6\,\text{mm}$$

$$F_{Rd} := \frac{f_{yw} \cdot L_{eff} \cdot t_w}{\gamma_{M1}} \qquad F_{Rd} = 8.97\,\text{MN}$$

$$\eta_2 := \frac{F_{Ed.web}}{F_{Rd}} \qquad \eta_2 = 1.132$$

As $\eta_2 = 1.132 > 1.0$ the patch loading verification can not be fulfilled and thus also the interaction cases are not fulfilled. Instead they are shown for the sake of completeness using the value of the patch loading resistance according to Davaine [9].

Example calculation based on the procedure according to Davaine [9] (cont.)

Based on the recommended procedure in EN 1993-1-5, the patch loading verification can not be fulfilled and a solution would be to increase the web thickness t_w to 30 mm. When using EN 1993-1-5, another stiffener position or longer loading length would not increase the calculated resistance decisively. However,the design models developed in [9] and [5] which are summarised in [7] allow to asses the existing higher patch loading resistance without using numerical simulation tools. Here, the procedure acc. to [9] has been shown to improve the patch loading resistance with regard to the drawbacks described in the remark to the determination of the critical load F_{cr}.

Interaction between transverse force and bending moment

In Section 7.2(1), EN 1993-1-5 , the interaction should be determined as follows:

$$\eta_2 + 0.8 \cdot \eta_1 \leq 1.4$$

If $\eta_2 = 1.0$ is assumed, it can be shown that the influence of bending moment must be taken into account only for $\eta_1 > 0.5$.

Interaction between transverse force and shear force

In the frame of the COMBRI project, experimental and numerical studies on steel plated girders have been conducted in order to review and to propose an interaction equation for combined shear and patch loading. From the investigations, it is obvious that the interaction between shear and patch loading is not negligible. Although the interaction might appear severely at first sight, the specific conditions during bridge launching have to be taken into account. For this reason, the figurebelow shows two relevant construction stages: a) when the bridge girder is about to arrive at the support and a cantilever is existent; b) when the bridge girder has reached the pier. In stage a) the introduced patch load is almost equally equilibrated resulting in a pure patch loading situation where the shear is already considered in the patch load model.

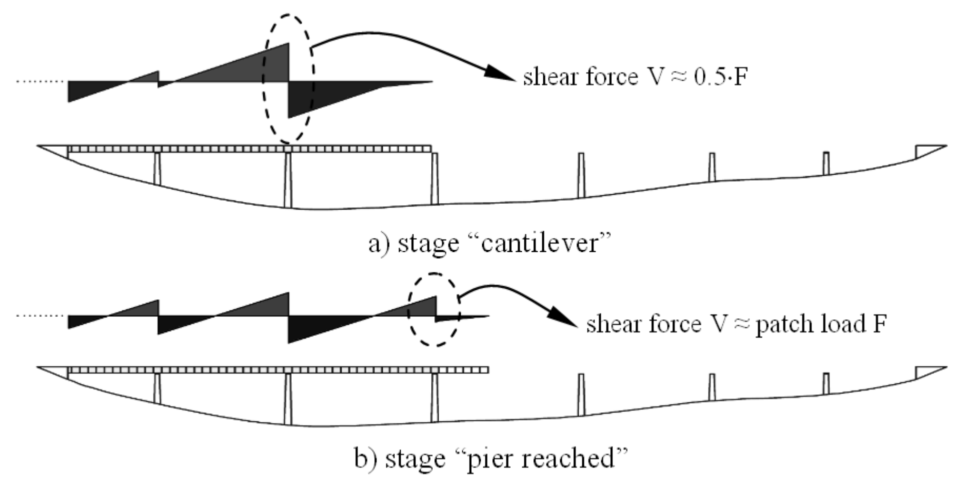

Interaction between transverse force and bending moment

Here, $\eta_1 = 0.580 > 0.5$ so that the interaction with bending moment has to be considered.

$$\sigma_{x.Ed} := \frac{M_{Ed}}{W_{bot}} \qquad \sigma_{x.Ed} = 189.42\,\text{MPa}$$

$$\eta_1 := \frac{\sigma_{x.Ed}}{\dfrac{f_{yf}}{\gamma_{M0}}} \qquad \eta_1 = 0.58$$

$$\eta_2 + 0.8 \cdot \eta_1 = 1.60$$

W_{bot} takes into account the effects of plate buckling in the bottom flange and in the webs.

Interaction between transverse force and shear force

Although the considered panel is subjected to an additional shear force of $V_{Ed} = 0.83$ MN which is not induced by the patch loading, this interaction is not taken into account in EN 1993-1-5.

Interaction between transverse force and shear force (cont.)

In stage b) the maximum internal shear force approximates the value of the applied patch load which leads to an asymmetric patch loading condition. For this situation the interaction becomes relevant, however, the average will result in reductions of around 10%, see interaction diagram below.

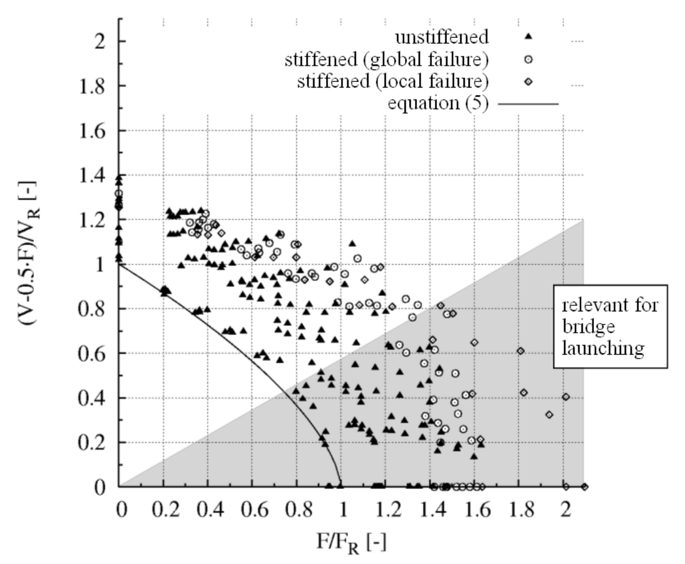

Interaction equation proposed in [7]: $\left(\frac{V - 0.5 \cdot F}{V_R}\right)^a + \left(\frac{F}{F_R}\right)^b \leq 1.0$ with $a = 1.6$, $b = 1.0$ which gives in this example with the patch loading resistance according to [9]:

$$\left(\frac{0.83}{20.71}\right)^{1.6} + \left(\frac{10.15}{14.77}\right) = 0.01 + 0.67 = 0.68 < 1.0$$

4.2.2.2 Launching situation “2”

The results for launching situation “2” are summarised below:

$F_{cr} = 4.19\,\text{MN} \qquad F_y = 27.60\,\text{MN}$

$F_{Rd} = 4.89\,\text{MN} \qquad \eta_2 = 1.413$

$\eta_1 = 0.456$

Here, $\eta_1 = 0.456 < 0.5$ so that the interaction with bending moment is not considered.

The cross-section cannot be verified for launching situation “2”, see also Figure 4-4 of the summary.

4.2.2.3 Launching situation “3”

The results for launching situation “3” are summarised below:

$F_{cr} = 3.05\,\text{MN} \qquad F_y = 24.84\,\text{MN}$

$F_{Rd} = 3.96\,\text{MN} \qquad \eta_2 = 1.510$

$\eta_1 = 0.294$

Here, $\eta_1 = 0.294 < 0.5$ so that the interaction with bending moment is not considered.

The cross-section cannot be verified for launching situation “3”, see also Figure 4-4 of the summary.

4.2.3 Verifications according to Section 10, EN 1993-1-5

4.2.3.1 Webpanel (Launching situation “1” only)

In the following, the patch loading resistance according to Section 10, EN 1993-1-5 is determined. For this example launching situation “1” has been chosen. The resulting stress field acting at the studied panel is shown in Figure 4-3.

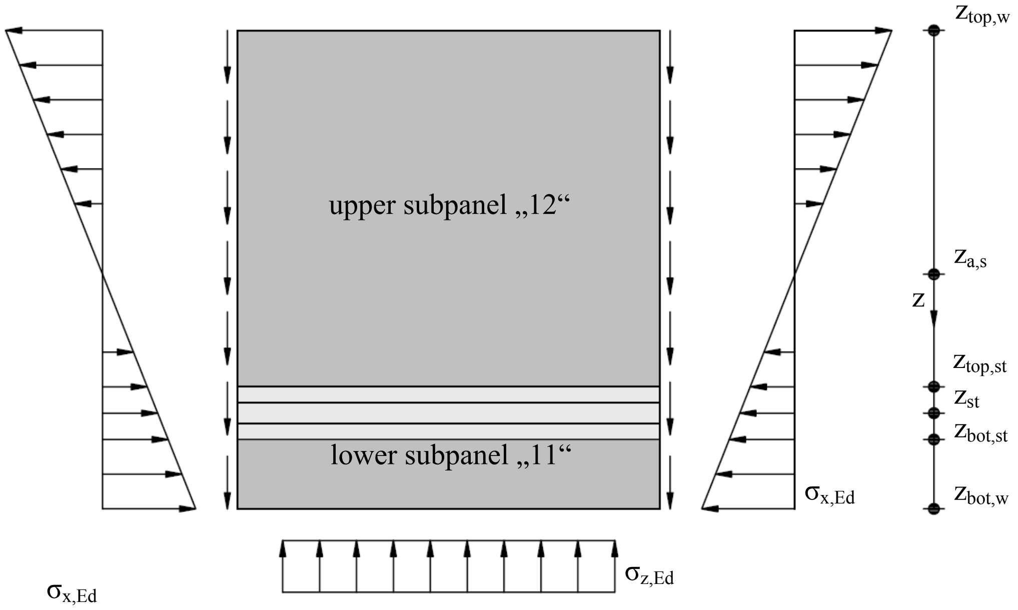

Figure 4-9: Stress field acting on the studied panel.

The moment of inertia of the gross steel section at position x = 448 m is $I_a = 4.524 \cdot 10^8$ cm^4. Shear lag does not have to be considered because $b_0 < L_e/50$, cf. EN 1993-1-5, Section 3.1, so that the values according to Table 4-3 have been determined directly.

$b_p := 6.5\text{m}$ $\qquad$ $L_3 := 92\text{m}$

$b_0 := \frac{b_p}{2}$ $\qquad$ $b_0 = 3.25\ \text{m}$

$L_e := 2 \cdot L_3$ $\qquad$ $\frac{L_e}{50} = 3.68\ \text{m}$

Table 4-3: Values of the studied panel, see Figure 4-3 (compression is taken as positive).

Position [Index]	z-axis [mm]	W [cm^3]	$\sigma_{x,Ed}$ [MPa]	$\sigma_{,z,Ed}$ [MPa]
“top,w”	-1906.3	-1186573	-183.7	0.0
“top,st”	880.5	2569047	84.8	72.9
“st”	1086.5	2081882	104.7	81.7
“bot,st”	1292.5	1750027	124.5	87.7
“bot,w”	1834.7	1232880	176.8	98.4

From section 4.2.1 the following dimensions are already known.

Subpanel widths: $b_{11} = b_1 = 657.9$ mm

$b_{12} = 3381.5$ mm

Subpanel widths up to centreline of stiffener: $b_{11,st} = 907.9$ mm

$b_{12,st} = 3631.5$ mm

The value of additional shear stress is $\tau_{Ed} = 0.6$ MPa.

The stress ratios can be determined from Table 4-3:

Overall: $\psi_{ov} = -1.04$

Lower subpanel “11”: $\psi_{11} = 0.70$

Upper subpanel “12”: $\psi_{12} = -2.17$

In the following verification procedure, the subpanels “11” and “12” and the longitudinal stiffener are verified individually.

4.2.3.1.1 Verification of subpanel “11”

The subpanel aspect ratio is $\alpha_{11} = 6.1$.

Determination of α_{cr}

The determination of the minimum load amplifier α_{cr} for the design loads to reach the elastic critical load of the plate under the complete stress field can be either determined

- **for each component of the stress field (e.g. by a hand-calculation)**

$$\sigma_{E.11} := 189800\text{MPa}\cdot\left(\frac{t_w}{b_{11}}\right)^2 \qquad \sigma_{E.11} = 319.7\,\text{MPa}$$

Elastic critical longitudinal stress acc. to Table 4.1, Section 4.4, EN 1993-1-5

$$k_{\sigma.x.11} := \begin{vmatrix} \dfrac{8.2}{1.05 + \psi_{11}} \text{ if } 1 \geq \psi_{11} > 0 \\ 7.81 - 6.29\psi_{11} + 9.78\psi_{11}^{\,2} \text{ if } 0 \geq \psi_{11} > -1 \\ 5.98\cdot\left(1 - \psi_{11}\right)^2 \text{ if } -1 \geq \psi_{11} > -3 \end{vmatrix} \qquad k_{\sigma.x.11} = 4.674$$

$$\sigma_{cr.x.11} := k_{\sigma.x.11}\cdot\sigma_{E.11} \qquad \sigma_{cr.x.11} = 1494.2\,\text{MPa}$$

$$\alpha_{cr.x.11} := \frac{\sigma_{cr.x.11}}{\sigma_{x.Ed.bot.w}} \qquad \alpha_{cr.x.11} = 8.453$$

Elastic critical transverse stress acc. to EBPlate

Because of the large subpanel aspect ratio of $\alpha = 6.1$, the determination of the elastic critical transverse stress is not possible by a hand-calculation. Thus, in this case software EBPlate has been used:

$$\sigma_{cr.z.11} := 360.7\text{MPa}$$

$$\alpha_{cr.z.11} := \frac{\sigma_{cr.z.11}}{\sigma_{z.Ed}} \qquad \alpha_{cr.z.11} = 3.67$$

Elastic critical shear stress acc. to Eq. (A.5), Annex A.3, EN 1993-1-5

$$k_{\tau.11} := \begin{cases} 5.34 + 4.00 \cdot \left(\dfrac{b_{11}}{a}\right)^2 & \text{if } \dfrac{a}{b_{11}} \geq 1 \\ 4.00 + 5.34 \cdot \left(\dfrac{b_{11}}{a}\right)^2 & \text{if } \dfrac{a}{b_{11}} < 1 \end{cases} \qquad k_{\tau.11} = 5.448$$

$$\tau_{cr.11} := k_{\tau.11} \cdot \sigma_{E.11} \qquad \tau_{cr.11} = 1741.8\,\text{MPa}$$

$$\alpha_{cr.\tau.11} := \frac{\tau_{cr.11}}{\tau_{Ed}} \qquad \alpha_{cr.\tau.11} = 3162.6$$

Minimum load amplifier acc. to Eq. (10.6), Section 10, EN 1993-1-5

$$\alpha_{cr.11} := \frac{1}{\dfrac{1+\psi_{11}}{4\alpha_{cr.x.11}} + \dfrac{1}{2\alpha_{cr.z.11}} + \sqrt{\left(\dfrac{1+\psi_{11}}{4\alpha_{cr.x.11}} + \dfrac{1}{2\alpha_{cr.z.11}}\right)^2 + \dfrac{1-\psi_{11}}{2\cdot\alpha_{cr.x.11}^{\;2}} + \dfrac{1}{\alpha_{cr.\tau.11}^{\;2}}}}$$

$$\alpha_{cr.11} = 2.638$$

- **for the complete stress field (e.g. by using appropriate software)**

  In case e.g. software EBPlate is used, the minimum load amplifier can be determined in a single step as $\alpha_{cr} = 3.490$.

In the following calculations, the value $\alpha_{cr} = 2.638$ is further used.

Elastic critical column-buckling stress $\sigma_{cr,c}$

The determination of $\sigma_{cr,c}$ in the transverse direction should take into account the nonlinear stress distribution in the web for which no hand-calculation method exists at the moment. Instead, a common approach is to assume a linearly varying stress distribution for a pin-ended strut which is zero at one end and for which the buckling length s_k can be calculated acc. to DIN 4114 as follows:

$$s_k := b_{11} \cdot \sqrt{\frac{1 + 0.88 \cdot \dfrac{\sigma_{z.Ed.bot.st} \cdot s_{bot.st}}{\sigma_{z.Ed} \cdot \left(s_s + 2 \cdot t_f\right)}}{1.88}}$$

It should be noted that this simplification may lead to unsafe results because $\sigma_{cr,c}$ is underestimated and in turn the ratio $\sigma_{cr,p}/\sigma_{cr,c}$, is overestimated so that column-like behaviour is not detected correctly. The shorter the loading lengths is, the larger this deviation is.

Reduction curve for transverse stresses, column-like behaviour and interpolation function

In the COMBRI project it has been shown that the interpolation function acc. to Eq. (4.13), Section 4.5.4, EN 1993-1-5, which takes into account column-like buckling, is not appropriate for patch loading stresses in the transverse direction. Moreover, the ratio of $\sigma_{cr,p}/\sigma_{cr,c}$, for which column-like buckling needs to be considered, should be 2.7 (and not 2.0 as given in Eq. (4.13)).

Basically, either a new interpolation function is required or a reduction curve should be used which can be used with the existing interpolation function. A new interpolation function has been derived e.g. by Seitz [40] and this method is introduced in the COMBRI Final report [7]. However, e.g. for the new German DIN-Fachbericht 103 [12], it has been decided to use the reduction curve of Annex B, EN 1993-1-5, for transverse stresses because this approach complies well with current Eurocode rules and could be easier implemented. Thus, for a welded girder Table B.1, Annex B.1, EN 1993-1-5 gives:

$$\bar{\lambda}_{p0} := 0.80 \qquad \alpha_p := 0.34 \qquad \phi_{p.} := 0.5 \cdot \left[1 + \alpha_p \cdot \left(\lambda_p - \lambda_{p0}\right) + \lambda_p\right]$$

which is to be used in

$$\rho := \frac{1}{\phi_{p.} + \sqrt{\phi_{p.}^{\;2} - \lambda_p}}$$

This reduction curve is used on the right hand-side instead of Eq. (4.13), Section 4.5.4,
EN 1993-1-5.

Determination of $\alpha_{ult,k}$

$$\sigma_{eq.11} := \sqrt{\sigma_{x.Ed.bot.w}^2 + \sigma_{z.Ed}^2 - \sigma_{x.Ed.bot.w}\cdot\sigma_{z.Ed} + 3\cdot\tau_{Ed}^2} \qquad \sigma_{eq.11} = 153.4\,\text{MPa}$$

$$\alpha_{ult.k.11} := \frac{f_{yw}}{\sqrt{\sigma_{x.Ed.bot.w}^2 + \sigma_{z.Ed}^2 - \sigma_{x.Ed.bot.w}\cdot\sigma_{z.Ed} + 3\cdot\tau_{Ed}^2}} \qquad \alpha_{ult.k.11} = 2.249$$

Determination of the slenderness parameter $\bar{\lambda}_p$

$$\lambda_{p.11} := \sqrt{\frac{\alpha_{ult.k.11}}{\alpha_{cr.11}}} \qquad \lambda_{p.11} = 0.923$$

Determination of the reduction factors

The determination of the reduction factors for the design loads to reach the elastic critical load of the plate under the complete stress field can be either determined

- **using different buckling curves**

  Longitudinal stress acc. to Eq. (4.2), Section 4.4, EN 1993-1-5

$$\rho_{x.11} := \frac{\lambda_{p.11} - 0.055\cdot\left(3 + \psi_{11}\right)}{\lambda_{p.11}^2} \qquad \rho_{x.11} = 0.844$$

Check of column-like behaviour in the longitudinal direction

Column-like buckling in the longitudinal direction for plates under pure bending is only relevant for panel aspect ratios $\alpha < 0.15$. Therefore column-like behaviour is not calculated in detail here.

Transverse stress acc. to Annex B.1, EN 1993-1-5

$$\rho_{z.} := \frac{1}{\phi_{p..} + \sqrt{\phi_{p..}^2 - \lambda_{p.11}}} \quad \text{with} \quad \phi_{p..} = 0.983 \qquad \rho_{z.} = 0.842$$

Check of column-like behaviour in the transverse direction

Due to the nonlinear distribution of transverse stresses in the web, the determination of the critical column-buckling stress has been done here most accurately based on the energy method which takes into account the nonlinear stress distribution.

$$\sigma_{cr.c.11} = 333.2\,\text{MPa}$$

$$\frac{\sigma_{cr.z.11}}{\sigma_{cr.c.11}} = 1.08 \qquad \xi_{11} := \frac{\sigma_{cr.z.11}}{\sigma_{cr.c.11}} - 1 \qquad \xi_{11} = 0.08$$

Use of the corrected interpolation function

For comparison, here the use of the newly derived interpolation function acc. to Seitz [40] is used. The calculation gives:

$$\eta_{Seitz.11} = 0.598$$

Here ξ is close to 0.0, i.e. pure column-like behaviour.

$$\lambda_{c.11} := \sqrt{\frac{f_{yw}}{\sigma_{cr.c1.11}}} \qquad \lambda_{c.11} = 1.051$$

$$\Phi_{11} := 0.5\cdot\left[1 + 0.21\cdot\left(\lambda_{c.11} - 0.2\right) + \lambda_{c.11}{}^{2}\right] \qquad \Phi_{11} = 1.142$$

$$\chi_{c.11} := \frac{1}{\Phi_{11} + \sqrt{\Phi_{11}{}^{2} - \lambda_{c.11}{}^{2}}} \qquad \chi_{c.11} = 0.630$$

$$\rho_{c.z.11} := \left(\rho_{z.11.} - \chi_{c.11}\right)\cdot\xi_{11}\cdot\left(2 - \xi_{11}\right) + \chi_{c.11} \qquad \rho_{c.z.11} = 0.663$$

Shear stress acc. to Table 5.1, section 5.3, EN 1993-1-5

$$\chi_{w.11} := \begin{array}{|l} 1.0 \quad \text{if } \lambda_{p.11} < 0.83 \\ \dfrac{0.83}{\lambda_{p.11}} \quad \text{if } \lambda_{p.11} \geq 0.83 \end{array} \qquad \chi_{w.11} = 0.899$$

- **using a single buckling curve**

  According to Table B.1, Annex B.1, EN 1993-1-5

$$\lambda_{p0} := 0.80 \qquad \alpha_{p} := 0.34$$

$$\phi_{p.11.} := 0.5\cdot\left[1 + \alpha_{p}\cdot\left(\lambda_{p.11} - \lambda_{p0}\right) + \lambda_{p.11}\right] \qquad \phi_{p.11.} = 0.983$$

$$\rho_{11} := \frac{1}{\phi_{p.11.} + \sqrt{\phi_{p.11.}{}^{2} - \lambda_{p.11}}} \qquad \rho_{11} = 0.842$$

$$\rho_{c.11.} := \chi_{c.11} + \left(\rho_{11} - \chi_{c.11}\right)\cdot f_{11} \qquad \rho_{c.11.} = 0.651$$

Determination of the patch loading resistance

- **using different buckling curves**

$$\eta_{diff.11} := \sqrt{\left(\frac{\sigma_{x.Ed.bot.w}}{\rho_{x.11}\cdot\frac{f_{yw}}{\gamma_{M1}}}\right)^{2} + \left(\frac{\sigma_{z.Ed}}{\rho_{c.z.11}\cdot\frac{f_{yw}}{\gamma_{M1}}}\right)^{2} - \left(\frac{\sigma_{x.Ed.bot.w}}{\rho_{x.11}\cdot\frac{f_{yw}}{\gamma_{M1}}}\right)\cdot\left(\frac{\sigma_{z.Ed}}{\rho_{c.z.11}\cdot\frac{f_{yw}}{\gamma_{M1}}}\right) + 3\cdot\left(\frac{\tau_{Ed}}{\chi_{w.11}\cdot\frac{f_{yw}}{\gamma_{M1}}}\right)^{2}}$$

$$\eta_{diff.11} = 0.595$$

- **using a single buckling curve**

$\alpha_{Rd.11} = \frac{\rho_{c.11} \cdot \alpha_{ult,k.11}}{\gamma_{M1}}$ $\alpha_{Rd.11} = 1.332$ $\eta_{single.11} = \frac{1}{\alpha_{Rd.11}} = 0.751$

4.2.3.1.2 Verification of subpanel "12"

The subpanel aspect ratio is $\alpha_{12} = 1.18$.

In the following only the results of the calculation are shown. For further information the reader is referred to the previous section "verification of subpanel "11".

Determination of α_{cr}

The determination of the minimum load amplifier α_{cr} for the design loads to reach the elastic critical load of the plate under the complete stress field can be either determined

- **for each component of the stress field (e.g. by a hand-calculation)**

  Elastic critical longitudinal stress acc. to Table 4.1, Section 4.4, EN 1993-1-5

  $k_{\sigma.x.12} = 59.907$ $\sigma_{cr.x.12} = 724.9\,\text{MPa}$ $\alpha_{cr.x.12} = 8.546$

  Elastic critical transverse stress with k = 3.8 acc. to Table 8.12 [38]

  $\sigma_{cr.z.12} := k_{12} \cdot \sigma_{E.12} \cdot a \cdot \frac{1}{s_{top.st}}$ $\sigma_{cr.z.12} = 58.05\,\text{MPa}$

  $\alpha_{cr.z.12} := \frac{\sigma_{cr.z.12}}{\sigma_{z.Ed.top.st}}$ $\alpha_{cr.z.12} = 0.60$

  Elastic critical shear stress acc. to Eq. (A.5), Annex A.3, EN 1993-1-5

  $k_{\tau.12} = 8.199$ $\tau_{cr.12} = 99.2\,\text{MPa}$ $\alpha_{cr.\tau.12} = 180.137$

  Minimum load amplifier acc. to Eq. (10.6), Section 10, EN 1993-1-5

  $\alpha_{cr.12} = 0.616$

- **for the complete stress field (e.g. by using appropriate software)**

  In case e.g. software EBPlate is used, the minimum load amplifier can be determined in a single step as $\alpha_{cr} = 0.889$.

In the following calculations, the value $\alpha_{cr} = 0.616$ is further used.

Determination of $\alpha_{ult,k}$

$\sigma_{eq.12} = 91.3\,\text{MPa}$ $\alpha_{ult.k.12} = 3.735$

Elastic critical column-buckling stress $\sigma_{cr,c}$

The determination of $\sigma_{cr,c}$ in the transverse direction should take into account the nonlinear stress distribution in the web for which no hand-calculation method exists at the moment. Instead, a common approach is to assume a linearly varying stress distribution for a pin-ended strut which is zero at one end and which can be calculated acc. to DIN 4114 as follows:

$$\sigma_{cr,c} = 1.88 \cdot \sigma_E$$

It should be noted that this simplification may lead to unsafe results because $\sigma_{cr,c}$ is underestimated and in turn the ratio $\sigma_{cr,p}/\sigma_{cr,c}$, is overestimated so that column-like behaviour is not detected correctly. The shorter the loading lengths is, the larger this deviation is.

Reduction curve for transverse stresses, column-like behaviour and interpolation function

In the COMBRI project it has been shown that the interpolation function acc. to Eq. (4.13), Section 4.5.4, EN 1993-1-5, which takes into account column-like buckling, is not appropriate for patch loading stresses in the transverse direction. Moreover, the ratio of $\sigma_{cr,p}/\sigma_{cr,c}$, for which column-like buckling needs to be considered, should be 2.7 (and not 2.0 as given in Eq. (4.13)).

Basically, either a new interpolation function is required or a reduction curve should be used which can be used with the existing interpolation function. A new interpolation function has been derived e.g. by Seitz [40] and this method is introduced in the COMBRI Final report [7]. However, e.g. for the new German DIN-Fachbericht 103 [12], it has been decided to use the reduction curve of Annex B, EN 1993-1-5, for transverse stresses because this approach complies well with current Eurocode rules and could be easier implemented. Thus, for a welded girder Table B.1, Annex B.1, EN 1993-1-5 gives:

$$\lambda_{p0} := 0.80 \qquad \alpha_p := 0.34 \qquad \phi_{p.} := 0.5 \cdot \left[1 + \alpha_p \cdot \left(\lambda_p - \lambda_{p0}\right) + \lambda_p\right]$$

which is to be used in

$$\rho := \frac{1}{\phi_{p.} + \sqrt{\phi_{p.}^{\,2} - \lambda_p}}$$

This reduction curve is used on the right hand-side instead of Eq. (4.13), Section 4.5.4,
EN 1993-1-5.

Determination of the slenderness parameter $\bar{\lambda}_p$

$\lambda_{p.12} = 2.462$

Determination of the reduction factors

The determination of the reduction factors for the design loads to reach the elastic critical load of the plate under the complete stress field can be either determined

- **using different buckling curves**

  Longitudinal stress acc. to Eq. (4.2), Section 4.4, EN 1993-1-5

  $\rho_{x.12} = 0.399$

  Check of column-like behaviour in the longitudinal direction

  Column-like buckling in the x-direction for plates under pure bending is only relevant for panel aspect ratios a < 0.15. Therefore column-like behaviour is not calculated in detail here.

  Transverse stress acc. to Annex B.1, EN 1993-1-5

  $\rho_{z.12.} = 0.305$

  Check of column-like behaviour in the transverse direction

  Due to the nonlinear distribution of transverse stresses in the web, the determination of the critical column-buckling stress has been done here most accurately based on the energy method which takes into account the nonlinear stress distribution.

  $\sigma_{cr.c.12} = 27.86\,\text{MPa} \qquad \frac{\sigma_{cr.z.12}}{\sigma_{cr.c.12}} = 2.08 \qquad \xi_{12} = 1.08$

  Because $\xi > 1.0$, column-like behaviour does not have to be considered according to the code calculation. However, as shown by Seitz, the interpolation function is not safe-sided.

  Shear stress acc. to Table 5.1, section 5.3, EN 1993-1-5

  $\chi_{w.12} = 0.337$

- **using a single buckling curve**

  According to Table B.1, Annex B.1, EN 1993-1-5

  $\phi_{p.12.} = 2.014 \qquad \rho_{12} = 0.305$

Use of the corrected interpolation function

For comparison, here the use of the newly derived interpolation function acc. to Seitz [40] is used. The calculation gives:

$$\eta_{\mathrm{Seitz.12}} = 0.915$$

DIN 18800 Part 3, Element (801)
Additional verification for plates with transverse stresses σ_y

For longitudinally stiffened plates with transverse stresses σ_y, the longitudinal stiffeners should be verified using a second order elastic method of analysis based on the following assunptions:

- The considered longitudinal stiffener is treated as simply supported member with an initial sinusoidal imperfection w0 equal to bik/250, where bik is the smallest width of the adjacent subpanels.
- The adjacent longitudinal boundaries are straight, simply supported and rigid.
- Hinged boundaries are usually assumed between the subpanels and the longitudinal stiffener. If the subpanels are considered to be rigidly connected to the longitudinal stiffener, the loading on the subpanels when they act together with the longitudinal stiffener should be taken into account.

Determination of the patch loading resistance

- **using different buckling curves**

  $\eta_{\text{diff.12}} = 0.897$

- **using a single buckling curve**

  $\alpha_{\text{Rd.12}} = 1.037$ $\eta_{\text{single.12}} = \dfrac{1}{\alpha_{\text{Rd.12}}} = 0.965$

4.2.3.1.3 Verification of the longitudinal stiffener

Generally, the resistance of the longitudinal stiffener can be either calculated according to second-order theory or with the help of a buckling coefficient and a reduction curve. In the latter case, it is of utmost importance to determine the buckling coefficient correctly to which advanced analysis software such as EBPlate [13] is able to highly contribute nowadays. However, in this example, a buckling coefficient for the longitudinal stiffener could not be explicitly determined because the stiffener deflection was always found in combination with local subpanel eigenmodes of higher order. Thus, a verification on the basis of second-order theory is followed here.

In contrast to EN 1993-1-5, in German standard DIN 18800 Part 3, Element (801) [10] rules are provided for the verification of longitudinal stiffeners in panels which are subjected to transverse loading. These complementary rules will be used to determine the stiffener resistance in this example.

Determination of the initial stiffener imperfection

$w_0 := \min\left(\dfrac{b_{11.st}}{250}, \dfrac{b_{12.st}}{250}\right)$ $w_0 = 3.63\,\text{mm}$

Normal force acting on the stiffener

The stiffener force is calculated with the direct stress $\sigma_{x,st}$ and the gross cross-section of the stiffener A_{st}. The gross cross-section of the stiffener is determined according to EN 1993-1-5, Figure A.1:

$b_{11.part} := \dfrac{3 - \psi_{11}}{5 - \psi_{11}} \cdot b_{11}$ $b_{11.part} = 351.6\,\text{mm}$

$b_c := b_{12} - |z_{top.w}|$ $b_c = 1475.2\,\text{mm}$

$b_{c.part} := 0.4 \cdot b_c$ $b_{c.part} = 590.1\,\text{mm}$

$A_{st} := A_{sl.1} + t_w \cdot (b_{11.part} + b_{st} + b_{c.part})$ $A_{st} = 575.84\,\text{cm}^2$

$N_{x.st} := A_{st} \cdot \sigma_{x.Ed.st}$ $N_{x.st} = 6.03\,\text{MN}$

Transverse loading acting on the stiffener

The transverse stress $\sigma_{z,Ed,st}$ acts on the stiffener along the loading length s_{st} only. It can be recalculated to an equivalent transverse stress $\sigma_{z,Ed,st,eq}$ which acts on the whole stiffener length and a factor q as follows:

$$\sigma_{z.Ed.st.eq} := \sigma_{z.Ed.st} \cdot \left(\frac{s_{st}}{a} + \frac{1}{\pi} \cdot \sin\left(\frac{\pi \cdot s_s}{a} \right) \right) \qquad \sigma_{z.Ed.st.eq} = 80.4\,\text{MPa}$$

$$q := \sigma_{z.Ed.st.eq} \cdot t_w \cdot \left(\frac{1}{b_{11.st}} + \frac{1}{b_{12.st}} \right) + \left(\frac{\pi}{a} \right)^2 \cdot N_{x.st} \qquad q = 6.706\,\text{MPa}$$

Second-order theory verification of the stiffener

With the critical force $N_{x,cr}$ of the stiffener and the influence of the elastic foundation c_f, the elastic deformation $w_{el,II}$ and the bending moment M_{II} according to second-order theory can be determined and with the maximum distance $z_{st,1}$ = 393.3 mm to the outer fibre and the moment of inertia $I_{sl.1}$ = 154894 cm^4 of the longitudinal stiffener, the verification can be done.

$$N_{x.cr} := \frac{\pi^2 \cdot 210000\text{MPa} \cdot I_{sl.1}}{a^2} \qquad N_{x.cr} = 200.65\,\text{MN}$$

$$c_f := \left(\frac{\pi}{a} \right)^2 \cdot N_{x.cr} \qquad c_f = 123.8\,\text{MPa}$$

$$w_{el.II} := \frac{q \cdot w_0}{c_f - q} \qquad w_{el.II} = 0.21\,\text{mm}$$

$$M_{II} := N_{x.cr} \cdot w_{el.II} \qquad M_{II} = 0.042\,\text{MNm}$$

$$\sigma := \sigma_{x.Ed.st} + \frac{M_{II}}{I_{sl.1}} \cdot z_{st.1} \qquad \sigma = 115.3\,\text{MPa}$$

$$\eta := \frac{\sigma}{\frac{f_{yw}}{\gamma_{M1}}} \qquad \eta = 0.37$$

4.2.3.2 Bottom plate

4.2.3.2.1 Application of Sections 3, 9 and 10, EN 1993-1-5 to launching situation “1”

In the following, the ultimate resistance of the longitudinal stiffened bottom plate is determined acc. to Sections 3, 9 and 10 of EN 1993-1-5. Resistance is calculated for the erection phase, taking into account the horizontal component of the patch load, cp. Section 4.2.2.1.

Specific cross-section parameters of considered bottom plate (cp. Section 2.2.3):

Thickness of bottom plate:	$t_f = 75$ mm
Number of stiffeners:	$n_{st} = 6$ (Geometry cp. Figure 2-9)
Yield strength of steel:	$f_{yf} = 325$ N/mm²

Determination of the stress field components acc. to elastic bending theory:

Bending moment in cross-section:	$M_{Ed} = 217.93$ MNm
Section modulus at bottom plate:	$W_{bot} = 1150500$ cm³
Resulting axial stress in bottom plate:	$\sigma_{x.Ed} = 189.4$ N/mm²
Horizontal component of patch load:	$F_{Ed.bot} = 5.75$ MN
Loading length:	$s_s = 3.0$ m
Resulting transverse stress:	$\sigma_{y.Ed} = 25.6$ N/mm²

Remark: The above used „section modulus at bottom plate“y takes conservatively into account shear lag effect. In disregard to the consistency this fact is neglected in the following to provide an entire design example.

Figure 4-10 shows the idealized assumption of the stress distribution in the bottom plate acc. to the elastic bending theory. The next required calculation steps are:

1. Correction of the axial stress distribution due to shear lag effect, acc. to EN 1993-1-5 Section 3, if required.
2. Verification of the subpanel resistance acc. to EN 1993-1-5, Section10.
3. Verification if the longitudinal stiffeners fulfil the minimum requirements to act as fix supports for the subpanels acc. to EN 1993-1-5, Section 9.

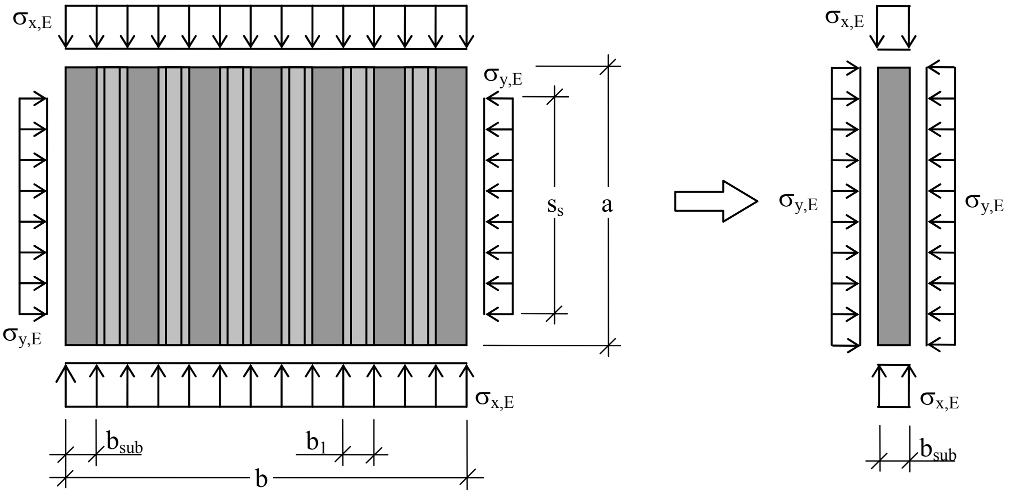

Figure 4-10: Stress field in bottom plate acc. to elastic bending theory (left hand side) and resulting conservative assumption for stress field in subpanel (right hand side).

EN 1993-1-5, 3.1, General

(1) Shear lag in flanges may be neglected if $b_0 < L_e/50$ where b_0 is taken as the flange outstand or half the width of an internal element and L_e is the length between points of zero bending moment, see 3.2.1(2).

EN 1993-1-5, 3.2.1, Effective width

(2) Provided adjacent spans do not differ more than 50% and any cantilever span is not larger than half theadjacent span the effective lengths L_e may be determined from Figure 3.1. For all other cases L_e should betaken as the distance between adjacent points of zero bending moment.

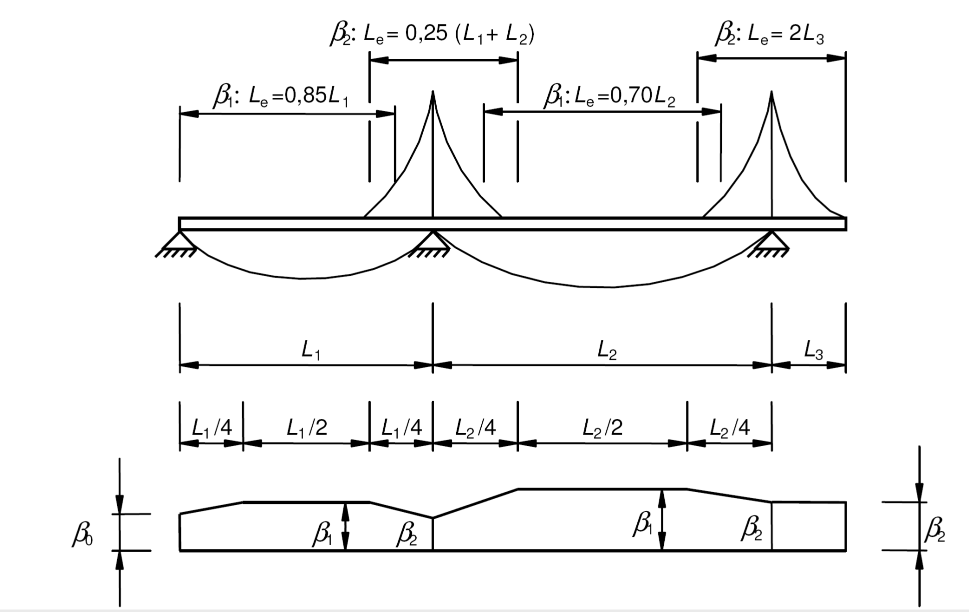

Figure 3.1: Effective length L_e for continuous beam and distribution of effective^{s} width

Table 3.1: Effective^{s} width factor β

κ	Verification	β – value
$\kappa \le 0{,}02$		$\beta = 1{,}0$
$0{,}02 < \kappa \le 0{,}70$	sagging bending	$\beta = \beta_1 = \frac{1}{1 + 6{,}4\,\kappa^2}$
	hogging bending	$\beta = \beta_2 = \frac{1}{1 + 6{,}0\left(\kappa - \frac{1}{2500\,\kappa}\right) + 1{,}6\,\kappa^2}$
$> 0{,}70$	sagging bending	$\beta = \beta_1 = \frac{1}{5{,}9\,\kappa}$
	hogging bending	$\beta = \beta_2 = \frac{1}{8{,}6\,\kappa}$
all κ	end support	$\beta_0 = (0{,}55 + 0{,}025 / \kappa)\,\beta_1$, but $\beta_0 < \beta_1$
all κ	Cantilever	$\beta = \beta_2$ at support and at the end
$\kappa = \alpha_0\, b_0 / L_e$ with $\alpha_0 = \sqrt{1 + \frac{A_{s\ell}}{b_0 t}}$ in which $A_{s\ell}$ is the area of all longitudinal stiffeners within the width b_0 and other symbols are as defined in Figure 3.1 and Figure 3.2.		

Verification if shear lag effect has to be taken into account (EN 1993-1-5, 3.1):

Effective length: $L_e = 120$ m (conservative assumption)

Considered width: $b_0 = b_p/2 = 3.25$ m

⇒ $b_0 < L_e/50$ requirement not fulfilled! Shear lag effect has to be taken into account.

Correction of axial stress distribution due to shear lag effect:

Gross area of longitudinal stiffeners:

$$A_{sl} := n_{st} \cdot t_{st} \cdot (b_2 + 2 \cdot b_3) = 0.109\,\mathrm{m}^2$$

Shear lag parameters:

$$\alpha_0 := \sqrt{1 + \frac{A_{sl}}{b_p \cdot t_f}} = 1.106$$

$$\kappa := \alpha_0 \cdot \frac{b_0}{L_e} = 0.03$$

$$\beta := \begin{cases} 1 & \text{if } \kappa \le 0.02 \\ \dfrac{1}{1 + 6 \cdot \left(\kappa - \dfrac{1}{2500 \cdot \kappa}\right) + 1.6 \cdot \kappa^2} & \text{if } 0.02 < \kappa \le 0.7 \\ \dfrac{1}{8.6 \cdot \kappa} & \text{otherwise} \end{cases}$$

$$\beta = 0.908$$

The axial stress $\sigma_{1.x.Ed}$ in the bottom plate (at location of web) is that value, which deliveres a mean stress value $\sigma_{x.mean}$ in the bottom plate, which is equal to the axial design stress $\sigma_{x.Ed}$ derived by the elasic bending theory. The mean stress $\sigma_{x.mean}$ in the bottom plate is given by the integral

$$\sigma_{x.mean} = \frac{1}{b_0} \int_0^{b_0} \sigma(y)\,dy$$

which results in

$$\sigma_{x.mean} := \sigma_{1.x.Ed} - \frac{4}{5} \cdot (\sigma_{1.x.Ed} - \sigma_{2.x.Ed})$$

with the axial stress $\sigma_{2.x.Ed}$ in the middle of the bottom plate

$$\sigma_{2.x.Ed} := \left| \, 1.25 \cdot (\beta - 0.2) \cdot \sigma_{1.x.Ed} \quad \text{if } \beta > 0.2 \right.$$

the mean stress $\sigma_{x.mean}$ becomes equal to the axial stress $\sigma_{x.Ed}$ for the following value of $\sigma_{1.x.Ed}$:

$$\sigma_{1.x.Ed} := \frac{\sigma_{x.Ed}}{\beta} = 208.6 \cdot \mathrm{N} \cdot \mathrm{mm}^{-2}$$

Cross-check:

$$\sigma_{x.mean} := \sigma_{1.x.Ed} - \frac{4}{5} \cdot (\sigma_{1.x.Ed} - \sigma_{2.x.Ed}) = 189.4 \cdot \mathrm{N} \cdot \mathrm{mm}^{-2} \overset{!}{=} \sigma_{x.Ed} = 189.4 \cdot \mathrm{N} \cdot \mathrm{mm}^{-2}$$

EN 1993-1-5, 3.2.2, Stress distribution due to shear lag

(1) The distribution of longitudinal stresses across the flange plate due to shear lag should be obtained from Figure 3.3.

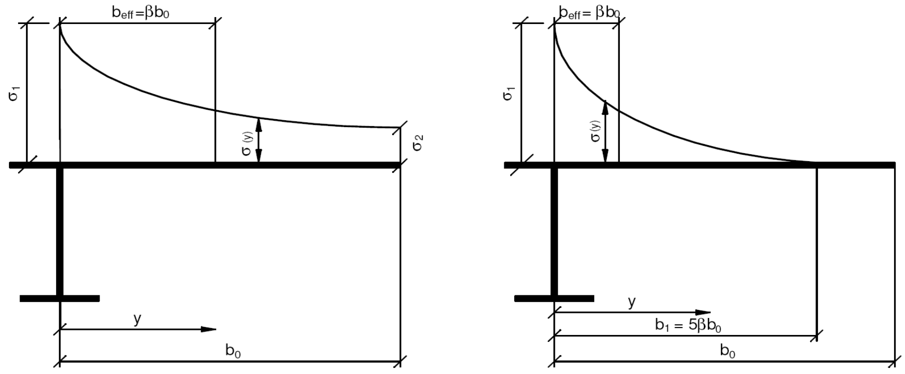
$b_{eff}=\beta b_0$
σ_1
$\sigma(y)$
σ_2
y
b_0
$b_{eff}=\beta b_0$
σ_1
$\sigma(y)$
y
$b_1 = 5\beta b_0$
b_0

$$\beta > 0{,}20:$$
$$\sigma_2 = 1{,}25\,(\beta - 0{,}20)\,\sigma_1$$
$$\sigma(y) = \sigma_2 + (\sigma_1 - \sigma_2)\,(1 - y/b_0)^4$$

$$\beta \le 0{,}20:$$
$$\sigma_2 = 0$$
$$\sigma(y) = \sigma_1 (1 - y/b_1)^4$$

Figure 3.3: Distribution of stresses due to shear lag

EN 1993-1-5, 10, Reduced stress method

(4) In determining $\alpha_{ult,k}$ the yield criterion may be used for resistance:

$$\frac{1}{\alpha_{ult,k}^2} = \left(\frac{\sigma_{x,Ed}}{f_y}\right)^2 + \left(\frac{\sigma_{z,Ed}}{f_y}\right)^2 - \left(\frac{\sigma_{x,Ed}}{f_y}\right)\left(\frac{\sigma_{z,Ed}}{f_y}\right) + 3\left(\frac{\tau_{Ed}}{f_y}\right)^2 \qquad (10.3)$$

where $\sigma_{x,Ed}$, $\sigma_{z,Ed}$ and τ_{Ed} are the components of the stress field in the ultimate limit state.

NOTE: By using the equation (10.3) it is assumed that the resistance is reached when yielding occurs withoutplate buckling.

EN 1993-1-5, 4.4, Plate elements without longitudinal stiffeners

(4) …k_σ is the buckling factor corresponding to the stress ratio ψ and boundary conditions. For long plates k_σ is given in Table 4.1 or Table 4.2 as appropriate;

Table 4.1: Internal compression elements

Stress distribution (compression positive)	Effective^p width b_{eff}
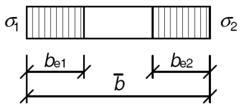 σ_1 σ_2 b_{e1} b_{e2} $\bar{b}$	$\psi = 1$: $b_{eff} = \rho\,\bar{b}$ $b_{e1} = 0{,}5\,b_{eff}$ $b_{e2} = 0{,}5\,b_{eff}$
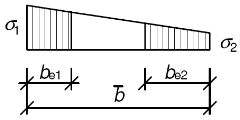 σ_1 σ_2 b_{e1} b_{e2} $\bar{b}$	$1 > \psi \ge 0$: $b_{eff} = \rho\,\bar{b}$ $b_{e1} = \dfrac{2}{5-\psi} b_{eff}$ $b_{e2} = b_{eff} - b_{e1}$
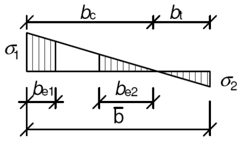 b_c b_t σ_1 σ_2 b_{e1} b_{e2} $\bar{b}$	$\psi < 0$: $b_{eff} = \rho\,b_c = \rho\,\bar{b}\,/\,(1-\psi)$ $b_{e1} = 0{,}4\,b_{eff}$ $b_{e2} = 0{,}6\,b_{eff}$

$\psi = \sigma_2/\sigma_1$	1	$1 > \psi > 0$	0	$0 > \psi > -1$	-1	$-1 > \psi > -3$
Buckling factor k_σ	4,0	$8{,}2\,/\,(1{,}05 + \psi)$	7,81	$7{,}81 - 6{,}29\psi + 9{,}78\psi^2$	23,9	$5{,}98\,(1 - \psi)^2$

Axial stress distribution in bottom flange (half bottom plate):

$$\sigma_x(y) := \begin{cases} \sigma_{2.x.Ed} + \left(\sigma_{1.x.Ed} - \sigma_{2.x.Ed}\right)\cdot\left(1 - \dfrac{y}{b_0}\right)^4 & \text{if } \beta > 0.2 \\ \sigma_{1.x.Ed}\cdot\left(1 - \dfrac{y}{5\cdot\beta\cdot b_0}\right)^4 & \text{otherwise} \end{cases}$$

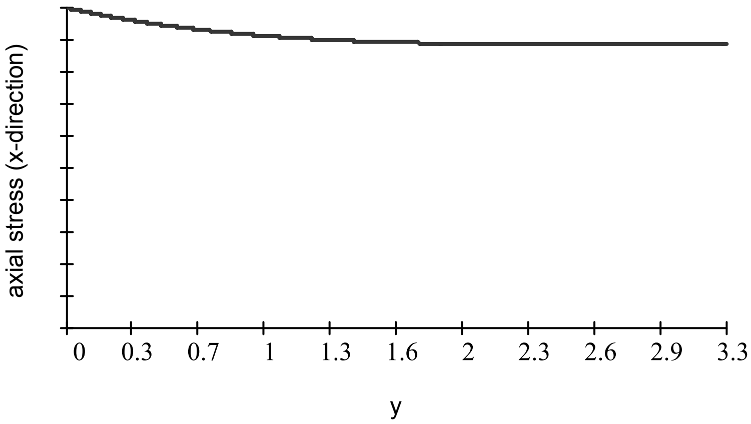

Figure 4-11: Axial stress distribution in bottom flange.

Buckling verification of subpanels:

- Minimum load amplifier $\alpha_{ult,k}$ of subpanel:

$$\alpha_{ult.k} := \frac{f_{yf}}{\sqrt{\sigma_{1.x.Ed}^2 + \sigma_{y.Ed}^2 - \left(\sigma_{1.x.Ed}\cdot\sigma_{y.Ed}\right)}} = 1.649$$

Stress distibution in subpanel:

$$\sigma_{1.sub} := \sigma_{1.x.Ed} = 208.6\cdot N\cdot mm^{-2}$$

$$\sigma_{2.sub} := \sigma_x\left(b_{sub}\right) = 196.7\cdot N\cdot mm^{-2}$$

$$\psi := \frac{\sigma_{2.sub}}{\sigma_{1.sub}} = 0.943$$

Buckling factor for internal compression elements:

$$k_\sigma := \frac{8.2}{1.05 + \psi} = 4.115$$

Critical local buckling stress in x-direction:

$$\sigma_{cr.p.sub.x} := \frac{\pi^2\cdot E\cdot t_f^2}{12\cdot\left(1 - \nu^2\right)\cdot b_{sub}^2}\cdot k_\sigma = 16701.1\cdot N\cdot mm^{-2}$$

Remark from author

The exact elastic critical plate buckling stress $\sigma_{cr,x}$ for a plate with an aspect ratio $\alpha \leq 1$ results from:

$$\sigma_{cr,x} = \frac{\pi^2 \cdot E \cdot t^2}{12 \cdot \left(1 - \mu^2\right) \cdot b^2} \cdot \left[\alpha + \frac{1}{\alpha}\right]^2$$

where a length of the panel in direction of load

b width of panel (transvers to load-direction)

α $= a/b$

EN 1993-1-5, 10, Reduced stress method

(6) Where α_{cr} values for the complete stress field are not available and only $\alpha_{cr,i}$ values for the arious components of the stress field $\sigma_{x,Ed}$, $\sigma_{z,Ed}$ and τ_{Ed} can be used, the α_{cr} value may be determined from:

$$\frac{1}{\alpha_{cr}} = \frac{1+\psi_x}{4\alpha_{cr,x}} + \frac{1+\psi_z}{4\alpha_{cr,z}} + \left[\left(\frac{1+\psi_x}{4\alpha_{cr,x}} + \frac{1+\psi_z}{4\alpha_{cr,z}}\right)^2 + \frac{1-\psi_x}{2\alpha_{cr,x}^2} + \frac{1-\psi_z}{2\alpha_{cr,z}^2} + \frac{1}{2\alpha_{cr,\tau}^2}\right] \qquad (10.6)$$

$$\alpha_{cr,x} = \frac{\sigma_{cr,x}}{\sigma_{x,Ed}}$$

where $$\alpha_{cr,z} = \frac{\sigma_{cr,z}}{\sigma_{z,Ed}}$$

$$\alpha_{cr,\tau} = \frac{\tau_{cr}}{\tau_{Ed}}$$

and $\sigma_{cr,x}$, $\sigma_{cr,z}$, τ_{cr}, ψ_x, ψ_z are determined from Section 4 and Section 6.

EN 1993-1-5, 10, Reduced stress method

(3) The plate slenderness $\bar{\lambda}_p$ should be taken from

$$\bar{\lambda} = \sqrt{\frac{\alpha_{ult,k}}{\alpha_{cr}}} \qquad (10.2)$$

where α_{cr} is the minimum load amplifier for the design loads to reach the elastic critical load of the plate under the complete stress field, see (6)

NOTE1: For calculating α_{cr} for the complete stress field, the stiffened plate may be modelled using the rules in section 4 and 5 without reduction of the second moment of area of longitudinal stiffeners as specified in 5.3(4).

NOTE2: When α_{cr} cannot be determined for the panel and its subpanels as a whole, separate checks for the subpanel and the full panel may be applied.

Minimum load amplifier $\alpha_{cr,sub,x}$:

$$\alpha_{cr.sub.x} := \frac{\sigma_{cr.p.sub.x}}{\sigma_{1.sub}} = 80.063$$

Critical local buckling stress in y-direction:

$$\sigma_{cr.p.sub.y} := \frac{\pi^2 \cdot E \cdot t_f^{\,2}}{12 \cdot \left(1 - \nu^2\right) \cdot a^2} \cdot \left(\frac{b_{sub}}{a} + \frac{a}{b_{sub}}\right)^2 = 4193.6 \cdot N \cdot mm^{-2}$$

Minimum load amplifier $\alpha_{cr,sub,y}$:

$$\alpha_{cr.sub.y} := \frac{\sigma_{cr.p.sub.y}}{\sigma_{y.Ed}} = 164.041$$

Resulting minimum load amplifier α_{cr} for local subpanel bucking (with $\psi \approx 1$):

$$\alpha_{cr.sub} := \frac{1}{\dfrac{1}{\alpha_{cr.sub.x}} + \dfrac{1}{\alpha_{cr.sub.y}}} = 53.803$$

- Interaction between plate and column-type buckling behaviour:

The buckling behaviour in x-direction of the subpanel is pure plate-like, due to ist aspect ratio.

The buckling behaviour in y-direction of the subpanel has to be checked.

Critical local column buckling stress in y-direction:

$$\sigma_{cr.c.sub.y} := \frac{\pi^2 \cdot E \cdot t_f^{\,2}}{12 \cdot b_{sub}^{\,2}} = 3693.8 \cdot N \cdot mm^{-2}$$

Weighting factor ξ:

$$\xi := \frac{\sigma_{cr.p.sub.y}}{\sigma_{cr.c.sub.y}} - 1$$

$$\xi = 0.135$$

- Reduction due to local buckling of subpanels:

Global plate slenderness of subpanel:

$$\lambda := \sqrt{\frac{\alpha_{ult.k}}{\alpha_{cr.sub}}} = 0.175$$

Reduction factor for internal compression elements:

$$\rho_{sub}(\lambda, \psi) := \left| \begin{array}{ll} 1 \ \text{ if } \ \lambda < 0.673 & \\ \dfrac{\lambda - 0.055 \cdot (3 + \psi)}{\lambda^2} & \text{otherwise} \end{array} \right.$$

EN 1993-1-5, 10, Reduced stress method

(5) The reduction factor ρ may be determined using either of the following methods:

a) the minimum value of the following reduction factors:

ρ_x for longitudinal stresses from 4.5.4(1) taking into account column-like behaviour where relevant;

ρ_z for transverse stresses from 4.5.4(1) taking into account column-like behaviour where relevant;

χ_w for shear stresses from 5.2(1);

each calculated for the slenderness $\bar{\lambda}_p$ according to equation (10.2). [..]

b) a value interpolated between the values of ρ_x, ρ_z and χ_w as determined in a) by using the formula for $\alpha_{ult,k}$ as interpolation function

NOTE: This method leads to the verification format:

$$\left(\frac{\sigma_{x,Ed}}{\rho_x f_y / \gamma_{M1}}\right)^2 + \left(\frac{\sigma_{z,Ed}}{\rho_z f_y / \gamma_{M1}}\right)^2 - \left(\frac{\sigma_{x,Ed}}{\rho_x f_y / \gamma_{M1}}\right)\left(\frac{\sigma_{z,Ed}}{\rho_z f_y / \gamma_{M1}}\right) + 3\left(\frac{\tau_{Ed}}{\chi_w f_y / \gamma_{M1}}\right)^2 \le 1$$

(10.5)

NOTE 1: Since verification formulae (10.3), (10.4) and (10.5) include an interaction between shear force, bending moment, axial force and transverse force, section 7 should not be applied.

NOTE 2: The National Annex may give further information on the use of equations (10.4) and (10.5). In case of panels with tension and compression it is recommended to apply equations (10.4) and (10.5) only for the compressive parts.

EN 1993-1-5, 9.2.1, Minimum requirements for transverse stiffeners

(1) In order to provide a rigid support for a plate with or without longitudinal stiffeners, intermediate transverse stiffeners should satisfy the criteria given below.

(2) The transverse stiffener should be treated as a simply supported member subject to lateral loading with an initial sinusoidal imperfection w_0 equal to s/300, where s is the smallest of a_1, a_2 or b, see Figure 9.2, where a_1 and a_2 are the lengths of the panels adjacent to the transverse stiffener under consideration and b is the height between the centroids of the flanges or span of the transverse stiffener. Eccentricities should be accounted for.

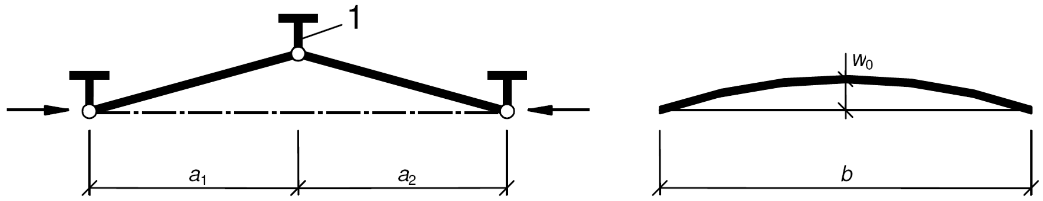

1 Transverse stiffener

Figure 9.2: Transverse stiffener

(3) The transverse stiffener should carry the deviation forces from the adjacent compressed panels under the assumption that both adjacent transverse stiffeners are rigid and straight together with any external load and axial force according to the NOTE: to 9.3.3(3). The compressed panels and the longitudinal stiffeners are considered to be simply supported at the transverse stiffeners.

(4) It should be verified that using a second order elastic method analysis both the following criteria are satisfied at the ultimate limit state:

Reduction factor for column buckling:

$$\chi_{sub}(\phi) := \begin{cases} 1 & \text{if } \lambda < 0.2 \\ \dfrac{1}{\phi + \sqrt{\phi^2 - \lambda^2}} & \text{otherwise} \end{cases}$$

$$\phi := 0.5 \cdot \left[1 + 0.34 \cdot (\lambda - 0.2) + \lambda^2\right] = 0.511$$

$$\chi_{sub} := \chi_{sub}(\phi) = 1$$

Resulting reduction factors

$$\rho_{sub.x} := \rho_{sub}(\lambda, \psi) = 1$$

$$\rho_{sub.y} := \rho_{sub}(\lambda, 1.0) = 1$$

$$\rho_{c.sub.y} := \left(\rho_{sub.y} - \chi_{sub}\right) \cdot \xi \cdot (2 - \xi) + \chi_{sub} = 1$$

Subpanel verification:

$$\eta := \left(\frac{\sigma_{1.sub}}{\rho_{sub.x} \cdot \frac{f_{yf}}{\gamma_{M1}}}\right)^2 + \left(\frac{\sigma_{y.Ed}}{\rho_{c.sub.y} \cdot \frac{f_{yf}}{\gamma_{M1}}}\right)^2 - \left(\frac{\sigma_{1.sub}}{\rho_{sub.x} \cdot \frac{f_{yf}}{\gamma_{M1}}}\right) \cdot \left(\frac{\sigma_{y.Ed}}{\rho_{c.sub.y} \cdot \frac{f_{yf}}{\gamma_{M1}}}\right) = 0.445$$

Global buckling verification of longitudinal stiffener:

- General: Local subpanel bucking is governing, if the longitudinal stiffeners statisfy the criteria of a rigid support. Therefore the minimum requirements for transverse stiffeners given in EN 1993-1-5 Section 9.2 are applied to the longitudinal stiffeners. As the bottom plate is designed for the Ultimate Limit State, it can be expected that for the launching loads the stiffeners fulfill the simplified conservative check acc. to Section 9. In case that this hand-calculation check fails, an exact buckling check, using an appropiate computer program (e.g. EBPlate), has to be performed.

- Minimum requirements for the longitudinal stiffener:

Maximum stress in stiffener:

$$\sigma_{max} \le \frac{f_{yf}}{\gamma_{M1}}$$

Maximum additional deflection:

$$w := \frac{a}{300}$$

- Simplified second order elastic analysis of longitudinal stiffener:

Discription of used parameters:

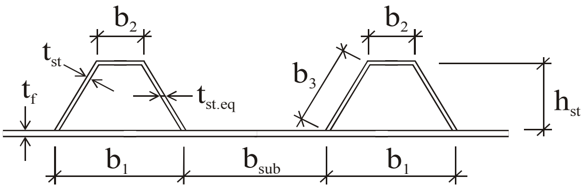

Figure 4-12: Detail of bottom plate cross-section with trapezoidal stiffeners.

EN 1993-1-5, 9.2.1, Minimum requirements for transverse stiffeners

(6) If the stiffener carries axial compression this should be increased by $\Delta N_{st} = \sigma_m \cdot b^2/\pi^2$ in order to account for deviation forces. The criteria in (4) apply but ΔN_{st} need not be considered when calculating the uniform stresses from axial load in the stiffener.

from (5) [..] where $$\sigma_m = \frac{\sigma_{cr,c}}{\sigma_{cr,p}} \frac{N_{Ed}}{b} \left(\frac{1}{a_1} + \frac{1}{a_2} \right)$$

N_{Ed} is the maximum compressive force of the adjacent panels but not less than the maximum compressive stress times half the effective^p compression area of the panel including stiffeners;

$\sigma_{cr,c}$, $\sigma_{cr,p}$ are defined in 4.5.3 and Annex A.

Commentary and worked examples to EN 1993-1-5 “Plated structural elements", 9.2.1 [34] Minimum requirements for transverse stiffeners (p. 110-111)

[..] For single sided transverse stiffeners the mechanical model is shown in Figure 9.2. The equilibrium equation (9.10) is still valid; only the boundary conditions change due to end moments $M_{EN} = N_{st,Ed}\, e_o$, where e_o is the eccentricity of the centroid of single sided stiffener relative to the mid-plane of the web. With new boundary conditions the solution of (9.10) becomes much more complicated than the solution given by (9.17) and is not suitable for practical use. To overcome this problem, a simplified approach may be used, based on the expression for maximum displacements and stresses at mid height of double sided stiffeners (9.19) and (9.20).

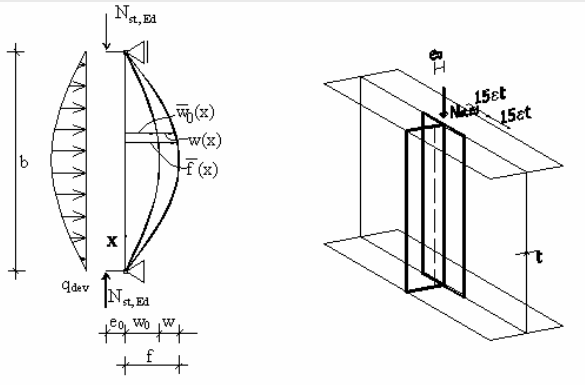

Figure 9.2: The mechanical model of a single sided stiffener

It is considered that $N_{st,Ed}$ is related to the maximum eccentricity $e_o + w_o$ and $\Delta N_{st,Ed}$ from deviation force only to w_o. In this case expression (9.20) rewrites as follows:

$$\sigma_{\max} = \frac{N_{st,Ed}}{A_{st}} + \frac{e_{\max}}{I_{st}} \left(\Sigma N_{st,Ed}\; w_0 \cdot \frac{1}{1 - \dfrac{\Sigma N_{st,Ed}}{N_{cr,st}}} + N_{st,Ed}\; e_0 \cdot \frac{1}{1 - \dfrac{\Sigma N_{st,Ed}}{N_{cr,st}}} \right) \tag{9.21}$$

and after rearranging:

$$\sigma_{\max} = \frac{N_{st,Ed}}{A_{st}} + \frac{\Sigma N_{st,Ed}\; w_0 \cdot e_{\max}}{I_{st}} \cdot \frac{1}{1 - \dfrac{\Sigma N_{st,Ed}}{N_{cr,st}}} \cdot \left(1 + q_m\right) \le \frac{f_y}{\gamma_{M1}} \tag{9.22}$$

where:

$$q_m = \frac{N_{st,Ed}\; e_0}{\Sigma N_{st,Ed}\; w_0}$$

Gross cross-section of stiffener:

$$b_{st.1} := \begin{pmatrix} 2\cdot 15\cdot \varepsilon \cdot t_f \\ b_{sub} \end{pmatrix} = \begin{pmatrix} 1.913 \\ 0.513 \end{pmatrix} m$$

$$b_{st.2} := \begin{pmatrix} 2\cdot 15\cdot \varepsilon \cdot t_f \\ b_1 \end{pmatrix} = \begin{pmatrix} 1.913 \\ 0.485 \end{pmatrix} m$$

$$b_{st} := \min\left(b_{st.1}\right) + \min\left(b_{st.2}\right) = 0.998\,m$$

$$A_{st} := t_{st}\cdot\left(b_2 + 2\cdot b_3\right) + t_f\cdot b_{st} = 93059.4\cdot mm^2$$

$$z_{st} := \frac{h_{st}\left(t_{st.eq}\cdot h_{st} + t_{st}\cdot b_2\right)}{A_{st}} = 55.6\cdot mm$$

$$I_{st} := \left[2\cdot\left[\frac{h_{st}{}^3\cdot t_{st.eq}}{12} + h_{st}\cdot t_{st.eq}\cdot\left(\frac{h_{st}}{2} - z_{st}\right)^2\right] + b_2\cdot t_{st}\cdot\left(h_{st} - z_{st}\right)^2\right] + \frac{b_{st}\cdot t_f{}^3}{12} + b_{st}\cdot t_f\cdot z_{st}{}^2$$

Eccentricity of single sided stiffener:

$$e_0 := z_{st} = 0.056\,m$$

Maximum eccentricity of stiffener:

$$e_{max} := z_{st} + \frac{t_f}{2} = 0.093\,m$$

Amplitude of inital imperfection:

$$w_0 := \min\left[\frac{a}{300}, \frac{\left(b_{sub} + \frac{b_1}{2}\right)}{300}\right] = 2.52\cdot mm$$

Axial load in stiffener:

$$N_{st.Ed} := A_{st}\cdot\sigma_{x.Ed} = 17.63\cdot MN$$

Reduction due to plate type behaviour of the adjacent panels (subpanels):

$$\frac{\sigma_{cr.c.sub.y}}{\sigma_{cr.p.sub.y}} \geq 0.5$$

Deviation force from patch load:

$$N_{Ed} := F_{Ed.bot} = 5.75\cdot MN$$

Maximum deviation stress from patch load:

$$\sigma_m := \frac{\sigma_{cr.c.sub.y}}{\sigma_{cr.p.sub.y}}\cdot\frac{N_{Ed}}{a}\cdot\left(\frac{2}{b_{sub} + \frac{b_1}{2}}\right) = 3.35\cdot N\cdot mm^{-2}$$

If the same amplification factor (1+q_m) is applied to the displacements, equation (9.19) rewrites as follows:

$$w = w_0 \frac{1}{\dfrac{N_{cr,st}}{\Sigma N_{st,Ed}} - 1}\left(1 + q_m\right) \;\leq\; \frac{b}{300} \tag{9.23}$$

Expressions (9.21) and (9.22) were tested against the solution of the equilibrium equation (9.10). Based on an extensive parametric study it was found (Beg and Dujc [1]), that safe and very accurate results are obtained, when q_m is multiplied by a factor 1,11 in (9.22) and by a factor 1,25 in (9.23). This means that single sided transverse stiffeners may be checked to fulfil the requirements (9.1) with the following simplified expressions:

$$\sigma_{\max} = \frac{N_{st,Ed}}{A_{st}} + \frac{\Sigma N_{st,Ed}\, e_{\max}\, w_0}{I_{st}} \cdot \frac{1}{1 - \dfrac{\Sigma N_{st,Ed}}{N_{cr,st}}} \cdot \left(1 + 1{,}11\, q_m\right) \leq \frac{f_y}{\gamma_{M1}} \tag{9.24}$$

$$w = w_0 \frac{1}{\dfrac{N_{cr,st}}{\Sigma N_{st,Ed}} - 1}\left(1 + 1{,}25 q_m\right) \;\leq\; \frac{b}{300} \tag{9.25}$$

For single sided stiffeners $e_{\max}$ has to be understood as the distance from the web surface (opposite to the stiffener) to the stiffener centroid, if this distance is smaller than $e_{\max}$. This is due to the fact that the most unfavourable situation is present when the initial bow imperfection w_0 extends to the stiffener side of the web. In this case compression stresses from the axial force and from bending sum up at the web side of the stiffener.

See also [1].

Additional axial force in stiffener:

$$\Delta N_{st.Ed} := \frac{\sigma_m \cdot a^2}{\pi^2} = 5.44 \cdot MN$$

Resulting axial force in stiffener:

$$\Sigma N_{st.Ed} := N_{st.Ed} + \Delta N_{st.Ed} = 23.06 \cdot MN$$

Euler load of stiffener:

$$N_{cr.st} := \frac{\pi^2 \cdot E \cdot I_{st}}{a^2} = 216.29 \cdot MN$$

Amplifier of deviation force:

$$q_m := \frac{N_{st.Ed} \cdot e_0}{\Sigma N_{st.Ed} \cdot w_0} = 16.864$$

Maximum axial stress in striffener:

$$\sigma_{max} := \frac{N_{st.Ed}}{A_{st}} + \frac{\Sigma N_{st.Ed} \cdot e_{max} \cdot w_0}{I_{st}} \cdot \frac{\left(1 + 1.11 \cdot q_m\right)}{1 - \frac{\Sigma N_{st.Ed}}{N_{cr.st}}}$$

$$\sigma_{max} = 260.9 \cdot N \cdot mm^{-2} \qquad \le \qquad \frac{f_{yf}}{\gamma_{M1}} = 295.5 \cdot N \cdot mm^{-2}$$

→ Minimum requirement for „maximum allowable stress“ fulfilled!

Maximum additional deflection:

$$w := w_0 \cdot \frac{\left(1 + 1.25 \cdot q_m\right)}{\frac{N_{cr.st}}{\Sigma N_{st.Ed}} - 1}$$

$$w = 6.6 \cdot mm \qquad \le \qquad \frac{a}{300} = 13.3 \cdot mm$$

→ Minimum requirement for „maximum allowable additional deflection“ fulfilled!

Final conclusion:

The bottom plate fulfilles the verification acc. to Sections 9 and 10 for the launching situation “1”.

Remark 1: The performed verification via hand-calculation acc. to Section 9 is a safe but conservative approach. In case that the longitudinal stiffeners do not satisfy these requirements, an exact global buckling analysis via appropriate computer software has to be performed.

Remark 2: The verification of the local buckling resitance of the trapezoidal stiffeners can be done separately, whereas the minimum load amplifier is governing the design of the whole cross-section. This calculation is not covered by the calculation example given above.

Parameter study

Table 4-4: Summary of parameter study for launching situation “1”; Variation parameter n_{st}.

Number of stiffeners n_{st}	**[-]**	**2**	**3**	**4**	**5**	**6**
Subpanel width b_{sub}	[m]	1.84	1.26	0.91	0.68	0.51
Maximum axial stress in bottom plate due to shear lag effect $\sigma_{1.x.Ed}$	[N/mm²]	205.4	206.2	207.0	207.8	208.6
Axial stress in bottom plate due to shear lag effect at location of 1st stiffener $\sigma_{2.x.Ed}$	[N/mm²]	185.5	185.2	185.0	184.8	184.6
Minimum load amplifier $\alpha_{ult,k}$	[-]	1.676	1.669	1.663	1.656	1.649
Minimum load amplifier $\alpha_{cr.sub}$	[-]	4.732	9.520	17.611	31.111	53.803
Weighting factor ξ	[-]	0.615	0.328	0.216	0.163	0.135
Global plate slenderness of subpanel $\bar{\lambda}$	[-]	0.595	0.419	0.307	0.231	0.175
Ultilisation level of subpanel η	[-]	0.430	0.432	0.437	0.441	0.445
Ultilisation level of maximum allowable axial stress in stiffener $\eta_{\sigma.max}$	[-]	0.828	0.834	0.848	0.865	0.883
Ultilisation level of maximum allowable additional deflection in stiffener η_{w}	[-]	0.549	0.511	0.496	0.496	0.496

4.2.3.2.2 Application of Sections 3, 9 and 10, EN 1993-1-5 to launching situation "2"

Specific cross-section parameters of considered bottom plate (cp. Section 2.2.3):

Thickness of bottom plate: $t_f = 35$ mm

Geometry of stiffeners: cp. Figure 2-9

Yield strength of of steel: $f_{yf} = 345$ N/mm²

Determination of the stress field components acc. to elastic bending theory:

Bending moment in cross-section: $M_{Ed} = 99.35$ MNm

Section modulus at bottom plate: $W_{bot} = 630829$ cm³

Resulting axial stress in bottom plate: $\sigma_{x.Ed} = 157.5$ N/mm²

Horizontal component of patch load: $F_{Ed.bot} = 3.912$ MN

Loading length: $s_s = 3.0$ m

Resulting transverse stress: $\sigma_{y.Ed} = 37.3$ N/mm²

Verification if shear lag effect has to be taken into account:

Effective length: $L_e = 120$ m (conservative assumption)

Considered width: $b_0 = b_p/2 = 3.25$ m

→ $b_0 < L_e/50$ requirement not fulfilled! Shear lag effect has to be taken into account.

Table 4-5: Summary of parameter study for launching situation "2"; Variation parameter n_{st}.

Number of stiffeners n_{st}	[-]	2	3	4	5	6
Subpanel width b_{sub}	[m]	1.84	1.26	0.91	0.68	0.51
Maximum axial stress in bottom plate due to shear lag effect $\sigma_{1.x.Ed}$	[N/mm²]	172.3	173.7	175.0	176.3	177.5
Axial stress in bottom plate due to shear lag effect at location of 1st stiffener $\sigma_{2.x.Ed}$	[N/mm²]	153.8	153.5	153.1	152.9	152.6
Minimum load amplifier $\alpha_{ult,k}$	[-]	2.197	2.178	2.161	2.144	2.128
Minimum load amplifier $\alpha_{cr.sub}$	[-]	1.033	2.026	3.704	6.501	11.2
Weighting factor ξ	[-]	0.615	0.328	0.216	0.163	0.135
Global plate slenderness of subpanel $\bar{\lambda}$	[-]	1.458	1.037	0.764	0.574	0.436
Ultilisation level of subpanel η	[-]	0.726	0.428	0.287	0.259	0.264
Ultilisation level of maximum allowable axial stress in stiffener $\eta_{\sigma.max}$	[-]	0.713	0.710	0.708	0.731	0.760
Ultilisation level of maximum allowable additional deflection in stiffener η_w	[-]	0.444	0.436	0.436	0.444	0.457

4.2.3.2.3 Application of Sections 3, 9 and 10, EN 1993-1-5 to launching situation “3”

Specific cross-section parameters of considered bottom plate (cp. Section 2.2.3):

Thickness of bottom plate: $t_f = 25$ mm

Geometry of stiffeners: cp. Figure 2-9)

Yield strength of of steel: $f_{yf} = 345$ N/mm²

Determination of the stress field components acc. to elastic bending theory:

Bending moment in cross-section: $M_{Ed} = 50.62$ MNm

Section modulus at bottom plate: $W_{bot} = 499908$ cm³

Resulting axial stress in bottom plate: $\sigma_{x.Ed} = 101.3$ N/mm²

Horizontal component of patch load: $F_{Ed.bot} = 3.38$ MN

Loading length: $s_s = 3.0$ m

Resulting transverse stress: $\sigma_{y.Ed} = 45.1$ N/mm²

Verification if shear lag effect has to be taken into account:

Effective length: $L_e = 60$ m

Considered width: $b_0 = b_p/2 = 3.25$ m

→ $b_0 < L_e/50$ requirement not fulfilled! Shear lag effect has to be taken into account.

Table 4-6: Summary of parameter study for launching situation “3”; Variation parameter n_{st}.

Number of stiffeners n_{st}	**[-]**	**2**	**3**	**4**	**5**	**6**
Subpanel width b_{sub}	[m]	1.84	1.26	0.91	0.68	0.51
Maximum axial stress in bottom plate due to shear lag effect $\sigma_{1.x.Ed}$	[N/mm²]	134.2	136.1	137.9	139.6	141.2
Axial stress in bottom plate due to shear lag effect at location of 1st stiffener $\sigma_{2.x.Ed}$	[N/mm²]	93.0	92.6	92.2	91.7	91.3
Minimum load amplifier $\alpha_{ult,k}$	[-]	2.917	2.873	2.833	2.796	2.762
Minimum load amplifier $\alpha_{cr.sub}$	[-]	0.588	1.117	2.005	3.477	5.939
Weighting factor ξ	[-]	0.615	0.328	0.216	0.163	0.135
Global plate slenderness of subpanel $\bar{\lambda}$	[-]	2.228	1.604	1.189	0.897	0.682
Ultilisation level of subpanel η	[-]	0.844	0.482	0.304	0.206	0.150
Ultilisation level of maximum allowable axial stress in stiffener $\eta_{\sigma.max}$	[-]	0.513	0.512	0.511	0.511	0.526
Ultilisation level of maximum allowable additional deflection in stiffener η_w	[-]	0.308	0.308	0.308	0.308	0.316

4.2.4 Results

In Figure 4-4 the distribution of the patch loading resistances is summarised along the whole bridge length. It can be shown that with the current resistance model of Section 6, EN 1993-1-5 the patch loading resistance cannot be verified for any of the cases. It can be however shown that the improvements made in the COMBRI project [7] lead to increase in the calculated resistances so that launching situation “1” can be verified as it is. For launching situations “2” and “3” a small increase in web thickness from $t_{w(2)}$ = 20 mm to 22 mm and $t_{w(3)}$ = 18 mm to 20 mm allows for a verification against patch loading.

The calculation according to Section 6, EN 1993-1-5 showed that at least for launching situation “1” the patch loading resistance could be verified, see Section 4.2.3.1.

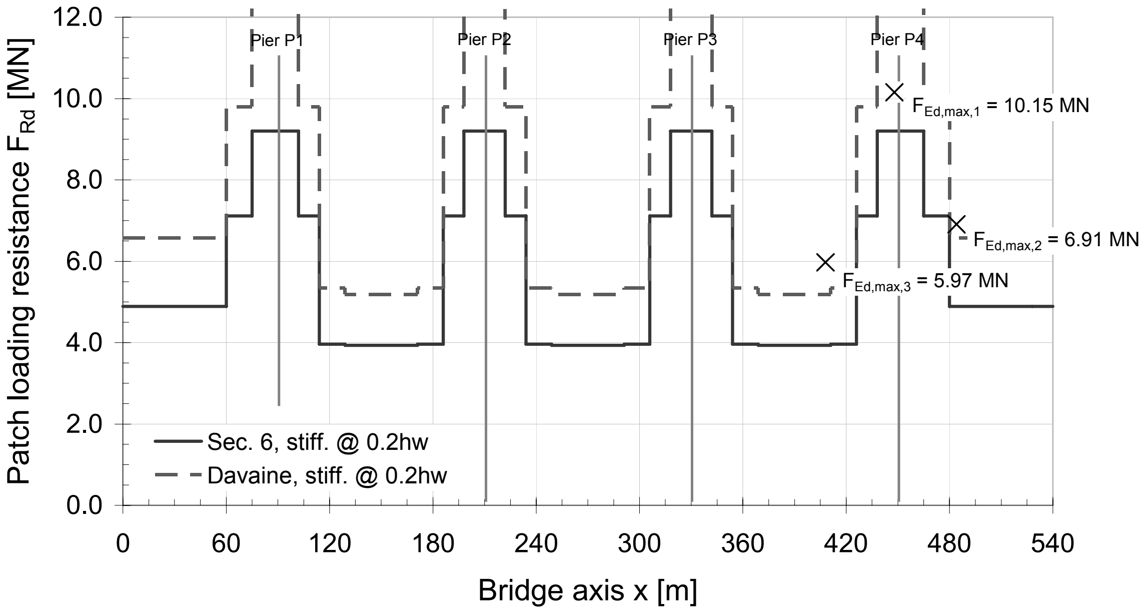

Figure 4-13: Distribution of patch loading resistances according to EN 1993-1-5 [23] along the bridge length.

Figure 4-14 and Figure 4-15 summarise the results of all parameter variations described in Section 4.2.3.2 with regard to the bottom plate. It can be seen that, in spite of the conservatism of the used hand-calculation approach and the used “section modulus at bottom plate”, the level of utilisation for subpanel and stiffener resistance is always below 100%, even if only two stiffeners are used. This means in fact, that for the bottom plate the erection phase is not governing the design.

Furthermore it can be seen that:

1) for thin bottom plates (launching situation “2”, launching situation “3”) the number of stiffeners play a significant roll for its resistance.
2) with increasing number of stiffeners the maximum axial stress in the stiffeners is increasing. This is due to the fact that with decreasing width of the plate the buckling behaviour of the subpanel becomes more column-like. The ratio $\sigma_{cr.c}/\sigma_{cr.p}$ in the hand-calculation approach accounts for the influence of column type behaviour in the subpanels transverse direction that increases deviation forces and thus the equivalent axial stress in the stiffener.

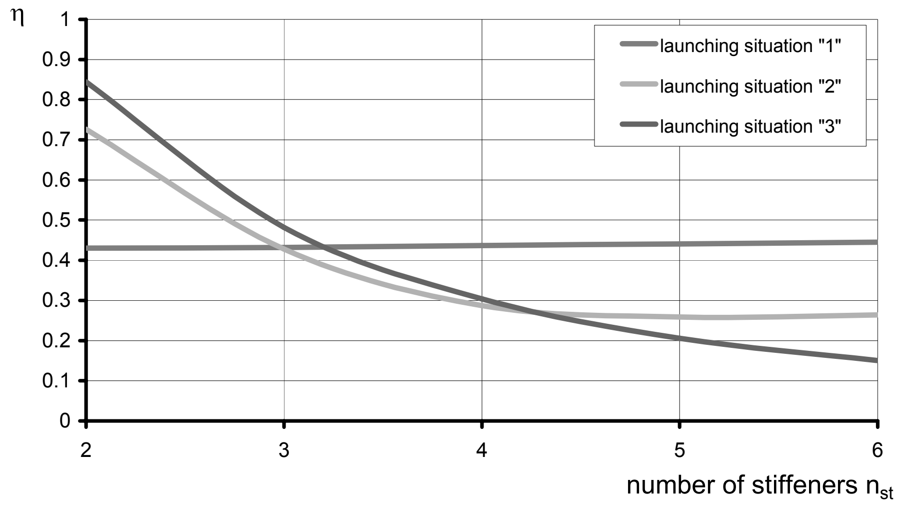

Figure 4-14: Utilisation level of subpanel resistance η in function of number of stiffeners.

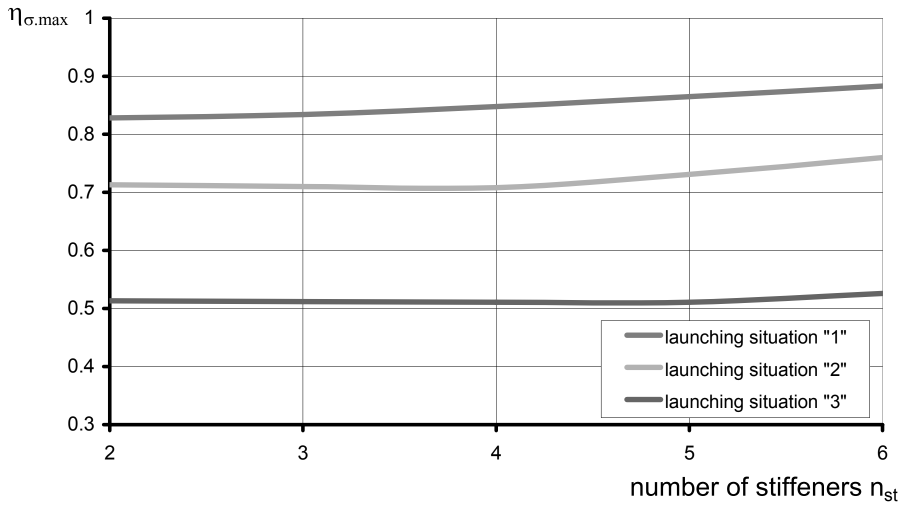

Figure 4-15: Utilisation level of stiffener resistance $\eta_{\sigma.max}$ in function of number of stiffeners.

5 Summary

This publication is Part I of the Design Manual based on results from the research project „Competitive Steel and Composite Bridges by Improved Steel Plated Structures - COMBRI“ [7] and the subsequent dissemination project “Valorisation of Knowledge for Competitive Steel and Composite Structures - COMBRI+“, both sponsored by RFCS. Part II is a separate publication [8], which shows the state-of-the-art and the conceptual design of steel bridges and the steel parts of composite bridges and it is based on the rules in EN 1993-1-5, EN 1993-2 and EN 1994-2. This Part I focuses in detail on the application of Eurocodes on a composite I-girder bridge and a composite box-girder bridge which are related to plate buckling verifications but an overall view on bridge design could not be covered in depth due to its very wide field.

In Chapter 2 the deck of the twin-girder and the box-girder bridge were described and the global analysis of both bridges were introduced. For this purpose, an overview on the bridge geometry, material distribution and construction sequences were firstly given. Secondly, a general section followed in which common data such as material properties and actions as well as combinations thereof were given. The global analysis were presented for both bridges and the relevant results - internal forces and moments - were summarised and set the basis for the verifications in Chapters 3 and 4 which look at the verifications during the final stage and the execution stage.

In Part II of the Design Manual [8] the standard design of the calculation examples of this Part I is enhanced with regard to the conceptual possibilities of the Eurocode rules and the application of results of the COMBRI research project [7]. Part II of the Design Manual is structured according to certain main topics such as steel grades, flanges, webs, cross bracings and diaphragms as well as launching of steel- and composite bridges. Besides general design recommendations in these chapters, relevant parts of the calculation examples of this Part I are recalculated in order to compare and to show the application of new rules or proposals. Especially the following topics related to this Part I are addressed in Part II of the Design Manual [8]:

- Hybrid girders with higher strength in the flanges than in the webs are economic in many applications. Thus, the box-girder is redesigned from S355 to a hybrid girder with S460 and S690 and it will be shown that the cost of the material is reduced by 10% in the spans and 25% at the piers.
- Double composite action with both top and bottom flanges being composite has been used for some large bridges in Germany and France. The top flange is as usual the bridge deck and the bottom flange has a concrete slab at the piers where the bottom flange is in compression. The design of bridges with double composite action is more complicated than the design of a normal composite bridge so that past experience is summarised and recommendations for design are given.
- Here and in general, it is common that transverse stiffeners are used at the locations of the cross bracings of which the transverse stiffeners form a part. Besides that. the effect of the transverse stiffeners on the resistance of the web is basically an increase in the shear buckling resistance. However, unless the distance between the transverse stiffeners is very short this effect is small and it does not justify the cost of the stiffeners. The possibility of omitting the transverse stiffeners ise discussed. Moreover, longitudinal stiffeners on webs increase the resistance for bending as well as for shear so that the economy of using longitudinal stiffeners and their detailing is studied.
- Cross-bracings and diaphragms are to prevent lateral torsional buckling and to transfer lateral loads on the girders to the deck. As used in Chapter 3, traditional cross bracings can be of truss

type or frame type including transverse stiffeners on the webs. Although it is not much material used for cross bracings, from an economical point of view it is important to minimize the man hours for fabrication. This is discussed in terms of eliminating parts and possibly also the transverse stiffeners leading to straightforward solutions.

- The technique of launching bridges has become very popular. As shown in Chapter 4, the resistance to patch loading is of importance as very high support reactions have to be resisted in combination with high bending moments. This has been studied in the COMBRI research project and it resulted in improved design rules. These rules allow the utilisation of quite long loaded lengths and accordingly quite high resistance can be achieved. This may make it possible to launch bridges with parts of the concrete slab or the reinforcement in place. For the twin-girder bridge of this Part I, these two possibilities are studied and the results are compared.

References

[1] Beg, D.; Dujc, J.: Eccentric loading on single sided transverse stiffeners. Background document DB-C008 to EN 1993-1-5, 2005.

[2] Beg, D.; Kuhlmann, U.; Davaine, L.: Design of Plated Structures. Eurocode 3: Design of Steel Structures, Part 1-5 - Design of Plated Structures. ECCS (in preparation).

[3] Calgaro, J.-A.: The design of bridges with the EN Eurocodes. Workshop "Eurocodes: Building the future in the Euro-Mediterranean Area", November 27th-29th, 2006, Varese, Italy.

[4] Calgaro, J.-A.; Tschumi, M.; Shetty, N.; Gulvanessian, H.: Designers' Guide to EN 1992-2, 1991-1.3 and 1991-1.5 to 1.7 Eurocode 1: Actions on Structures - Traffic Loads and other actions on bridges. Thomas Telford, London, 2007.

[5] Clarin, M.: Plate Buckling Resistance - Patch Loading of Longitudinally Stiffened Webs and Local Buckling. Doctoral Thesis 2007:31, Division of Steel Structures, Luleå University of Technology, 2007.

[6] Cook, N.: Designers' Guide to EN 1991-1-4 Eurocode 1: Actions on structures, general actions part 1-4. Wind actions. Thomas Telford, London, 2007.

[7] COMBRI: Competitive Steel and Composite Bridges by Improved Steel Plated Structures. Final Report, RFCS research project RFS-CR-03018, 2007.

[8] COMBRI+: COMBRI Design Manual - Part II: State-of-the-Art and Conceptual Design of Steel and Composite Bridges. RFCS project RFS2-CT-2007-00031, 2008.

[9] Davaine, L.: Formulation de la résistance au lancement d'une âme métallique de pont raidie longitudinalement. Doctoral Thesis D05-05, INSA de Rennes, France, 2005.

[10] DIN 18800 Teil 3: Stahlbauten - Stabilitätsfälle, Plattenbeulen, November 1990.

[11] DIN EN 1993 NA: National Annex - Nationally determined parameters: Eurocode 3: Design of steel structures – Part 1-5 NA: Plated structural elements (in preparation).

[12] DIN-Fachbericht 103: Stahlbrücken. Revised version (in preparation).

[13] EBPlate: A piece of software developed in the frame of the COMBRI research project [7]. Its aim is to assess the elastic critical stresses of plates. *EBPlate* is free of charge and can be downloaded from the web site of cticm: www.cticm.com

[14] EN 1990/A1: Eurocode: Basis of structural design – Application for bridges, December 2005.

[15] EN 1991-1-1: Eurocode 1: Actions on structures – Part 1-1: General actions - Densities, self-weight, imposed loads for buildings, April 2002.

[16] EN 1991-1-3: Eurocode 1: Actions on structures – Part 1-3: General actions, Snow loads, July 2003.

[17] EN 1991-1-4: Eurocode 1: Actions on structures – Part 1-4: General actions, Wind actions, April 2005.

[18] EN 1991-1-5: Eurocode 1: Actions on structures – Part 1-5: General actions, Thermal actions, November 2003.

[19] EN 1991-1-6: Eurocode 1: Actions on structures – Part 1-6: General actions, Actions during execution, June 2005.

[20] EN 1991-1-7:Eurocode 1: Actions on structures – Part 1-7: General actions, Accidental Actions, July 2006.

[21] EN 1991-2: Eurocode 1: Actions on structures – Part 2: Traffic loads on bridges, September 2003.

[22] EN 1993-1-1: Eurocode 3: Design of steel structures – Part 1-1: General rules and rules for buildings, May 2005.

[23] EN 1993-1-5: Eurocode 3: Design of steel structures – Part 1-5: Plated structural elements, October 2006.

[24] EN 1993-2: Eurocode 3: Design of steel structures – Part 2: Steel Bridges, October 2006.

[25] EN 1994-1: Eurocode 4: Design of composite steel and concrete structures – Part 1-1: General rules and rules for building, December 2004.

[26] EN 1994-2: Eurocode 4: Design of composite steel and concrete structures – Part 2: General rules and rules for bridges, October 2005.

[27] EN 1997-1: Eurocode 7: Geotechnical design – Part 1: General rules, November 2004.

[28] EN 1998-1: Eurocode 8: Design of structures for earthquake resistance – Part 1: General rules, seismic actions and rules for buildings.

[29] EN 1998-2: Eurocode 8: Design of structures for earthquake resistance – Part 2: Bridges, November 2005

[30] EN 1998-5: Eurocode 8: Design of structures for earthquake resistance – Part 5: Foundations, retaining structures and geotechnical aspects, November 2004.

[31] Gozzi, J.: Patch Loading Resistance of Plated Girders - Ultimate and serviceability limit state. Doctoral Thesis 2007:30, Division of Steel Structures, Luleå University of Technology, 2007.

[32] Hendy, C.R.; Johnson, R.: Designers' Guide to EN 1994-2 Eurocode 4: Design of composite steel and concrete structures Part 2, General rules and rules for bridges. Thomas Telford, London, 2006.

[33] Hendy, C.R.; Murphy, C.J.: Designers' Guide to EN 1993-2 Eurocode 3: Design of steel structures. Part 2: Steel bridges. Thomas Telford, London, 2007.

[34] Johansson, B.; Maquoi, R.; Sedlacek, G.; Müller, C.; Beg, D.: Commentary and worked examples to EN 1993-1-5 "Plated structural elements". Joint report JRC-ECCS, 2007.

[35] Leitfaden zum DIN-Fachbericht 101: Einwirkungen auf Brücken. Verlag Ernst & Sohn, Berlin, 2003.

[36] Leitfaden zum DIN-Fachbericht 103: Stahlbrücken. Verlag Ernst & Sohn, Berlin, 2003.

[37] Leitfaden zum DIN-Fachbericht 104: Verbundbrücken. Verlag Ernst & Sohn, Berlin, 2003.

[38] Protte, W.: Beulwerte für Rechteckplatten unter Belastung beider Längsränder. Stahlbau 62 (1993), No. 7, pp.189-194.

[39] Sedlacek, G.; Feldmann, M.; Naumes, J.; Müller, Ch.; Kuhlmann, U.; Braun, B.; Mensinger, M; Ndogmo, J.: Entwicklung und Aufbereitung wirtschaftlicher Bemessungsregeln für Stahl- und Verbundträger mit schlanken Stegblechen im Hoch- und Brückenbau. AiF-project 14771, Final Report, Oktober 2007.

[40] Seitz, M.: Tragverhalten längsversteifter Blechträger unter quergerichteter Krafteinleitung. Doctoral Thesis, Universität Stuttgart, Mitteilung des Instituts für Konstruktion und Entwurf Nr. 2005-2, 2005.

[41] Sétra: Guidance book Eurocodes 3 and 4 - Application to steel-concrete composite road bridges. Sétra (Service d'Etudes techniques des routes et autoroutes), July 2007.

List of figures

Figure 1-1: Eurocodes to be used in a composite bridge design. 1

Figure 2-1: Elevation of the twin-girder bridge. 5

Figure 2-2: Cross-section with traffic data of the twin-girder bridge...7

Figure 2-3: Transverse cross-bracing on supports of the twin-girder bridge. 7

Figure 2-4: Structural steel distribution for a main girder of the twin-girder bridge. 9

Figure 2-5: Order for concreting the slab segments of the twin-girder bridge..11

Figure 2-6: Elevation of the box-girder bridge...15

Figure 2-7: Cross-section with traffic data of the box-girder bridge...15

Figure 2-8: Transverse cross-bracings on supports of the box-girder bridge..17

Figure 2-9: Detail of a bottom flange longitudinal stiffener of the box-girder bridge. 19

Figure 2-10: Structural steel distribution for a main girder of the box-girder bridge..............................21

Figure 2-11: Order for concreting the slab segments of the box-girder bridge.......................................23

Figure 2-12: Location of mid-span and support sections for longitudinal reinforcing steel of the twin-girder bridge...25

Figure 2-13: Location of mid-span and support sections for longitudinal reinforcing steel of the box-girder bridge..25

Figure 2-14: Modelling the concrete slab for the longitudinal global bending (twin-girder bridge). 27

Figure 2-15: Modelling the concrete slab for the longitudinal global bending (box-girder bridge). 27

Figure 2-16: Non-structural bridge equipment details. 35

Figure 2-17: Traffic lanes positioning for calculating the girder no.1. 39

Figure 2-18: Calculation of the box-girder for eccentric concentrated load. 41

Figure 2-19: Traffic lanes positioning for calculating the box-girder...41

Figure 2-20: Tandem TS loading on the deck for the twin-girder bridge. 43

Figure 2-21: Tandem TS loading on the deck for the box-girder bridge...43

Figure 2-22: UDL tranverse distribution on the bridge deck for the twin-girder bridge..........................45

Figure 2-23: UDL tranverse distribution on the bridge deck for the box-girder bridge...........................45

Figure 2-24: Effective slab width for a main girder in a given cross-sectionof the twin-girder bridge...57

Figure 2-25: Effective slab width for a main girder in a given cross-section of the box-girder bridge...59

Figure 2-26: Cracked zonesof the twin-girder bridge used in the global analysis. 63

Figure 2-27: Cracked zones of the box-girder bridge used in the global analysis. 63

Figure 2-28: Global analysis organisation chart...67

Figure 2-29: Isostatic and hyperstatic bending moments due to the long-term concrete shrinkage for the twin-girder bridge..69

Figure 2-30: Bending moments under the uniformly distributed load and tandem traffic load (frequent and characteristic LM1) for the twin-girder bridge. 69

Figure 2-31: Bending moments under the fundamental ULS and characteristic SLS combinations of actions for the twin-girder bridge. 71

Figure 2-32: Shear forces under the fundamental ULS and characteristic SLS combinations of actions for the twin-girder bridge. 71

Figure 2-33: Isostatic and hyperstatic bending moments due to the long-term concrete shrinkage for the box-girder bridge. 73

Figure 2-34: Bending moments under the uniformly distributed load and tandem traffic load (frequent and characteristic LM1) for the box-girder bridge 73

Figure 2-35: Torque under characteristic LM1 for the box-girder bridge. 75

Figure 2-36: Bending moments under the fundamental ULS and characteristic SLS combinations of actions for the box-girder bridge. 75

Figure 2-37: Shear forces under the fundamental ULS and characteristic SLS combinations of actions for the box-girder bridge. 77

Figure 3-1: Position of vertical stiffeners of the twin-girder bridge. 79

Figure 3-2: Checked sections of the twin-girder bridge. 79

Figure 3-3: Different subpanels on the internal support P2. 81

Figure 3-4: Cross-section at the end support C0. 81

Figure 3-5: Design Plastic resistance moment at external support C0. 89

Figure 3-6: Cross-section at mid-span P1-P2. 97

Figure 3-7: Cross-section at the internal support P2. 109

Figure 3-8: Design Plastic resistance moment $M_{f,Rd}$ of the flanges only at internal support support P2. 121

Figure 3-9: Checked sections of the box-girder bridge. 139

Figure 3-10: Cross-section of the box-girder bridge at mid-span P1-P2. 141

Figure 3-11: Cross-section of the box-girder bridge at the internal support P3. 153

Figure 3-12: Geometry of the trapezoidal stiffeners. 159

Figure 3-13: Utilisation level (left ordinate) and effective^p area (right ordinate) of bottom plate in function of bottom plate thickness t_p; curve parameter = number of stiffeners n_{st}. 169

Figure 4-1: Most unfavourable launching situation. 195

Figure 4-2: Dimensions of the studied panel in [m]. 197

Figure 4-3: Stress field acting at the studied panel. 197

Figure 4-4: Distribution of patch loading resistances according to EN 1993-1-5 along the bridge length. 209

Figure 4-5: Launching situation “1” (most unfavourable both for maximum bending and pier cross-section). 211

Figure 4-6: Launching situation “2” (most unfavourable for weakest end-span cross-section). 213

Figure 4-7: Launching situation “3” (most unfavourable for weakest mid-span cross-section). 213

Figure 4-8: Notations of the studied panel in [mm]. 215

Figure 4-9: Stress field acting on the studied panel. 225

Figure 4-10: Stress field in bottom plate acc. to elastic bending theory (left hand side) and resulting conservative assumption for stress field in subpanel (right hand side). 243

Figure 4-11: Axial stress distribution in bottom flange. 247

Figure 4-12: Detail of bottom plate cross-section with trapezoidal stiffeners.......................................251

Figure 4-13: Distribution of patch loading resistances according to EN 1993-1-5 [23] along the bridge length. 263

Figure 4-14: Utilisation level of subpanel resistance η in function of number of stiffeners. 265

Figure 4-15: Utilisation level of stiffener resistance $\eta_{\sigma.max}$ in function of number of stiffeners. 265

List of tables

Table 2-1: Age of concrete slab segments at the end of the construction phasing of the twin-girder bridge. 13

Table 2-2: Age of concrete slab segments at the end of the construction phasing of the box-girder bridge. 23

Table 2-3: Areas of the steel reinforcement. 29

Table 2-4: Decrease of fy and fu according to the plate thickness t. 29

Table 2-5: Partial safety factors for materials (ULS). 31

Table 2-6: Partial safety factors for materials (SLS). 31

Table 2-7: Loads of the non-structural equipment (twin-girder bridge). 33

Table 2-8: Loads of the non-structural equipment (box-girder bridge). 33

Table 2-9: Shrinkage at traffic opening for the persistent design situation at traffic opening (tini). 35

Table 2-10: Shrinkage at infinite time. 37

Table 2-11: Modular ratio for long-term loading (twin-girder bridge). 37

Table 2-12: Modular ratio for long-term loading (box-girder bridge). 37

Table 2-13: Adjustment coefficients for LM1 39

Table 3-1: Resulting effectivep width of subpanels and stiffener plates 161

Table 4-1: Dimensions of the studied panels in [mm] 215

Table 4-2: Internal design forces. 215

Table 4-3: Values of the studied panel, see Figure 4-3 (compression is taken as positive). 225

Table 4-4: Summary of parameter study for launching situation “1”; Variation parameter nst. 257

Table 4-5: Summary of parameter study for launching situation “2”; Variation parameter nst. 259

Table 4-6: Summary of parameter study for launching situation “3”; Variation parameter nst. 261